GEORGIA DOT RESEARCH PROJECT 13-09

FINAL REPORT

ASSESSMENT OF LIMESTONE BLENDED CEMENTS FOR TRANSPORTATION APPLICATIONS

OFFICE OF RESEARCH
15 KENNEDY DRIVE
FOREST PARK, GA 30297-2534

1. Report No.: FHWA-GA-17-13-09	2. Government Accession No.:	3. Recipient's Catalog No.:
4. Title and Subtitle: Assessment of Limestone Blended Cements for Transportation Applications	5. Report Date: September 2017	
	6. Performing Organization Code:	
7. Author(s): Kimberly E. Kurtis, Lawrence F. Kahn, Ahmad Shalan, Behnaz Zaribaf, Elizabeth Nadelman	8. Performing Organ. Report No.:	
9. Performing Organization Name and Address: Georgia Institute of Technology 790 Atlantic Drive, Atlanta, GA 30332	10. Work Unit No.:	
	11. Contract or Grant No.:	
12. Sponsoring Agency Name and Address: Georgia Department of Transportation Office of Research15 Kennedy Drive Forest Park, GA 30297-2534	13. Type of Report and Period Covered: Draft; May 2013-September 2017	
	14. Sponsoring Agency Code:	
15. Supplementary Notes:		

16. Abstract:

This research assessed the applicability of Type IL cements satisfying AASHTO M 240 specifications for use in transportation applications in place of Type I/II cements which satisfy AASHTO M 85 specifications for construction of transportation structures. Type I/II and Type IL cements from five producers were investigated. The cements and both mortars and concretes made with these cements were studied to determine material characteristics; material properties including setting time, strength development, shrinkage, and permeability; and mechanical properties. The results showed the performance of concrete made with Type IL cement was affected by the cement fineness which increased strength and drying shrinkage. Type IL cement may be used in place of Type I/II cement when fineness values are specified.

17. Key Words: performance-based specification, mix-design, concrete, durability, limestone blended cement	18. Distribution Statement:		
19. Security Classification (of this report): Unclassified	20. Security Classification (of this page): Unclassified	21. Number of Pages: 265	22. Price:

Final Report

ASESSMENT OF LIMESTONE BLENDED CEMENTS FOR TRANSPORTATION
APPLICATIONS

By
Kimberly E. Kurtis
Lawrence F. Kahn
Ahmad Shalan
Behnaz Zaribaf
Elizabeth Nadelman

Georgia Institute of Technology

Contract with

Georgia Department of Transportation

In cooperation with

U.S. Department of Transportation
Federal Highway Administration

September 2017

TABLE OF CONTENTS

LIST OF TABLES

LIST OF FIGURES

EXECUTIVE SUMMARY

This research compared the performance of Type IL limestone blended cements satisfying AASHTO M 240 to conventional Type I/II portland cements satisfying AASHTO M 85 in pastes and in concretes designed to meet GDOT specifications for Classes A, AA, and AA1 or AAA concrete. Five cement producers provided both Type IL and Type I/II cements; all were investigated and compared. Substitution of Type I/II cement with Type IL cement resulted in concretes of all GDOT classes which satisfied GDOT specifications.

In general, differences in mechanical properties of concretes made with each cement type were higher between plants than between Type I/II and Type IL cement from the same plant. The fineness of the portland cement and of the interground limestone had the most significant effect on paste and concrete properties; each cement plant provided cements with different fineness.

Blaine fineness was shown to be an inadequate measure of fineness when comparing Type IL cements. Fineness parameters obtained by laser diffraction analysis were found to be comparatively more sensitive to changes in the particle size distributions and correlated well with the resulting dilution- or nucleation-dominated behaviors. Based on this preliminary study, it is recommended that "fine" Type IL cements be classified as those cements having median particle sizes $D_{50} < 10$ μm or 90th percentile particle sizes $D_{90} < 30$ μm.

Use of interground limestone in the cement had a dilution effect (weakening the concrete) when the cement factor was high and the water-to-binder ratio (w/b) was low,

such as in Class A concrete. Yet, the same use of a fine interground limestone in the cement had a nucleation effect (stronger early age concrete) when the cement factor was high and the *w/b* ratio was low, such as in Class AAA concrete. The figure below presents the compressive strength results for Class A (blue), AA (black), and AAA (red) concretes made with Type I/II cement (solid) and Type IL cement (cross-hatched) from a single plant; this plant produced Type IL cements in which the fineness of the interground limestone was about the same as that of the cement. Often the fineness of the interground limestone is significantly less than that of the portland cement.
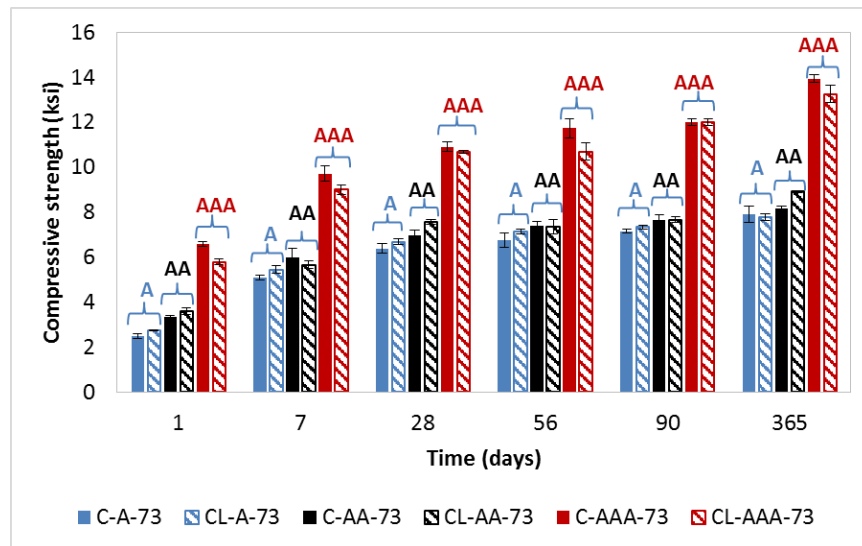
Pastes and concretes made with high fineness of Type IL cements demonstrated greater chemical and autogenous shrinkage at early ages than those with coarser interground limestone.

The use of Class C fly ash, Class F fly ash, and blast furnace slag demonstrated that the increases in compressive strength and reductions in permeability of the concretes tended to be greater in blends using these supplementary cementitious materials (SCMs) with portland-limestone cements (PLCs) than in blends with ordinary portland cements

(OPCs) due to the synergetic interactions between the limestone and the alumina within the SCM. While the synergetic interactions beneficially refined the porosity of the systems, these refinements were accompanied by often substantial increases in early-age shrinkage in PLC-SCM blended systems. In applications where low shrinkage is required, it is *not* recommended that combinations of PLCs with Class C fly ash or high volumes of slag be used. Concretes made with PLC and Class F fly ash showed similar drying shrinkage and strength to concretes made with OPCs and Class F fly ash.

PLC and PLC-SCM blended systems have comparable or slightly improved resistance to the ingress of contaminants when compared to neat OPC and OPC-SCM blended systems at $w/b = 0.445$. When adequately air-entrained, PLC concrete showed good resistance to freezing and thawing cycles under accelerated testing. Results of the rapid chloride ion penetration resistance (RCPT, AASHTO T277) showed there was little difference between the electrical properties for the Type I/II and Type IL concretes and that, in general, concretes had similar charges passed suggesting similar permeabilities. Nevertheless, it is recommended that the surface resistivity and RCPT tests only be used in quality control applications where samples of field-batched concrete are compared to laboratory-prepared reference samples having similar compositions and pore solution chemistries or that variations in these be accounted for appropriately, such as through the use of Formation factor limits.

Overall, the performance of concrete made with Type IL cement was affected by the cement fineness which increased strength and drying shrinkage. Type IL cement may be used in place of Type I/II cement when performance requirements such as shrinkage are specified.

ACKNOWLEDGMENTS

Administration, the Georgia Department of Transportation, or any other sponsoring or cooperating organization.

LIST OF SYMBOLS AND ABBREVIATIONS

AASHTO   American Association of State Highway and Transportation Officials

ASTM   American Society for Testing and Materials

BET   Brunauer-Emmett-Teller

BJH   Barrett, Joyner, Halenda

BSE   Backscattered electron

COD   Crystallography Open Database

CSA   Canadian Standards Association

DOT   Department of Transportation

DTG   Thermogravimetric derivative

EPA   United States Environmental Protection Agency

GDOT   Georgia Department of Transportation

GHG   Greenhouse gas

HDPE   High-density polyethylene

LS   Limestone

NIST   National Institute of Standards and Technology

OPC   Ordinary portland cement

PLC   Portland limestone cement

RCP(T)   Rapid chloride permeability test

SCM   Supplementary cementitious material

SD   Standard deviation

SEM   Scanning electron microscopy

SFF   ratio of the Blaine surface area (m^2/kg) to the percent passing No. 325 sieve

SG   Specific gravity

SR   Surface resistivity

SSA   Specific surface area

TGA   Thermogravimetric analysis

VP-SEM   Variable pressure scanning electron microscopy

QXRD   Quantitative X-ray diffraction

XRD   X-ray diffraction

Cement Chemistry Abbreviations

AFm   Alumina-ferrite-monosulfate

AFt   Alumina-ferrite-trisulfate

C_2S Dicalcium silicate ($2CaO \cdot SiO_2$)

C_3A Tricalcium aluminate ($3CaO \cdot Al_2O_3$)

C_3S Tricalcium silicate ($3CaO \cdot SiO_2$)

C_4AF Tetracalcium aluminoferrite ($4CaO \cdot Al_2O_3 \cdot Fe_2O_3$)

$C\bar{C}$ Calcium carbonate ($CaCO_3$)

CH   Calcium hydroxide ($Ca(OH)_2$)

C-S-H   Calcium-silicate-hydrate

Hc   Hemicarboaluminate hydrate (hemicarbonate)

Mc   Monocarboaluminate hydrate (monocarbonate)

Ms   Monosulfoaluminate hydrate (monosulfate)

Symbols

a Probe spacing

C/C_0 Degree of supersaturation (C = concentration)

D_{10} 10th percentile particle diameter

$D_{3,2}$ Surface area-weighted mean particle size

$D_{4,3}$ Volume-weighted mean particle size

D_{50} 50th percentile particle diameter

D_{90} 90th percentile particle diameter

D_a Apparent diffusion coefficient

E Elastic modulus

F Formation factor

f_c' Specified compressive strength of concrete

f_{sp}	Splitting tensile strength of concrete
h	Height of capillary rise in a porous material
$H(t)$	Cumulative heat of hydration through time t
H_∞	Total heat of hydration upon complete hydration
H_{cem}	Total heat of hydration upon complete hydration of cement
H_{FA}	Total heat of hydration upon complete hydration of fly ash
h_s	Height of capillary rise at the surface of a porous material
H_{slag}	Total heat of hydration upon complete hydration of slag
I	Current (Chapter 7 only)
I	Total absorption (Chapter 8 only)
I_{eff}	Effective total absorption
J	Flux
k	Permeability
p	Initial volume fraction of water (Powers' model)
p_c	Crystallization pressure
p_{cap}	Capillary pressure
p_i	Mass fraction of phase i in system of interest
p_w	Pore wall pressure
Q_t	Total charge passed by RCP test
r	Pore radius
R	Universal gas constant, 8.314 J/mol·K
RH	Relative humidity
S	Sorptivity
SG	Specific gravity
SG_b	Specific gravity of binder
T	Temperature
V	Voltage (Chapter 7 only)
V_{cs}	Volume fraction of chemical shrinkage
V_{cw}	Volume fraction of capillary water (capillary porosity)
V_f	Volume fraction of filler

V_{hp}	Volume fraction of hydration product
V_{uc}	Volume fraction of unhydrated cement
w/b	Water-to-binder mass ratio, where the "binder" includes the cement and limestone , and any supplementary cementitious materials
α	Degree of hydration
α_u	Ultimate degree of hydration
β	Hydration shape parameter
γ	Surface energy
η	Viscosity
θ	Contact angle (of a liquid-solid interface)
κ	Curvature (of a crystal)
ρ	Density
ρ	Electrical resistivity
σ	Electrical conductivity
τ	Hydration time parameter
ϕ or φ	Porosity

Chapter 1. INTRODUCTION

1.1 Motivation

Concrete is the most widely used construction material in the world, with an estimated 34 billion metric tons produced worldwide in 2015 [1]. Of those 34 billion tons, approximately 12%, or 4.1 billion metric tons is portland cement, whose production is estimated to contribute 5-8% of all anthropogenic CO_2 emissions each year [2]. Worldwide, cement production ranks first among industrial processes in total greenhouse gas (GHG) emissions, with only fuel combustion ranking higher (Figure 1-1) [3].
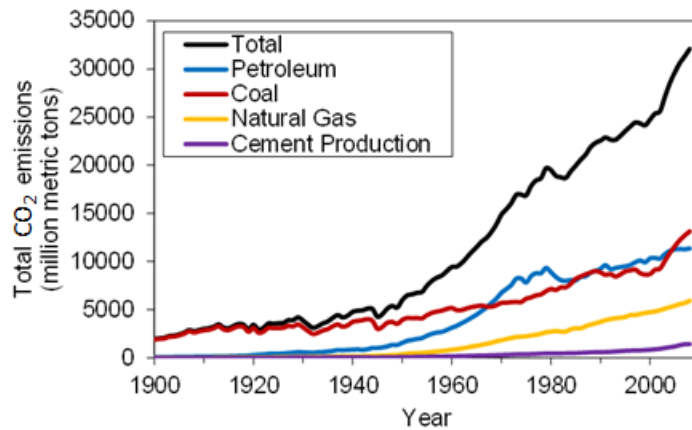
Figure 1.1: Global anthropogenic CO_2 emissions from four largest contributors, 1900-2009 [4]

Altogether, the production of one ton of portland cement releases between 0.65 and 0.95 tons of CO_2, with production in the United States averaging about 0.89 tons of CO_2 per ton of cement [5]. While long-term options to curb CO_2 emissions include improving the operating efficiency of the kilns and converting to less CO_2-intensive fuel sources for heating and energy, more immediate reductions in CO_2 emissions can be

realized by (1) reducing the amount of cement used in concrete or (2) reducing the amount of clinker used in the cement.

This research focuses on the latter of these two options, with a particular emphasis on portland limestone or limestone blended cements, which, in North America, contain nominally 80-90 wt.% portland cement clinker and 6-15 wt.% finely divided limestone powder [6].

Both AASHTO and ASTM have recently approved significant changes to their specification for cements or blended cements. Most recently, both have adopted changes to existing specifications – ASTM C595 [7] and AASHTO M240 [8] – allowing an increase in the allowable mass of ground limestone ($CaCO_3$) in some Portland cement to approximately 15% by mass (Figure 1-2). This new Class of "limestone blended cements" or Type IL cements are anticipated to have significantly different behavior than currently available binders due to the higher limestone fraction. Until recently, ground limestone had not been permitted in US Portland cements. However, in 2007, ASTM specifications were altered to allow up to 5% ground limestone by mass under its C150 specification [9]. AASHTO followed in 2008 and modified its M85 specification in a similar manner [10].

Acceptance of Portland Limestone Cement
Tentative data: May 2015
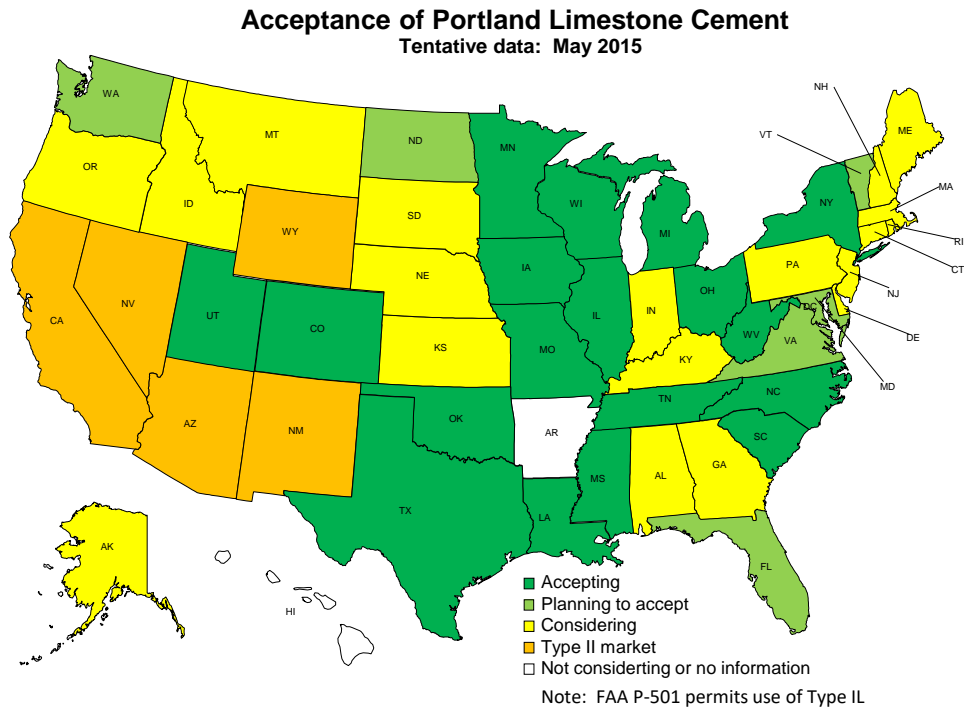
Figure 1.2: Map of states who are accepting or planning/considering to accept portland limestone cement, Map courtesy of Steven Wilcox.

The partial replacement of cement clinker with ground limestone is associated with contributions to sustainability due to reduced energy consumption during cement manufacture and reduced emissions of carbon dioxide, other gases, and particulates during production. In part to address these concerns, European and Canadian specifications [11] allow up to 15% and 35% by mass in certain cement Classes, and the use of such cements is growing.

While ground limestone is largely chemically inert, its presence in cement has been shown to alter the rate of cement reaction, time to set, and early age shrinkage, among other properties, at the 5% replacement level previously allowed [12]. Others have suggested that the limestone itself may react to some degree and may densify the cement paste. Relatively less research has been conducted on the durability of such cements,

3

although some results do suggest that resistance to sulfate attack may be negatively impacted in limestone-blended cements as the limestone addition rate increases. Further, other recent research has suggested that ground limestone and supplementary cementitious materials (SCMs), like fly ash, may be used synergistically to better replicate the behavior of traditional cement formulations. The effects of higher replacement levels, such as those recently approved, on the early and long-term performance of concrete have been less examined, particularly in the presence of SCMs, than usage rates of 5% or less. However, additional examination of the range of behavior of the higher limestone blended cements must be assessed independently, to ensure that their performance can meet state and federal specifications. In particular, studies are needed on concrete mixtures of particular relevance to GDOT [13], including evaluation of Type IL cements for use in leaner (i.e., lower cement fraction) Class A concretes and in Class AA and AA1 or AAA mixes. Also, examination of lower fly ash content (15%) and higher slag (50%) content, to match Section 500 specifications [13], in combination with Type IL cements is needed. In addition, data for very early age compressive strength (<1 day), elastic modulus, and tensile and/or flexural strengths are needed for design and operation. Examination of varying field conditions, particularly high and low temperature, on performance of these cements is also needed. Moreover, the observed decreased air content with Type IL cement concrete suggests that additional studies of admixture compatibility and freezing/thawing resistance are needed, again for a range of concrete Classes. The variability in shrinkage and permeability suggests that more data are needed to better understand the implications of Type IL cement usage on performance, for a range of concrete Classes. From these additional studies, a greater

understanding can be gained about how to address Type IL cements and their use with SCMs in current Georgia DOT specifications.

Yet despite recent provisions allowing the Type IL cement use, there is still widespread uncertainty regarding the performance and long-term durability of concretes made with limestone-blended cements. Type IL cement originated during an era in which it was widely believed that suitable performance could be achieved through the design of high-strength concrete mixtures, and less consideration was paid to factors such as permeability and cracking resistance, which can have significant impacts on the service life of a structure. The focus has shifted in the last few decades, however, to a more performance-based philosophy, in which durability and service life are considered along with strength. Thus, this research serves to fill the gaps in the knowledge by investigating how the fundamental mechanisms of cement hydration and microstructural development are influenced by the presence of finely divided limestone powders.

1.2 Research Objectives

The objectives of this research are to (1) compare regionally produced limestone blended cements with conventional portland cements in terms of composition and fineness, (2) evaluate the influence of increasing ground limestone addition rates through the assessment of key material properties (e.g., setting time, strength development, shrinkage, permeability, air content, and durability to freezing/thawing cycling), (3) examine the relative sensitivity of those properties to field conditions (e.g., variations in temperature), and (4) assess the combinations of limestone blended cements with fly ash (15%) and slag (50%). The overall objective will be to compare the performance of limestone blended cements to conventional portland cements in concretes designed to

5

meet GDOT specifications for Class A, AA, and AA1 or AAA concrete [13]. Results will be used to better understand the implications of the recent changes in cement compositions and to provide guidance of how these changes can or should be accommodated in the state's Section 500 specifications.

Additional research may be necessary to better understand the impacts of using limestone blended cements on durability in marine and other aggressive environments (e.g., chloride diffusion rate, carbonation rate, sulfate resistance) and in pavements (e.g., wear resistance, resistance to curling), as well as their appropriateness for pre-stressed concrete applications (e.g., creep resistance, early strength development with accelerated curing, bond development length). Such research might be conducted as a pooled-fund study.

Chapter 2. LITERATURE REVIEW

2.1 Cement hydration in the presence of limestone fillers

When it was first incorporated into portland cements, finely divided limestone was believed to act as a chemically inert filler, occupying space that would otherwise be filled by either unhydrated cement grains or capillary porosity. However, recent research has shown that limestone "fillers" play several important roles in the early hydration of portland cement pastes, not only physically but chemically, as well [14]. The combination of physical and chemical effects alters both the kinetics and the thermodynamics of cement hydration, changing the reaction rates of the raw cement phases and forming additional carbonate phases within the hydrated cement paste. As a result, hydrated pastes of portland limestone cement have differences in physical microstructure – and consequently differences in performance – when compared to traditional portland cement pastes. The following sections discuss the influence of finely divided limestone on the hydration of portland limestone cements and the implications therein for their mechanical properties, dimensional stability, and ultimate durability.

2.2 Portland limestone cement hydration

2.2.1 Chemical effects

In the presence of calcium carbonate ($C\bar{C}$), the hydration reactions are slightly altered. While the C_3S, C_2S, and the initial C_3A reactions all proceed in the same manner as in ordinary portland cements, thermodynamic models [14, 15] have suggested that the secondary conversion of ettringite into monosulfate will not occur when sufficient calcium carbonate is present. Rather, once the sulfate has been depleted, the remaining

unhydrated C_3A will preferentially react with the calcium carbonate to form monocarbonate ($C_4A\bar{C}H_{11}$) and hemicarbonate ($C_4A\bar{C}_{0.5}H_{12}$) phases, in proportions that depend on the ratio of carbonate to alumina [14]:

$$C_3A + C\bar{C} + 11\ H \rightarrow C_4A\bar{C}H_{11} \qquad (2.5)$$

$$C_3A + 0.5\ C\bar{C} + 0.5\ CH + 11.5\ H \rightarrow C_4A\bar{C}_{0.5}H_{12} \qquad (2.6)$$
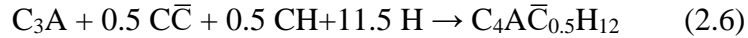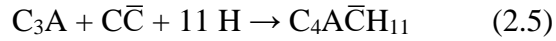
These models not only suggest that limestone stabilizes the ettringite that has already formed, preventing it from converting into monosulfate, but also that it replaces the monosulfate with a less soluble and more thermodynamically stable monocarbonate or hemicarbonate compound [14, 16]. The stabilization of the ettringite and the additional formation of carboaluminate phases is consequently believed to increase the volume of hydration products relative to ordinary cement pastes, leading to an overall reduction in the capillary porosity of the hydrated cement paste; however, such effects have not been experimentally demonstrated. Further work is needed not only to verify that the carboaluminate phases are formed in real cement systems, but also to quantify their effect on the overall microstructure of the hydrated cement paste.

2.2.2 Physical effects

The fineness of limestone powders and their dispersion throughout the cement paste also result in physical effects that may alter the kinetics of cement hydration. These physical effects include filler effects, nucleation effects, and dilution effects, each of which is illustrated in Figure 2.1.
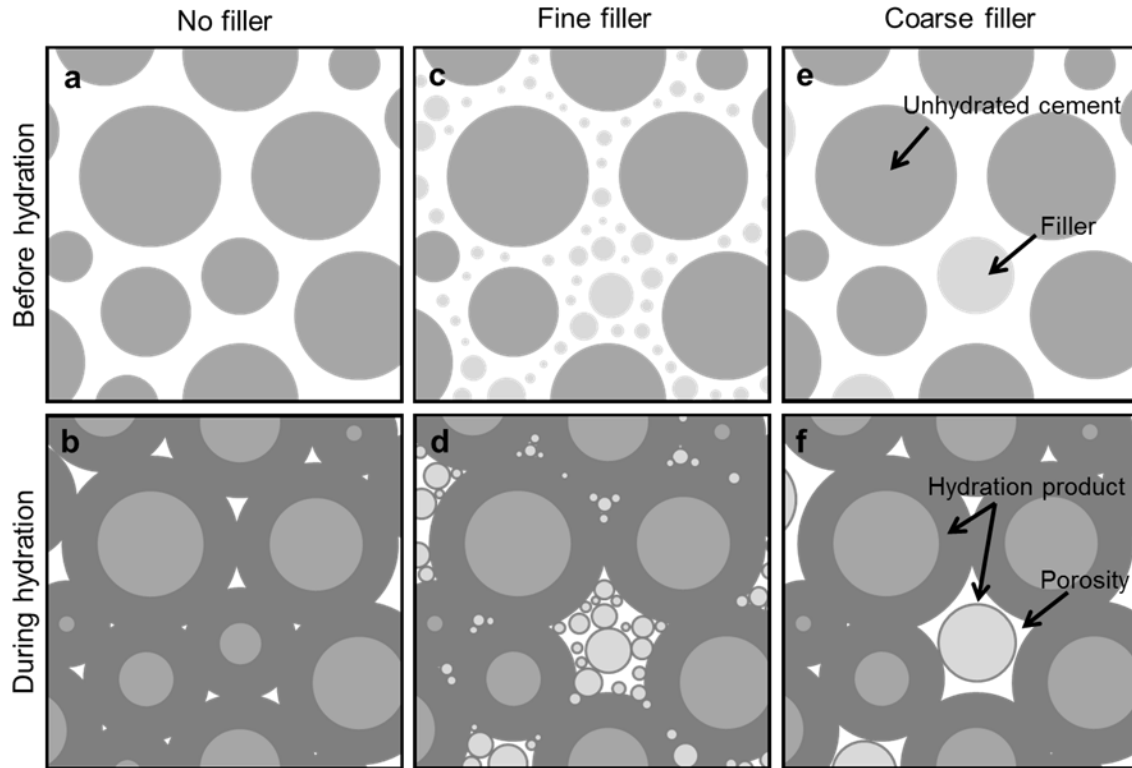
Figure 2.1: Schematic representation of the effect of a 10% volumetric filler replacement on cement hydration. Filler effects dominate in the presence of fine fillers (c & d), while dilution effects dominate in the presence of coarse fillers (e & f) [17].

The filler effect, shown in Figure 2.1-c and d, refers to the wider dispersion of the cement grains and the improved packing of the solid phases that result from the change in particle size distribution [18]. It is typically observed for cements in which the limestone filler is ground more finely than the cement clinker, resulting in a wider particle size distribution for the overall system [19]. The wider dispersion of the cement grains helps to improve material homogeneity by reducing flocculation, which in turn helps to improve the efficiency of the clinker dissolution and hydration. Additionally, the denser particle size distribution helps to fill the gaps in the hydrated cement paste, leading to overall decreases in porosity.

Nucleation effects (Figure 2.1-d and f) are caused by the increase in solid surface area due to the fine limestone addition. The increased surface area provides additional sites for the precipitation of hydration products (especially calcium hydroxide, CH), which leads to a net acceleration of the hydration reaction [20, 21]. While nucleation effects are known to occur for many mineral fillers (e.g., quartz [20], TiO_2 [22, 23], and C-S-H [24]), they are especially pronounced for limestone additions [25, 26], which some researchers have attributed to the unique interfacial properties of limestone that significantly reduce the energy barrier (activation energy) for heterogeneous nucleation of cement hydration products [26]. As a result, limestone fillers may promote the hydration of cement clinker at earlier ages more effectively than other fillers.

Accompanying – and possibly counteracting – the filler and nucleation effects is the dilution effect (Figure 2.1-e and f), which results from the substitution of the reactive cement clinker by a less reactive limestone filler. This substitution reduces or dilutes the amount of cement that is available for hydration and increases the effective water-to-binder ratio (w/b) of the cement paste. The increase in effective w/b may improve the efficiency of the hydration reaction by allowing a greater portion of the cement to hydrate, but the reduction in clinker content decreases the total volume of hydration products that may be formed, which could result in an increase in porosity and a decrease in strength. Some cement producers will compensate for this potential decrease in strength by increasing the fineness of the cement, effectively enhancing the nucleation effect and increasing strength at early ages. However, studies have shown that despite having higher early-age strengths, ordinary portland cements with higher fineness tend to

have lower strengths at later ages [27], and so it is unlikely that the nucleation effect can fully compensate for the dilution of the portland cement.

Finally, additional ancillary improvements in particle packing can occur as a result of the lower specific gravity of the limestone. Whereas portland cement clinker typically has a specific gravity of about 3.15, limestone has a specific gravity of only about 2.7 [28], which increases the volume of solids in the system when the limestone is used as a partial clinker replacement on an equivalent-mass basis. Replacing 10% of the clinker by mass, for example, will increase the solid volume of the system by approximately 1.6%. The increase in the solid volume creates a slightly denser packing of solid particles in the initial cement paste matrix, resulting in a secondary filler effect that is independent of particle size.

Analogously, when the limestone is substituted for cement on an equivalent-volume basis, the mass of cementitious "binder" in the system is decreased, leading to an increase in the water-to-binder ratio (w/b)[1] for the system. A portland limestone cement containing 10% limestone by volume, for instance, will weigh 1.4% less than an ordinary portland cement and increase the effective w/b by the same amount. The net result is a slight dilution effect, again independent of particle size.

2.3 Influence of limestone on mechanical properties of concrete

At the level of interground limestone less than 5 % (LS <5%), some modification of the heat of hydration at early ages may be observed depending on the fineness of the limestone but the long and short term properties of concrete made with portland

---

[1] The "binder" refers to the cement, fillers, and any supplementary cementitious materials

limestone cement (PLC) such as compressive, flexural strength and drying shrinkage are similar to that of portland cement (PC) concrete [29]. Some studies showed that the PLC concrete with higher limestone cement (>15%) had lower strength, compared to that of portland cement concrete at all ages, with the reduction in strength increasing with LS content [30]. It is believed that the reduction in concrete strength with higher portion of limestone can be due to the significant lower cement content known as dilution effect. Due to the significant strength loss generated using LS, several studies and national standards have set the optimum replacement level of PC by LS to 20% [31]. Some studies have reported that addition of fine limestone powder up to 15% could improve the early age hydration of portland cement [32] and may reduce the total porosity and shorten the initial and final setting time as well [33] while the mechanical properties of portland-limestone mortar and concrete are slightly improved or similar to those of a portland cement concrete [34]. It was also observed that increasing the fineness of LS could enhance its reactivity and consequently improve the compressive strength of the PLC concrete mix [35]. The obtained results indicate that to limit the reduction effect on the compressive strength, using a maximum of 15% limestone as a partial substitute for portland cement is recommended [36] .

2.3.1 Setting time

Setting time was lower for all samples containing limestone filler when compared to unblended samples [37]. However, El-Didamony et al. [38] found that the setting time was higher with 5% limestone and got lower with higher filler content when compared to unblended cement (Figure 2.2). The difference in values when compared to those of Tsivilis et al. [39] is most probably from the fact that different fineness that El-Didamony

12

et al. used (3000 ±50 cm^2/g) compared to that of Tsivilis et al. (3800 to 4300 cm^2/g). Other factors may include the C$_3$A content of clinker and the chemical composition of limestone (high calcite, dolomite, or quartz/clay).
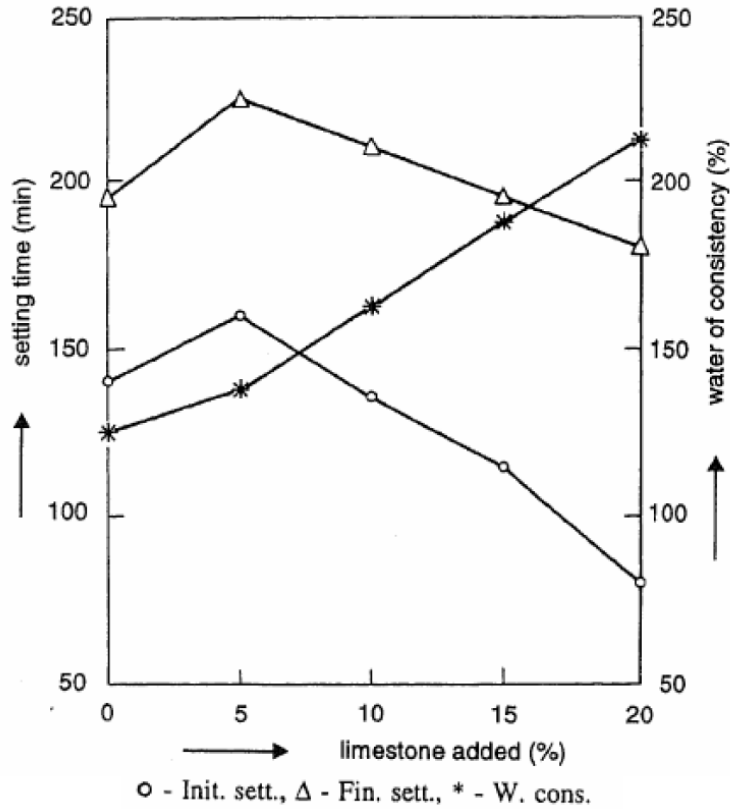
Figure 2.2: Setting time and water demand of portland-limestone cement pastes [38]

2.3.2 Mechanical properties

Tsivilis et al. [39] compared the compressive strength of pure samples with ones having limestone filler content ranging from 5% to 35% and interground to varying fineness with clinker of two chemical compositions (Figure 2.3).

A) $C_3S=65\%$, $C_2S=13\%$, $C_3A=8\%$, $C_4AF=11\%$

B) $C_3S=58\%$, $C_2S=19\%$, $C_3A=12\%$, $C_4AF=6\%$
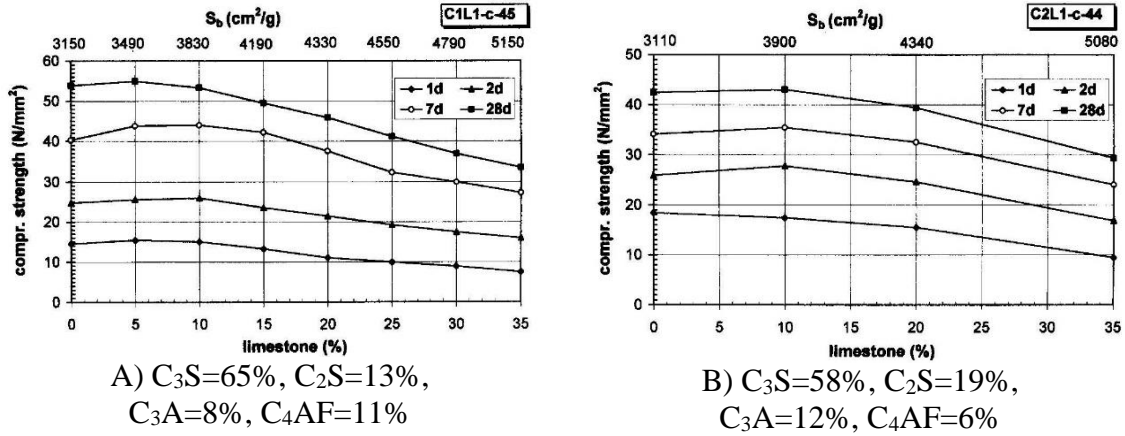
Figure 2.3: Influence of limestone content on strength development [39]

The results showed that limestone was more reactive with clinker having higher C_3A content, and that fineness has an optimum value to produce higher compressive strength. The addition of up to 10% limestone did not significantly affect the compressive strength at any age.

Hydrated cementing materials content in concrete depends on cement content and the degree of hydration. Compressive strength of concrete with filler is less at later stages than concrete without filler since less hydrated cementing materials are produced and higher effective w/b due to cement replacement with filler (Figure 2.4). Gel-space ratio measures the combined effects of addition of limestone: acceleration of hydration, dilution, and higher effective w/b. The higher the gel-space ratio, the higher the compressive strength of the concrete (Figure 2.5). Optimum value of limestone filler content can be estimated using the gel-space ratio concept.

14
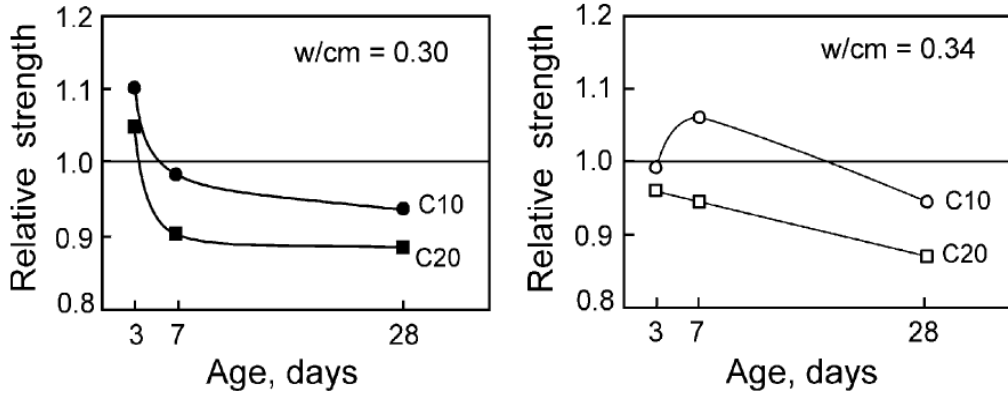
Figure 2.4: Relative compressive strength of concrete [40]
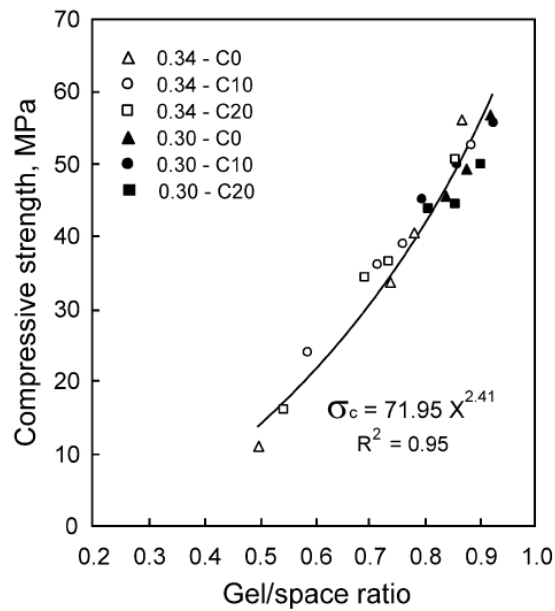
Figure 2.5: Compressive strength of concrete as function of the gel–space ratio [40]

2.4 Concrete durability

The early-age hydration and microstructural development of a cement-based material are critical in determining its permeability and ultimate durability. Permeability is a function of the size, interconnectivity, and tortuosity of the porosity, so materials with high porosity are more likely to have large, interconnected pores through which contaminants, such as chlorides or sulfates dissolved in water, may flow [17].

Permeability is most strongly a function of the interconnectivity of the porosity. Theoretical simulations have demonstrated that the porosity of portland cement paste becomes disconnected for a capillary porosity of about 18% [41], while experimental observations have suggested that this threshold is somewhere in the range of 20-40% for real cement paste systems [42]. If a conservative percolation threshold of 18% is assumed, Powers' model can be used to show that an ordinary portland cement paste system can achieve disconnected porosity for *w/b* below about 0.51 [43]. This, again, assumes only the dilution effect and becomes more complicated as additional physical and chemical interactions are considered.

One interesting feature of the percolation threshold is that it is universal; that is, it does not depend on the presence (or absence) of fillers – reactive or inert, coarse or fine [44]. This means that as the limestone addition rate increases, a portland limestone cement paste will require a lower *w/b* to achieve disconnected porosity as a consequence of the dilution effect previously discussed. For example, while less than 18% capillary porosity can be achieved in an ordinary portland cement paste with w/b below 0.51, it cannot be achieved in a portland limestone cement paste containing 20% limestone (by mass) until the w/b drops below 0.42 [43]. Similarly, for limestone replacements of 5, 10, 20, and 35% by mass, a

16

disconnected porosity may be obtained for maximum w/b's of approximately 0.50, 0.48, 0.43, and 0.34, respectively [45]. Thus, for a constant w/b, an increase in limestone content should similarly increase the permeability of the cement paste.

In reality, permeability does not always increase with increasing limestone content due to the additional physical and chemical effects of the limestone fillers. Trends in porosity that were discussed previously can be applied again to trends in permeability because of the constant 18% threshold for disconnected capillary porosity. When the limestone content is less than or approximately equal to the unhydrated cement content, the possible decreases in capillary porosity that may occur will additionally reduce pore interconnectivity and overall permeability; however, when the limestone content is greater than the unhydrated cement content, the resulting increase in capillary porosity will further increase both interconnectivity and permeability.

These general trends are supported by water penetration and sorptivity experiments performed by Ramezanianpour, et al., [46] and Dhir, et al. [47], on concretes prepared over a range of typical *w/b*'s (0.37-0.79) and limestone contents (0-45 wt.%). In both studies, decreases in water penetration and sorptivity were observed after 28, 90, and 180 days of curing for low limestone replacement levels (5-15 wt.%, depending on the *w/b*), but marked increases were observed at higher levels (20-45 wt.%). On the other hand, when Tsivilis [48] and colleagues measured gas and water permeability on concretes prepared at *w/b* = 0.62 and 0.70, they found that although gas permeability was higher for concretes containing limestone, water permeability was lower at all limestone replacement levels.

One possible explanation for this seemingly anomalous behavior comes from the work of Pipilikaki and Beazi-Katsioti [49], who observed that although concretes with high limestone addition rates exhibited higher capillary porosities (related to gas permeability), they also

17

tended to exhibit lower "threshold diameters", below which the pores are no longer continuous (related to water permeability). An ordinary portland cement paste with $w/b = 0.50$, for example, has a threshold diameter on the order of 1000 nm, while a paste with 35% limestone addition has a threshold diameter on the order of 100 nm [49]. This tenfold decrease in threshold diameter means that it is significantly more difficult for water to penetrate the 35% limestone mixture, since it may need to enter pores 100 nm in size – rather than 1000 nm – in order to percolate through the material. In other words, although the dilution effect may increase the total porosity of the cement paste matrix, particle packing and filler effects may still decrease the average size of the interconnected pores, making fluid penetration more difficult overall. It is therefore possible, as Tsivilis and others [39] have observed, that gas permeability may increase with increasing limestone rate, but because of improvements in particle packing, water penetration may become more difficult. Additional study is needed to fully understand the influence of limestone on the microstructural development – and interconnectivity of the porosity, in particular – of portland limestone cement pastes.

The transport properties of concrete control many aspects of its durability, from resistance to chloride and sulfate ion penetration to resistance to damage by freezing and thawing cycles or by internal salt crystallization, among others. The most commonly characterized transport properties for concrete are permeability (the rate of pressure-driven fluid flow through the material) and diffusivity (the rate of concentration-driven ion flow through saturated porosity), but other transport processes such as electromigration (flow of ions under an electric field) and thermal migration (flow of fluids and ions under a temperature gradient), may also influence the long-term durability of the concrete [50]. The concrete's transport properties are a function of several microstructural parameters, including

the size, interconnectivity, and tortuosity of the porosity. Materials with large pore volumes are more likely to have larger and more interconnected pores through which water and ionic species can flow [50]. Likewise, materials with low porosity are more likely to have more tortuous, less interconnected pore networks, which could help to protect against damage caused by transport-related phenomena.

It was established in the previous studies that limestone substitutions to portland cement can have significant impacts on microstructural development [48] [49]. In particular, dilution effects were found to reduce the total volume of hydration products formed, thereby increasing the total porosity of the cement paste matrix, while filler and ancillary specific gravity effects were found to improve the efficiency of particle packing within the matrix, thereby reducing the average size of the pores. The balance between these two competing microstructural effects has important implications for the transport processes – and therefore the long-term durability – of PLC-based materials and warrants further investigation. Specifically of interest is whether the overall increase in porosity dominates the behavior such that permeability and diffusivity are also increased, or whether the reduction in average pore size dominates such that the interconnectivity and therefore the permeability and diffusivity are instead reduced.

The permeability of PLC concrete can be measured by the rapid chloride penetration test (RCPT) and surface resistivity (SR). Previous studies show that PLC concrete containing 15% of limestone filler with a *w/b* of 0.6 with regard to the plain concrete, showed an increased chloride ion permeability factor of 67% and 135% at 28 days and 90 days, respectively. These results were similar to the results of Bonavetti et al. [51] who reported that the penetration of chloride ion increased from 43% to 114% for concretes containing 10% and 20% of limestone, respectively. They reported that the higher chloride ion

permeability of the concrete containing limestone, as compared to that of plain concrete, might be related to the higher level of OH^- ions present in the pore solution of the concrete made with limestone filler. On the other hand, the higher chloride ion permeability could be attributed to the porous and connected paste–aggregate interfacial transition zone (ITZ) associated with limestone filler particles addition. The water permeability of concrete containing limestone was also found to be greater than that of plain concrete [52]. The surface resistivity of PLC concrete were evaluated in previous studies. Ramezanianpour et al. [53] showed that the partial replacement of cement with limestone reduces the electrical resistivity of concrete. The electrical resistivity decreased with increasing limestone replacement with PLC concretes containing 10% and 20% limestone replacement showing the maximum and minimum resistivity values respectively [53].

2.5 Creep and drying shrinkage

Dhir et al. [30] measured the effect of increasing limestone content from 0% to 45% on the creep and drying shrinkage of concrete. They found that the higher the limestone content, the lower the creep and the drying shrinkage as shown in Table 2.1. The creep results were within the precision of the test and therefore the effect of limestone filler was negligible. They concluded that both properties depend on the restraining effects of aggregates and that the limestone filler resulted in similar or reduced volume when compared to portland cement.

Table 2.1: Comparison of 90 day deformation properties of concrete made with portland cement and limestone-blended portland cement [30]

Property	Concrete type				
	PC	PLC			
		LS15	LS25	LS35	LS45
Cube strength[a], N/mm^2	41.0	36.5	30.5	23.5	17.0
Creep[b], $\times 10^{-6}$	790	780	775	770	760
Drying shrinkage[c], $\times 10^{-6}$	680	630	605	590	575

[a]28 days, 20°C water cured
[b]Creep loading at 28 days, $0.40f_{cu}$
[c]Shrinkage at 20°C, 55% RH

Adams et al. [54] discussed the effect of limestone on the drying shrinkage of cement mortar. They concluded that drying shrinkage increased as the surface area (fineness) increased. They also recommended that shrinkage had a better correlation Southwestern fineness factor (SFF) than with Blaine surface area, where the SFF is the ratio of the Blaine surface area (m^2/kg) to the percent passing No. 325 sieve. The SFF ratio gives a bigger contribution to the very fine fraction which has a significant effect on shrinkage.

Bentz et al. [36] conducted restrained shrinkage tests on mortar rings made with cements without limestone and with cements with 10% limestone that was ground at three fineness levels (fine, intermediate, and coarse). The results, shown in Figure 2.6, showed that finer limestone resulted in higher tensile stresses due to shrinkage than the coarsest limestone.
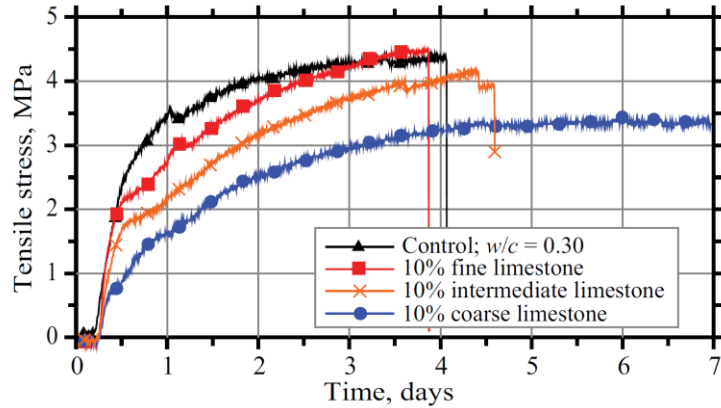
Figure 2.6: Stress development versus time of plain mortar rings and mortar rings containing 10% replacement by mass of different fineness limestone powders [36].

Alunno-Rosseti and Curcio [55] compared drying shrinkage of concretes made with cements with and without 20% limestone from two plant sources. Their results showed increased shrinkage with higher cement content but the difference between concretes made with and without limestone was negligible (Table 2.2).

Table 2.2: One-year drying shrinkage (UNI Standard 6555) of concretes made with cements with or without 20% limestone [55]

	Plant B				Plant G			
Cement content, kg/m^3	270		330		270		330	
Limestone content of cement, % by mass	0	20	0	20	0	20	0	20
Shrinkage, µm/m	635	640	680	690	540	560	615	595

Detwiler [56] measured the drying shrinkage according to ASTM C157 [57] of concrete made without and with 2.5% limestone, as well as mixes with Class C fly ash. The results showed that 2.5% limestone did not affect the shrinkage of mixes with or without fly ash (Table 2.3).

22

Table 2.3: Drying shrinkage (ASTM C157 [57]) of concrete mixes with and without
2.5% limestone and with and without Class C fly ash [56]

Mix	4 days	7 days	14 days	28 days	8 weeks	16 weeks	32 weeks
Type I (control)	0.002	0.009	0.015	0.025	0.039	0.044	0.049
LS	0.003	0.008	0.017	0.025	0.038	0.046	0.051
Type I with 15% Class C fly ash	0.004	0.019	0.019	0.02	0.023	0.046	0.061
LS with 15% Class C fly ash	0.003	0.011	0.022	0.026	0.029	0.046	0.058

Chapter 3. MATERIALS CHARACTERIZATION

3.1 Materials

Eleven cements from five sources in the southeastern United States (Figure 3-1) were considered for this study. Sources were randomly assigned designations A-E to preserve anonymity. One ASTM C150 Type I/II ordinary portland cement (LS ≤ 5%) and at least one companion ASTM C595 Type IL portland limestone cement (LS ≤ 15%) produced from the same clinker were provided from each source. One Type IL cement was received from each source A-D, while two Type IL cements of identical composition and varying fineness (designated CG for more coarsely ground and FG for more finely ground) were received from source E. In the analysis and discussion that follows, Type I/II cements are indicated by their single letter source name (e.g., cement A), while Type IL cements are indicated by their single letter source name plus the letter "L" (e.g., cement AL). For this study, 33 cement paste mixtures and 12 concrete mixtures were developed using the eleven commercially produced cements combined with either Class F fly ash, Class C fly ash, or blast-furnace slag.
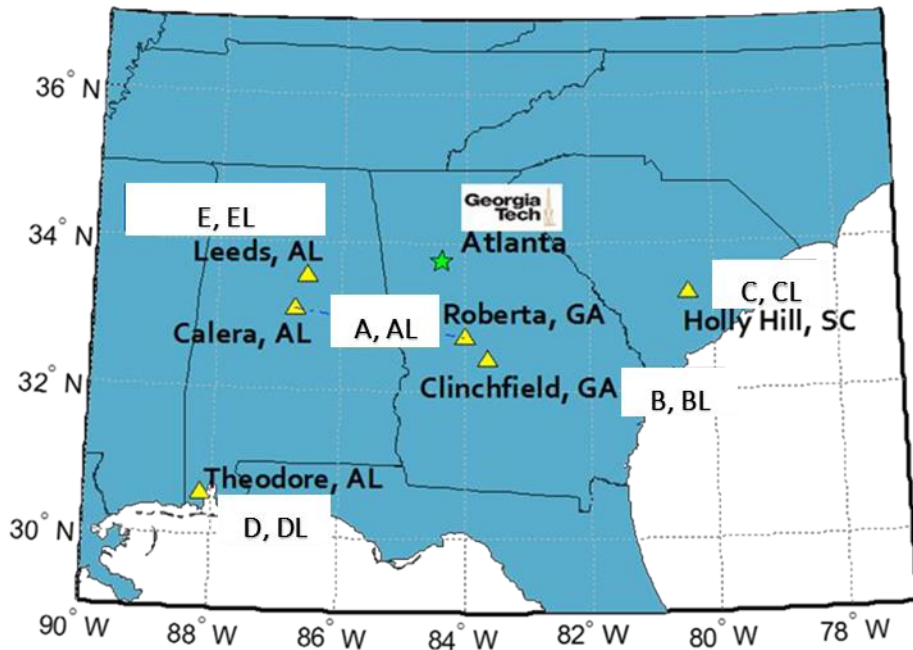
Figure 3.1: Geographic sources for cements investigated. Cements A and AL were produced in Calera, AL and finished in Roberta, GA

3.2 Chemical composition

The chemical compositions of each cement were obtained by oxide analysis (ASTM C114 [58]) and quantitative x-ray diffraction (XRD) (ASTM C1365 [59]). Primary phase distributions (i.e., the relative quantities of C_3S, C_2S, C_3A, and C_4AF phases) were determined either by application of the Bogue equations to oxide compositions or by Rietveld analysis of the x-ray diffraction patterns. While oxide analysis is more commonly used to estimate the primary phase distributions in cement, application of the Bogue equations to limestone cements requires a priori knowledge of the limestone composition and content [60]. For this reason, the Bogue potential compositions are only provided for the Type I/II cements. Complete results from the XRD and oxide analyses are provided in Table 3.1 and Table 3.2, respectively. The

similarities in chemical analyses between cements from the same source confirm that each of the paired cements likely originated from similar clinker, as had been planned by the producers. The differences between relative C_3S and C_2S quantities determined by the two methods can be partially attributed to the pure-phase assumptions implicit in the Bogue equations; since the XRD quantifications are based on the impure "alite" and "belite" phases of C_3S and C_2S, respectively (which are found in real cements), it is believed that they are more indicative of the true composition of the cement and will therefore be used in most future compositional inquiries.

Table 3.1: Cement phase compositions as determined by Rietveld analysis of XRD patterns, % by mass. A non-zero portlandite content indicates that the cement is slightly pre-hydrated.

Component	Type I/II					Type IL				
	A	B	C	D	E	AL	BL	CL	DL	EL
C_3S	52.1	55.9	60.9	55.5	64.3	50.8	54.3	52.7	53.5	61.9
C_2S	24.2	21.6	16.4	17.4	13.1	17.3	15.3	17.9	15.3	7.6
C_3A	3.0	3.0	1.9	5.0	4.2	3.3	2.6	1.5	5.0	3.9
C_4AF	10.3	12.9	12.2	12.1	10.6	9.3	13.5	12.1	10.8	10.3
Calcite ($CaCO_3$)	3.2	1.0	4.2	4.2	2.4	12.2	7.9	10.8	10.5	9.8
Gypsum ($CaSO_4 \cdot 2H_2O$)	0.3	0.0	0.0	0.0	0.0	0.8	0.0	0.0	0.0	0.1
Hemihydrate ($CaSO_4 \cdot 0.5H_2O$)	2.0	3.2	2.5	3.9	1.6	1.6	3.3	3.0	2.9	1.1
Anhydrite ($CaSO_4$)	0.1	1.6	0.1	0.1	0.2	0.1	0.9	0.0	0.0	2.3
Arcanite (K_2SO_4)	0.3	0.3	0.0	0.3	1.1	1.1	1.3	0.2	0.4	1.8
Periclase (MgO)	3.1	0.2	0.8	0.3	1.0	2.2	0.3	0.5	0.1	1.4
Lime (CaO)	0.3	0.3	0.3	0.4	0.3	0.1	0.2	0.2	0.3	0.0
Quartz (SiO_2)	0.0	0.1	0.2	0.4	0.1	0.1	0.3	0.3	0.8	0.2
Portlandite ($Ca(OH)_2$)	1.3	0.0	0.6	1.7	1.2	1.2	0.2	0.8	1.5	1.3

Table 3.2: Cement oxide composition, % by mass. LOI is loss on ignition at 1000°C.

Component	Type I/II					Type IL				
	A	B	C	D	E	AL	BL	CL	DL	EL
C_3S	62.9	62.3	57.4	57.5	57.5	-	-	-	-	-
C_2S	7.6	10.5	13.6	13.6	14.0	-	-	-	-	-
C_3A	6.9	6.6	7.2	7.1	7.0	-	-	-	-	-
C_4AF	9.2	12.1	11.1	10.7	9.3	-	-	-	-	-
SiO_2	19.2	20.1	19.9	19.9	20.0	17.1	18.2	18.6	18.5	18.2
Al_2O_3	4.5	5.0	5.0	4.9	4.6	4.2	4.6	4.6	4.5	4.3
Fe_2O_3	3.0	4.0	3.6	3.5	3.1	2.9	4.2	3.5	3.3	3.2
CaO	62.8	64.7	63.4	63.8	63.0	62.1	62.9	62.4	63.3	62.2
MgO	3.6	1.1	1.5	1.1	2.5	3.1	1.1	1.5	1.0	2.8
Na_2O_e	0.5	0.4	0.5	0.4	0.5	0.4	0.3	0.4	0.4	0.5
TiO_2	0.3	0.3	0.3	0.3	0.3	0.3	0.3	0.3	0.2	0.2
Mn_2O_3	0.1	0.1	0.1	0.0	0.1	0.1	0.1	0.1	0.0	0.1
SO_3	3.1	3.1	2.9	3.2	3.2	3.3	3.2	3.1	3.2	3.0
Free CaO	0.9	0.1	0.7	1.0	0.7	0.6	0.1	0.2	0.9	0.6
LOI	2.6	0.8	2.3	2.5	2.4	6.3	4.7	5.1	5.2	5.3

In terms of chemical composition, all five portland cements conform to ASTM C150 Type I/II specifications [61], but contain a range of C_3S, C_2S, C_3A, and C_4AF contents. Based on the XRD analyses, the cements from source E contain the highest amount of C_3S (contributing to early strength and microstructural development), while the cements from sources A and B have more C_2S (contributing to later age strength and microstructural development). The cements from source D, meanwhile, have the most C_3A, possibly leading to more favorable conditions for carboaluminate formation, while the cements from source B have the most C_4AF. Given the range of compositions examined, it will be important to compare the behavior between pairs of cements to better understand the role of the limestone, as well as among all eleven cements to better understand the behavior of limestone cements as a whole.

The limestone content of each cement additionally was measured by thermogravimetric analysis (TGA) under nitrogen environment, using a Hitachi EXSTAR TG/DTA 7300. Three replicate cement samples weighing approximately 20 mg were heated from ambient temperature to 900°C at a rate of 10°C/min, with a 30-minute hold at 105°C to remove any free moisture from the powder. $CaCO_3$ contents were calculated based on the mass loss between approximately 600°C and 750°C, wherein $CaCO_3$ thermally decomposes into CaO and $CO_2\uparrow$. The calculation is shown in Equation 3.1 below, where $m600$ indicates the mass of the sample at 600°C, and the molecular weights of $CaCO_3$ and CO_2 are taken to be 100.09 g/mol and 44.01 g/mol, respectively:

$$\%CaCO_3 = \frac{m_{600} - m_{750}}{m_{105}} \times \frac{MW_{CaCO_3}}{MW_{CO_2}}$$

The $CaCO_3$ contents as determined by TGA are shown in Figure 3.2. While the true "limestone" contents of the cements cannot be determined without also knowing the $CaCO_3$ contents of each interground limestone, it can nonetheless be observed that four of the five Type I/II cements contained small quantities of limestone as permitted under ASTM C150 specifications [12], while all five Type IL cements contained limestone contents within the 5-15% permissible range of ASTM C595 [7].
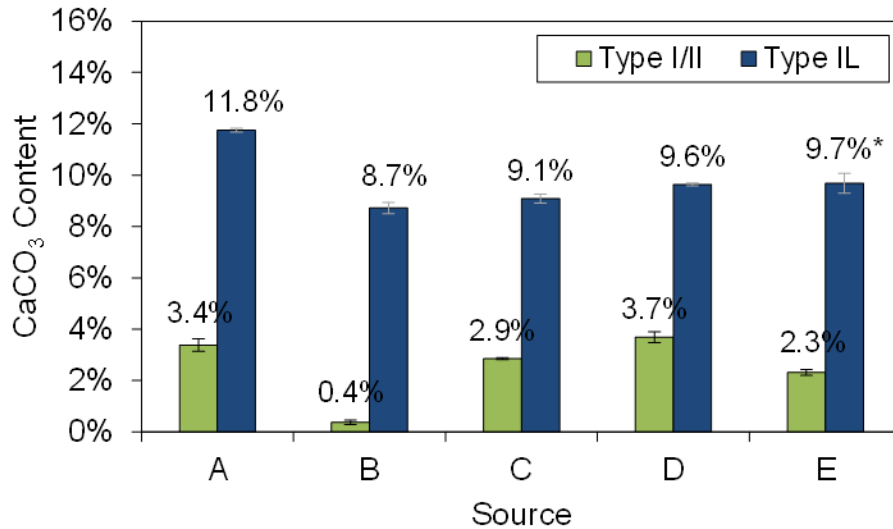
Figure 3.2: CaCO$_3$ contents of cements A-E determined by TGA. Error bars indicate one standard deviation. Values for cement EL represent the average of both CG and FG cements.

3.3 Particle size distribution

Many of the physical effects of limestone fillers depend on the relative sizes of the cement and the limestone inclusions. It is therefore important to characterize the particle sizes of the Type I/II and Type IL cement pairs in order to better understand the role of nucleation, filler, and dilution effects in commercially produced cements. In terms of the physical effects of limestone fillers, it is believed that parameters related to the surface area of the material (e.g., SSA and $D_{3,2}$) are likely to govern surface nucleation effects, while parameters related to the distribution of volumes (e.g., D_{10}, D_{50}, and D_{90}) are likely to govern filler and dilution effects.

The Blaine fineness of cements were obtained according to ASTM C204 [62], while the particle size parameters for the eleven cements were obtained by laser diffraction in ethanol using a Malvern Mastersizer 3000E. The particle size measurement was carried out by adding a small amount of each cement while dispersed in ethanol until

30

a laser obscuration of approximately 7% was obtained. The dispersed material was sonicated for 1 min then stirred at a rate of 840 rpm for approximately 10 min to reduce agglomeration. Particle size distributions were determined as the average of five samples, each collected over a 60 s interval, assuming smooth (but not necessarily spherical) particles and using Mie theory. 4 Refractive indices of 1.68 and 1.36 were selected for cement and ethanol, respectively, from the database included in the Mastersizer software. The resulting differential and cumulative particle size distributions for the eleven cements are shown in Figure 3.3 and Figure 3.4, respectively, with Type I/II cements shown in solid black lines and Type IL cements shown in colored dashed lines. A summary of relevant size parameters is given in Table 3.3.

Based on the particle size distributions, it can be observed that there are generally two categories of Type IL cements considered in this study: those with significantly finer particle size distributions than their Type I/II companion cements (cements AL, DL, and EL, both CG and FG), and those with broader but similar particle size distributions to their Type I/II companion cements (cements BL and CL). A working hypothesis is that Type IL cements in the former group will exhibit filler-dominated behavior, which would be evidenced by accelerated hydration rates and decreased porosity early ages, while Type IL cements in the latter group will exhibit dilution-dominated behavior, which would be evidenced by decreased hydration rates and increased porosity. Finally, since it was determined that all of the Type IL cements have higher specific surface areas and smaller surface-weighted mean particle sizes than their Type I/II companions, it is also hypothesized that nucleation effects will be observed at early ages for all six Type IL

cements. This hypothesis is further supported by the Blaine fineness results, which similarly show higher relative specific surface areas for all six Type IL cements.

Finally, the specific gravity (SG) of each cement was measured by displacement in kerosene at $23 \pm 2°C$ according to ASTM C188 (Table 3.3) [57]. The SG for cement is typically assumed to be 3.15, but values ranging from 3.04 to 3.17 were measured for the Type I/II cements considered in this study. Because limestone has a lower density than cement (typically ~2.7 g/cm3 [63]), limestone substitutions of only a few percent by mass can cause significant reductions in the SG of the cementitious binder, accounting for the lower SGs for Type IL cements. If it is assumed that the limestone has SG = 2.7 and is composed 100% of the $CaCO_3$ measured by TGA, it can be further demonstrated that the Type I/II and Type IL cements for each source originate from clinkers having approximately the same specific gravity, and that they therefore likely originate from the same clinker.
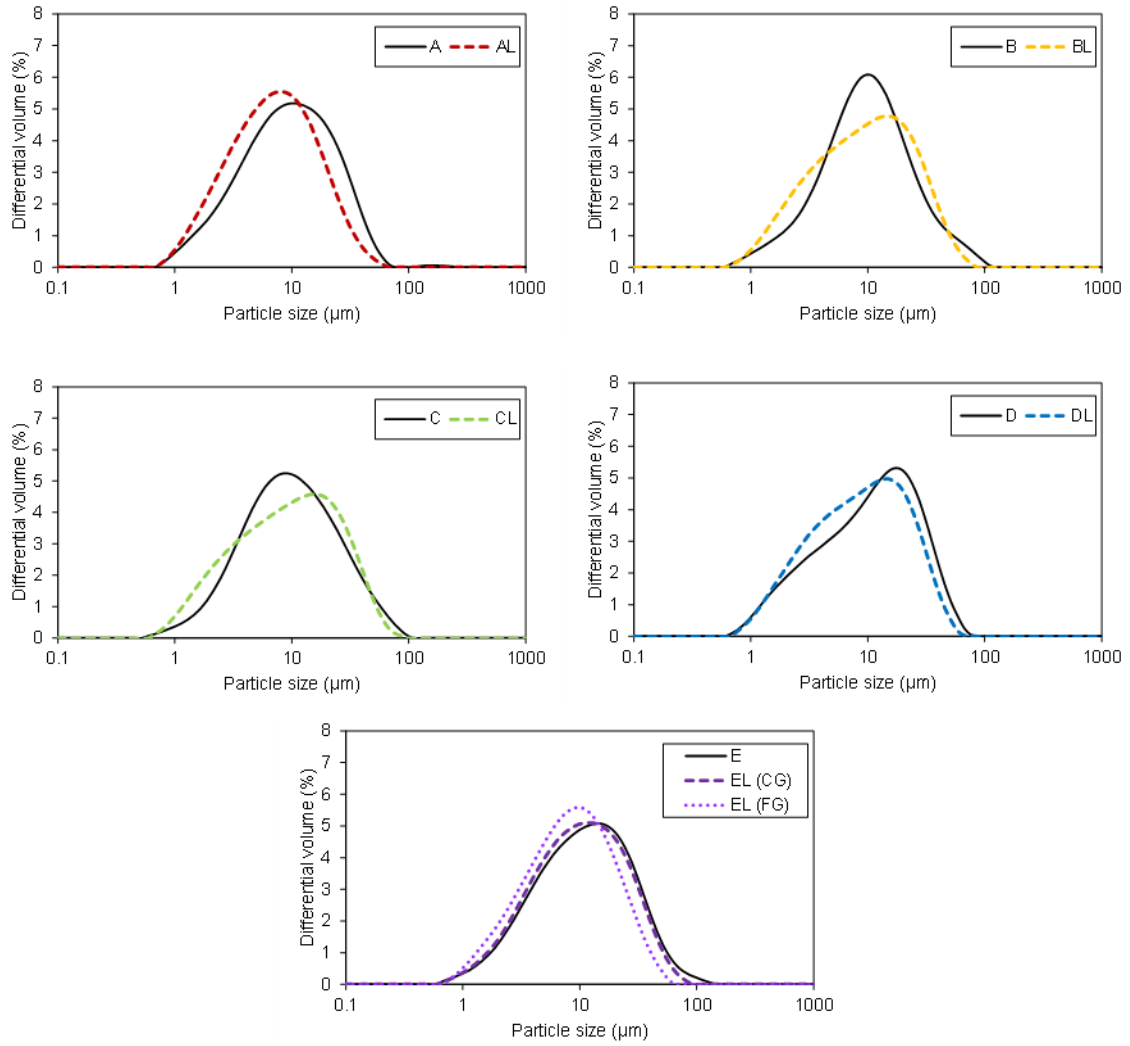
Figure 3.3: Differential particle size distributions for cements A-E
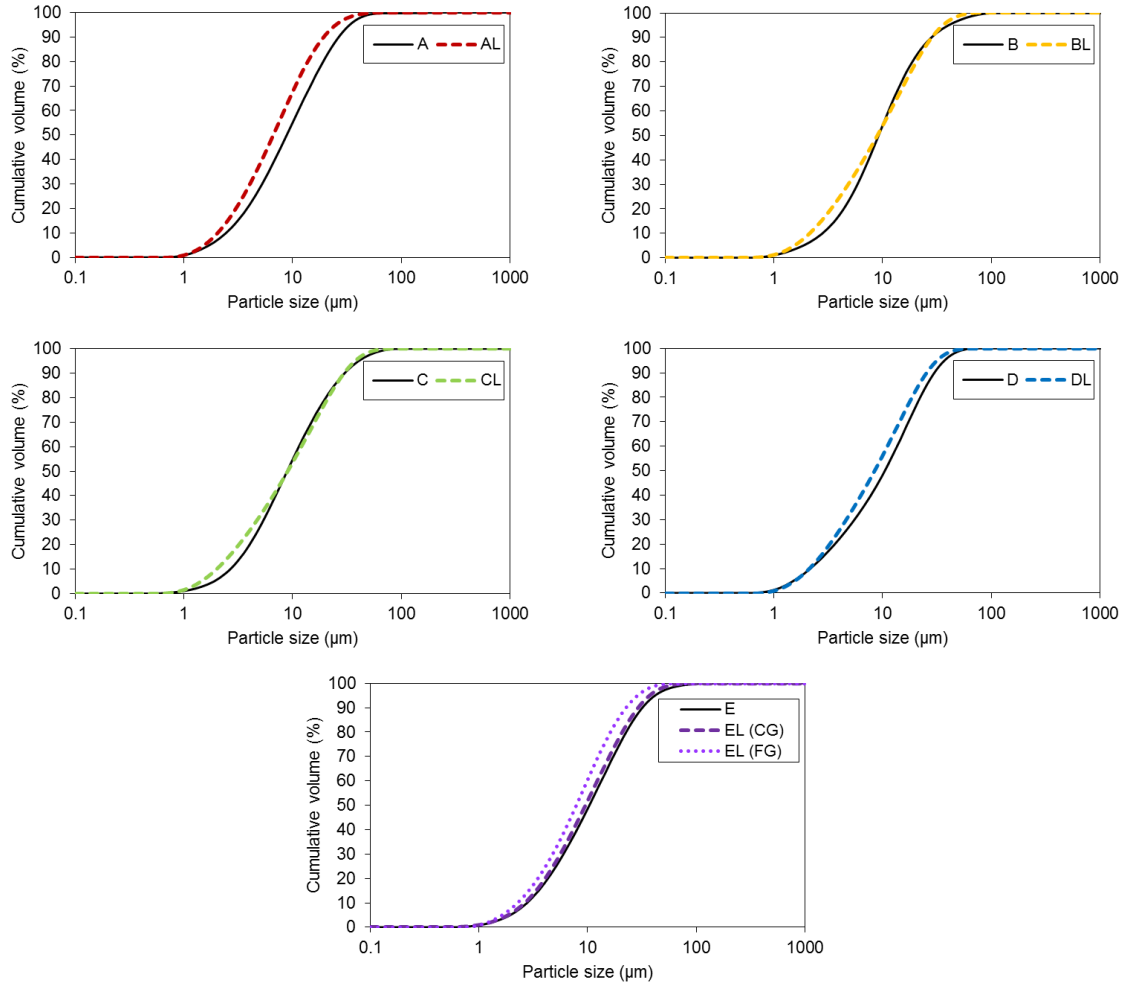
Figure 3.4: Cumulative particle size distributions for cements A-E

Table 3.3: Summary of physical properties for Type I/II and Type IL cements.

Cement	D_{10} μm	D_{50} μm	D_{90} μm	$D_{3,2}$ μm	$D_{4,3}$ μm	SSA m^2/kg	SG	Blaine m^2/kg
A	2.77	10.0	30.2	6.28	14.1	288	3.08	448
AL	2.29	7.5	21.8	5.09	10.2	356	3.05	597
B	3.17	10.4	31.9	6.71	15.1	282	3.17	416
BL	2.41	10.1	32.1	5.83	14.3	326	3.11	600
C	3.03	10.1	34.1	6.53	15.1	278	3.04	465
CL	2.25	10.2	33.6	5.60	14.6	324	3.01	606
D	2.45	11.9	34.0	6.19	15.5	293	3.10	460
DL	2.37	9.5	28.6	5.66	12.9	321	3.07	574
E	3.15	11.8	36.2	7.07	16.8	257	3.10	428
EL (CG)	2.99	10.8	32.8	6.69	14.9	271	3.05	511
EL (FG)	2.54	8.9	25.4	5.72	11.8	317	3.10	553

Chapter 4. EARLY AGE HYDRATION

4.1   Materials and methods

Cement pastes with w/b = 0.40 were prepared from each of the eleven commercially produced cements discussed in Chapter 3, where again the mass of the binder was taken to be the mass of the cement as received, including interground limestone. The mixing procedure consisted of manual stirring the cement in deionized water for 30 s, followed by mechanical mixing of the paste mixture with a 5-speed hand mixer at low speed for 60 s and at medium speed for 60 s. Immediately after mixing, specimens were cast and cured in their respective environments at 25°C.

The kinetics of cement hydration were measured indirectly by isothermal calorimetry, by examining the rate of heat release for each cement paste as it hydrates. Isothermal calorimetry was performed in accordance with ASTM C1679 [64] on pastes prepared at a water-to-binder ratio (w/b) of 0.40, where the binder consists of both the cement and its interground limestone. The mixing procedure consisted of manual stirring of the cement in deionized water for 30 s, followed by mechanical mixing of the paste mixture with a 5-speed hand mixer at low speed for 60 s and at medium speed for 60 s. Two samples, each weighing 7.0 ± 0.5 g, were transferred to glass vials and then placed into the isothermal calorimeter (TA Instruments TAM Air). The rate of heat evolution and the cumulative heat released were measured at 25°C for the first 7 days of hydration.

Chemical shrinkage was measured by dilatometry according to ASTM C1608 [65]; 9.5 ± 0.5 g of paste was added to each of at least three glass vials, which were then filled with de-aerated deionized water and capped with a rubber stopper fitted with a

capillary pipette. A colored droplet of hydraulic oil was added to the top of each pipette, so that the change in water volume over time, which indicated the amount of chemical shrinkage in the paste, could be easily monitored. The capped vials were placed into a water bath maintained at 25°C, and measurements were recorded at 30 minute intervals for 7 days, using an automated camera acquisition system as shown in Figure 4.1. For each set of tests performed, one additional set of empty vials – containing only de-aerated deionized water – was also placed into the water bath to measure incidental volume changes due to evaporation of water from the capillary tubes; the average evaporation-induced volume change at each sampling age was subtracted from the raw testing data prior to analysis.

Figure 4.1. Experimental set-up used for chemical shrinkage test. Shrinkage was monitored by tracking the heights of red oil droplets atop the water within the capillary pipettes. Image acquisition software was used to automatically record images at 30 min intervals.

Autogenous shrinkage was measured for each cement paste in accordance with ASTM C1698 [66]. Three specimens were cast for each mixture in corrugated tube molds and stored in their sealed conditions in an environmental chamber at 25°C. The length change of each sample was measured by dilatometry, as shown in Figure 4.2, from the time of final setting to an age of 56 days. The time of final setting was determined by penetration of a Vicat needle in accordance with ASTM C191 [67]. Measurements of autogenous shrinkage were taken every 2 hr for the first 6 hr, once daily until 7 days, bi-weekly until 28 days, and then weekly until 56 days.

The initial and final set time of all Types I/II and IL cements were measured by auto Vicat apparatus in accordance with ASTM C191[67]. A constant *w/b* ratio of 0.31 was used for the setting time measurements.

Figure 4.2: Autogenous shrinkage measured on a corrugated tube specimen, in accordance with ASTM C1698 [66].

Vicat time of setting (ASTM C191 [68]) was conducted for all cements at 40 °F, 73 °F, and 90 °F to compare the initial and final setting times of limestone cements to Type I/II cements at different temperatures. In addition to that, the effect of blending secondary cementitious materials (SCMs) was examined at 73 °F, where 15% Class F fly ash, 15% Class C fly ash, and 50% slag replaced the cement (by weight) for each sample. Three samples were made for each variable and the average values were reported.

The instrument used was ToniSET (Figure 4.3) which is an automatic Vicat needle instrument at Heidelberg Technology Center. In the testing protocol, a penetration of 25 mm was defined as the initial time of setting, and a penetration of 2 mm was defined as the final time of setting.

Figure 4.3: ToniSET automatic Vicat instrument

A *w/b* ratio of 0.31 was used for samples. This was based on the *w/b* needed to achieve normal consistency for cement C and was close to the normal consistency of several of the cement samples from sources A to E. One specific *w/b* was used to allow

comparing different cement sources with each other. Three samples per cement source were prepared. The rest of the procedure followed ASTM C191.

The test matrix was designed to investigate the effect of temperature and the effect of SCMs on the setting time of Type I/II and Type IL cements. In order to achieve that, the test matrix consisted of four main groups. The first group consisted of plain mixes (i.e. cement paste without SCMs) where samples from sources A to E were prepared and tested at 73 °F. The second group consisted of plain mixes from sources A to E and tested at 90 °F. The third group consisted of plain mixes from sources A to E and tested at 40 °F. The forth group consisted of cements from sources A to E blended with SCMs. The SCMs used were fly ash (Class F and Class C) and slag. The SCMs replacements were 15% by mass for the fly ash and 50% by mass for slag. The SCMs were added to the cement and dry blended before mixing with water. Figure 4.4 shows a schematic of the test matrix.
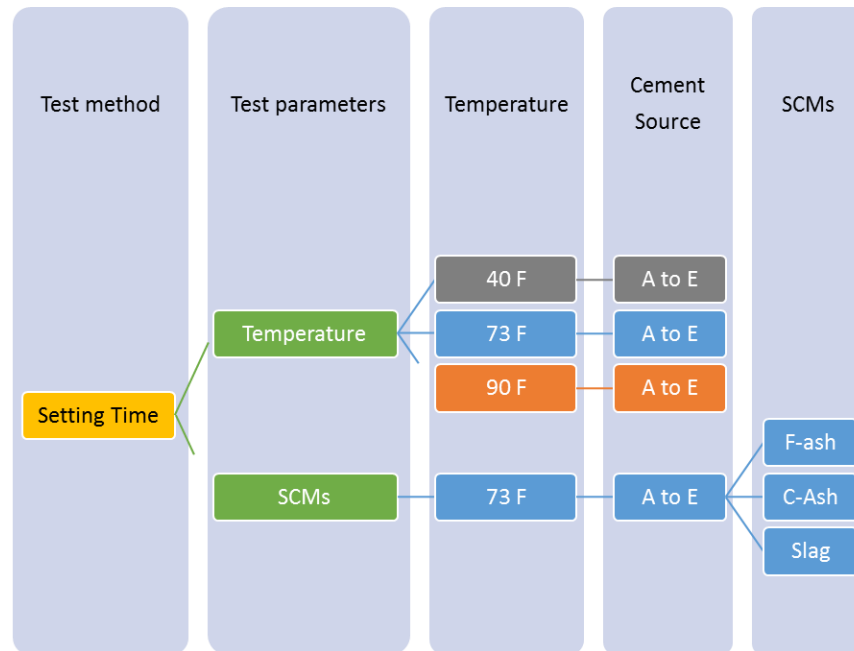
Figure 4.4: Schematic of the test matrix for Vicat time of set

The time at which the first measurement for the tests done at 73 °F was taken at 30 minutes. However, for the tests at 40 °F, the first measurement was taken at 120 minutes. This was done since there are limited number of testing points available on the surface of the specimen (ASTM C191 requires a minimum spacing of 5 mm between previous penetrations, and to prevent depleting those testing points on the sample surface by the time an initial set and a final set have been reached). Subsequent measurements were taken at a 10 minutes increment for all tests.

4.2 Results

4.2.1 Hydration kinetics

The kinetics of cement hydration were measured by isothermal calorimetry, by examining the rate of heat release for each cement paste as it hydrates. Three calorimetric peaks are typically observed during the hydration of a portland cement: the first corresponding to the dissolution of the clinker phases in the first ~30 minutes of hydration; the second corresponding to the hydration of the C_3S phase, after about 4-6 hours; and the third corresponding to the hydration of the C_3A phase, sometimes overlapping with the C_3S peak. A fourth broad shoulder may also appear after 24-36 hours, corresponding to the formation of AFm phases such as monosulfate and monocarbonate, but this peak is not always apparent [69]. By comparing the calorimetric heat profiles of the Type IL cement pastes to those of their Type I/II companions, the differences in hydration kinetics between Type I/II and Type IL cements can be assessed. Isothermal calorimetry was performed in accordance with ASTM C1679 [64] on pastes prepared at a water-to-binder ratio (*w/b*) of 0.40, where the binder consists of both the cement and its interground limestone. The mixing procedure consisted of manual stirring of the cement in deionized water for 30s, followed by mechanical mixing of the paste mixture with a 5-speed hand mixer at low speed for 60 s and at medium speed for 60 s. Two samples, each weighing 7.0 ± 0.5 g, were transferred to glass vials and then placed into the isothermal calorimeter (TA Instruments TAM Air). The rate of heat evolution and the cumulative heat released were measured at 25°C for the first 7 days of hydration.

The rates of heat evolution over the first 72-hour and the cumulative heats of hydration over the entire testing period are shown in Figure 4-5. The rate of heat

evolution and cumulative heat are both normalized with respect to the mass of the binder, such that dilution effects are indicated by a reduction in the amount of heat released. A summary of important calorimetric results is given in Table 4-1. For consistency, the "peak" heat release tabulated corresponds to the peak typically associated with C_3S hydration (second peak).
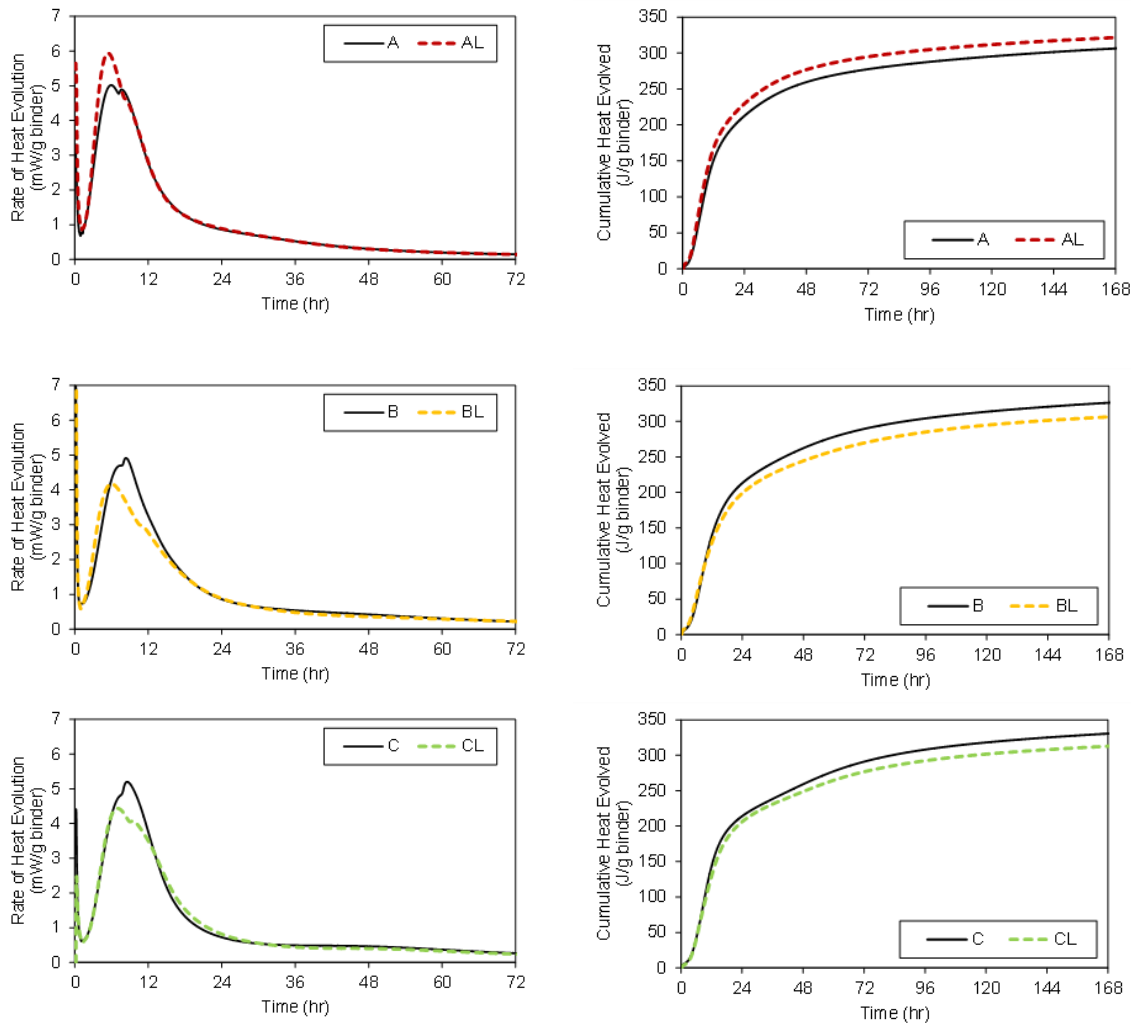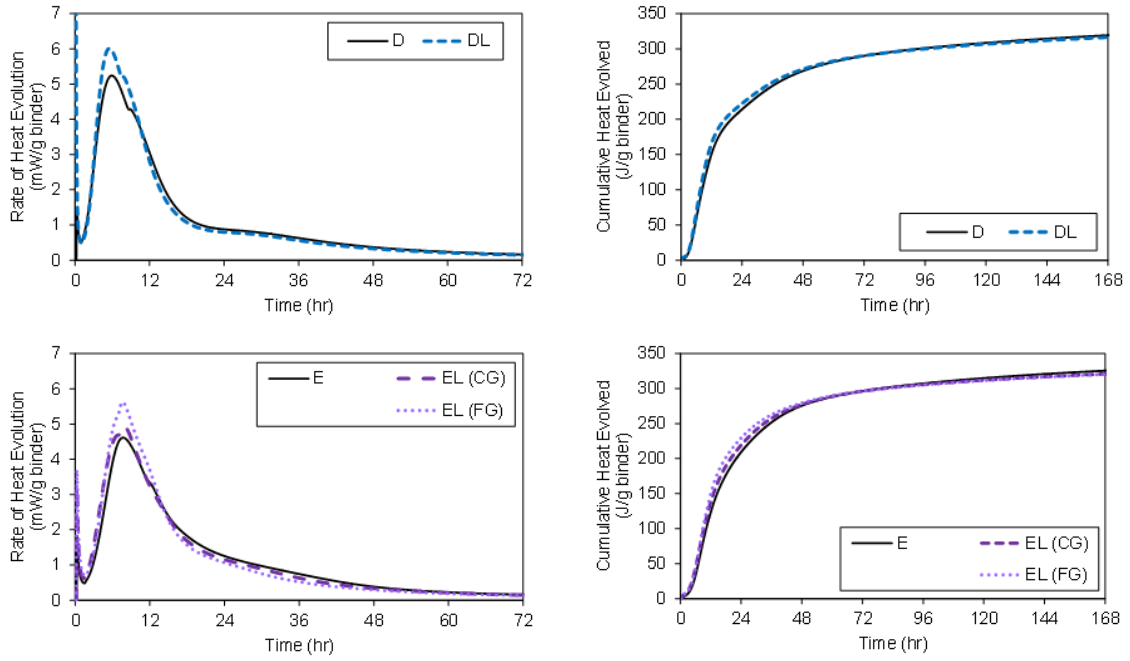
Figure 4.5: Heat evolution for cement pastes A-E at *w/b* = 0.40 and 25°C through 72 hr and cumulative heat evolved for cement pastes A-E through 168 hr (7 days).

Table 4.1: Summary of calorimetric results for cement pastes A-E with $w/b = 0.4$ at 25°C. Peak heat release parameters are given for the C_3S (second) peak.

Cement	Time to peak heat release (hr)	Peak heat release (mW/g)	Cumulative heat (J/g)			
			24 hr	48 hr	72 hr	168 hr
A	5.9	5.0	213	259	277	306
AL	5.4	5.9	230	277	295	321
B	7.5	4.7	213	262	290	326
BL	5.9	4.2	199	245	270	306
C	7.8	4.9	214	259	291	331
CL	7.0	4.4	306	249	277	313
D	5.9	5.2	214	269	290	319
DL	5.5	6.0	222	271	290	316
E	7.8	4.8	209	276	296	325
EL (CG)	7.5	4.8	219	277	296	321
EL (FG)	7.1	5.4	230	280	296	320

The results of the calorimetry experiments suggest that the rate of hydration in the first 24 hr is directly related to the relative fineness of the cement. When the Type IL cement is ground to a finer median particle size than its companion Type I/II cement (as illustrated by cements from sources A, D, and E), the peak heat release is increased, which indicates more rapid hydration rates, consistent with nucleation-dominated behavior [70]. Meanwhile, when the Type IL cement is ground to a similar median particle size as its companion Type I/II cement (as illustrated by cements from sources B

and C), the peak heat release is reduced, consistent with dilution effect-dominated behavior [71]. Additionally, all six Type IL cement pastes show accelerated times to C_3S hydration, consistent with nucleation effects arising from the increase in surface area [70].

After the first 24 hr of hydration, the rates of heat evolution for all six Type IL cement pastes were lower than for their Type I/II counterparts due to the dilution of the cement. The consequences of the later-age dilution effects can be seen in the cumulative heat curves (Figure 4.5). For the two dilution-dominated cements, BL and CL, an approximate 6% relative decrease in total heat release was observed at 7 days. For the four filler effect-dominated cements AL, DL, and EL (CG and FG), the early nucleation and filler effects were enough to overcome the later decreases in hydration rate, leading to a relative increase in total heat of 5% for cement AL, and only a 1% decrease in total heat release for the DL and EL cements by 7 days. Thus, while nucleation effects appear to have a potentially significant effect on hydration behavior in the first 24 hr, the dilution of the reactive clinker by the relatively inert limestone appears to have the more significant effect on the longer term heat of hydration.

4.2.2 Autogenous shrinkage

Changes to cement hydration and microstructural development have important implications for the early-age shrinkage of cement-based materials. Autogenous shrinkage is the volumetric contraction of the cement paste generated by the consumption of capillary pore water during hydration.

Cement pastes with *w/b* = 0.40 were prepared from each of the eleven commercially produced cements where again the mass of the binder was taken to be the mass of the cement as received, including interground limestone. The mixing procedure was the combination of manual and mechanical mixing previously described in this chapter.

Autogenous shrinkage was measured for each cement paste in accordance with ASTM C1698 [60]. Three specimens were cast for each mixture in corrugated tube molds and stored in their sealed conditions in an environmental chamber at 25°C. The length change of each sample was measured by dilatometry, as shown in Figure 4.2, from the time of final setting to an age of 56 days. The time of final setting was determined by penetration of a Vicat needle in accordance with ASTM C191 [68]. Measurements of autogenous shrinkage were taken every 2 hr for the first 6 hr, once daily until 7 days, bi-weekly until 28 days, and then weekly until 56 days.

The autogenous shrinkage results (Figure 4.6) also indicate that the more finely ground Type IL cements (from sources A, D, and E) tend to experience greater degrees of autogenous shrinkage when compared to Type I/II cements of the same clinker composition. Linear strains were increased by as much as 200 μm/m by 56 days for cement pastes AL, DL and EL, suggesting that the more refined microstructures and more rapid rates of hydration for the finely ground Type IL cement pastes result in greater contractions than would be expected for conventional Type I/II cement pastes at the same age.

For the cements from sources B and C, the autogenous shrinkage of the more coarsely ground Type IL cement pastes was lower in magnitude than the autogenous shrinkage of the Type I/II companion pastes through the first 7 days of hydration. Generally,

lower magnitudes of autogenous shrinkage can be attributed to the slower rates of hydration and larger porosities for these pastes [45].

After 7 days of hydration, however, the autogenous shrinkage of cement paste CL continued to be of lower magnitude compared to its Type I/II counterpart, the autogenous shrinkage of cement paste BL was found to increase in magnitude relative to its Type I/II counterpart. The cements from sources B and C had nearly identical particle size parameters to one another so the differences between the autogenous shrinkages of the two Type IL cements suggest that particle size alone is not a suitable predictor for autogenous shrinkage. Rather, the results suggest that significant hydration and microstructural changes are still occurring in cement paste BL due to primary (AFt-producing) and secondary (AFm-producing) reactions of the more slowly hydrating C_4AF phase, which was previously proposed to alter later-age chemical and microstructural evolution for cement paste BL. Thus, it cannot be predicted on the basis of particle size alone whether a Type IL cement will be more or less susceptible to autogenous shrinkage compared to a traditional Type I/II cement – both chemical and physical properties must be considered.

In summary, it was observed that while a relative increase in cement fineness increased autogenous shrinkage at $w/b = 0.40$, a relative decrease in cement fineness did not necessarily decrease autogenous shrinkage. Recommendations to limit early-age shrinkage in PLC-based materials, therefore, cannot rely solely upon limiting the fineness of the cement, as the chemistry of the clinker also has an important impact on the early-age deformation of PLC pastes that must be considered.
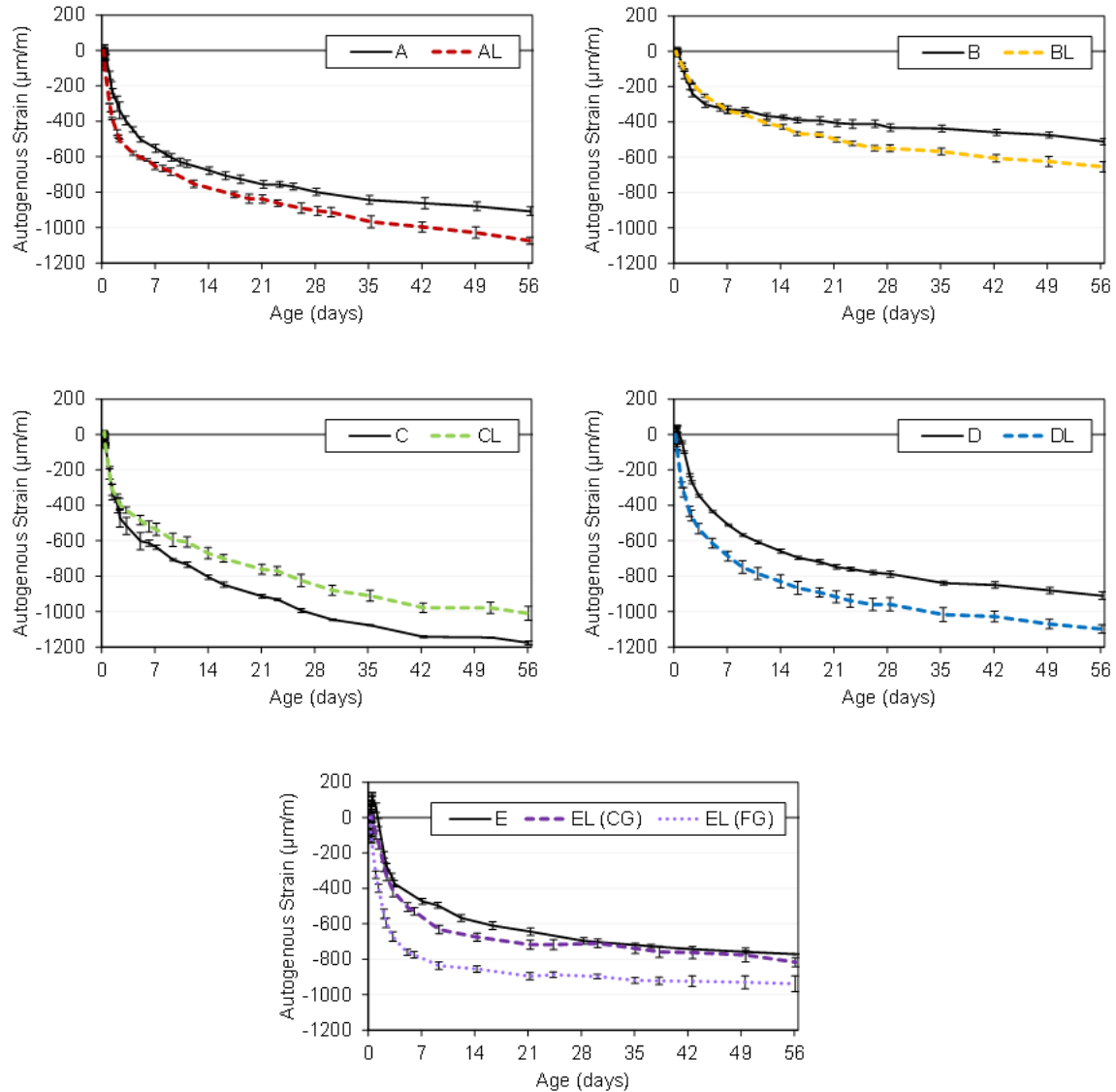
Figure 4.6: Autogenous shrinkage of cement pastes A-E at 25°C with w/b = 0.40.

4.2.3 Chemical shrinkage

The results of the chemical shrinkage test, in units of mL shrinkage per g binder, are presented in **Error! Reference source not found.**. For clarity, error bars are not shown, but the average coefficient of variation over the 7 day testing period was less than 5% for each of the pastes examined.
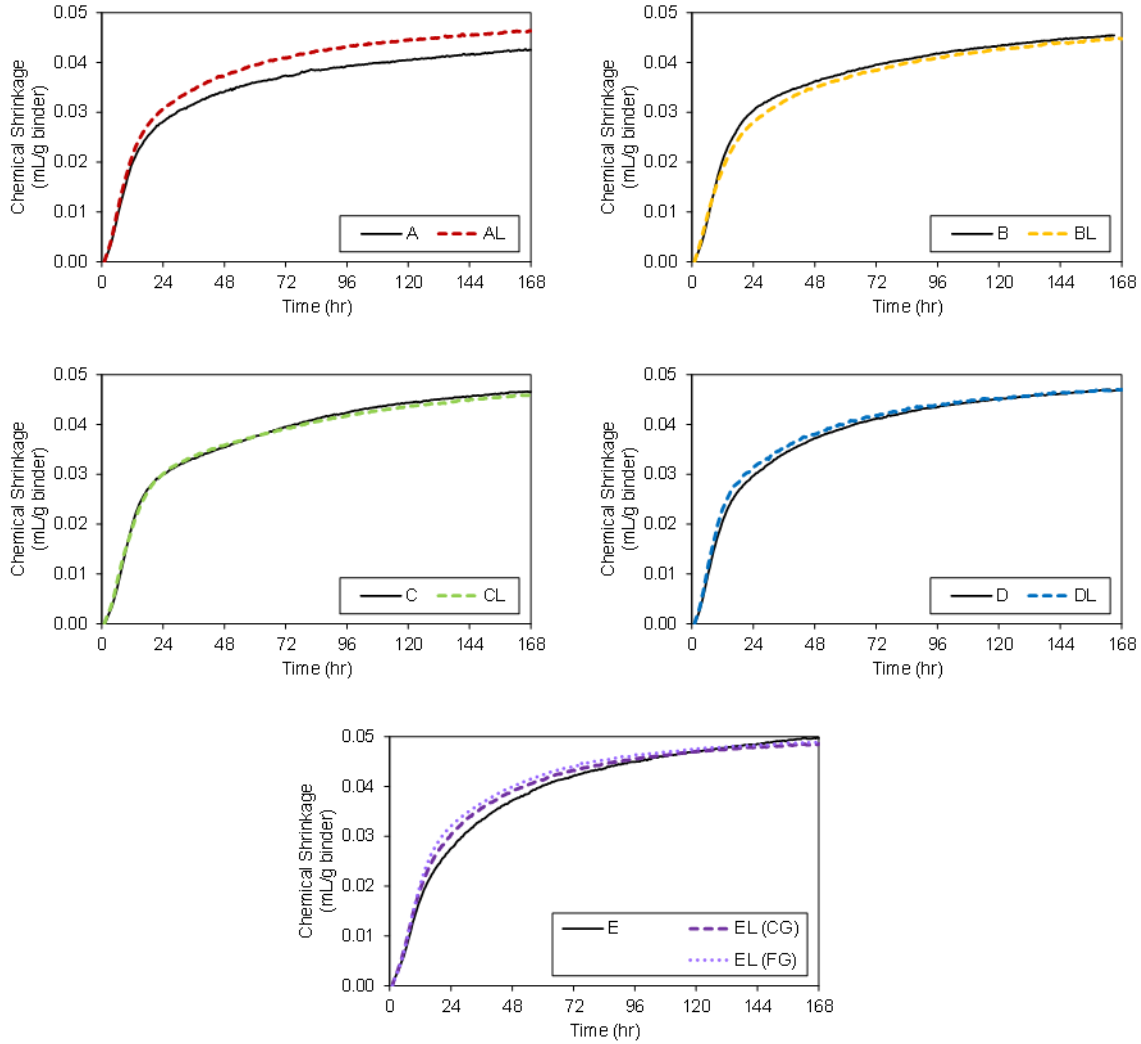
Figure 4.7: Chemical shrinkage measured, in mL/g binder, for cement pastes A-E at *w/b* = 0.40 and 25°C for 7 days (168 hr).

The chemical shrinkage results showed that the more finely ground Type IL cements from sources A, D, and E exhibited greater amounts of chemical shrinkage relative to their Type I/II counterparts, while the more coarsely ground Type IL cements from sources B and C exhibited lesser amounts of chemical shrinkage relative to their Type I/II counterparts. Intuitively, this makes sense, as an increase in hydration rate would imply an increase in the rate of hydration product formation and, by extension, an

increase in the rate of volume loss (due to chemical shrinkage), as well. Therefore, it is not surprising that the four cements that exhibited nucleation-dominated behavior (AL, DL, ELC, and ELF) in calorimetric studies also exhibited a higher degree of chemical shrinkage during that period, which was also found in previous research [72]. Neither is it surprising that the two Type IL cements that exhibited dilution-dominated hydration behavior (cements BL and CL) also exhibited a lower degree of chemical shrinkage than their Type I/II counterparts, since the reduction in reactive material implies a reduction in the relative volume of hydration product and therefore a reduction in chemical shrinkage, as well. Interestingly, although the trends in chemical shrinkage were generally consistent with what was observed through isothermal calorimetry, the relative magnitudes of chemical shrinkage were not as significantly different between Type I/II and Type IL cement pastes as were the relative magnitudes of cumulative heat. In particular, it was observed that at 7 days the cumulative heats of hydration for cement pastes BL and CL were approximately 6% lower than for their companion cement pastes B and C, while the chemical shrinkages for the same two cement pastes were only 2% lower than their Type I/II counterparts. Such a result suggests that the limestone addition may have a greater impact on heat of hydration than it does on chemical shrinkage, which has important implications for the prediction of chemical shrinkage of Type IL cements by Powers' model.

4.2.4 Setting time

Figure 4.8 shows the results of the time of setting for the group of samples from sources A to E and tested at 73 °F.

The results show that Type IL cement showed faster setting time (10% to 20%) for finer limestone cements (such as AL and ELF) and similar setting time for the coarser ones (CL). Higher fineness provides more nucleation sites and therefore increases the rate of hydration, which explains the faster setting.

In contrast to the trends related to cement fineness, cement BL showed faster setting time than cement B (~25%) although cements B and BL were of similar fineness. Also, cement D and DL showed similar setting times although cement DL was finer. This may have occurred due to a sulfate imbalance. QXRD analysis showed that Cements B, BL, D, and DL had higher orthorhombic C_3A than the rest of the cement sources.
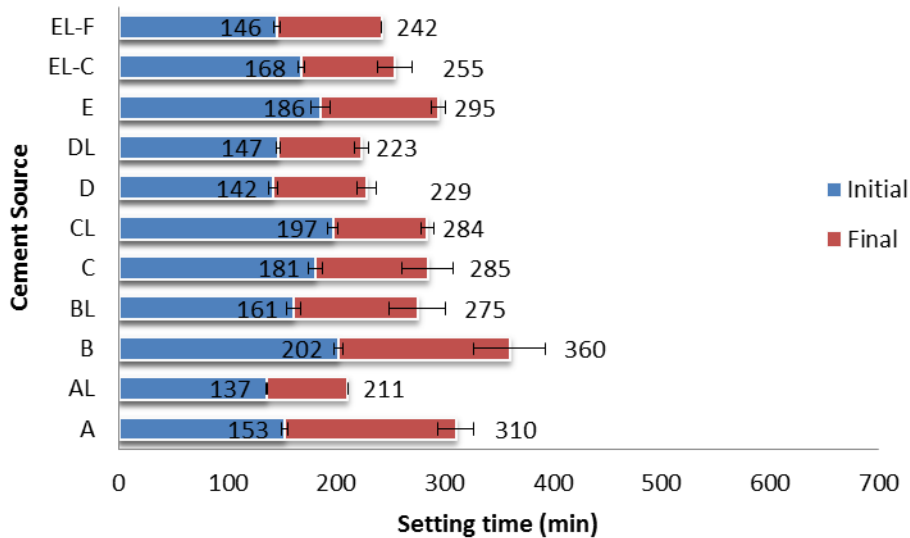
Figure 4.8: Time of setting of cements A to E at 73 °F

The data in Figure 4.8 were then used with the QXRD results to create Figure 4.9 which shows a scatter plot of the relation between calcite content and setting time together with linear regression best fit lines. The results show that the setting time

generally decreased with higher calcite content. The slope of the linear best fit line for the final setting was steeper than the one for the initial setting, indicating a higher effect of the calcite content on the final setting time. However, low R^2 values indicate that other factors (such as fineness and chemical composition) also contribute to the observed behavior.
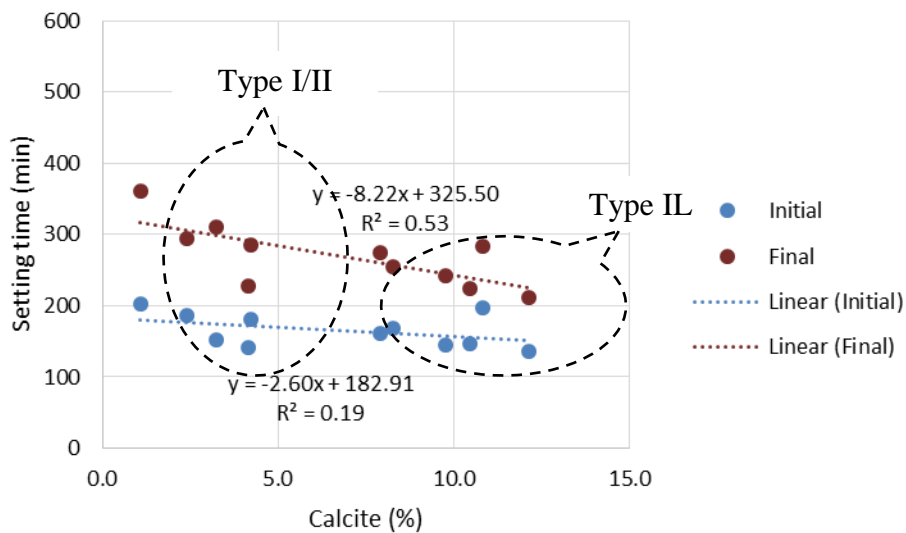
Figure 4.9: Effect of calcite content on setting time at 73 °F

Figure 4.10 shows the effect of the particle size on the setting time at 73 ºF. The results show that larger particle size led to slower setting time. When the data for Type I/II and Type IL cements were separated, as shown in Figure 4.11, the results showed that the particle size had a more significant effect on Type IL cements than Type I/II cements.
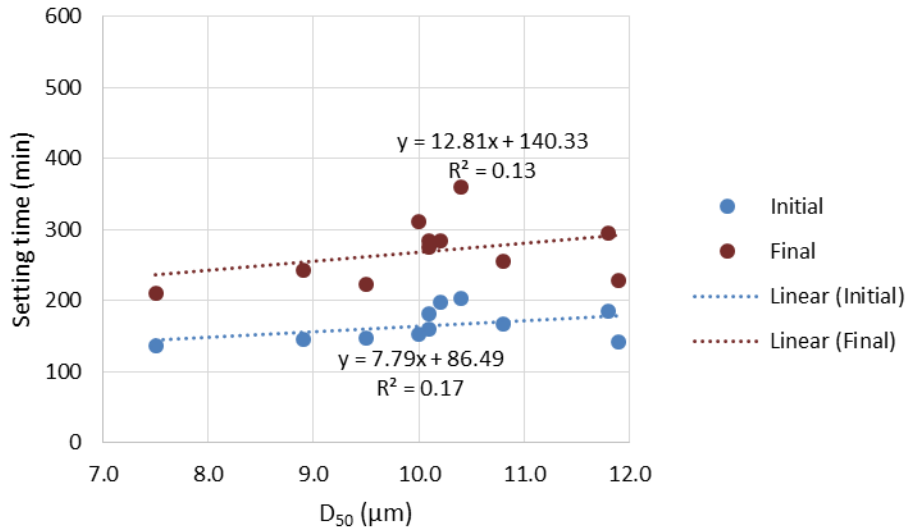
Figure 4.10: Effect of particle size on the setting time at 73 ℉
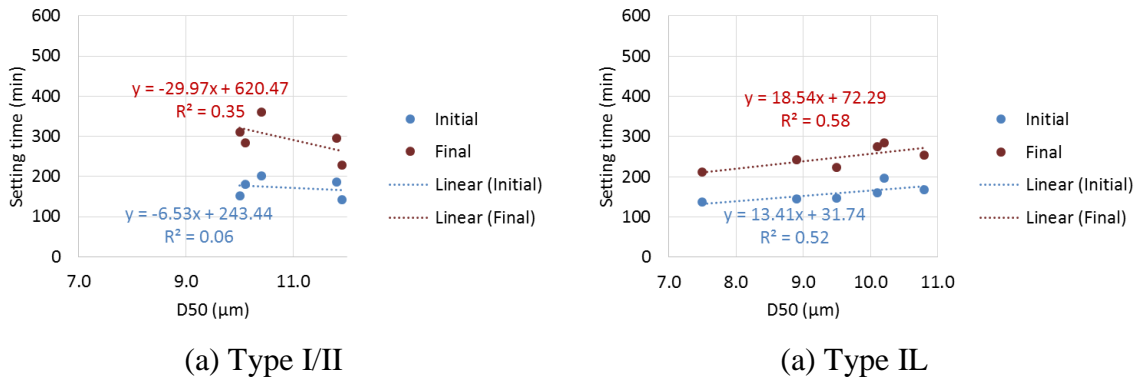
(a) Type I/II   (a) Type IL

Figure 4.11: Effect of particle size of Type I/II and Type IL cements on the setting time at 73 ℉

In general, the values of the setting times are relatively close to those reported in the literature (but with lower limestone replacements). Table 4.2 shows the results reported by Hawkins et al. [29]. The data showed that Type IL cement (limestone content > 5%) resulted in faster setting time.

54

Table 4.2: Vicat Setting Times for interground Cements at Constant Blaine (Hawkins et al. [29])

% Limestone by mass of total cement	Initial Set (min)	Final Set (min)
0	160	300
3	170	300
5.5	170	295
8	165	290

Chapter 5. DEVELOPMENT AND PRODUCTION OF CONCRETE MIXES

The concrete mix designs were developed based on Georgia Department of Transportation (GDOT) Section 500 specifications [73]. Three Classes of concrete - A, AA, and AAA - were cast with the *w/b* ratios of 0.490, 0.445, and 0.320, respectively, which satisfy the requirements of the GDOT specifications as given in Table 5.1.

Eleven concrete mixtures were prepared using the Type I/II cements from sources A to E, along with their companion Type IL cements. Mixtures were designed to meet the highest *w/b* ratio and the minimum total cementitious materials content for each GDOT Class (Table 5.1). Crushed granite coarse aggregates (Lithia Springs, GA; #67 stone, dry-rodded unit weight = 98 lb/ft^3, SG = 2.61) and natural sand fine aggregates (Byron, GA; fineness modulus = 2.4, SG = 2.65) were proportioned at 1889 lb/yd^3 (1120 kg/m^3) and 1260 lb/yd^3 (750 kg/m^3), respectively, for each of the 11 mixtures. A mid-range water reducer (Sika SikaPlast-300GP) was used for Class A and AA and high range water reducer (Sika Viscocrete 2100) was used for AAA concrete to ensure adequate workability. The dosages of admixtures were adjusted to achieve the slump in the range of 2-4 inches required by GDOT section 500 (Table 5.1). The concrete mix design for the three concrete Classes are shown in Table 5.2.

The raw materials were mixed in 5 ft^3 batches in a 9 ft^3 rotating drum mixer, following ASTM standard practices [74]. Cylindrical specimens were cast in cylinders measuring 4-in. (diameter) by 8-in. (length) for compressive and tensile strength testing and 6 in (diameter) by 12-in. (length) for elastic modulus measurements. Concrete prisms 3-in. square cross-section and approximately 11 ¼ in. long were cast for drying

shrinkage tests according to ASTM C157 [57]. Specimens were removed from their molds 24 hours after casting and cured in a saturated calcium hydroxide (limewater) solution at 70 ± 3°F until testing. Other concrete mixes were cured at 40 °F and at 90 °F in temperature controlled curing boxes. These concrete mixes are discussed in more detail in chapter 9.

Table 5.1: Concrete mix requirements from GDOT specification section 500 [73]

Class of Concrete	Coarse Aggregate Size No.	Min. Cement Factor lbs/yd^3	Max. w/b	Slump acceptance Limits (in) Lower-Upper	Entrained Air Acceptance Limits (%) Lower-Upper	Minimum Compressive Strength at 28 days (psi)
A	56, 57, 67	611	0.490	2-4"	2.5-3	3000
AA	56, 57, 67	635	0.445	2-4"	3.5-7	3500
AAA	67,68	675	0.440	2-4"	2.5-6	5000

Table 5.2: Concrete mix designs for Class A, AA and AAA concretes

Material	Weight (pcy)		
	Class A	Class AA	Class AAA
Cement	611	635	800
Water	299	283	256
Coarse Aggregate (#67 granite)	1890	1890	1890
Fine Aggregate (natural sand)	1230	1253	1096
Water reducer	Mid-range WR (SikaPlast -300GP) 2 fl. oz/100 lb cement	Mid-range WR (SikaPlast -300GP) 8-12 fl. oz/100 lb cement	High-range WR (Sika Viscocrete 2100) 4 fl. oz./ 100 lb cement

The slump of fresh concrete was measured following ASTM C143 [75], the unit weight (gravimetric method) was measured following ASTM C138 [76], and the air content was measured by the pressure method according to ASTM C231 [77].

Initially, Class AA concrete was tested extensively since it is for general use concrete. The fresh concrete properties for Class AA concrete from different cement sources are shown in Table 5.3. The slumps of the concrete were in the range of 2-8 in for all concretes and exhibited good cohesion, and the air contents were in the range of 2-3%.

Class AA concrete was made using cement from all the five cement producers mentioned earlier. After examining the properties and performance of all cements, it was

found that cement fineness had significant effects on the performance of concrete. Cement producer "A" had finer Type IL cement while producer "C" had Type IL cement with a fineness more similar to that of the Type I/II cement. Cements from producers A and C became the representative types for further tests. Those cements were selected for producing the samples of Class A and Class AAA concretes.

Table 5.3: Fresh concrete properties for Class AA concrete

Cement source	Mid-range water reducer (fl. oz/100 lb cement)	Slump (in)	Unit Weight (pcf)	Air content (%)
A	12	7.75	150.1	2.6
AL	12	7.25	146.1	3.3
B	8	4	148.7	2.6
BL	8	5.25	146.9	3.2
C	8	2.75	147.7	3.0
CL	8	3	147.4	2.4
D	8	3	150.4	2.0
DL	8	2.25	151.2	2.5
E	8	5.25	149.1	2.2
EL (CG)	8	2	150.1	2.1
EL (FG)	8	2	151.6	2.0

The fresh properties of Classes A and AAA concrete are shown in Table 5.4 and Table 5.5, respectively.

Table 5.4: Fresh concrete properties for Class A concrete

Cement source	Mid-range water reducer (fl. oz/100 lb cement)	Slump (in)	Unit Weight (pcf)	Air content (%)
A	2	3	147.4	2.6
AL	2	3.75	148.4	2.1
C	2	6	145.8	3.2
CL	2	4	147.6	2.7

Table 5.5: Fresh concrete properties for Class AAA concrete

Cement source	Mid-range water reducer (fl. oz/100 lb cement)	Slump (in)	Unit Weight (pcf)	Air content (%)
A	5	8	153.3	1.2
AL	5	6.5	151.8	1.7
C	5	8	152.6	1.6
CL	5	6	152.3	2.6

Chapter 6. ASSESSMENT OF MECHANICAL PROPERTIES AND DRYING SHRINKAGE

6.1 Experimental Program

In this research, the assessment of concrete was organized into two main categories: mechanical properties, and long-term effects. These are discussed in more details in subsequent sections. Figure 6.1 shows a schematic of the test program for concrete assessment. The effect of curing temperature and SCMs are discussed in Chapters 8 and 9.
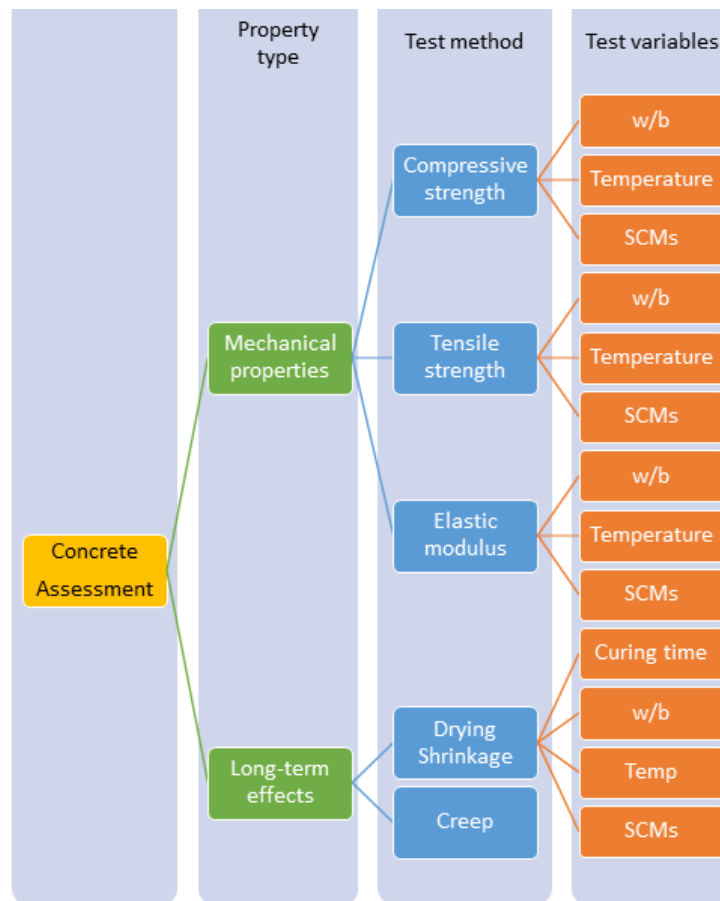
Figure 6.1: Schematic of the test program for concrete assessment

6.1.1 Mechanical properties

The mechanical properties tested were compressive strength (ASTM C39 [78]), elastic modulus (ASTM C469 [79]), and splitting tensile strength (ASTM C496 [80]). Each test method is discussed in detail below.

6.1.1.1 Compressive strength

Compressive strength of concrete cylinders (4 in. x 8 in.) was measured for Class A, AA, and AAA concrete at 1 day, 7 days, 28 days, 56 days, 90 days, and 1 year according to ASTM C39 [78] (AASHTO T22 [81]). Figure 6.2 shows the experimental program for the compressive strength tests.
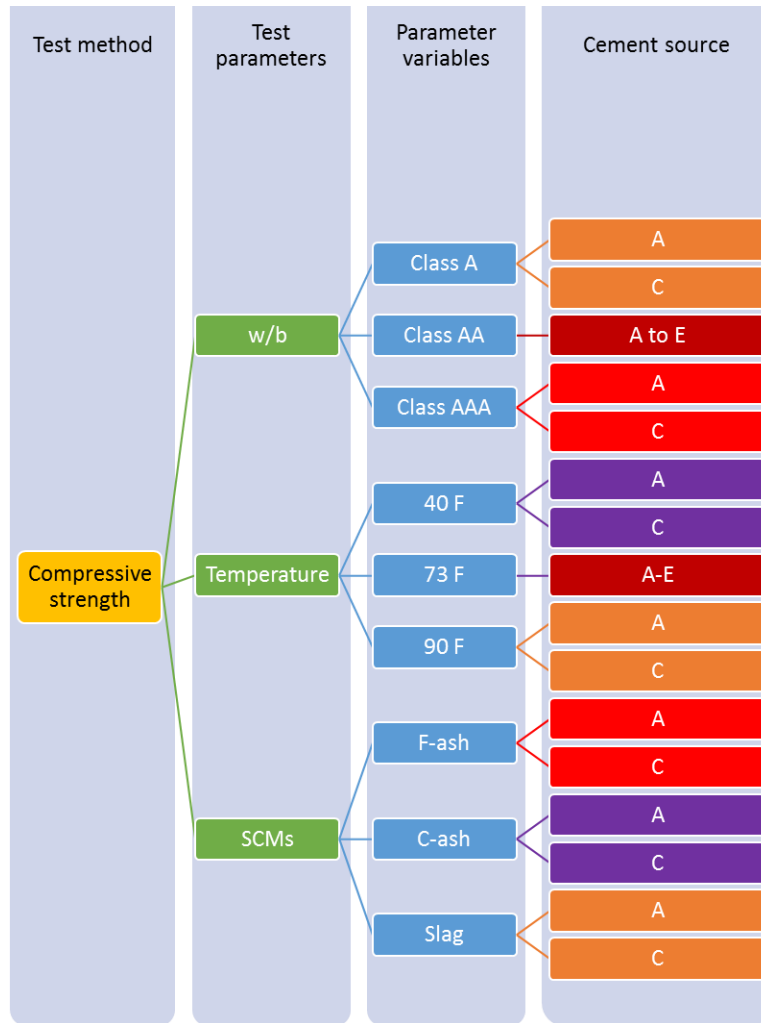
Figure 6.2: Experimental program of the compressive strength of concrete

6.1.1.2 Elastic modulus

Elastic modulus (ASTM C469 [79]) was measured using concrete cylinders (6 in. x 12 in.) at 28 days of age. Figure 6.3 shows the experimental program for the elastic modulus tests.
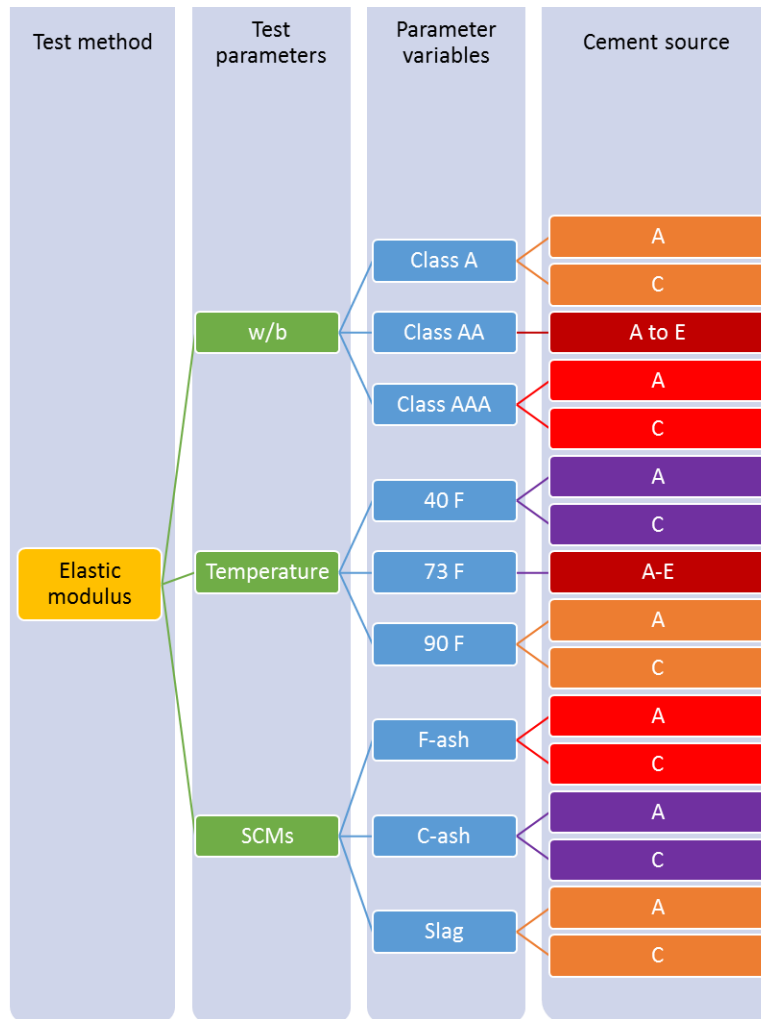
Figure 6.3: Experimental program for the elastic modulus of concrete

6.1.1.3 Splitting tensile strength

Splitting tensile strength (ASTM C496 [80], AASHTO T 198 [82]) was measured using concrete samples (4 in. x 8 in.) at 28 days of age. Figure 6.4 shows the experimental program for the splitting tensile strength tests.
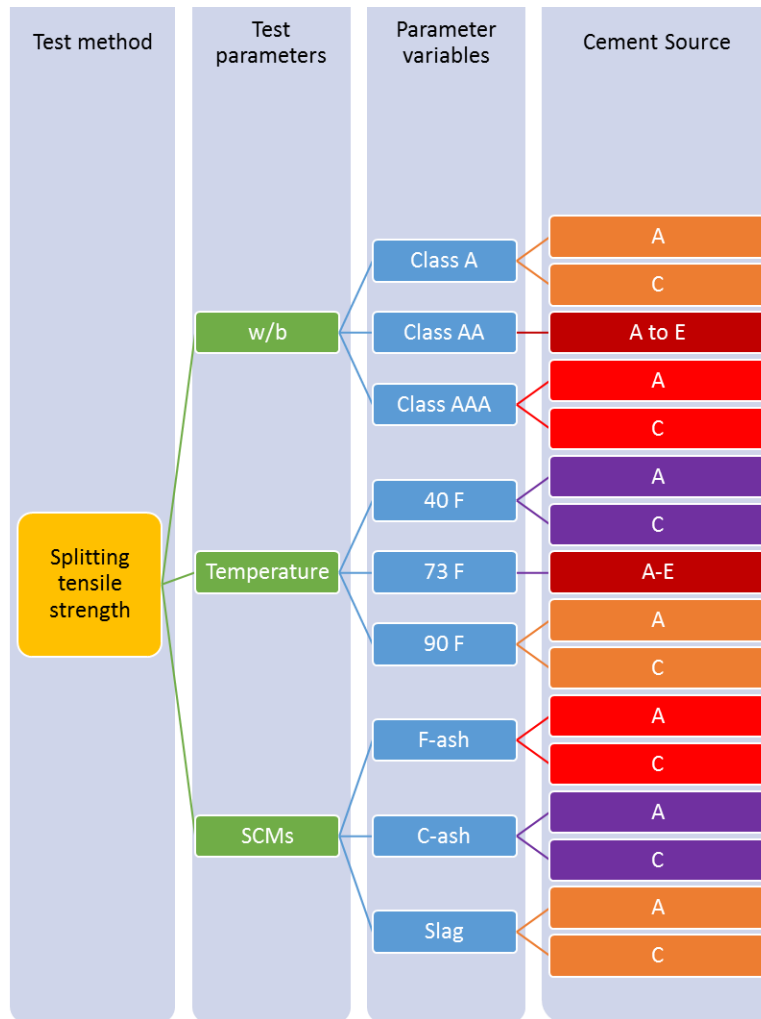
Figure 6.4: Experimental program for the splitting tensile strength of concrete

6.1.2 Drying shrinkage

Drying shrinkage prisms (3 in. x 3 in. x 10 in.) were cured in lime-saturated water for 28 days (ASTM C157 [57]), and then drying initiated at standard room temperature and humidity. Measurements were then taken at 4 days, 7 days, 14 days, 4 weeks, 8 weeks, 16 weeks, and 32 weeks using a length comparator (Figure 6.5).

A second group of samples was only cured for 7 days (Alabama DOT Standard Specifications for Highway Construction, Section 501 [83]), and then drying was measured at the same drying times given above. Curing for only 7 days was used since the shorter curing time more accurately reflects field curing conditions. Figure 6.6 shows the experimental program for the drying shrinkage tests.

Figure 6.5: Drying shrinkage sample with length comparator

Figure 6.6: Experimental program for the drying shrinkage of concrete

6.2   Mechanical properties results

6.2.1 Compressive strength

6.2.1.1 Class AA concrete

Initially, all of the cement sources (A to E) were used to produce Class AA concrete. Figure 6.7 shows the compressive strength values (up to 1 year) of Class AA concrete made with Type I/II and Type IL cements from plants A to E. The first group of

67

specimens was cured in saturated lime-water baths at room temperature (73 °F) until testing. Other samples were cured at 40 °F and at 90 °F as discussed in Chapter 9.
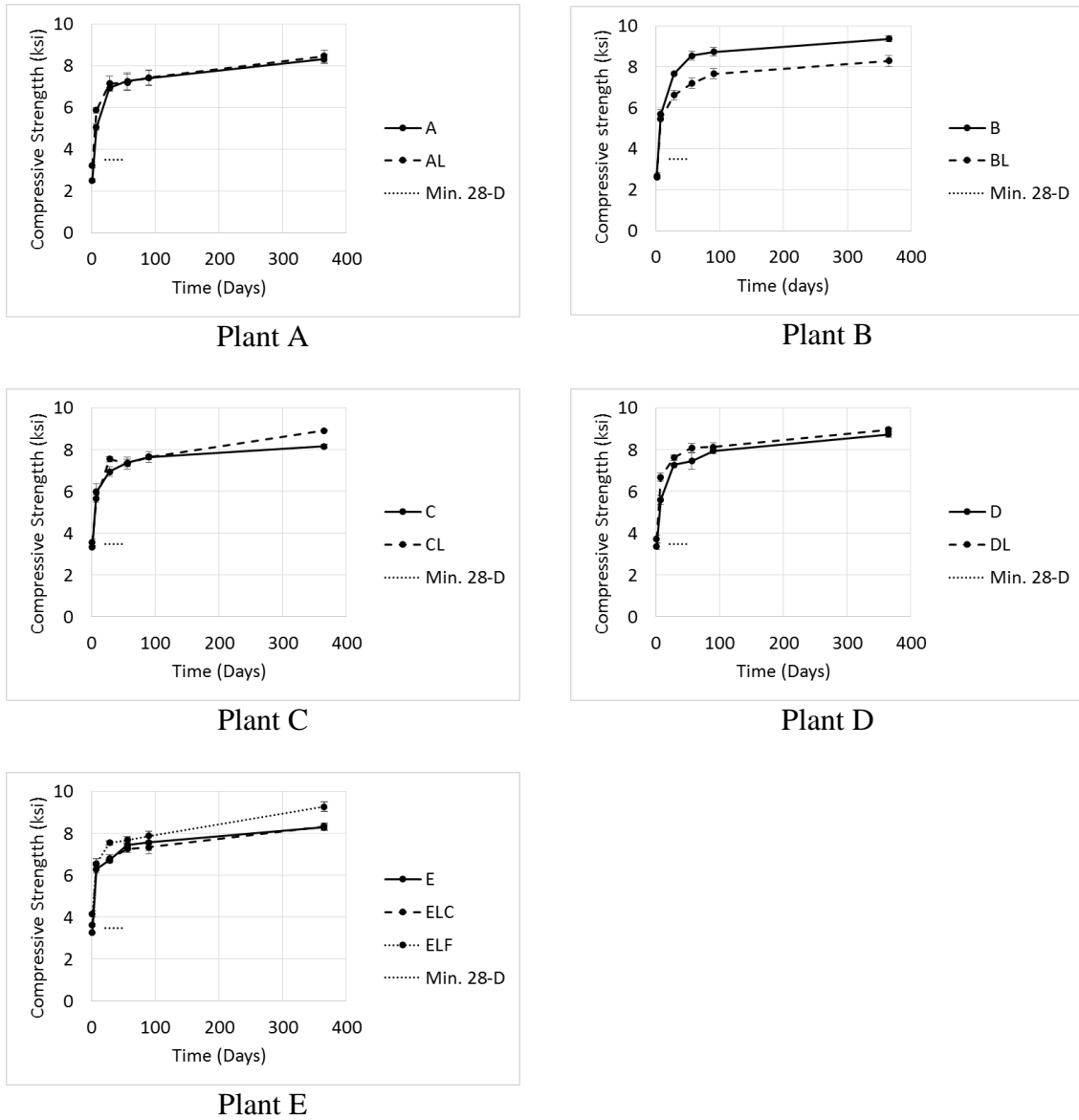
Figure 6.7: Compressive strength of Class AA concrete
The GDOT specified minimum strength of 3500 psi is shown as "Min 28-D"

At one day, the finer Type IL cements (AL, DL, ELC, and ELF) showed 10% to 35% higher compressive strength than their companion Type I/II cement. The coarser

Type IL cements showed values closer to Type I/II cement (~3% higher for CL). The authors hypothesize that the finer limestone cements provided additional nucleation sites which resulted in faster hydration and higher strength at early age.

At one year, all Type IL cements showed either equal or up to 20% higher strength when compared to their companion Type I/II cement. This indicated that the dilution effect had a negligible effect on the long term strength of Type IL cement. The percentage of cement phases (C_3S, C_2S, C_3A, and C_4AF), the average particle size, and the calcite content were investigated for their effects on the compressive strength.

Figure 6.8 shows a scatter plot of calcite content vs. the compressive strength of Class AA concrete at 1 day, 28 days, and 1 year. After applying a linear regression best fit line, it can be seen that the higher the calcite content, the greater the compressive strength, however the effect of calcite content diminishes for strength at 1 year. The data also suggest that for Type IL cement, about 10% calcite content produces a maximum strength for all ages.

The R^2 values with respect to the calcite content were higher for 1-day strength data than at other ages which indicates that calcite content has a higher influence on the early age strength than at later ages. Overall, the low R^2 values indicate that other factors (such as fineness and chemical composition) also contribute to the observed behavior.
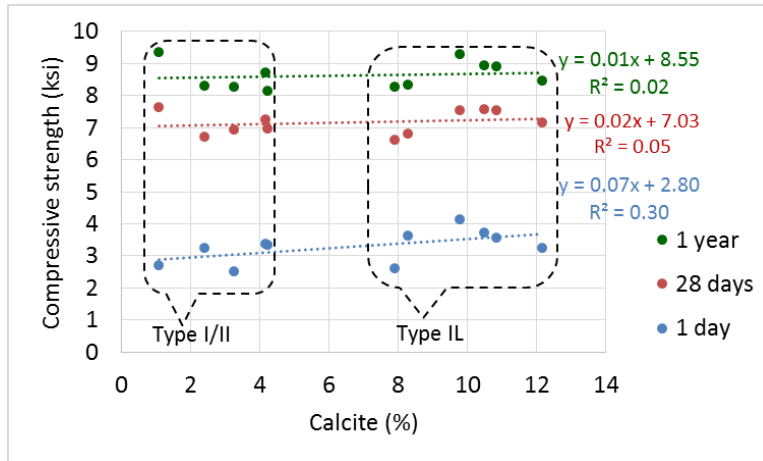
Figure 6.8: Effect of calcite content on compressive strength of Class AA concrete

Analysis of variance (ANOVA) was conducted to investigate the statistical significance of the difference in values of the compressive strength of Type I/II and Type IL cement of each plant. The null (no difference) hypothesis was that average strengths of Type I/II and Type IL are similar ($\mu1=\mu2$). A summary of the results for Class AA concrete is shown in Table 6.1. Accepting the null hypothesis indicates that there is no statistical significance in the difference between the strength of Type I/II and Type IL cements while rejecting the null hypothesis indicates that there is a significant statistical difference between the strength of Type I/II and Type IL cements.

Table 6.1: ANOVA results for comparing Type I/II and Type IL cements from each plant
for the compressive strength of Class AA concrete
(null hypothesis, strength of Type I/II = strength of Type IL, "Similar": $\mu1=\mu2$)

Time	Cement Source					
	A/AL	B/BL	C/CL	D/DL	E/ELC	E/ELF
7 days	Different	Similar	Similar	Different	Similar	Similar
28 days	Similar	Different	Different	Similar	Similar	Different
1 year	Similar	Different	Different	Similar	Similar	Different

70

The results showed that the fine-grade Type IL cement from plant E showed statistically significant different results when compared to Type I/II from the same plant, while there was no statistical significance in the difference between the strength of the coarse grade Type IL cement and Type I/II from plant E. In addition to that, the authors hypothesized that there are more differences between plant producers than there are between Type I/II and Type IL from the same plant. Table 6.2 shows the ANOVA results of comparing the compressive strength of Class AA concrete among different plants.

Table 6.2: ANOVA results for comparing the differences between plants for the compressive strength of Class AA concrete
(null hypothesis, concrete strength of cement from Plant 1 = concrete strength of cement from plant 2, "Similar": $\mu 1 = \mu 2$)

Time	Cement Source	
	Type I/II	Type IL
7 days	Different	Different
28 days	Different	Different
1 year	Different	Similar

The results show that difference in strength between plants was statistically significant in all cases except the 1 year strength of Type IL cement. This indicates that the difference between plants has a more significant effect on strength than the difference between Type I/II and Type IL. The results also show that there is no statistical significance difference of the strengths of Type IL cements from different producers at 1 year.

6.2.1.2 Class AAA concrete

After examining the properties and performance of all cements in the Class AA study, it was found that cement fineness had significant effects on the performance of

concrete. Cement producer "A" had finer Type IL cement while producer "C" had Type IL cement with a fineness more similar to that of the Type I/II cement. Based on that, cement from producers "A" and "C" were selected for the Class AAA study. Figure 6.10 shows the compressive strength of Class AA and AAA concretes from plants A and C, respectively. The concrete was cured at room temperature (73 °F) in a lime-saturated water bath until testing.
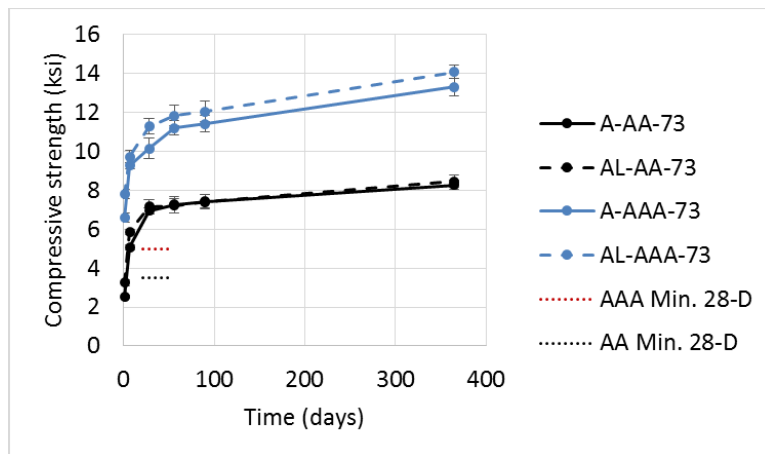
Figure 6.9: Compressive strength of Class AA and AAA concrete from Plant A
(GDOT Section 500 minimum required strength at 28 days is shown in dotted lines)
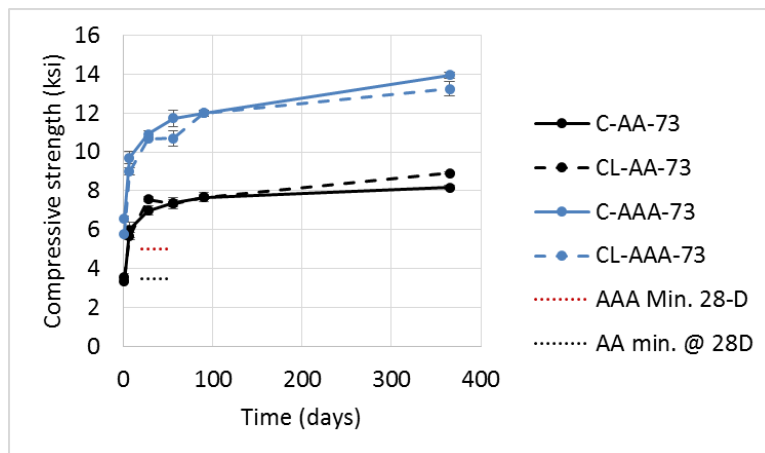
Figure 6.10: Compressive strength of Class AA and AAA concrete from Plant C
(GDOT Section 500 minimum required strength at 28 days shown in dotted lines)

When comparing Type I/II and Type IL cements of Class AAA concrete, cement AL showed higher strength than cement A at all ages. However, cement CL showed lower strength than cement C at all ages up to 90 days where the strength converged with cement C. Fineness had a significant effect for Class AAA concrete. The finer Type IL cement (cement AL) showed higher strength while the coarser Type IL (cement CL) showed a lower strength. The strength of cement CL later converged with that of cement C indicating negligible significance of the dilution effect at later ages. Another point to note is that the difference in strength of cement A and AL of Class AAA concrete was higher than the difference between cement A and AL of Class AA concrete.

Class AAA concrete showed higher strength than Class AA concrete for both plants. When comparing each cement of Class AAA concrete with the same one from Class AA concrete, the difference was about 60% for all cements at 90 days. However, at one day, there was a larger variability. Cements A and AL of Class AAA concrete showed a relatively larger difference than cements A and AL of Class AA (~160% and 140%, respectively). Cements C and CL of Class AAA concrete showed a relatively smaller difference than cements C and CL of Class AA concrete (~100% and ~60%, respectively). This implies that the effect of fineness is more significant at early ages.

Figure 6.11 shows a scatter plot of calcite content vs. the compressive strength of concrete Class AAA, at 1 day, 28 days, and 1 year. The higher the calcite content, the greater the compressive strength. This indicates that the nucleation effect was significant. However, low R^2 values indicate that other factors (such as fineness and chemical composition) also contribute to the observed behavior.
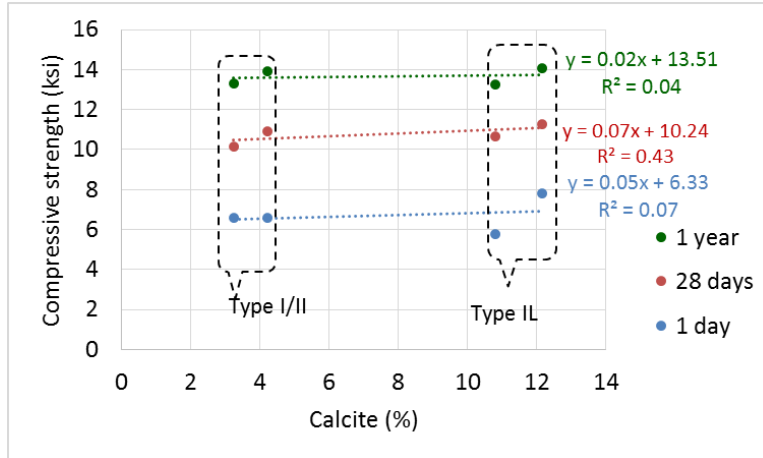
Figure 6.11: Effect of calcite content on the compressive strength of Class AAA concrete

Analysis of variance (ANOVA) was conducted to investigate the statistical significance of the difference in values of the compressive strength of Type I/II and Type IL cement of plants A and C. The null (no difference) hypothesis was that average strength of Type I/II and Type IL are similar ($\mu 1 = \mu 2$). A summary of the results for Class AAA concrete is shown in Table 6.3. Accepting the null hypothesis indicates that there is no statistical significance in the difference between the strength of Type I/II and Type IL cement while rejecting the null hypothesis indicates that there is a significant statistical difference between the strength of Type I/II and Type IL cement.

Table 6.3: ANOVA results for comparing Type I/II and Type IL cements from each plant
for the compressive strength of Class AAA concrete
(null hypothesis, strength of Type I/II = strength of Type IL, "Similar": $\mu 1 = \mu 2$)

Time	Cement source	
	A/AL	C/CL
7 days	Similar	Different
28 days	Different	Similar
1 year	Similar	Different

74

The results showed that the difference in strength between C and CL were statistically significant. Cement CL had a fineness similar to cement C but had a lower strength (dilution effect). Cement AL was finer and that increased the strength which also decreased the difference between A and AL leading to statistically insignificant differences between A and AL. In addition to that, the authors investigated the effect of different cement source on the strength of Type I/II and Type IL cements. Table 6.4 shows the ANOVA results of comparing the compressive strength of Class AAA concrete among plants A and C.

Table 6.4: ANOVA results for comparing the differences between plants for the compressive strength of Class AAA concrete
(null hypothesis, concrete strength of cement from Plant 1 = concrete strength of cement from plant 2, "Similar": $\mu 1 = \mu 2$)

Time	Cement Source	
	Type I/II	Type IL
7 days	Similar	Different
28 days	Similar	Similar
1 year	Similar	Different

The results show that difference in strength between plants was not statistically significant for Type I/II cement but was statistically significant for Type IL cement. This indicates that for Class AAA concrete, the difference in the cement source has a significant effect on concrete strength using Type IL cement but not on Type I/II cement for Class AAA concrete (due to the difference of fineness of cements AL and CL).

75

6.2.1.3 Class A concrete

Cement producers A and C were selected to produce Class A concrete for the same reasons mentioned for Class AAA concrete. Figure 6.12 and Figure 6.13 show the compressive strength of Class A and AA concrete from plants A and C, respectively.
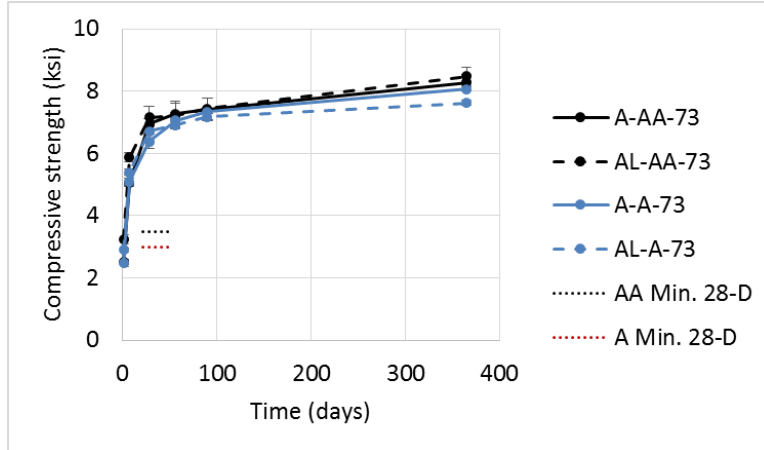
Figure 6.12: Compressive strength of Class A and AA concrete from Plant A
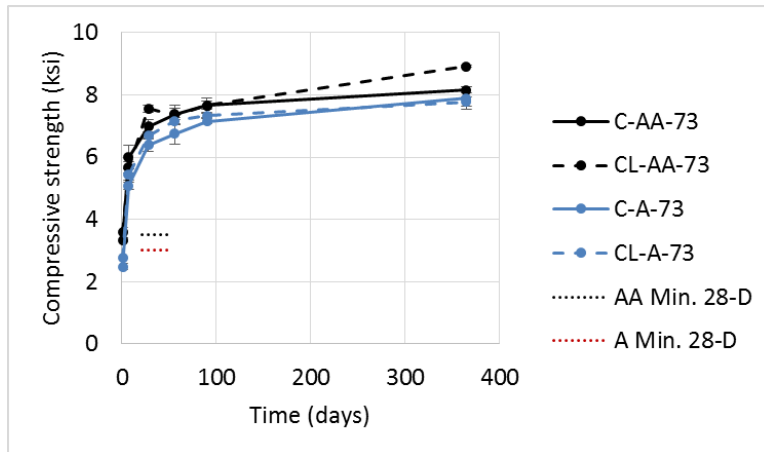
Figure 6.13: Compressive strength of Class A and AA concrete from Plant C

76

When comparing Type I/II and Type IL cements of Class A concrete, cement AL showed 16% higher strength than cement A. Similarly cement CL showed 11% higher strength at 1 day. However, the difference in strength continued to diminish with time. Cement A showed slightly higher strength after 56 days (5% at 1 year), and Cement C showed similar strength to CL at 1 year. This indicates that at this higher w/b ratio, Type IL cement increased the early age strength, but at later ages, the dilution effect was more significant than at lower w/b ratios. Class A concrete showed slightly lower strength than Class AA concrete for both plants. When comparing each cement of Class A concrete with the same one from Class AA concrete, the difference at 90 days was relatively low (~1% to 7%). However, at one day, there was a larger variability. Cement A and AL of Class A concrete showed a relatively smaller difference than cements A and AL of Class AA (~1% and 11%, respectively). Cement C and CL of Class A concrete showed a relatively larger difference than cements C and CL of Class AA concrete (26% and 23%, respectively). This implies that the effect of fineness is more significant at early ages.

Figure 6.14 shows a scatter plot of calcite content vs. the compressive strength of concrete Class A, at 1 day, 28 days, and 1 year. The higher the calcite content, the greater the compressive strength. This indicates that the nucleation effect was significant. The only exception was the 1-day strength values of Class A concrete, where the higher the calcite content, the lower the compressive strength, indicating that the dilution effect was significant.
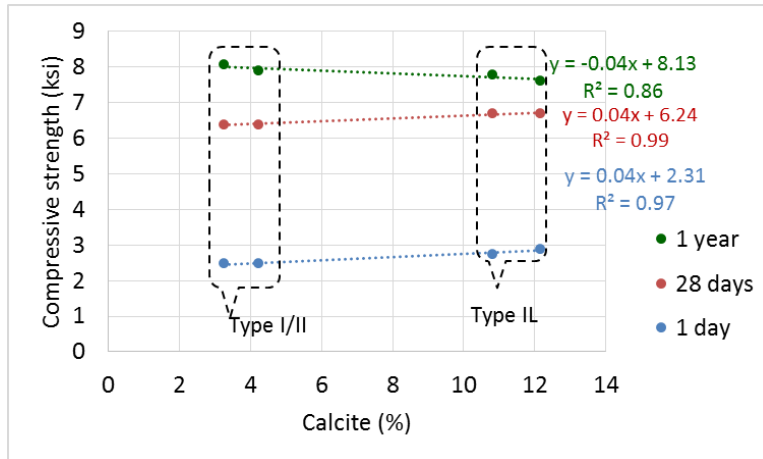
Figure 6.14: Effect of calcite content on the compressive strength of Class A concrete

Analysis of variance (ANOVA) was conducted to investigate the statistical significance of the difference in values of the compressive strength of Type I/II and Type IL cement of plants A and C. The null (no difference) hypothesis was that average strength of Type I/II and Type IL are similar ($\mu1=\mu2$). A summary of the results for Class A concrete is shown in Table 6.5. Accepting the null hypothesis indicates that there is no statistical difference between the strength of Type I/II and Type IL cement while rejecting the null hypothesis indicates that there is a significant statistical difference between the strength of Type I/II and Type IL cement.

Table 6.5: ANOVA results for comparing Type I/II and Type IL cements from each plant
for the compressive strength of Class A concrete
(null hypothesis, strength of Type I/II = strength of Type IL, "Similar": $\mu1=\mu2$)

Time	Cement source	
	A/AL	C/CL
7 days	Similar	Different
28 days	Similar	Similar
1 year	Different	Similar

78

The results showed that for Class A concrete, the difference in strength between Type I/II and Type IL was not statistically significant except for cement AL at 1 year (due to the higher fineness). The authors hypothesize that at this high *w/b* ratio and low cement factor, the effect of limestone replacement on the compressive strength diminishes.

In addition to that, the authors investigated the effect of different cement source on the strength of Type I/II and Type IL cements. Table 6.6 shows the ANOVA results of comparing the compressive strength of Class A concrete between plants A and C.

Table 6.6: ANOVA results for comparing the differences between plants for the compressive strength of Class A concrete
(null hypothesis, concrete strength of cement from Plant 1 = concrete strength of cement from plant 2, "Similar": $\mu 1 = \mu 2$)

Time	Cement Source	
	Type I/II	Type IL
7 days	Similar	Similar
28 days	Similar	Similar
1 year	Different	Similar

The results in Table 6.6 show that difference in strength between plants was not statistically significant for Type I/II and Type IL cements, except for the 1 year strength of Type I/II cement. This indicates that for Class A concrete, cement source has little effect on the compressive strength.

6.2.2 Elastic modulus

Elastic modulus was measured for concrete cylinders (6 in. x 12 in.) at 28 days of age. Figure 6.15 shows the elastic moduli for Class AA concrete measured at 28 days, along with theoretical values computed using ACI 318-14 section 19.2.2.1:

$$E = \frac{w_c^{1.5} 33\sqrt{f'_c}}{1000}$$

<div align="right">Equation 6.1</div>

where:

- E: modulus of elasticity (ksi)
- w_c: unit weight (pcf)
- f_c': compressive strength (psi)

Carrasquillo [84] showed that the ACI equation for predicting the modulus of elasticity over-predicted the values when the concrete compressive strength exceeded 6 ksi, and therefore concluded that a better equation is given by:

$$E = 40\sqrt{f'_c} + 10^3$$

<div align="right">Equation 6.2</div>

where:

- E: modulus of elasticity (ksi)
- f_c': compressive strength (psi)

The above equation is also adopted in ACI 363R-10 [85] (Equation 6-1 in ACI 363R-10) for high strength concrete and provides a better estimate for the measured values of the elastic moduli of all the samples mentioned in this report. Figure 6.15 shows the values calculated with Equation 6.2 which shows better prediction than Equation 6.1.

For Class AA concrete, the average elastic moduli of all Type IL samples varied from -5% to +18% compared to the companion Type I/II cement. The largest difference was between Type I/II cement from plant E and the fine-grade Type IL cement from that plant. This indicated that higher fineness increases the elastic modulus due to the

formation of more hydrated microstructure. The calculated values obtained using Equation 6.1 over-estimated the values for all cements by an average of 24% for Type I/II and 18% for Type IL mixes. However, the calculated values obtained using Equation 6.2 over-estimated the values for all cements by an average of 7% for Type I/II and 3% for Type IL mixes.
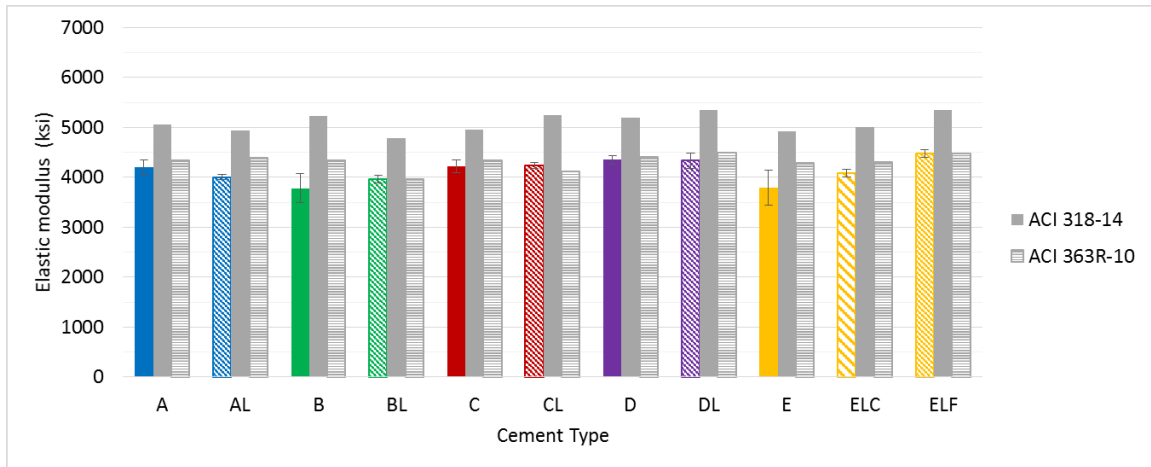
Figure 6.15: Elastic modulus values of Class AA concretes

Figure 6.16 shows a scatter plot of calcite content vs. the elastic modulus of Class AA concrete at 28 days. After applying a linear regression best fit line, it can be seen that there is an apparent slight correlation between calcite content and elastic modulus. This suggests that the limestone, whether through improvements in packing or microstructural refinement, decreased pre-existing microcracks and/or improved bonding in the aggregate/paste interface. However, low R^2 values indicate that other factors (such as fineness and chemical composition) also contribute to the observed behavior.
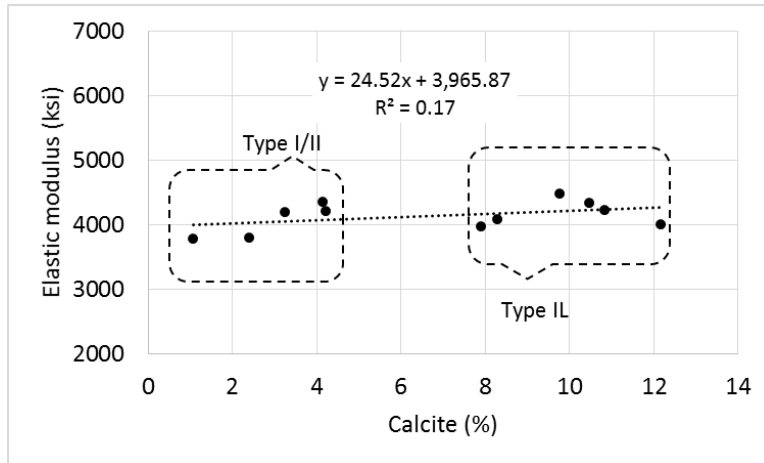
Figure 6.16: Effect of calcite content on elastic modulus of Class AA concrete

Figure 6.17 shows the effect of average particle size of cement on the elastic modulus of Class AA concrete. The results show no correlation between the average particle size and the elastic modulus.

(a) Type I/II   (b) Type IL
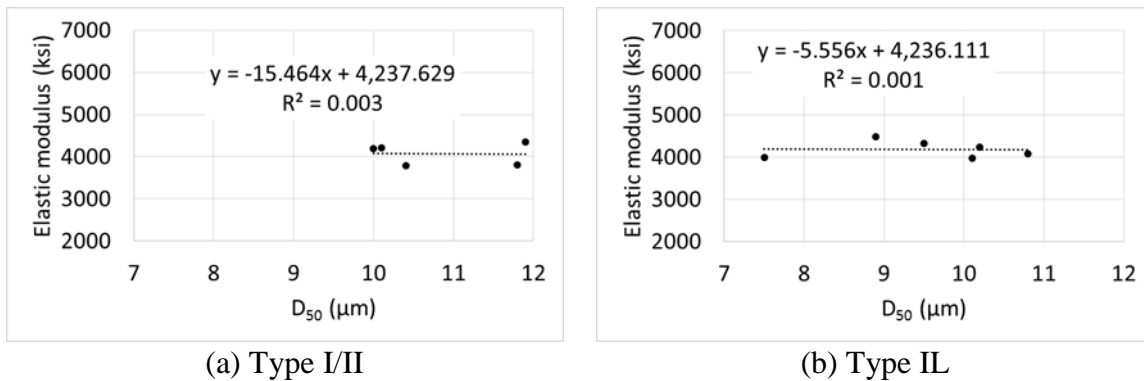
Figure 6.17: Effect of average particle size of cement on the elastic modulus of Class AA concrete

Analysis of variance (ANOVA) was conducted to investigate the statistical significance of the difference in values of the elastic modulus of Type I/II and Type IL cement from each plant. The null hypothesis was that average strength of Type I/II and Type IL are similar ($\mu 1=\mu 2$). A summary of the results for Class AA concrete is shown in Table 6.7. Accepting the null hypothesis indicates that there is no statistical significance in the difference between the modulus of Type I/II and Type IL cement while rejecting the null hypothesis indicates that there is a significant statistical difference between the strength of Type I/II and Type IL cement.

Table 6.7: ANOVA results for comparing the elastic moduli of Type I/II and Type IL cements from each plant of Class AA concrete
(null hypothesis, modulus of Type I/II = modulus of Type IL, "Similar": $\mu 1=\mu 2$)

Cement Source					
A/AL	B/BL	C/CL	D/DL	E/ELC	E/ELF
Similar	Different	Different	Similar	Similar	Different

The results showed that the fine-grade Type IL cement from plant E showed statistically significant different results when compared to Type I/II from the same plant, while there was no statistical significance in the difference between the strength of the coarse grade Type IL cement and Type I/II from plant E. In addition to that, the authors hypothesized that there are more differences between plant producers than there are between Type I/II and Type IL from the same plant.

Table 6.8 shows the ANOVA results of comparing the elastic modulus of Class AA concrete among different plants. The results show that difference in elastic modulus between plants was statistically significant for Type I/II but not statistically significant

for Type IL. This indicates that the difference between plants has a more significant effect on the elastic modulus of Type I/II cement.

Table 6.8: ANOVA results for comparing the differences between plants for the elastic modulus of Class AA concrete
(null hypothesis, modulus of Type I/II = modulus of Type IL, "Similar": $\mu1=\mu2$)

Cement Source	
Type I/II	Type IL
Different	Similar

Figure 6.18 and Figure 6.19 show the elastic moduli using cements from plants A and C for Class AAA and Class A concrete, respectively. For Class AAA concrete, Type IL showed 1% to 5% lower values (indicating that the dilution effect was significant in Class AAA concrete). The finer particle size of cement AL reduced the difference to only 1%. For Class A concrete, the results were relatively similar (differences were not statistically significant according to the ANOVA results discussed later).

84
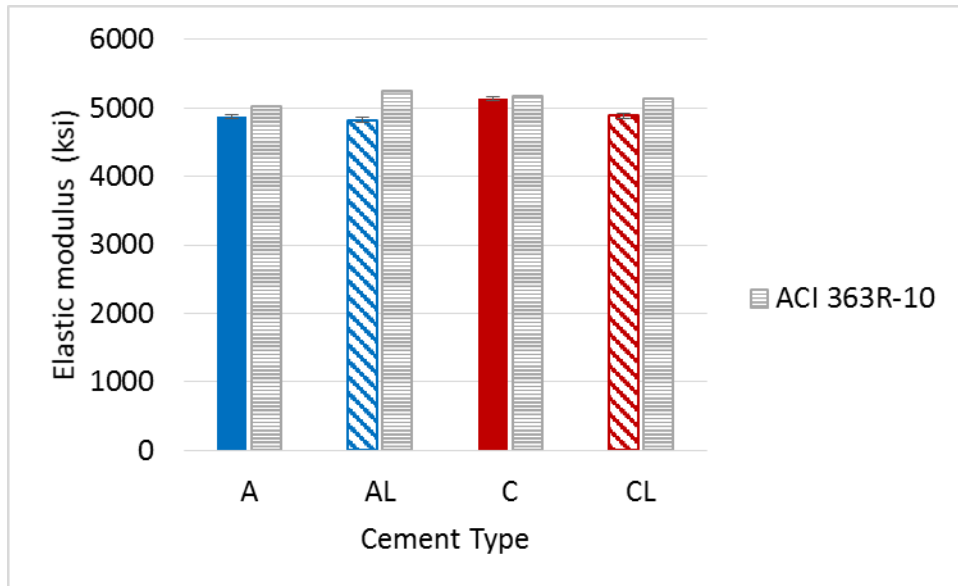
Figure 6.18: Elastic modulus values of Class AAA concretes
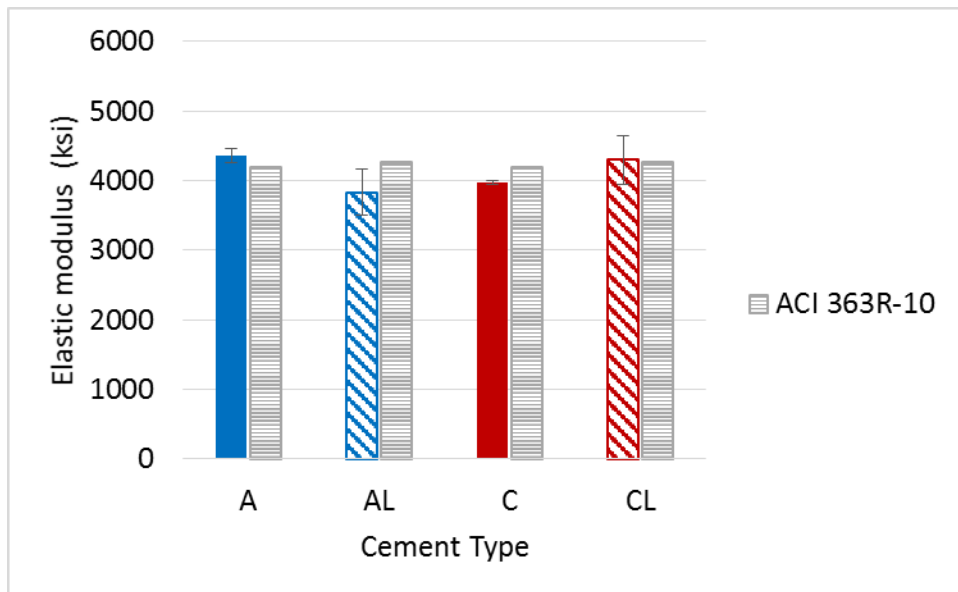
Figure 6.19: Elastic modulus values of Class A concretes

Figure 6.20 and Figure 6.21 show scatter plots of calcite content vs. the elastic

modulus of concrete Classes AAA and A, respectively, tested at 28 days. After applying

a linear regression best fit line, it can be seen that the higher the calcite content, the lower

85

the elastic modulus. However, low R^2 values indicate that other factors (such as fineness and chemical composition) also contribute to the observed behavior.
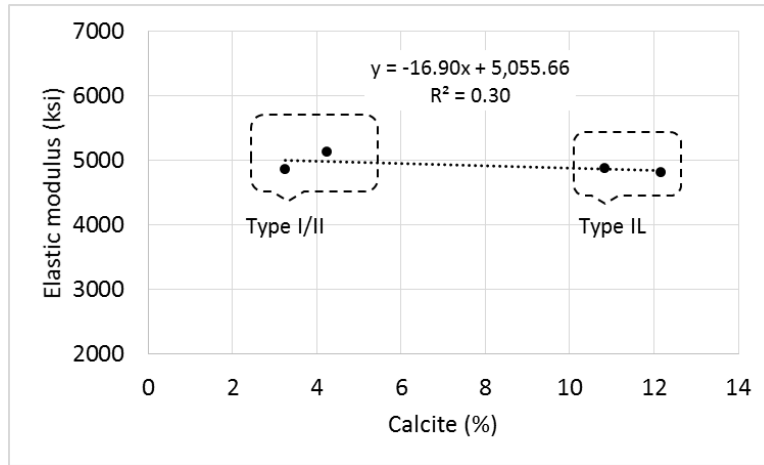
Figure 6.20: Effect of calcite content on elastic modulus of Class AAA concrete
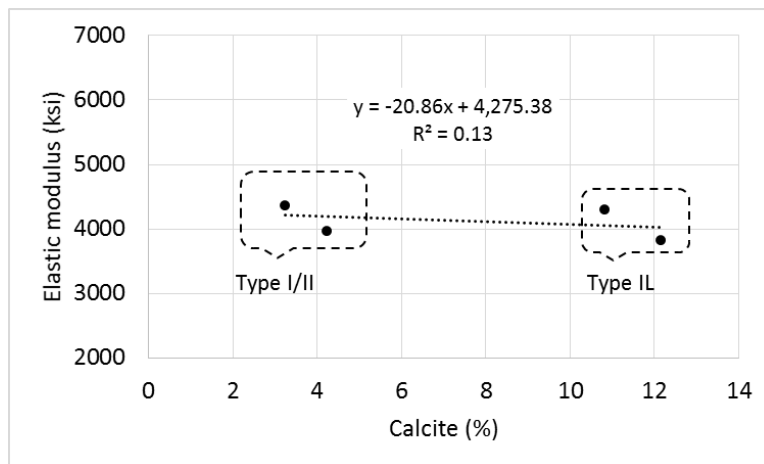
Figure 6.21: Effect of calcite content on elastic modulus of Class A concrete

Table 6.9 shows ANOVA results for all three concrete Classes. The results show that the differences between Type I/II and Type IL from plant A were not statistically significant. The differences between cement C and CL were statistically significant for

86

Classes AAA and AA, but not for Class A. Type IL cement showed lower elastic modulus values when of similar fineness to Type I/II (plant C). The finer Type IL cement, AL, reduced the differences between Type I/II and Type IL leading to no significant differences. The differences were not statistically significant for Class A concrete due to the low cement factor.

Table 6.9: ANOVA results for comparing the elastic modulus of Type I/II and Type IL cements from each plant of Classes A, AA, and AAA concrete
(null hypothesis, modulus of Type I/II = modulus of Type IL, "Similar": $\mu1=\mu2$)

Concrete Class	Cement Source	
	A/AL	C/CL
AAA	Similar	Different
AA	Similar	Different
A	Similar	Similar

Table 6.10 shows the ANOVA results of comparing the elastic modulus of Classes A, AA, and AAA concrete between plants A and C. For Classes A and AAA, the results show that difference in strength between plants was statistically significant for Type I/II but not statistically significant for Type IL. This indicates that for Classes A and AAA concrete, the difference between plants had a more significant effect on the elastic modulus of Type I/II cement than Type IL.

Table 6.10: ANOVA results for comparing the differences between plants A and C for the elastic modulus of Classes A, AA, and AAA concrete
(null hypothesis: concrete modulus of cement from plant 1 = concrete modulus of cement from plant 2, "Similar": $\mu1=\mu2$)

Concrete Class	Cement Type	
	Type I/II	Type IL
AAA	Different	Similar
AA	Similar	Different
A	Different	Similar

87

6.2.3 Splitting tensile strength

Splitting tensile strength [ASTM C496, AASHTO T 198] was measured for concrete samples (4 in. x 8 in.) at 28 days of age. Figure 6.22 shows splitting tensile strength values for Class AA concrete, along with calculated values computed using ACI 363R-10 equation 6-13 in section 6.6:

$$f_{sp} = 7.4\sqrt{f'_c} \qquad \text{Equation 6.3}$$

where:

- f_{sp} = splitting tensile strength (psi)
- $f_c{}'$ = compressive strength (psi)

The splitting tensile strength, f_{ct} , was related to the modulus of rupture, f_r , in ACI 318-95 with the following statement: *"f_r shall be modified by substituting $f_{ct}/6.7$ for $\sqrt{f'_c}$"*. That same relation for splitting tensile strength is given in ACI 318-14 section 19.2.4. That substitution results in the following, traditional relation for the splitting tensile strength:

$$f_{ct} = 6.7\sqrt{f'_c}$$

Oluokun et al. (1991) researched "Splitting Tensile Strength and Compressive Strength Relationship at Early Ages"; they recommend that f_{ct} equal to $0.584*(f_c{}')^{0.79}$ for $f_c{}'$ greater than 6000 psi, which applies to AA and AAA concrete in this current research. Results showed that the Oluokun et al. relation gave calculated results about equal to $7.4\sqrt{f'_c}$.

Because the current AASHTO Bridge Design Specifications (2016), and recent research suggested tensile strength be about $7.4\sqrt{f_c'}$, that relation was used for comparison to experimentally determined spilt tensile strengths (Figure 6.22).

No statistically significant differences were observed between Type I/II and Type IL cements for Class AA concrete.
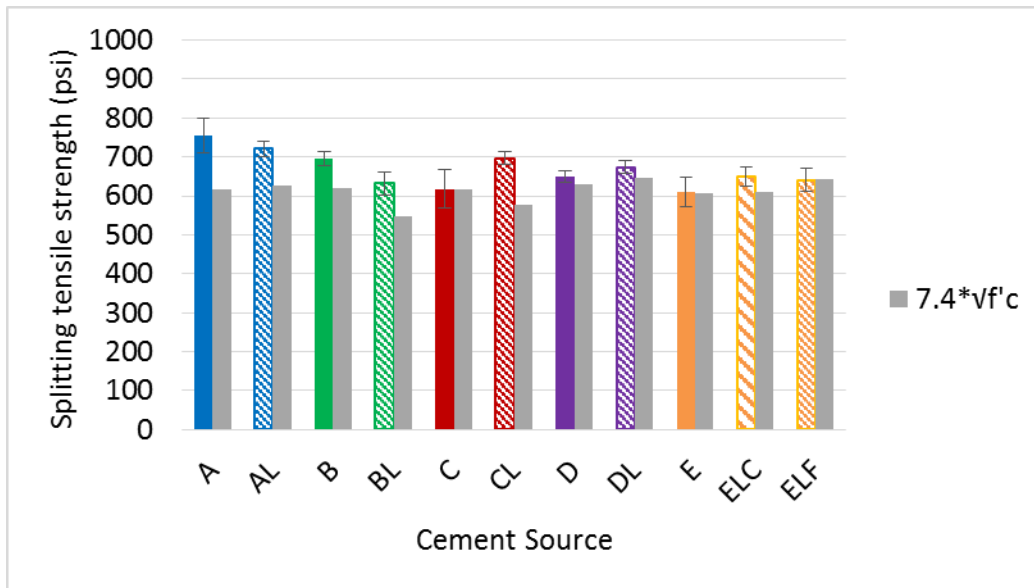
Figure 6.22: Splitting tensile strength of Class AA concrete

Figure 6.23 shows a scatter plot of calcite content vs. the splitting tensile strength of Class AA concrete at 28 days. After applying a linear regression best fit line, it can be that there is no relation between the calcite content and the splitting tensile strength. The calculated values obtained using ACI's equation under-estimated the values for concretes made with Type I/II by an average of 8% and for concretes made with Type IL cement by an average of 10%.
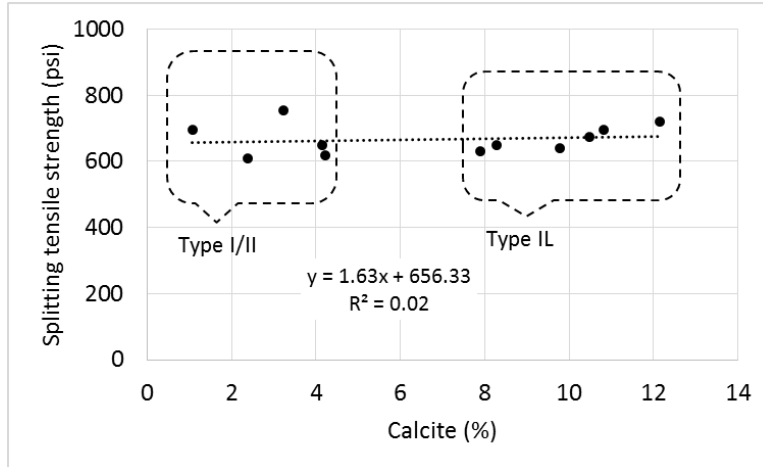
Figure 6.23: Effect of calcite content on the splitting tensile strength of Class AA concrete

Figure 6.24 shows the effect of average particle size of cement on the splitting tensile strength of Class AA concrete. The results show that larger particle size (i.e., lower fineness) leads to lower elastic modulus for Type I/II and Type IL cements. The slope of Type I/II cement is 115% steeper than that of Type IL cement, indicating a more significant effect of particle size on the splitting tensile strength of Type I/II cement. However, low R^2 values indicate that other factors (such as fineness and chemical composition) also contribute to the observed behavior.

(a) Type I/II   (b) Type IL
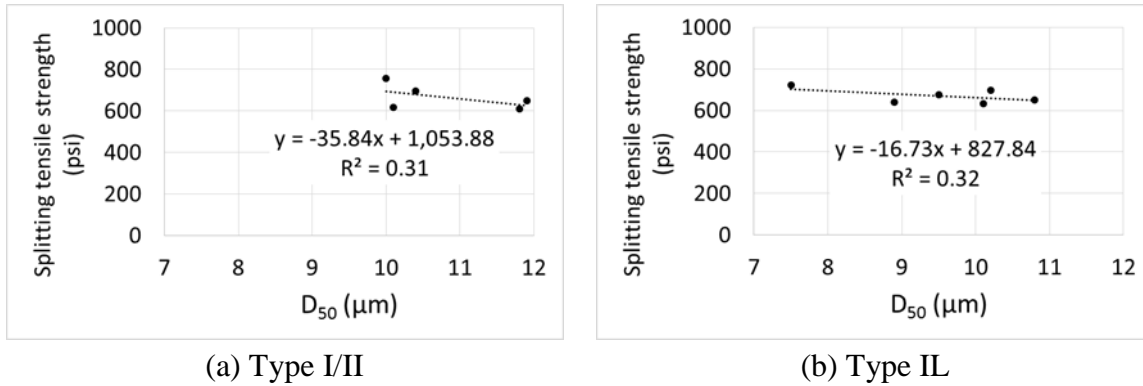
Figure 6.24: Effect of average particle size of cement on the splitting tensile strength of Class AA concrete

Analysis of variance (ANOVA) was conducted to investigate the statistical significance of the difference in values of the tensile strength of Type I/II and Type IL cement from each plant. The null hypothesis was that average strength of Type I/II and Type IL are similar ($\mu 1=\mu 2$). A summary of the results for Class AA concrete is shown in Table 6.11. Accepting the null hypothesis indicates that there is no statistical significance in the difference between the tensile strength of Type I/II and Type IL cement while rejecting the null hypothesis indicates that there is a significant statistical difference between the tensile strength of Type I/II and Type IL cement.

Table 6.11: ANOVA results for comparing Type I/II and Type IL cements from each plant for the tensile strength of Class AA concrete
(null hypothesis, tensile strength with Type I/II = tensile strength with Type IL, "Similar": $\mu 1=\mu 2$)

Cement Source					
A/AL	B/BL	C/CL	D/DL	E/ELC	E/ELF
Similar	Different	Similar	Similar	Similar	Similar

The results showed that there was no statistical difference between the tensile strength of Type I/II cement and Type IL from most plants. In addition to that, the authors hypothesized that there are more differences between Plant producers than there are between Type I/II and Type IL from the same plant.

Table 6.12 shows the ANOVA results of comparing the splitting tensile strength values of Class AA concrete among different plants. The results show that difference in tensile strength among all 5 plants was statistically significant for Type I/II and Type IL cement. This indicates that the source of the cement has a more significant effect on the splitting tensile strength than the type of cement.

Table 6.12: ANOVA results for comparing the differences among all 5 plants for the tensile strength of Class AA concrete
(null hypothesis: concrete tensile strength with cement from plant 1 = concrete tensile strength with cement from plant 2, "Similar": $\mu 1 = \mu 2$)

Cement Source	
Type I/II	Type IL
Different	Different

Figure 6.25 and Figure 6.26 show the splitting tensile strength using cements from plants A and C for Class AAA and Class A concrete, respectively. The results show that Type I/II and Type IL showed relatively similar values for both concrete Classes.
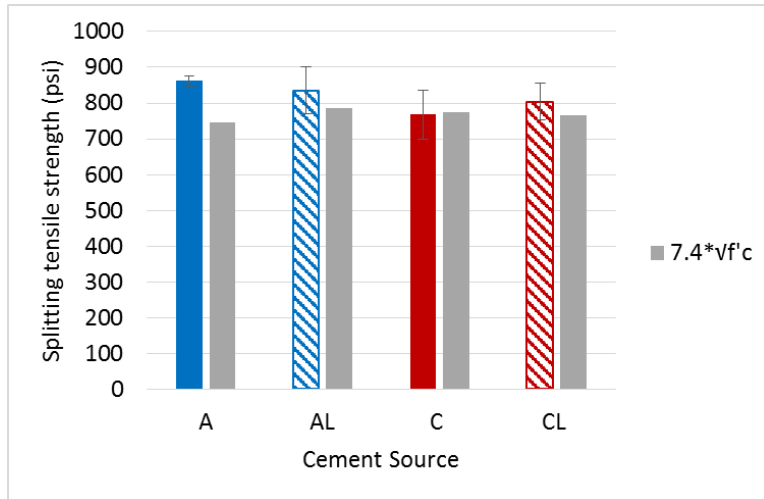
Figure 6.25: Splitting tensile strength of Class AAA concrete
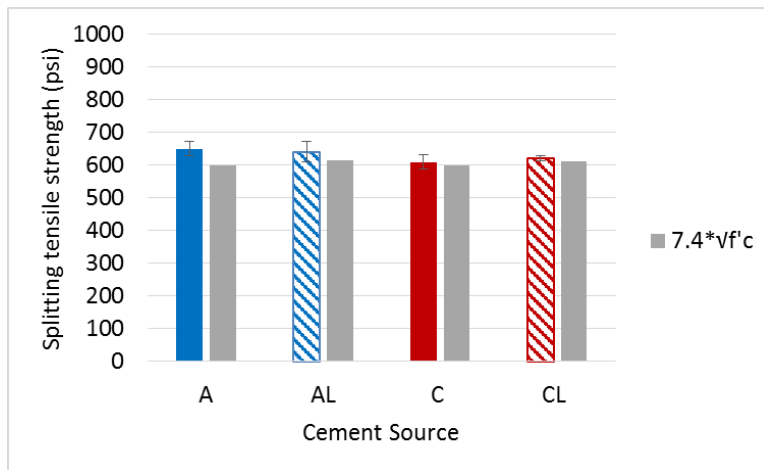
Figure 6.26: Splitting tensile strength of Class A concrete

Figure 6.27 and Figure 6.28 show scatter plots of calcite content vs. the tensile strength of concrete Classes AAA and A, respectively, tested at 28 days. After applying a linear regression best fit line, it can be seen that there is no relation between the calcite content and the splitting tensile strength.
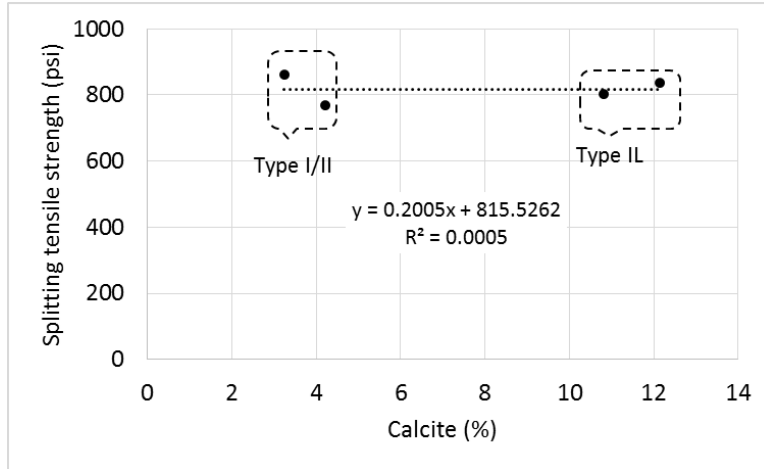
Figure 6.27: Effect of calcite content on splitting tensile strength of Class AAA concrete
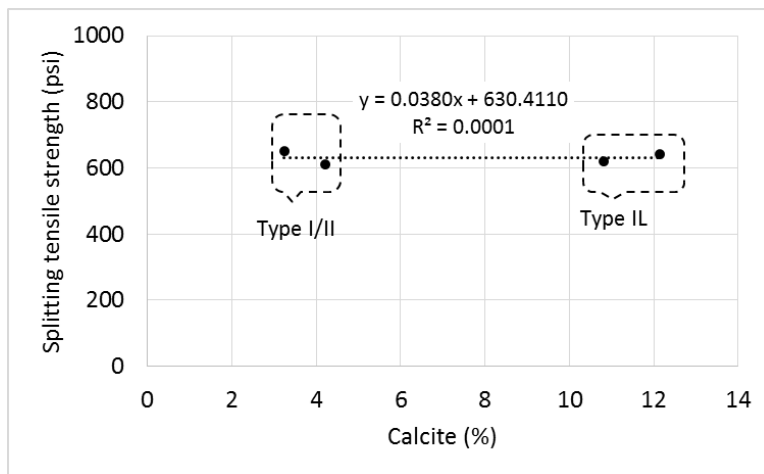
Figure 6.28: Effect of calcite content on splitting tensile strength of Class A concrete

Table 6.13 shows ANOVA results for all three concrete Classes. The results show that the differences between Type I/II and Type IL were not statistically significant for all concrete Classes.

Table 6.13: ANOVA results for comparing tensile strength of Type I/II and Type IL cements from each plant of Classes A, AA, and AAA concrete
(null hypothesis, concrete tensile strength with Type I/II = concrete tensile strength with Type IL, "Similar": $\mu 1 = \mu 2$)

Concrete Class	Cement Source	
	A/AL	C/CL
AAA	Similar	Similar
AA	Similar	Similar
A	Similar	Similar

Table 6.14 shows the ANOVA results of comparing the splitting tensile strength of Classes A, AA, and AAA concrete among different plants. For Classes A and AAA, the results show that difference in strength between plants were not statistically significant.

Table 6.14: ANOVA results for comparing the differences between plants for the splitting tensile strength of Classes A (plants A and C), AA (plants A to E), and AAA (plants A and C) concrete
(null hypothesis: concrete tensile strength with cement from plant 1 = concrete tensile strength with cement from plant 2, "Similar": $\mu 1 = \mu 2$)

Concrete Class	Cement Type	
	Type I/II	Type IL
AAA	Similar	Similar
AA	Different	Different
A	Similar	Similar

6.2.4 Mechanical properties conclusions (Concrete Class)

Figure 6.29 and Figure 6.30 summarize the compressive strength values of Classes A, AA, and AAA concrete, for plants A and C, respectively.
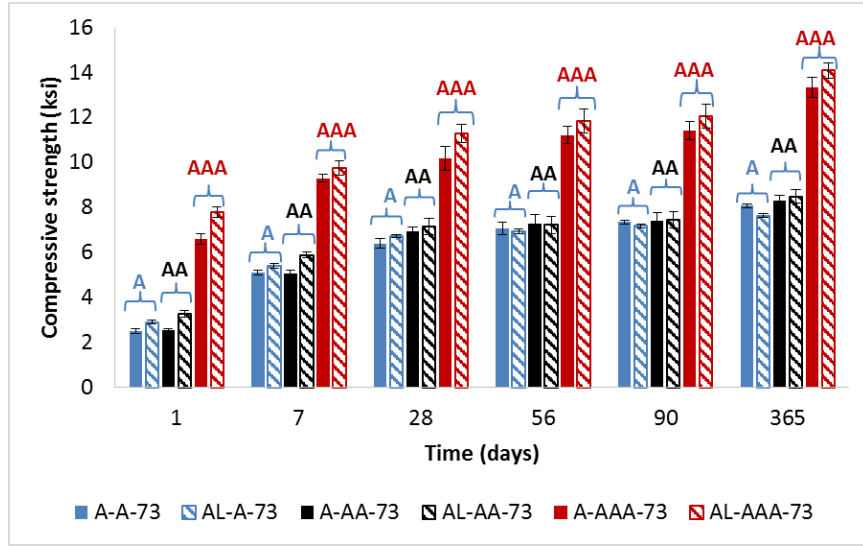
Figure 6.29: Compressive strength of Classes A, AA, and AAA concrete using Type I/II and Type IL cements from Plant A
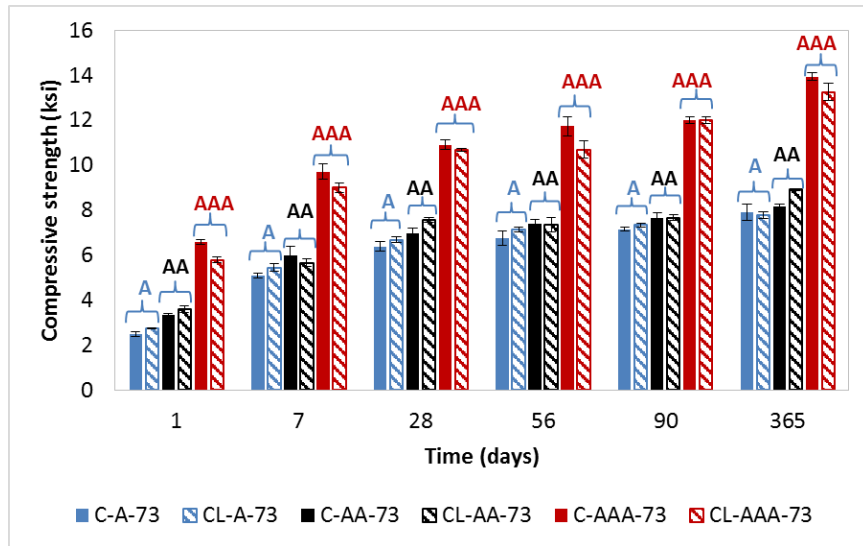
Figure 6.30: Compressive strength of Classes A, AA, and AAA concrete using Type I/II and Type IL cements from Plant C

The effects of several parameters on the compressive strength were investigated. It was found that the higher calcite content, the greater the compressive strength. Also, it was found that higher fineness of Type IL cement led to greater strength.

The effect of Type IL cement on the strength varied in different concrete Classes. It was found that the higher the concrete Class (i.e., higher cement factor and lower w/b ratio), the greater the effect of Type IL cement on the strength.

For Class A concrete, no statistically significant differences were found between use of Type I/II and Type IL cements. Also, for Class A concrete, the difference in strength among cement producers was not statistically significant.

For Class AA concrete, the difference in strength of fine-grade Type IL cement and Type I/II cement was significant while the difference in strength between coarse-grade Type IL cement and Type I/II was not significant. Also, for Class AA concrete, the difference in strength among cement producers was statistically significant.

For Class AAA concrete, the effect of Type IL cement was more significant than the other two Classes. Type IL cement led to lower strength (when having similar fineness to Type I/II). Higher fineness of Type IL cement increased the strength and resulted in statistically insignificant differences with Type I/II cement.

Figure 6.31 shows a comparison of the elastic modulus values of Classes A, AA, and AAA.
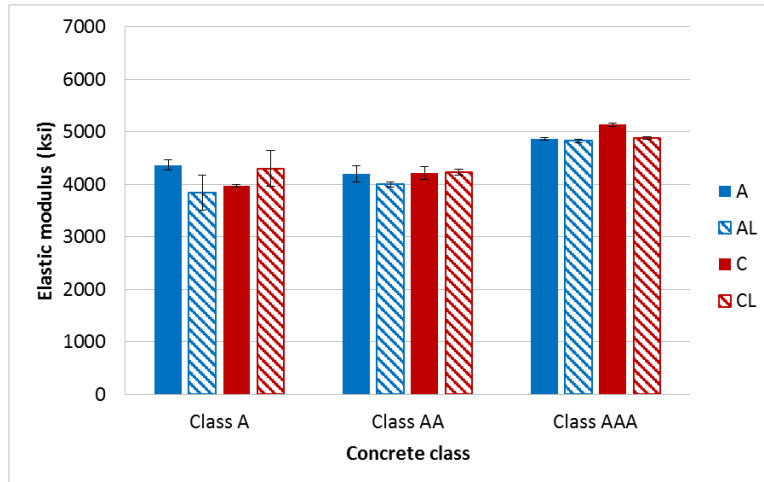
Figure 6.31: Elastic modulus values of Classes A, AA, and AAA concrete

The effect of several parameters on the elastic modulus was investigated. For Class AA concrete, it was found that the higher the calcite content, the higher the elastic modulus. However, for Classes A and AAA concrete, it was found that the higher the calcite content, the lower the elastic modulus. Also, it was found that concretes with higher fineness of Type IL cement showed greater elastic modulus. In general, the elastic modulus followed the trends of the compressive strength.

The effect of Type IL cement on the elastic modulus varied in different concrete Classes. For the finer Type IL cement (AL), the elastic modulus was similar for all three concrete Classes. However, for plant C (where the average particle size of Type I/II and Type IL were similar), cement CL resulted in a lower elastic modulus than C for Class AAA concrete while cement CL resulted in a higher elastic modulus for Class A concrete. The effect of nucleation was more dominant for Class A (lower cement factor and higher *w/b* ratio) while the dilution effect was more dominant for Class AAA concrete (higher cement factor and lower *w/b*).

For Class AA concrete, the finer Type IL cement (ELF) resulted in higher elastic modulus values than Type I/II (E) and the coarser Type IL from the same source (ELC). Also, the variation in results showed that the source of the cement had a more significant effect on the elastic modulus than the type of cement for this Class of concrete.

Regarding tensile strength, Figure 6.32 shows a comparison of the splitting tensile strength values of Classes A, AA, and AAA.
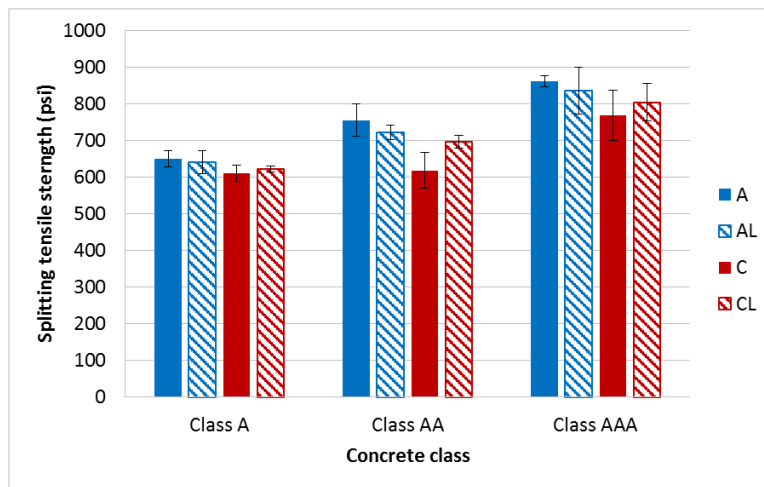
Figure 6.32: Splitting tensile strength values of Classes A, AA, and AAA concrete

The effect of several parameters on the splitting tensile strength was investigated. It was found that as the calcite content was increased, the splitting tensile strength slightly increased. Also, it was found that higher fineness of Type IL cement led to greater splitting tensile strength.

The effect of Type IL cement on the strength was similar in different concrete Classes. It was found that the effect of Type IL cement on the splitting tensile strength was not statistically significant for Class A, AA, and AAA concretes.

99

For Class AA concrete, the difference in splitting tensile strength values of Type IL cement among cement producers was statistically significant, indicating the source of the Type IL cement had a more significant effect on the splitting tensile strength values than the type of cement.

A general conclusion is that the behavior of Type IL cement differs in different w/b and cement content. As was discussed earlier, the difference was enhanced with low w/b and high cement factor.

6.3 Drying shrinkage results

Drying shrinkage prisms (ASTM C157 [57]) were lime water bath cured for 28 days, and then drying was initiated; shrinkage was measured at 4 days, 7, days, 14 days, 4 weeks, 8 weeks, 16 weeks, 32 weeks, and 1 year. Another group of samples was only lime water bath cured for 7 days, and then drying was measured at the same drying times mentioned before (Alabama DOT Standard Specifications for Highway Construction, Section 501).

The results show that higher calcite content and higher fineness of the cement resulted in higher shrinkage values. The results also showed that the shorter period of curing lead to higher drying shrinkage with the finer limestone cements.

The magnitudes of drying shrinkage were different for the three different Classes of concretes studied: Classes A, AA, and AAA. Extensive measurements were made using Class AA concrete while more cursory studies were conducted using Classes A and AAA.

6.3.1 Class AA concrete

Drying shrinkage was measured for Class AA concrete mixes made with Type I/II and Type IL cements from plant A to E. Samples were cured for 28 days in a saturated lime-saturated water bath (ASTM C157). After that, the concrete prisms were taken out to dry at 73 °F. The strain values were computed based on the length of the prism measured immediately after being removed from the lime-water bath.

Figure 6.33 shows the drying shrinkage values (ASTM C157) of Class AA concrete made with Type I/II and Type IL cements from Plants A to E and cured at 73 ºF. For Plant E, two Type IL cements with different fineness were provided. The coarse grade Type IL cement was labelled ELC, while the fine grade Type IL cement was labeled ELF.

The results show that the finer Type IL cements, i.e. from plants A, D and E, show relatively higher drying shrinkage after 1 year (~5% to ~15%) than Type I/II cement. The coarser Type IL cements, i.e. from plants B and C, show equivalent or lower drying shrinkage than Type I/II cement at one year (~15% for plant B).
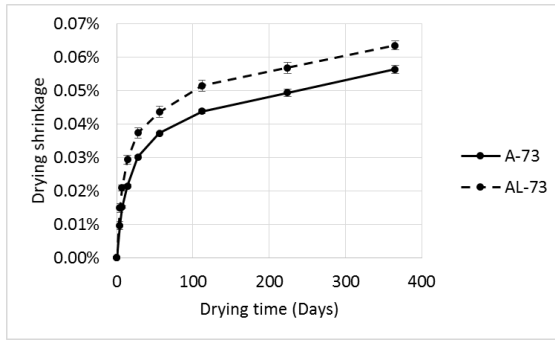
(a) Plant A
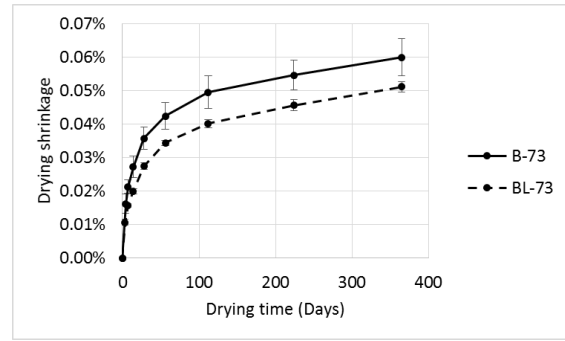
(b) Plant B
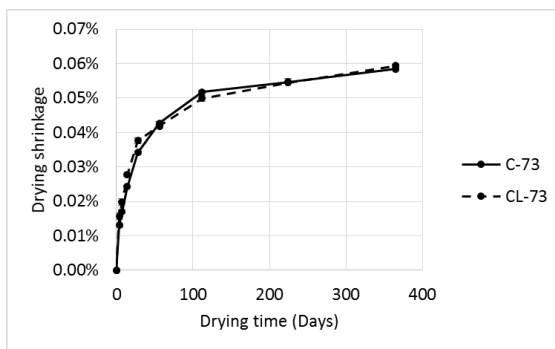
(c) Plant C
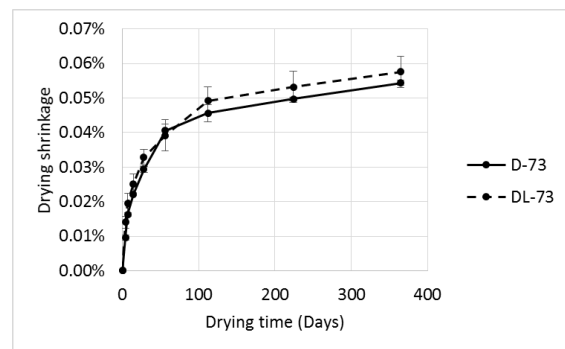
(d) Plant D
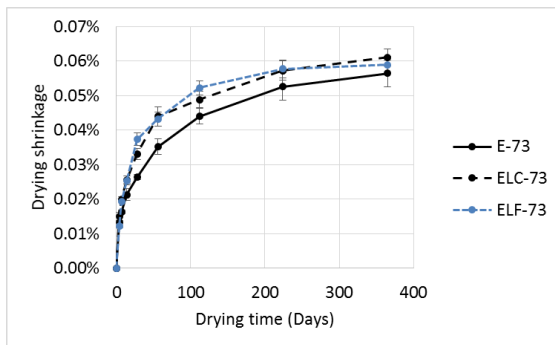
(e) Plant E

Figure 6.33: Drying shrinkage [ASTM C157] of Class AA concrete using Type I/II and Type IL cements from plants A to E and cured at 73 ℉

Figure 6.34 shows a scatter plot of calcite content vs. the drying shrinkage of Class AA concrete at 7 days, 28 days, and 1 year. After applying a linear regression best

fit line, it can be seen that the higher the calcite content, the larger the drying shrinkage. This indicates that the dilution effect due to limestone replacement is more significant on the drying shrinkage since it leaves a larger amount of free water that is able to escape through drying. Low R^2 values indicate that other factors (such as fineness and chemical composition) also contribute to the observed behavior.
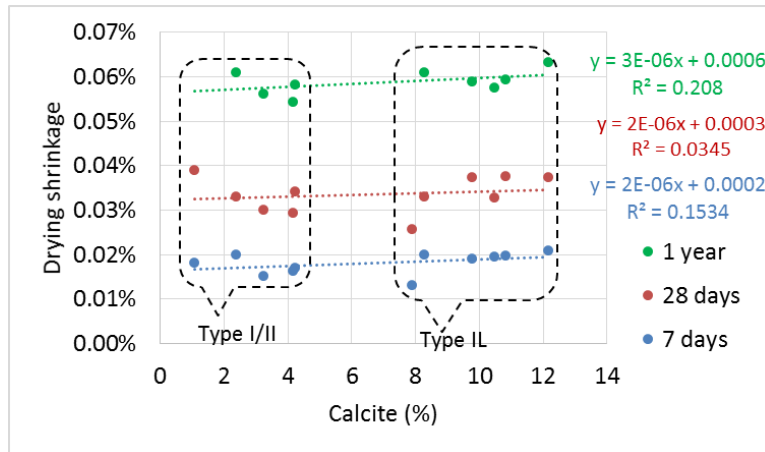
Figure 6.34: Effect of calcite content on drying shrinkage of Class AA concrete

Figure 6.35 and Figure 6.36 show scatter plots of the average particle size vs. the drying shrinkage of concrete Class AA at 7 days, 28 days, and 1 year for Type I/II and Type IL cements, respectively. For Type IL cement, larger average particle size resulted in lower drying shrinkage. However, low R^2 values indicate that other factors (such as fineness and chemical composition) also contribute to the observed behavior.
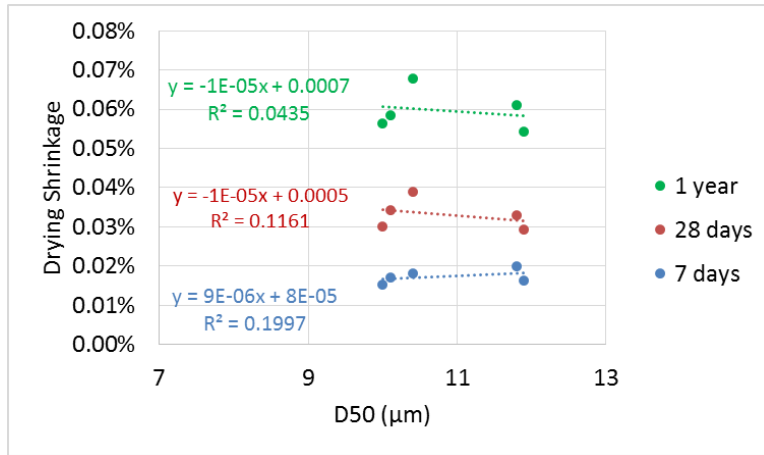
Figure 6.35: Effect of particle size on the drying shrinkage of Class AA concrete using Type I/II cement
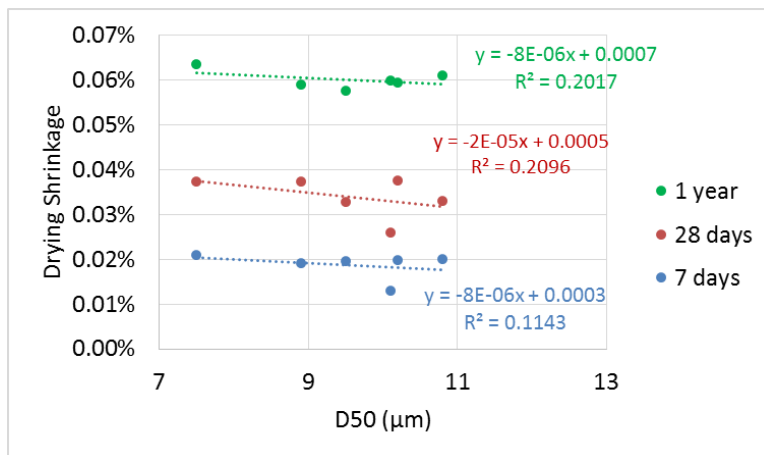
Figure 6.36: Effect of particle size on the drying shrinkage of Class AA concrete using Type IL cement

The effect of curing concrete for 28 days (per ASTM C157) on drying shrinkage was compared to curing concrete for only 7 days before start of drying at 73 °F (Alabama Specifications – Section 501). Figure 6.37 shows the effect of curing time on the drying shrinkage of Type IL and Type I/II cements from plant E. The Alabama Specifications limit of 0.04% (at 28 days of drying) is shown on Figure 6.37-b since it only applies for 7 days curing.
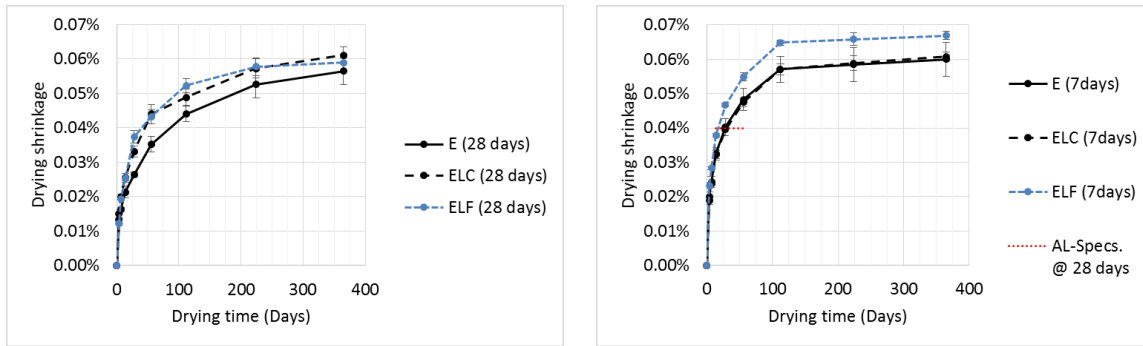
(a) 28 days curing	(b) 7 days curing

Figure 6.37: Effect of curing time on the drying shrinkage of Type I/II and Type IL cements (fine and coarse grade) from Plant E

The results show that when cured for just 7 days, the finer grade Type IL cement showed higher drying shrinkage (~10%) than Type I/II and the coarse grade Type IL cement. The coarse grade Type IL cement showed similar drying shrinkage values to Type I/II cement when cured for just 7 days. Alabama specifications for Class B concrete specifies a maximum drying shrinkage of 0.04%. The fine-grade Type IL cement (ELF) cured for 7 days did not exceed that maximum allowable shrinkage of Alabama specifications at 28 days of drying.

Note, Class B concrete in Alabama specifications is approximately equivalent to Class AA in GDOT Section 500 where Class B has a $w/b = 0.45$ and min. strength of 4 ksi at 28 days compared to a w/b of 0.445 and 3.5 ksi strength at 28 days for GDOT's Class AA concrete.

Analysis of variance (ANOVA) was conducted to investigate the statistical significance of the difference in values of the drying shrinkage of Type I/II and Type IL cement of each plant. The null (no difference) hypothesis was that average drying

105

shrinkage of Type I/II and Type IL are similar (μ1=μ2). A summary of the results for Class AA concrete is shown in Table 6.15. Accepting the null hypothesis indicates that there is no statistical significance in the difference between the shrinkage of Type I/II and Type IL cement while rejecting the null hypothesis indicates that there is a significant statistical difference between the shrinkage of Type I/II and Type IL cement.

Table 6.15: ANOVA results for comparing Type I/II and Type IL cements from each plant for the drying shrinkage of Class AA concrete
(null hypothesis, shrinkage of Type I/II = shrinkage of Type IL, "Similar": μ1=μ2)

Time	Cement Source					
	A/AL	B/BL	C/CL	D/DL	E/ELC	E/ELF
7 days	Different	Different	Different	Similar	Different	Different
28 days	Different	Different	Different	Similar	Different	Different
1 year	Different	Similar	Different	Similar	Similar	Similar

The results showed that Type IL cements from all plants (except plant D) showed statistically significant different results when compared to Type I/II from the same plant. Plant D showed similar shrinkage results for Type I/II and Type IL.

6.3.2 Class AAA concrete

Drying shrinkage was measured for Class AAA concrete mixes made with Type I/II and Type IL cements from plant A and plant C. Samples were cured for 28 days in a lime-saturated water bath [ASTM C157]. After that, the concrete prisms were taken out to dry at 73 °F.

Figure 6.38 shows the drying shrinkage results for Type I/II and Type IL cement from plant A (Cement A and AL) and plant C (cement C and CL) cured at 73 °F for Class AAA concrete.

For Class AAA concrete, cement AL (higher fineness) showed lower drying shrinkage than cement A (~10% at 1 year). For cements C and CL (similar fineness), cement C and CL showed similar shrinkage values at 1 year.

(a) Cement A/AL   (b) Cement C/CL
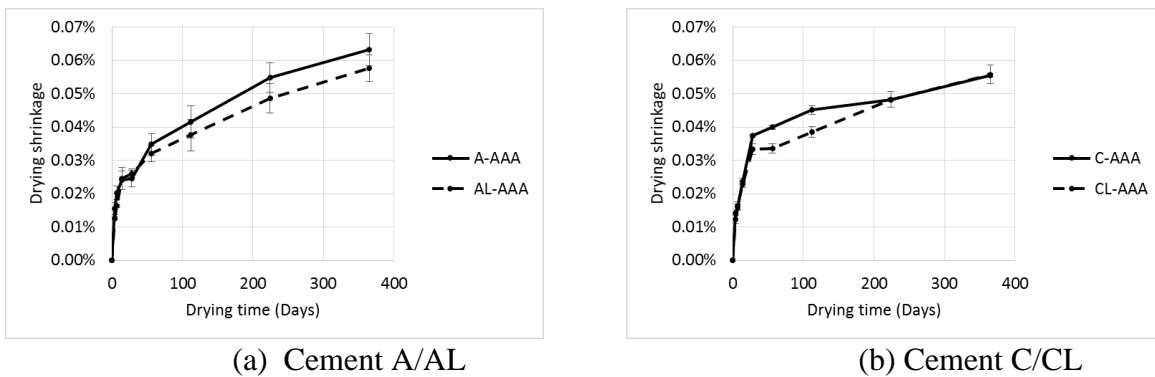
Figure 6.38: Drying shrinkage [ASTM C157] of Type I/II and Type IL cements from plants A and C with Class AAA concrete

A second group of Class AAA concrete prisms was cured for only 7 days in a lime- saturated water bath to show the effect of curing time on drying shrinkage. After curing, the concrete prisms were taken out to dry at 73 °F. Figure 6.39 shows the drying shrinkage results for concrete made with cement A/AL and C/CL and cured at 73 °F for 7 days as well as those cured for 28 days.

(a) Cement A/AL	(b) Cement C/CL
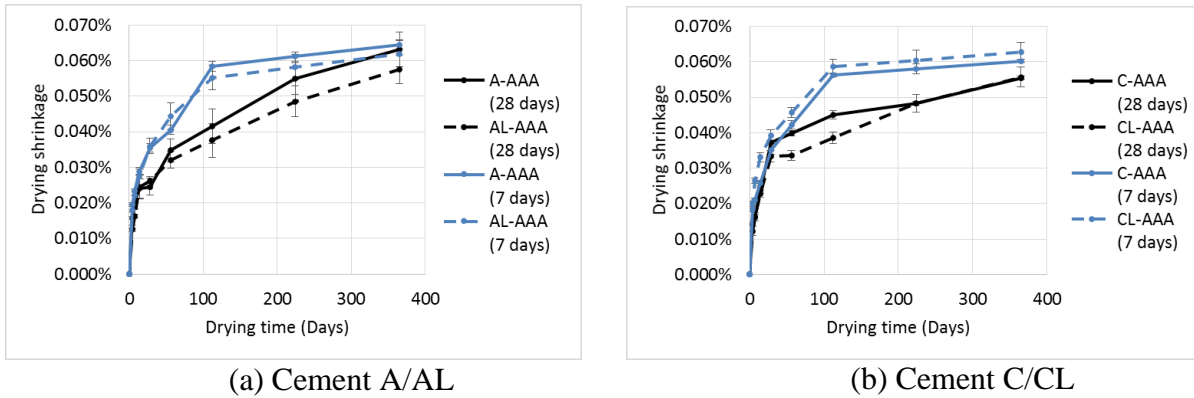
Figure 6.39: Drying shrinkage of Type I/II and Type IL cements from plants A and C cured for 7 days and 28 days with Class AAA concrete

For cements A and AL, the samples cured for 7 days showed higher drying shrinkage than samples cured for 28 days (~40% for Type I/II and ~45% for Type IL at 112 days). At one year, the difference became smaller (2% for Type I/II and 7% for Type IL). The drying shrinkage values of A and AL cured for 7 days differed by less than 5%.

For cements C and CL, the samples cured for 7 days also showed higher drying shrinkage than samples cured for 28 days (~25% for Type I/II and ~50% for Type IL at 112 days). At one year, the difference became smaller (9% for Type I/II and 12% for Type IL). The drying shrinkage values of C and CL cured for 7 days differed by less than 4%.

Analysis of variance (ANOVA) was conducted to investigate the statistical significance of the difference in values of the drying shrinkage of Type I/II and Type IL cement of plants A and C. The null (no difference) hypothesis was that average drying shrinkage of Type I/II and Type IL are similar ($\mu1=\mu2$). A summary of the results for Class AAA concrete is shown in Table 6.16. Accepting the null hypothesis indicates that

there is no statistical significance in the difference between the drying shrinkage of Type I/II and Type IL cement while rejecting the null hypothesis indicates that there is a significant statistical difference between the drying shrinkage of Type I/II and Type IL cement.

Table 6.16: ANOVA results for comparing Type I/II and Type IL cements from each plant for the drying shrinkage of Class AAA concrete
(null hypothesis, shrinkage of Type I/II = shrinkage of Type IL, "Similar": $\mu1=\mu2$)

Time	Cement source	
	A/AL	C/CL
7 days	Different	Similar
28 days	Similar	Different
1 year	Similar	Similar

For 7 days of drying, the results showed that the difference in drying shrinkage between A and AL (finer Type IL) were statistically significant. Cements and C and CL had a similar fineness and the differences in shrinkage were not statistically significant. However, at one year, both plants showed that the differences between Type I/II and Type IL cements were not statistically significant.

6.3.3 Class A concrete

Drying shrinkage was measured for Class A concrete mixes made with Type I/II and Type IL cements from plant A and plant C. Samples were cured for 28 days in a lime-saturated water bath [ASTM C157]. After that, the concrete prisms were taken out to dry at 73 °F.

Figure 6.40 shows the drying shrinkage results for Type I/II and Type IL cement from plant A (Cement A and AL) and plant C (cement C and CL) cured at 73 °F for Class A.

(a) Cement A/AL   (b) Cement C/CL
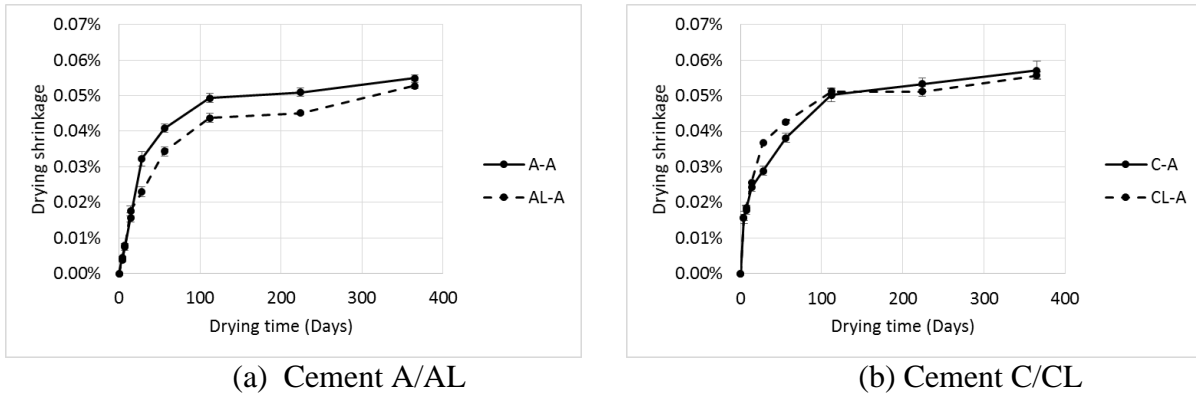
Figure 6.40: Drying shrinkage [ASTM C157] of Type I/II and Type IL cements from plants A and C with Class A concrete

For Class A concrete, cement AL showed lower drying shrinkage than cement A (5% at 1 year). Cements C and CL showed relatively similar values at most ages including one year. C and CL showed similar values at 4 days and 7 days, but CL showed higher values (10% at 56 days) from 14 days until 16 weeks (112 days), when the values converged with those of C.

A second group of Class A concrete prisms was cured for only 7 days in a lime-saturated water bath to show the effect of curing time on drying shrinkage. After curing, the concrete prisms were taken out to dry at 73 °F. Figure 6.41 shows the drying shrinkage results for concrete made with cement A/AL and C/CL and cured at 73 °F for 7 days as well as those cured for 28 days.
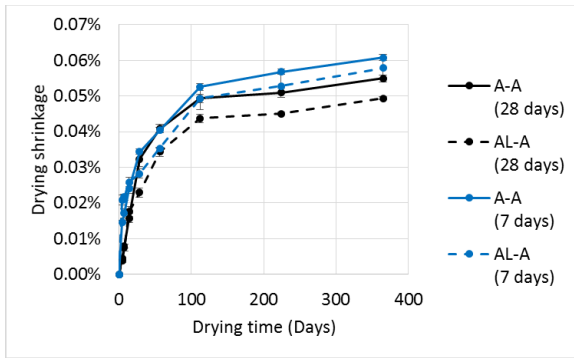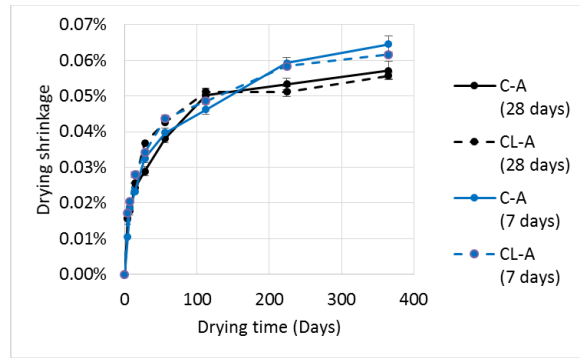
(a) Cement A/AL   (b) Cement C/CL

Figure 6.41: Drying shrinkage of Type I/II and Type IL cements from plants A and C cured for 7 days and 28 days with Class A concrete

For cements A and AL, the samples cured for 7 days showed higher drying shrinkage than samples cured for 28 days (10% at 1 year). The drying shrinkage values of A and AL cured for 7 days differed by 5% at 1 year.

For cements C and CL, the samples cured for 7 days showed higher drying shrinkage than samples cured for 28 days (12% at 1 year). The drying shrinkage values of C and CL cured for 7 days differed by 5% at 1 year. This indicates that shorter curing time results in higher drying shrinkage for this Class of concrete, but the trends between A and AL and C and CL were similar regardless of the curing time.

Analysis of variance (ANOVA) was conducted to investigate the statistical significance of the difference in values of the drying shrinkage of Type I/II and Type IL cement of plants A and C. The null (no difference) hypothesis was that average drying shrinkage of Type I/II and Type IL are similar ($\mu1=\mu2$). A summary of the results for Class AAA concrete is shown in Table 6.17. Accepting the null hypothesis indicates that

111

there is no statistical significance in the difference between the drying shrinkage of Type I/II and Type IL cement while rejecting the null hypothesis indicates that there is a significant statistical difference between the drying shrinkage of Type I/II and Type IL cement.

Table 6.17: ANOVA results for comparing Type I/II and Type IL cements from each plant for the drying shrinkage of Class A concrete
(null hypothesis, shrinkage of Type I/II = shrinkage of Type IL, "Similar": $\mu1=\mu2$)

Time	Cement source	
	A/AL	C/CL
7 days	Similar	Similar
28 days	Different	Different
1 year	Different	Similar

For 7 days of drying, the results showed that the difference in drying shrinkage between Type I/II and Type IL cements from both plants were not statistically significant. However, at one year, cement A and AL showed statistically significant differences while cement C and CL showed differences that were not statistically significant. This indicates that finer limestone cement has a more significant effect on the long-term drying shrinkage of concrete with higher w/c (i.e. Class A).

Figure 6.42 and Figure 6.43 show scatter plots of the *w/b* vs. the drying shrinkage of concrete at 7 days, 28 days, and 1 year for Type I/II and Type IL cements, respectively.
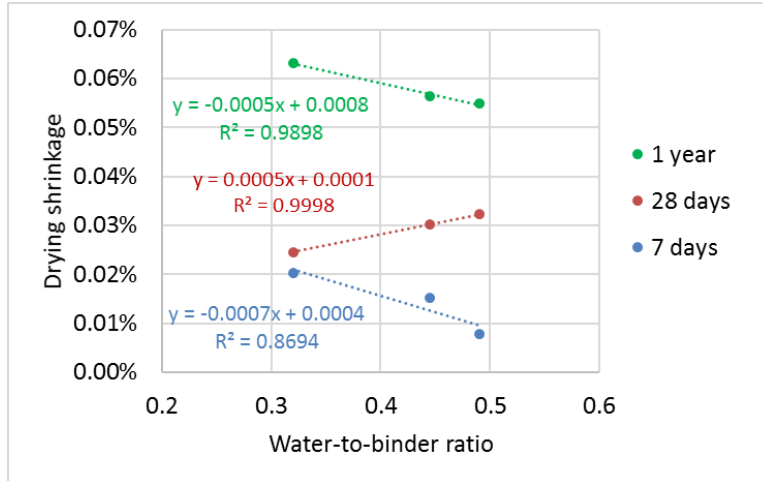
Figure 6.42: Effect of *w/b* on drying shrinkage of concrete using Type I/II cement
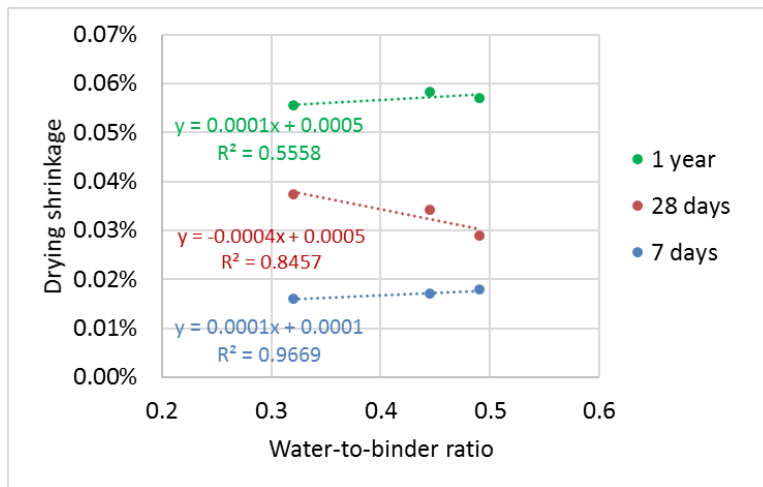
Figure 6.43: Effect of *w/b* on drying shrinkage of concrete using Type IL cement

The results show different behavior between Type I/II and Type IL cements. Higher values of *w/b* of concrete made with Type I/II cement resulted in higher drying shrinkage at 28 days but lower shrinkage values at 7 days and at 1 year. However, higher values of *w/b* of concrete made with Type IL cement resulted in lower drying shrinkage at 28 days but higher shrinkage values at 7 days and at 1 year. These conflicting results may be a result of the combined effects of other parameters on the drying shrinkage such as calcite content and the average particle size.

6.3.4 Drying shrinkage conclusions

To summarize the drying shrinkage values of Classes A, AA, and AAA concrete,

Figure 6.44 and Figure 6.45 show the values for plants A and C, respectively.
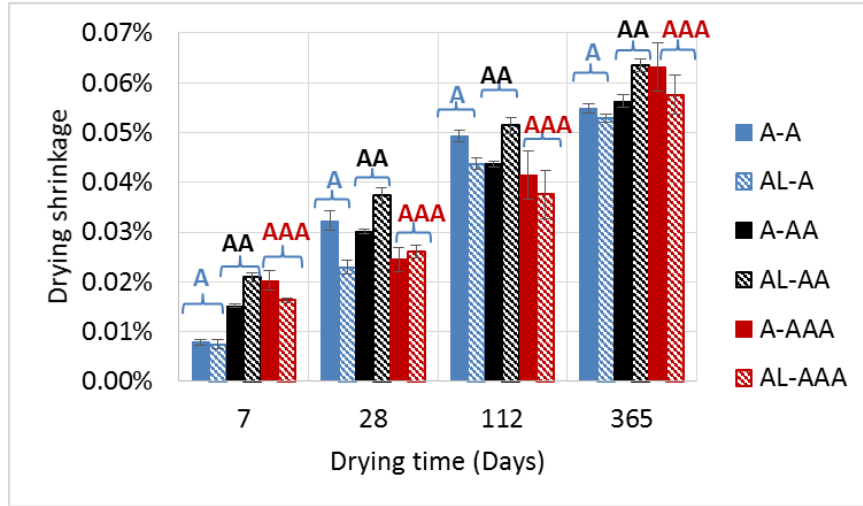
Figure 6.44: Drying shrinkage of Classes A, AA, and AAA concrete using Type I/II and Type IL cements from Plant A
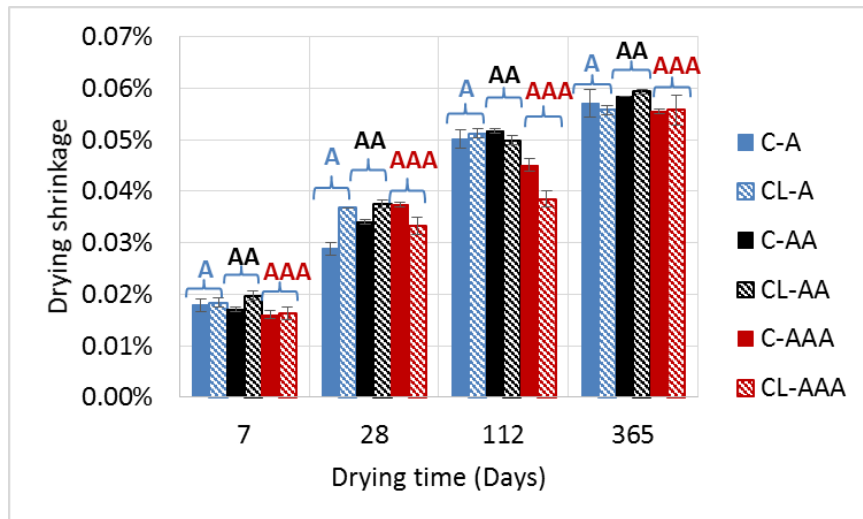
Figure 6.45: Drying shrinkage of Classes A, AA, and AAA concrete using Type I/II and Type IL cements from Plant C

The effects of several parameters on the drying shrinkage were investigated. It was found that higher fineness of Type IL cement led to higher shrinkage. At early age, Type I/II and Type IL cements showed conflicting relationships with the average particle size where finer Type I/II cements resulted in lower shrinkage while finer Type IL cements showed higher shrinkage values.

The effect of Type IL cement on the drying shrinkage varied in different concrete Classes. Type IL cement in Class AAA concrete showed lower shrinkage than Type IL in Class AA concrete. For Class A concrete (i.e. higher *w/b*), no statistically significant differences in shrinkage were found between Type I/II and Type IL cement at 7 days. However, finer limestone cement (AL) decreased the long-term drying shrinkage of this Class of concrete.

For Class AAA concrete (i.e. lower *w/b*), no statistically significant differences in shrinkage were found between Type I/II and Type IL cement at 1 year. However, finer limestone cement decreased the early age drying shrinkage of this Class of concrete.

Chapter 7. ASSESSMENT OF DURABILITY

The permeability of concrete is a key predictor of its durability, therefore, the permeability of Types I/II and IL cement concretes were measured at 56 days by the rapid chloride penetration test (ASTM C1202). For comparison, measurements were also carried out using the surface resistivity (SR) test method following AASHTO TP95-11 at 1, 3, 7, 14, 28, 56, and 90 days of hydration [86]. The results from these two indirect methods to assess permeability were compared to obtain greater insights into the influence of interground limestone on the microstructural development and long-term durability of Portland Limestone cement (PLC) concrete.

Another aspect of concrete durability is its resistance to the freezing and thawing cycles. The freezing and thawing resistance of Types I/II and IL cement concretes with and without air-entrainers were tested following ASTM C666 [87].

7.1 Materials and methods

Eleven concrete mixes were prepared with each of the Type I/II and their companion Type IL cements following the mix design explained in Chapter 5 for concrete Class AA according to Georgia Department of Transportation (GDOT) Section 500 specifications. Five 4 in. by 8 in. cylinders were cast for each mixture for use in permeability testing (RCPT and SR). After 24 hours, the cylinders were demolded, and an initial surface resistivity measurement was made on three of the specimens using a four-probed Wenner array, in accordance with AASTHO TP95-11 [88].

Measurements were made along lines drawn lengthwise at quarter-points around the circumference of the cylinders, with eight measurements being made for each

cylinder (two measurements per line), as depicted in Figure 7-1. The five samples were placed into a saturated calcium hydroxide (limewater) solution maintained at $70 \pm 3°F$. After 3, 7, 14, 28, 56, and 90 days of hydration, the surface resistivity was measured again on the same three specimens used for the 1-day measurement to obtain SR-development curves for each mix. SR values for limewater-cured specimens were multiplied by a factor of 1.1, as specified by the AASHTO provisional standard, to account for an assumed 10% decrease in pore solution resistivity caused by the limewater [89]. After 56 days of hydration, the two samples not used for resistivity testing were removed from the limewater bath, and a 2 in. disk was cut from near the top of each cylinder. The disks were vacuum-saturated for 18 ± 2 hr, and the rapid chloride permeability test was performed the following day in accordance with ASTM C1202/AASHTO T277 [90, 91].
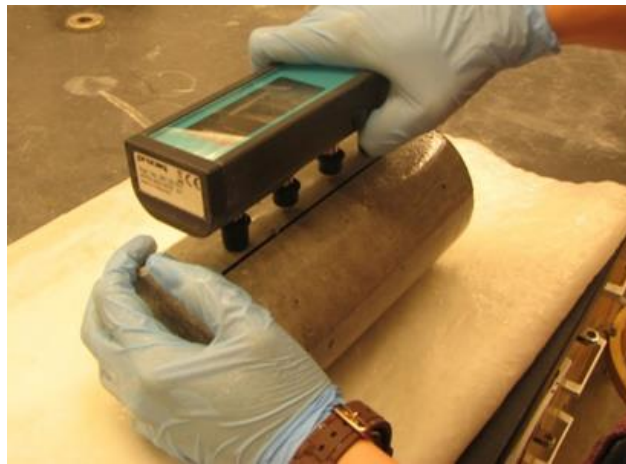
Figure 7.1: Surface resistivity test performed using four-probed Wenner array in accordance with AASHTO TP95-11.
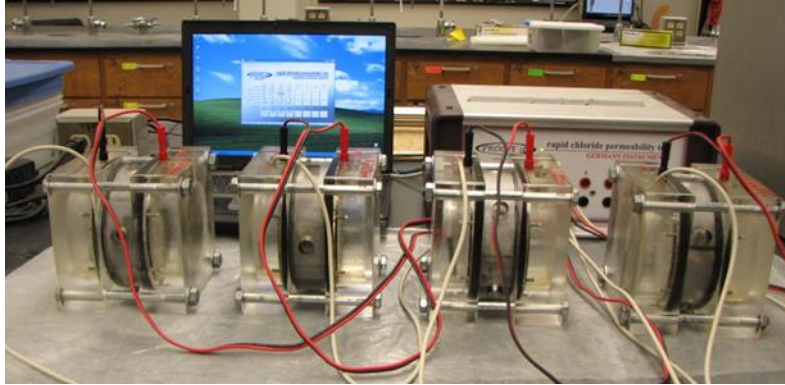
Figure 7.2: RCP test conducted in accordance with ASTM C1202/AASHTO T277.

Twelve mixes of Class AA concrete were cast for freezing and thawing resistance testing in twelve 4 by 8 in. cylinders and four 4-in square cross-section and approximately 11 ¼ in. long prisms. Four cement sources of A, AL, C, and CL and two types of air-entrainer admixtures (AEA), synthetic (A260) and organic (A14) both from Sika, chosen from GDOT qualified product list (QPL), were used. For air-entrained concrete, the dosage of AEA for each cement was adjusted to achieve the maximum allowable air content (5-7%) according to GDOT section 500 [13]. Mid-range water-reducer admixture (WRA) was used to improve the flowability to meet the 2-4 in. slump. The concrete mixes were Class AA concrete as shown before with the AEA added for air-entrained concrete.

As introducing air to concrete compromises its mechanical properties, compressive strength tests were carried out on 4 by 8 in. cylinders of air-entrained and non-air-entrained concrete at 1,7, and 28 days to evaluate if they still met the 3500 psi 28-day compressive strength, which is minimum strength for Class AA concrete required by GDOT section 500 [92]. Freezing and thawing resistance tests were carried out following

ASTM C666 method A, freezing and thawing in water, on air-entrained and non air-entrained concrete. Three concrete prisms for each mix were sent to TEC Service, Lawrenceville, GA for freezing and thawing testing. The relative dynamic modulii (RDM) were measured frequently after cycles of freezing and thawing up to 300 cycles specified by ASTM C666 and the results were reported based on the percentage of the initial RDM. Moreover, the concrete cylinders were cut and the cross sections were studied petrographically to measure the spacing factor (L bar), defined as the maximum distance in the cement paste from the periphery of an air void according to ASTM C457 [93].

7.2 Results

7.2.1 Rapid chloride permeability test

The results of the rapid chloride ion penetration tests are shown in Figure 7.3. The permeability Classifications defined by the ASTM and AASHTO standards (Table 7.1) are indicated in each figure by horizontal dashed lines. It is important to note that a lower total charge passed (which can be directly related to conductivity) indicates lower permeability concrete.

The results of the RCP test indicate that there is little difference between the electrical properties for the Type I/II and Type IL concretes. Slight reductions in total charge passed were observed for the more finely ground cements from sources D and E, but the cements from sources A, B, and C all yielded concretes having similar charges passed – suggesting similar permeabilities – to one another.

Table 7.1: Permeability Classifications for concrete tested according to the ASTM
C1202/AASHTO T277 rapid chloride penetration test.

Classification	Charge Passed (Coulombs)
High	> 4000
Moderate	2000-4000
Low	1000-2000
Very Low	100-1000
Negligible	< 100
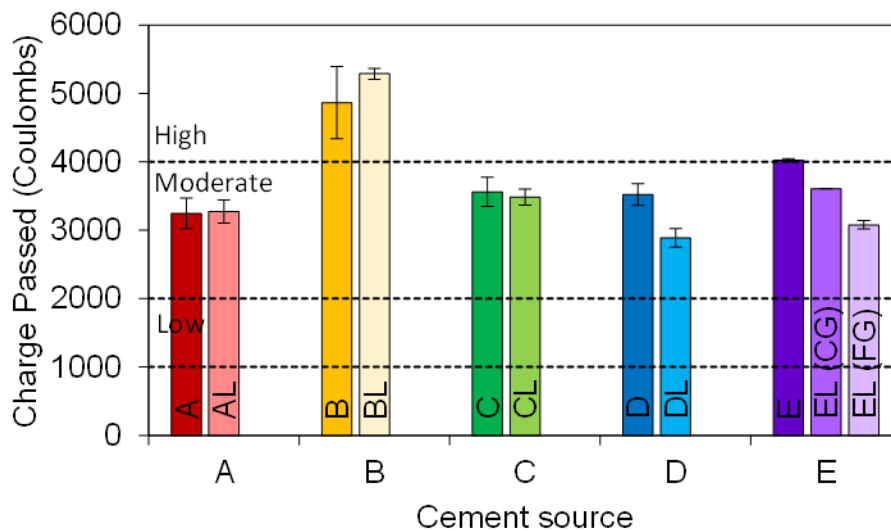
Figure 7.3: Total charge passed by RCPT for concretes A-E, after 56 days of hydration.
Error bars indicate the range of values obtained for each mixture.

7.2.2 Surface resistivity test

The evolution of surface resistivity over the first 90 days of hydration is shown in

Figure 7.4 for the 11 concrete mixtures. To aid in the interpretation of the results,

horizontal dashed lines are shown in all figures to indicate the permeability Classifications defined by the standard (Table 7-2).

Approximately 4 months after the first samples had been cast; the temperature of the curing room was reduced by an estimated 6-8°F while maintenance was performed on the thermal control unit. While most of the specimens tested had either reached 90 days of age by that time or had not yet been cast, the 56 and 90 day measurements for mix CL and the 90 day measurements for mix EL (FG) were performed under these lower temperature conditions. It was estimated based on an empirically-derived equation by Castellote, et al., [94] that such a temperature reduction increases SR values by approximately 10%;[2] the three affected SR values were therefore reduced by 10% to compensate for the thermal effect, and the adjusted values are reflected in Figure 7.4.

Table 7.2: Permeability Classifications for concrete tested according to the
AASHTO TP95 surface resistivity test.

Classification	SR limits (kOhm-cm)
High	< 12
Moderate	12 – 21
Low	21 – 37
Very Low	37 – 254
Negligible	> 254

---

[2] Castellote, et al., conducted temperature-dependence studies on 14 saturated concrete and mortar mixtures with similar w/b (0.45-0.5) to the mixtures considered in this study. They found that, for tests conducted below 25°C (77°F), the thermal adjustment factor, α, is approximately:

$$\alpha \approx (1 + 0.664 \cdot \Delta T - 0.825 \cdot W_g \cdot \Delta T)^{-1}$$

where ΔT is the temperature change (in °C) and W_g is the fraction of aggregates in the solids (cement + SCMs + aggregates). For $\Delta T = 4$°C and $W_g = 0.832$, $\alpha \approx 1.10$.
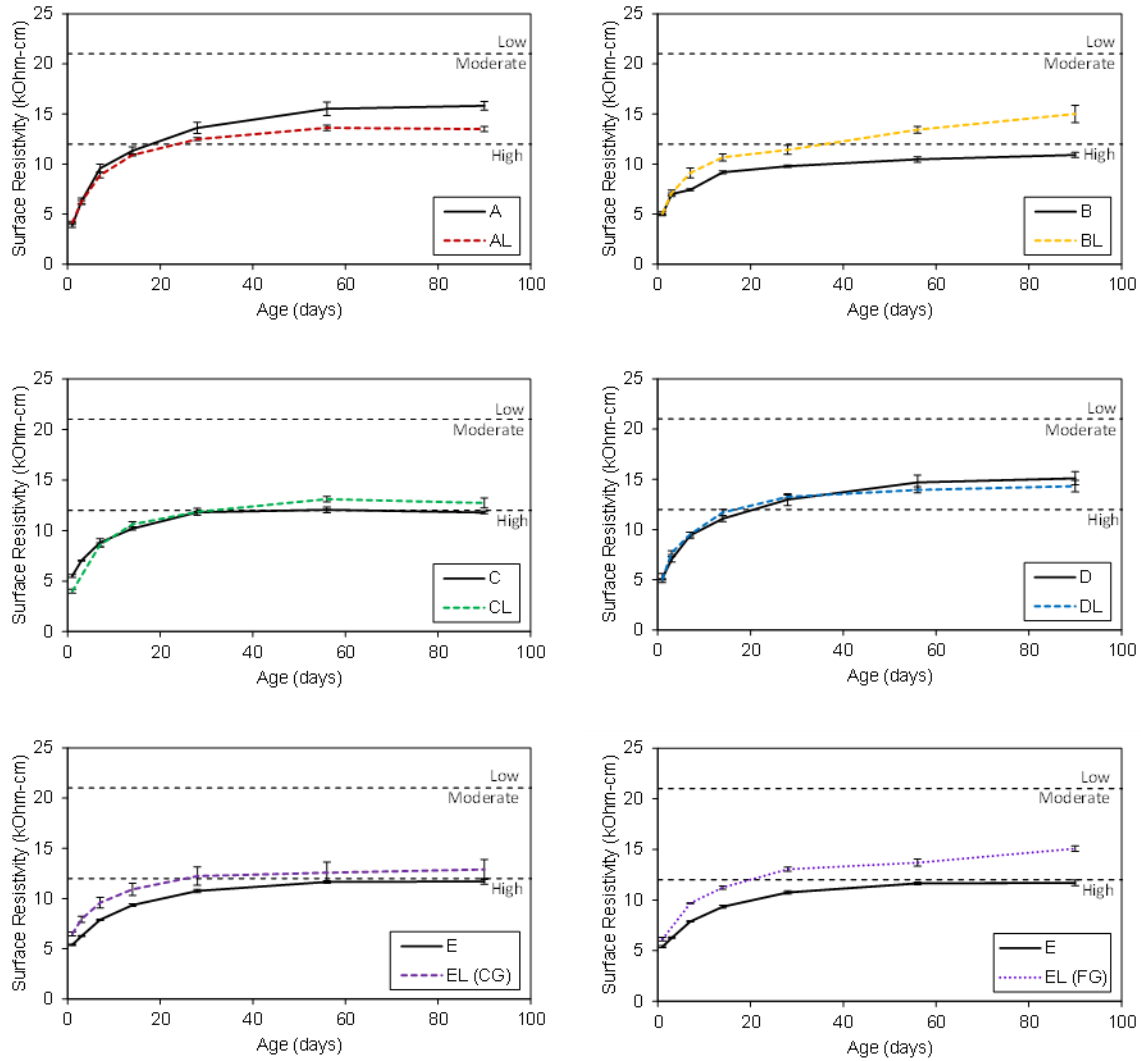
Figure 7.4: Surface resistivity measurements over the first 90 days of hydration for neat concretes A-E. Permeability Classifications, as specified by AASHTO TP95-11, are indicated by horizontal dashed lines in each figure.

In general, the 23 mixtures each show increasing resistivity with time as the primary hydration of the cement reduces and refines the porosity. While the neat OPC and PLC mixtures all tend to reach a plateau after about 28 days of hydration which is consistent with their slower rates of hydration and microstructural development at 28 days and which suggests continued microstructural development at later ages.

122

Comparing Type I/II and Type IL mixtures to one another, no consistent trends were observed based on limestone dosage or fineness. Cement AL, which had shown the greatest increases in hydration rate relative to its Type I/II counterpart, actually yielded consistently lower concrete surface resistivity values at all ages, by comparison. At 90 days, mix AL exhibited an SR reduction of 15% compared to mix A – greater, even, than the 8% dilution of the cement by the incorporation of limestone filler. By contrast, cement BL, which had shown reduced degrees of hydration compared to its Type I/II counterpart, was observed to yield concrete with consistently higher surface resistivity at all ages. At 90 days, it exhibited a 37% increase in SR relative to mix B. Cements from the other three sources also yielded inconsistent results based on limestone dosage and cement fineness, with the cements from source E producing the only mixtures to consistently show increases in degree of hydration, early-age shrinkage, and surface resistivity. Such generally inconsistent behavior suggests that the surface resistivity measurements may be additionally affected by changes to the pore solution chemistry caused by the limestone inclusion, and that therefore the permeability Classifications indicated in Table 7.2 may not be applicable to PLC systems.

Comparison of the 56 day SR and RCPT results to one another (Figure 7.5), show that the two tests have a nearly perfect inverse relationship to one another, as would be expected given the inverse relationship of conductivity (on which RCPT depends) and resistivity (measured directly by the SR test). Similar inverse relationships have been found by other authors [36, 95] although the line of best fit varies among studies. The results of this particular study are consistent with those obtained by Chini, et al.[96] on which the AASHTO TP95 guidelines for permeability Classification are based. Since the

two test methods yield consistent results, it is proposed that factors that affect the interpretation of results for the SR test (e.g., pore solution chemistry) equally affect the interpretation of results for the RCP test, such that the low total charges passed by mixes may be due to a combination of microstructural and pore solution effects [36, 95] which must also be de-coupled. Despite the similar results and interpretation of RCPT and the SR test, the SR test is a nondestructive test that can be carried out on the cylinders that can be used for other tests after 56 days (such as compressive test) while RCPT is a destructive test requires cutting cylinders to the exact size disc.
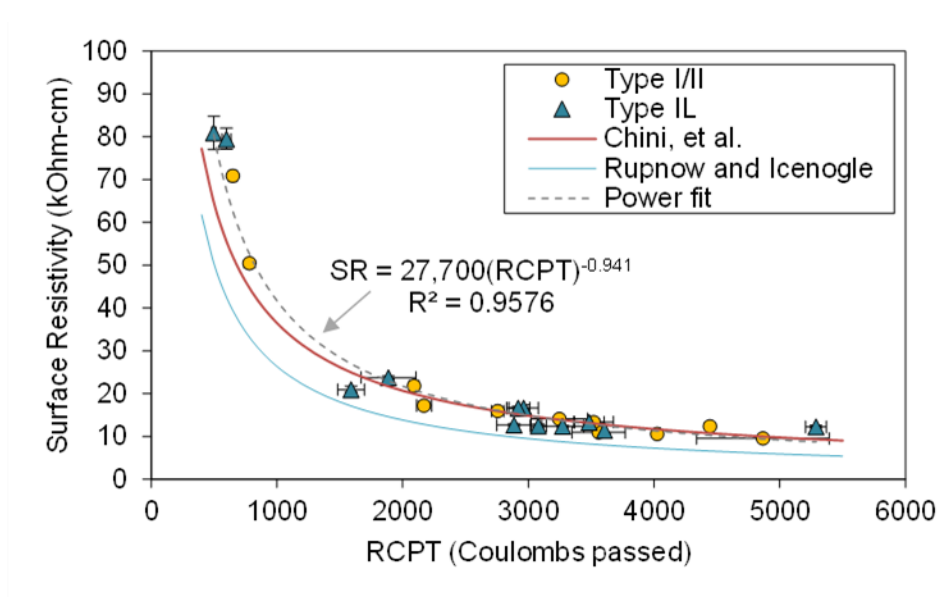
Figure 7.5: Correlation between SR and RCPT results. Fits obtained by Chini, et al., [96] and Rupnow and Icenogle [97] are shown for comparison.

7.2.3 Freezing and thawing resistance

The fresh concrete properties for air-entrained and non air-entrained concrete are shown in Table 7.3. It can be seen that with the same dosage of air-entrainer, a lower air content was attained for Type IL cement concrete compared to that of Type I/ II cement

124

concrete. The lower air content of Type IL cement concrete can be due to the finer particle sizes and higher surface area of Type IL cement (Table 3.3), a trend which was observed in previous studies as well [98]. The same WRA dosage was used for Types I/II and IL cements from the same clinker (A, AL or C and CL) and similar slumps were measured.

Table 7.3: Fresh concrete properties of air-entrained and non-air-entrained concrete

	Cement	AEA dosage (fl. oz. /100 lbs)	Water Reducer dosage (fl. oz./ 100 lbs)	Air (%) Pressure method	Slump (in.)
No Air-entrainer	A	0	12	2.6	7.75
	AL	0	12	3.3	7.25
	C	0	8	3.0	2.75
	CL	0	8	2.4	2.5
A260 [3]	A	1	6	7.5	2.8
	AL	1	6	6.0	2.5
	C	0.6	8	7.8	3.9
	CL	0.6	8	5.7	3.8
A14 [4]	A	1.5	7	7.9	4.25
	AL	1.5	7	7.5	4.5
	C	1.5	7	6.6	4
	CL	1.5	7	6.2	4.2

Freezing and thawing resistance of air-entrained and non air-entrained concrete in terms of percentage relative dynamic modulus (RDM) is shown in Figure 7.6. The solid horizontal line shows the minimum RDM of 60% required by ASTM C666 [87]. It can be seen that while none of the non-air-entrained concrete could pass the minimum retaining

[3] A260 is a synthetic air-entrainer
[4] A14 is an organic-based air-entrainer

of 60% RDM, all air-entrained concrete showed RDM of higher than 80% after 300 cycles of freezing and thawing. The freezing and thawing results show that although Type IL cement concrete exhibits a lower air content, its freezing and thawing resistance is similar to that of Type I/II cement concrete (Figure 7.6). The petrographic analysis for spacing factor measurements, shown as L bar, for air-entrained concrete is shown in Table 7.4. No direct relation between the L bar measurements and the RDM (%) was observed but the spacing factor shown as L bar for all air-entrained concrete is lower than 200µm which is the maximum suggested by ASTM C457[93] .
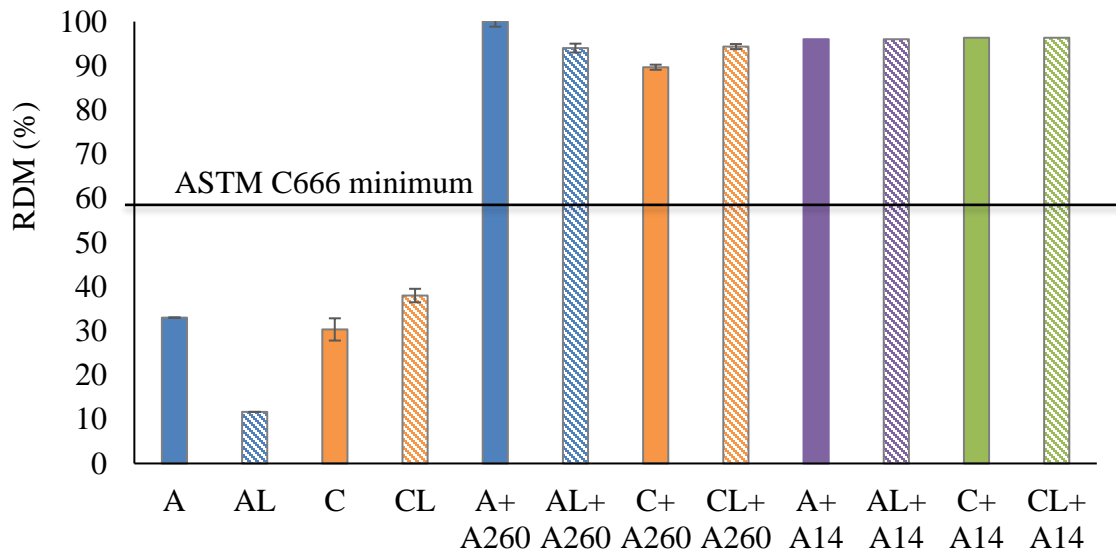
Figure 7.6: The relative dynamic modulus (RDM) of air-entrained and non air-entrained concrete after 300 cycles of freezing and thawing. The solid line shows the minimum RDM required by ASTM C666 after 300 cycles of freezing and thawing.

Table 7.4: The air content of fresh concrete, relative dynamic modulus (RDM) from freezing and thawing resistance tests, and L bar measurements from petrographic analysis of air-entrained concrete

	Air content (%)	L bar (μm)	RDM (%)
A+ A260	7.5%	105.0	100
AL+ A260	6.0%	93.3	94
C+ A260	7.8%	123.8	90
CL+ A260	5.7%	102.9	94
A+ A14	7.9%	86.6	96
AL+ A14	7.5%	118.7	96
C+ A14	6.6%	72.0	96
CL+ A14	6.2%	83.9	96

Compressive strength of air-entrained and non air-entrained concrete is shown in Figure 7.7. It can be seen that the compressive strength of air-entrained concrete (with 5-7% air) is lower than that of non air-entrained concrete with about 10% reduction in compressive strength per 1% increase in the air content. However, it should be noted that all entrained concrete passed the 28-day minimum requirement (3500 psi) by GDOT [92]. The compressive strength of air-entrained concrete with Type IL cement is similar or slightly higher than that of Type I/II cement concrete.
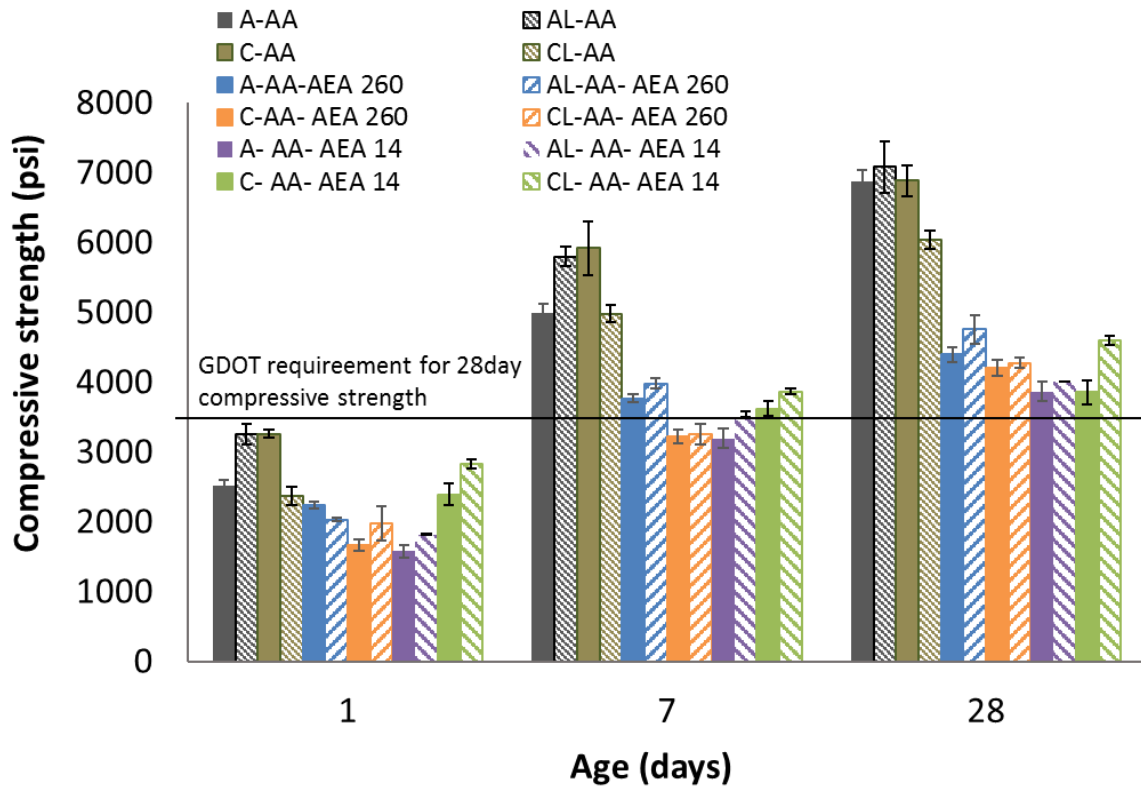
Figure 7.7: Compressive strength of air-entrained and non-air-entrained concrete at 1, 7, and 28 days. The horizontal line shows the GDOT minimum requirement for 28-day compressive strength (3500 psi) [92].

Chapter 8. EVALUATING THE EFFECT OF SCMS

The previous seven chapters investigated the influence of finely ground limestone powders on the hydration and microstructural development of neat portland limestone cement systems – that is, systems that contain only the PLC and water. In practice, however, cements are frequently blended with supplementary cementitious materials (SCMs) such as fly ash and slag, which react with the products of cement hydration to yield concrete with higher strengths, more refined porosities, and longer service lives in aggressive environments [99, 100]. Since portland limestone cements are intended to be used as direct alternatives to ordinary portland cements in concrete applications, it is therefore necessary to investigate how interactions between SCMs and limestone affect the hydration rate, early-age shrinkage, and microstructural development in PLC-SCM systems.

Supplementary cementitious materials fall into two general categories, based on their reactivity: pozzolanic materials, which contain reactive (glassy) silicates and produce additional C-S-H by reacting with the calcium hydroxide product of cement hydration; and latent hydraulic (or self-cementing) materials, which contain reactive calcium silicates or that produce additional C-S-H by their own reaction with water [2, 101]. Most SCMs exhibit some combination of both pozzolanic and latent hydraulic reactivity. Low-calcium (Class F [102]) fly ash, for example, is primarily pozzolanic due to its high concentration of aluminosilicate glass, while high-calcium (Class C) fly ash is both pozzolanic and latent hydraulic due to its high concentrations of aluminosilicate and calcium aluminosilicate glasses. Blast-furnace slag is similar to high-calcium fly ash and

129

exhibits primarily hydraulic behavior due to its high concentrations of calcium silicate and calcium-aluminosilicate glass [2, 99].

In typical portland cement-SCM systems, the pozzolanic and latent hydraulic reactions produce additional C-S-H beyond what is produced by cement hydration. This secondary C-S-H further densifies the microstructural skeleton created by the cement hydration, leading to reductions in porosity and corresponding increases in strength and impermeability. Additionally, the consumption of CH by the pozzolanic reaction, the improved alkali-binding of the secondary C-S-H [2, 101], and the more efficient particle packing of finer SCMs [18] all further enhance the ability of SCM-blended systems to resist degradation, such that blends containing SCMs are often recommended (or required) for use in applications where the concrete may be exposed to aggressive environments [99].

Recent studies have shown that when SCMs are combined with portland limestone cements, even greater improvements in durability will result from further refinements in porosity and increases in strength and impermeability [16, 103-105]. It is believed that these enhancements (commonly referred to as "synergies" in the literature) occur as a result of chemical reactions between the limestone and the aluminosilicate and calcium aluminosilicate phases in the SCMs [16, 106, 107], with higher alumina loadings hypothesized to yield greater "synergetic" interactions between PLCs and SCMs. Although several researchers have shown that limestone-SCM interactions can improve the strength and permeability characteristics of concrete mixtures, less research has been focused on their effects on early-age hydration rate and chemical and autogenous shrinkage. Since greater pore refinement often comes at the expense of greater

130

autogenous shrinkage (Chapter 4), these SCM-limestone "synergies" could lead to increased potential for cracking that counteracts any improvements in durability caused by the decrease in permeability. The objective of the research presented in this chapter is therefore to evaluate combinations of portland limestone cements and alumina-bearing SCMs in order to better understand how synergies between the limestone and the SCMs affect the early-age hydration and microstructural development of PLC-SCM blends.

8.1   Materials

For this study, 33 cement paste mixtures and 12 concrete mixtures were developed using the eleven commercially produced cements discussed in Chapter 3, combined with either Class F fly ash, Class C fly ash, or blast-furnace slag. Since it was desirable to investigate portland limestone cements in combination with SCMs for real structural applications, each SCM was dosed at the maximum replacement levels currently permitted by Georgia Department of Transportation (GDOT) specifications for concrete structures [108]: 15%, by weight, for each of the two fly ashes and 50%, by weight, for the slag.[5]

8.1.1   Composition

The oxide compositions (ASTM C114 [58]) for the three SCMs are shown in Table 8.1; trace amounts of Mn_2O_3, P_2O_5, SrO, and BaO were also found, but are not shown in the table. The high SiO_2 and low CaO content of the Class F fly ash suggest that

---

[5] GDOT Section 500 specifications permit replacements of fly ash at variable rates of 1.0-1.5 lb of fly ash to 1.0 lb of cement. Since an equivalent-mass substitution was used for this study in order to maintain a consistent *w/b* for all mixes, 1.0 lb of fly ash was substituted for 1.0 lb of cement.

it is primarily a pozzolanic material and will not hydrate until sufficient CH has been produced from primary cement hydration. Meanwhile, the SiO_2 and CaO contents of the Class C fly ash and the slag suggest that they are both primarily hydraulic materials, which can hydrate independently of the cement but more once sufficient CH has been produced. With respect to limestone synergies, the Class F fly ash contains the highest alumina (Al_2O_3) content at 23.3%, followed by the Class C fly ash at 18.8%, and the slag at 7.6%. Taking into account the different dosages used for the three SCMs, the total alumina loadings of the SCMs are found to be 3.5 g per 100 g cementitious material for the Class F fly ash, 2.8 g per 100 g cementitious material for the Class C fly ash, and 3.8 g per 100 g cementitious material for the slag. It is hypothesized that the higher alumina loadings for the Class F fly ash and slag blends will yield the greatest differences in early-age behavior for the Type I/II and Type IL cements.

Table 8.1: Chemical oxide analyses for SCMs. LOI indicates loss on ignition at 1000°C.

Component	Fly Ash (Class F)	Fly Ash (Class C)	Slag
SiO_2	51.30	34.57	38.77
Al_2O_3	23.32	18.78	7.62
Fe_2O_3	13.31	5.52	0.75
CaO	2.75	26.41	36.81
MgO	1.03	6.60	12.08
Na_2O	0.82	1.92	0.19
K_2O	2.43	0.47	0.48
TiO_2	1.25	1.39	0.26
SO_3	0.48	1.98	2.29
LOI	2.89	0.22	0.12

8.1.2 Particle size

The particle size distributions of the three SCMs, as measured by laser diffraction in ethanol (Section 3.3), are shown in Figure 8.1 (differential) and Figure 8.2 (cumulative); cement A is shown in each figure for comparison. A summary of relevant parameters is given in Table 8.2.

The Class F fly ash was found to be the coarsest of the four materials, having a median particle size 50% larger than that of cement A and nearly double those of the Class C fly ash and slag. It has similar surface area parameters ($D_{3,2}$ and SSA) to the cement when smooth particles are assumed for both materials, but has roughly half the specific surface area of the other two SCMs. The slag was found to be the finest of the three SCMs, having a median particle size nearly 30% finer than cement A and almost twice the specific surface area. Some of the increase in specific surface area can be attributed to the lower density of the slag compared to the cement; however, much of the increase is due to the finer size of the slag particles, as further evidenced by the 40% reduction in surface mean particle size ($D_{3,2}$). Based on the particle size distributions, it is hypothesized that the finer Class C fly ash and slag blends will likely exhibit further microstructural refinements due to the physical influence of filler effects [18], but since the SCMs are chemically reactive, these physical effects are not anticipated to dominate the hydration behavior like they did for the neat PLC systems.
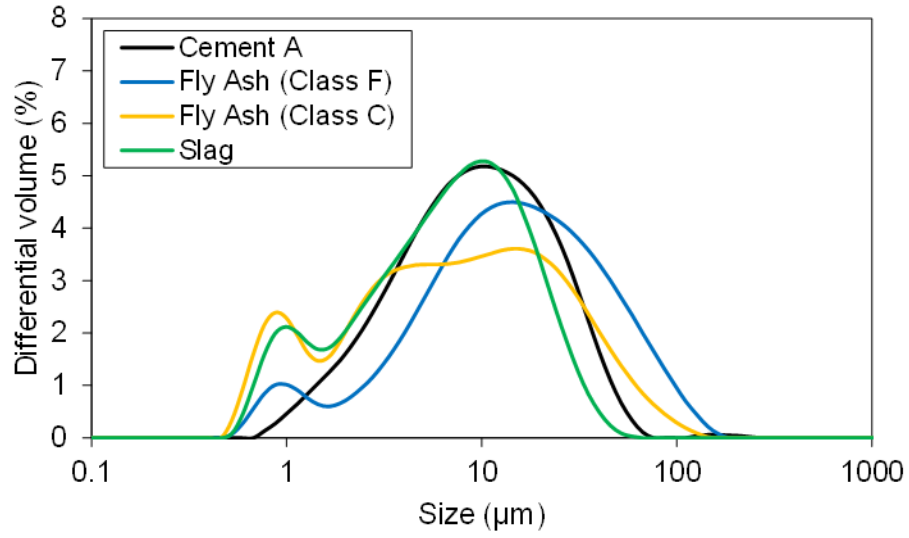
Figure 8.1: Differential particle size distributions for the three SCMs. Cement A is shown for comparison.
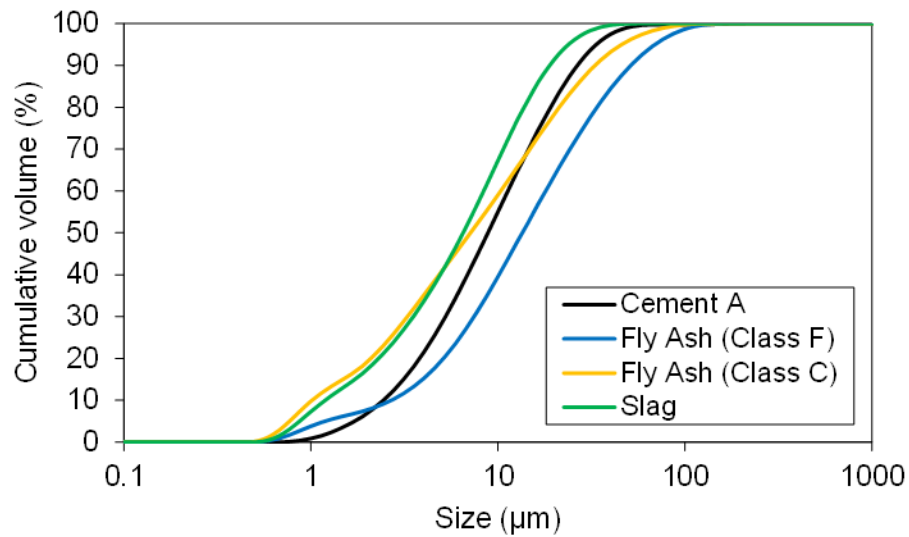
Figure 8.2: Cumulative particle size distributions for the three SCMs. Cement A is shown for comparison.

Table 8.2: Particle size distribution parameters for SCMs. Cement A is shown for comparison.

Parameter	Cement A	Fly Ash (Class F)	Fly Ash (Class C)	Slag
D_{10}, μm	2.77	3.05	1.15	1.35
D_{50}, μm	10.0	15.3	8.08	7.38
D_{90}, μm	30.2	58.3	37.5	21.4
$D_{3,2}$, μm	6.28	6.67	3.58	3.79
$D_{4,3}$, μm	14.1	24.3	15.0	9.78
SSA, m^2/kg	288	337	627	566

8.1.3 Specific gravity

The specific gravities of the three SCMs were measured by displacement in kerosene (ASTM C188 [57]) to be 2.35, 2.66, and 2.82 for the Class F fly ash, the Class C fly ash, and the slag, respectively. All three SCMs are lower in specific gravity than the Type I/II and Type IL cements, indicating that an equivalent mass substitution will increase the volume of the binder phase in the cement paste. The SCM blended cement pastes are therefore hypothesized to exhibit some reductions in average particle size due to ancillary particle-packing/filler effects in addition to the reductions generated by their pozzolanic and hydraulic reactions [18].

8.2   Experimental methods

8.2.1   Preparation of cement paste

Thirty-three cement paste mixtures were prepared from the eleven cements and three SCMs at a water-to-cementitious materials ratio (*w/b*) of 0.40, where the cementitious material was taken to be the combined Type I/II or Type IL cement and any SCM substitutions. The SCMs were first blended with the cement, then added to deionized water (18.2 MΩ-cm) and mixed following the procedures outlined in Section 8.2.1. Cement paste specimens were used for the investigation of hydration kinetics (isothermal calorimetry) and chemical and autogenous shrinkage.

8.2.2   Isothermal calorimetry

Isothermal calorimetry (ASTM C1679 [109]) was used to characterize the SCM-induced changes to hydration kinetics. Tests were performed on 7.0 ± 0.5 g of cement paste contained within high-density polyethylene (HDPE) ampules. Two replicate specimens of each mix were placed into a TAM Air isothermal calorimeter, held at 25°C for 72 hr. The rate of heat evolution was measured at 1 min intervals, and results were integrated to determine the cumulative heat of hydration over the 72 hr period.

The cumulative heat results were used to indirectly measure the degree of hydration of the SCM-blended cement pastes. For cement pastes containing additions of fly ash or slag, Equation 8.1 for the total heat of hydration at $\alpha = 100\%$ (H_∞) was modified as follows [110]:

$$H_\infty = H_{cem} p_{cem} + H_{FA} p_{FA} + H_{slag} p_{slag}$$
<div align="right">Equation 8.1</div>

where H_{cem} is the total heat of hydration for the cement, given in units of J/g; H_{FA} is the total heat of hydration of the fly ash, in units of J/g; H_{slag} is the total heat of hydration of the slag, assumed to be approximately 461 J/g [110]; and p_{cem}, p_{FA}, and p_{slag} are the mass fractions of cement, fly ash, and slag, respectively in the total cementitious binder. The total heat of hydration of fly ash depends on the mass fraction of CaO in the fly ash (p_{FACaO}), and can be approximated in units of J/g as [110]:

$$H_{FA} = 1800 p_{FACaO}$$ Equation 8.2

The estimated values for H_∞ for the 33 blended cement pastes are given in Table 8.3; the values for neat cement pastes are shown for comparison, and are generally similar to those of the blended cement pastes, with the exception of the Class F fly ash mixture, which releases less heat due to its lower CaO content.

Table 8.3: Predicted total heats of hydration, H_∞, for SCM-blended cement pastes, J/g cementitious material.

	A	AL	B	BL	C	CL	D	DL	E	EL
No SCMs	450.4	414.5	439.2	415.0	444.1	401.1	438.6	413.2	470.3	441.3
15% Fly Ash (Class F)	390.3	359.8	380.7	360.2	384.9	348.4	380.2	358.6	407.2	382.5
15% Fly Ash (Class C)	454.1	423.6	444.6	424.1	448.8	412.2	444.1	422.5	471.1	446.4
50% Slag	455.7	437.8	450.1	438.0	452.6	431.1	449.8	437.1	465.7	451.2

8.2.3 Chemical and autogenous shrinkage

Chemical shrinkage (ASTM C1608 [111]) was measured for the 33 blended cement pastes at 25°C, using the procedure described in Section 4.1. Measurements were recorded on a minimum of three replicate specimens, twice per hour for at least 48 hr, then once every 2 hr until 7 days. Units were converted from measured units of mL shrinkage per g of cementitious material to dimensionless % volume units, where the specific gravity of the binder was found using the inverse rule of mixtures for the cements and SCM additions.

Autogenous shrinkage (ASTM C1698 [112]) was measured by monitoring the length change of three replicate corrugated tube specimens cast as described in Section 4.1. Testing was performed on pastes made with cements from sources A and C only, due to the longer duration of the test. Length change was recorded at 2 hr intervals from the time of final set until 12 hr of hydration, then once daily until 7 days, bi-weekly until 28 days, and weekly until 56 days.

8.2.4 Setting time

Setting time for samples with SCMs was measured as described in Section 4.1 which also shows the test matrix.

8.2.5 Preparation of concrete specimens

Twelve concrete mixtures were also prepared using the cements from sources A and C, blended with the three SCMs at the replacement levels prescribed in Section 6.2. Mixtures were designed to meet the "worst-case" specifications for GDOT Class AA structural concrete [108], and were therefore mixed with the maximum permissible *w/b* of 0.445, and the minimum total cementitious materials content of 635 lb/yd^3 (375

kg/m^3). Crushed granite coarse aggregates (Lithia Springs, GA; #67 stone, dry-rodded unit weight = 98 lb/ft^3, SG = 2.61) and natural sand fine aggregates (Byron, GA; fineness modulus = 2.4, SG = 2.65) were proportioned at 1889 lb/yd^3 (1120 kg/m^3) and 1260 lb/yd^3 (750 kg/m^3), respectively, for each of the 12 mixtures. A mid-range water reducer (Sika SikaPlast-300GP) was used at dosages of 10-14 fl.oz./100 lb of cementitious material to ensure adequate workability.

The raw materials were mixed in 5 ft^3 batches in a 9 ft^3 rotating drum mixer, following ASTM standard practices [74]. Twenty cylindrical specimens measuring 4 in. (diameter) by 8 in. (length) were cast from the mixtures for compressive strength testing. Specimens were removed from their molds 24 hr after casting and cured in a saturated calcium hydroxide (limewater) solution at 70 ± 3°F until testing.

8.2.6   Mechanical properties

Compressive strength (ASTM C39) [113] of concrete cylinders (4 in. x 8 in.) was measured for Class AA concrete made with Type I/II and Type IL cements from plant A and plant C and with supplementary cementitious materials (SCMs). The SCMs were 15% Class F fly ash (Class F fly ash), 50% slag, and 15% Class C fly ash (Class C fly ash). The percentages mentioned here are the replacement of cement by weight. Compressive strength was measured at 1 day, 7 days, 28 days, 56 days, 90 days, and 1 year. Individual mixes used only a single SCM along with either Type I/II cement or Type IL cement. Table 8.4 explains the labels used for the SCM mixes.

Table 8.4: Labels used for SCM concrete mixes

SCM	Plant A		Plant C	
	Type /II	Type IL	Type /II	Type IL
Class F fly ash	A-F15	AL-F15	C-F15	CL-F15
Class C fly ash	A-C15	AL-C15	C-C15	CL-C15
Slag	A-S50	AL-S50	C-S50	CL-S50

Elastic modulus (ASTM C469 [79]) and splitting tensile strength (ASTM C496 [80]) tests were measured as described in Section 6.1.

8.2.7 Drying shrinkage

Drying shrinkage of concrete prisms (ASTM C157 [57]) was measured as described in Section 6.1.2. The samples were cured in a saturated lime-water bath until 28 days of age, after which drying was started.

8.3   Results

The interactions between PLCs and SCMs were monitored through a combination of hydration, shrinkage, and mechanical property studies. Hydration kinetics and chemical shrinkage were characterized to better understand how the interactions between the limestone and alumina-containing SCMs affect early-age hydration processes, while autogenous shrinkage and compressive strength were characterized in order to indirectly evaluate how the limestone-SCM interactions affect microstructural development.

8.3.1   Hydration

The rates of heat evolution for the 33 cement pastes over the first 48 hr are shown in Figure 8.3, and the cumulative heats of hydration over the first 72 hr are shown in Figure 8.4; the calorimetric results for the eleven neat cement pastes are also shown for

comparison. The results indicate that for all 33 mixtures, the partial substitution of cement by either fly ash or slag reduces the heat evolved relative to the neat cement paste mixtures throughout the first 72 hr of hydration, which would be expected given the slower rates of reaction of the three SCMs compared to the cement. By 72 hr, the cumulative heats released by the mixtures containing 15% Class F fly ash, 15% Class C fly ash, and 50% slag are reduced by an average of 10%, 5%, and 24%, respectively, when compared the neat cement paste controls. The reductions in heat evolution are less than the reduction in cement content, indicating that the three SCMs participate to some degree in the early-age hydration reactions.
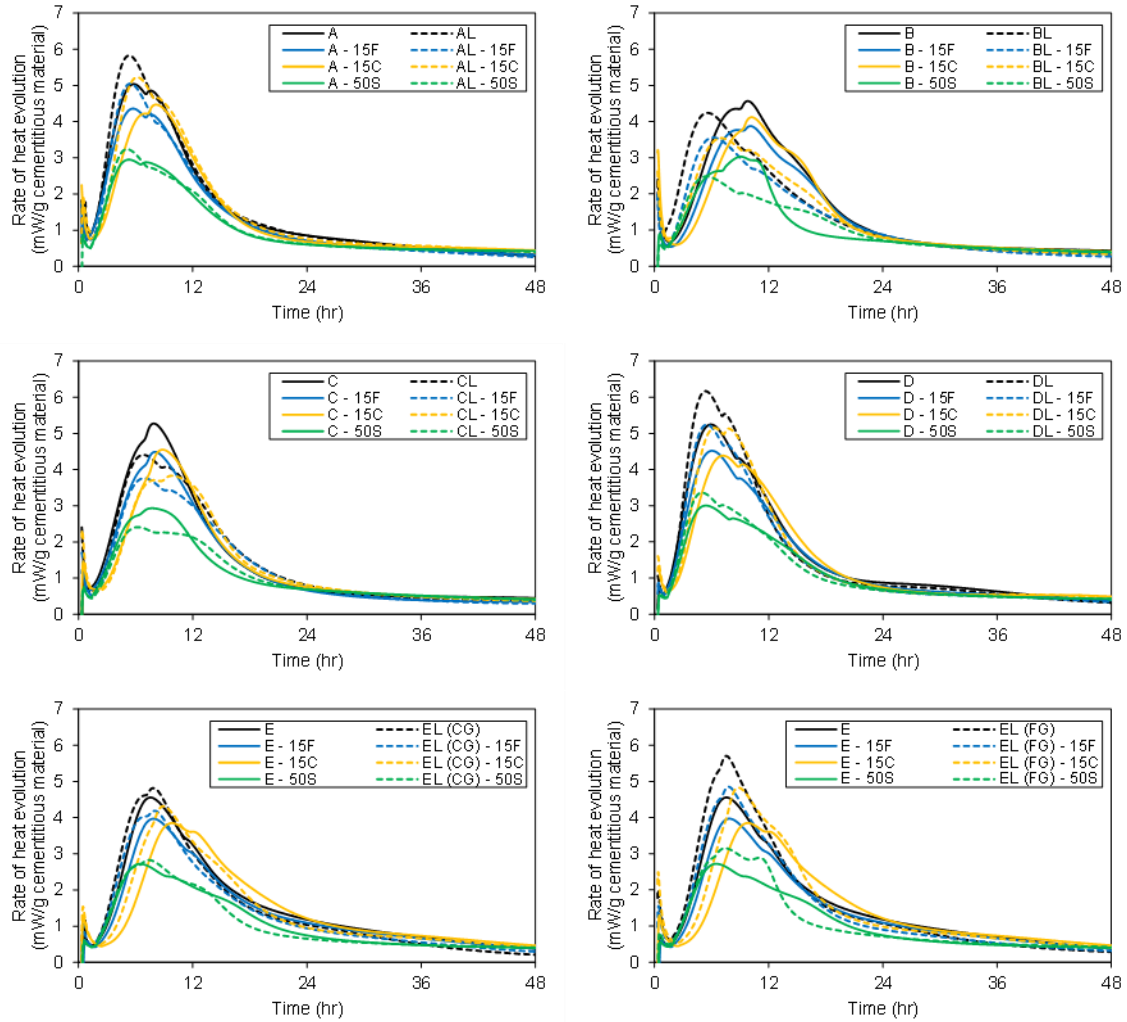
Figure 8.3: Rate of heat evolution for SCM-blended cement pastes, normalized by the mass of cementitious material.
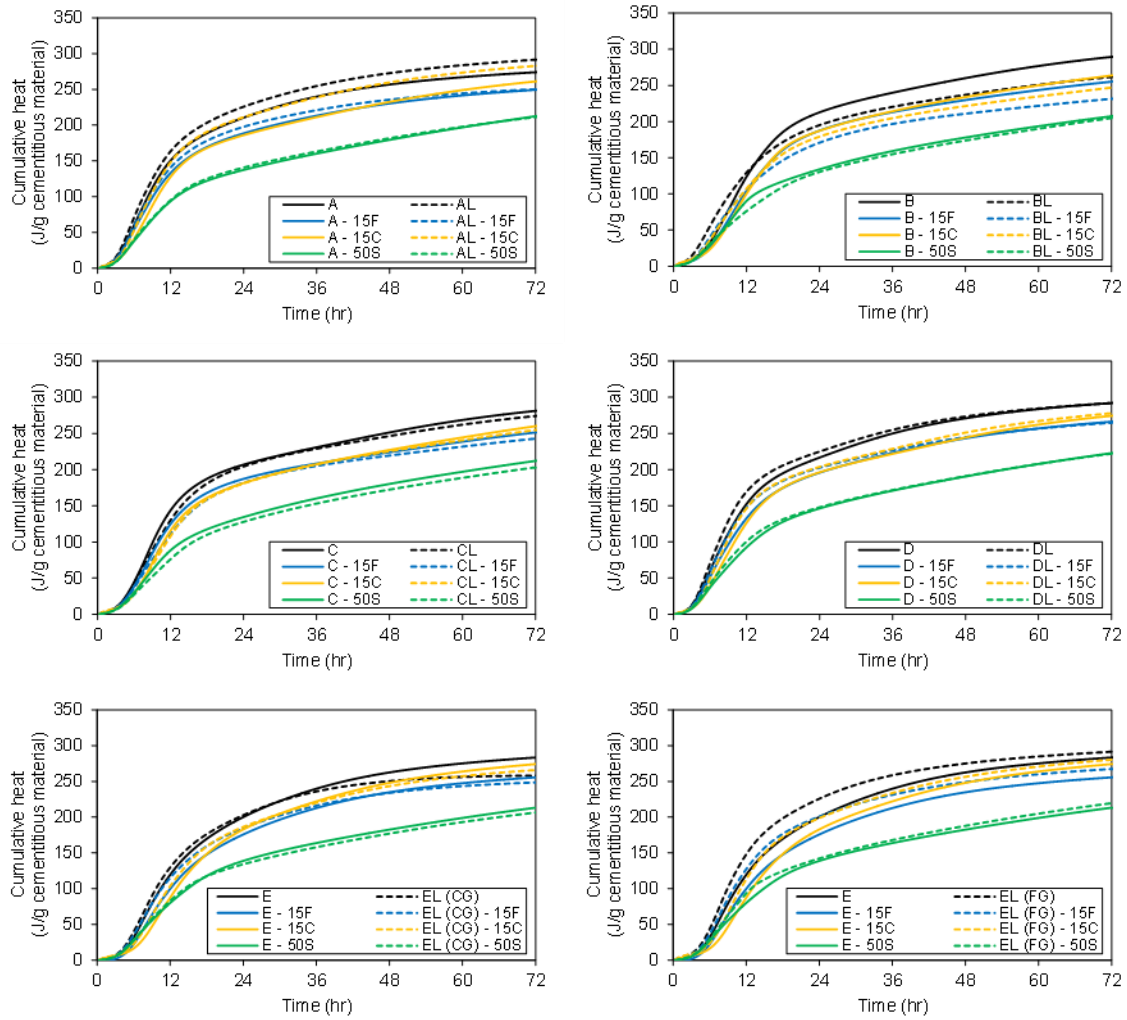
Figure 8.4: Cumulative heats of hydration for SCM-blended cement pastes, normalized by the mass of cementitious material.

The SCM-induced dilution effects can be removed by normalizing the heat by the mass of Type I/II or Type IL cement in the paste, rather than by the total mass of cementitious material. It can be seen from the resulting curves in Figure 8.5 that slag increases the rate of heat release per gram of cement by 15.4% (SD = 6.8%), while the Class F and Class C fly ash have no significant effects on rate of heat release (increases of $0.8 \pm 1.2\%$ and $1.7 \pm 3.2\%$, respectively). Thus, while most of the overall differences in hydration for the fly ash blended cement pastes appear to be related to the dilution of the cement by the more slowly reacting fly ash, the hydraulically reactive slag is found to contribute to the heat of hydration at early ages.

It can also be seen that the three SCMs each have a different accelerating or decelerating effect on hydration, as determined by the time to peak heat release. On average, it was found that a 15% substitution of cement by Class F fly ash delayed the time to peak heat release by less than 10 min, while a 50% substitution of cement by slag accelerated the time to peak heat release by approximately 25 min. By comparison, a 15% substitution of cement by Class C fly ash was found to have a significant retarding effect, delaying the time to peak heat release by more than 1 hour, on average. Since the slag and the Class C fly ash had similar (fine) particle size distributions, the retardation of the Class C fly ash mixtures is likely related to the chemistry of the fly ash, rather than to its particle size distribution.
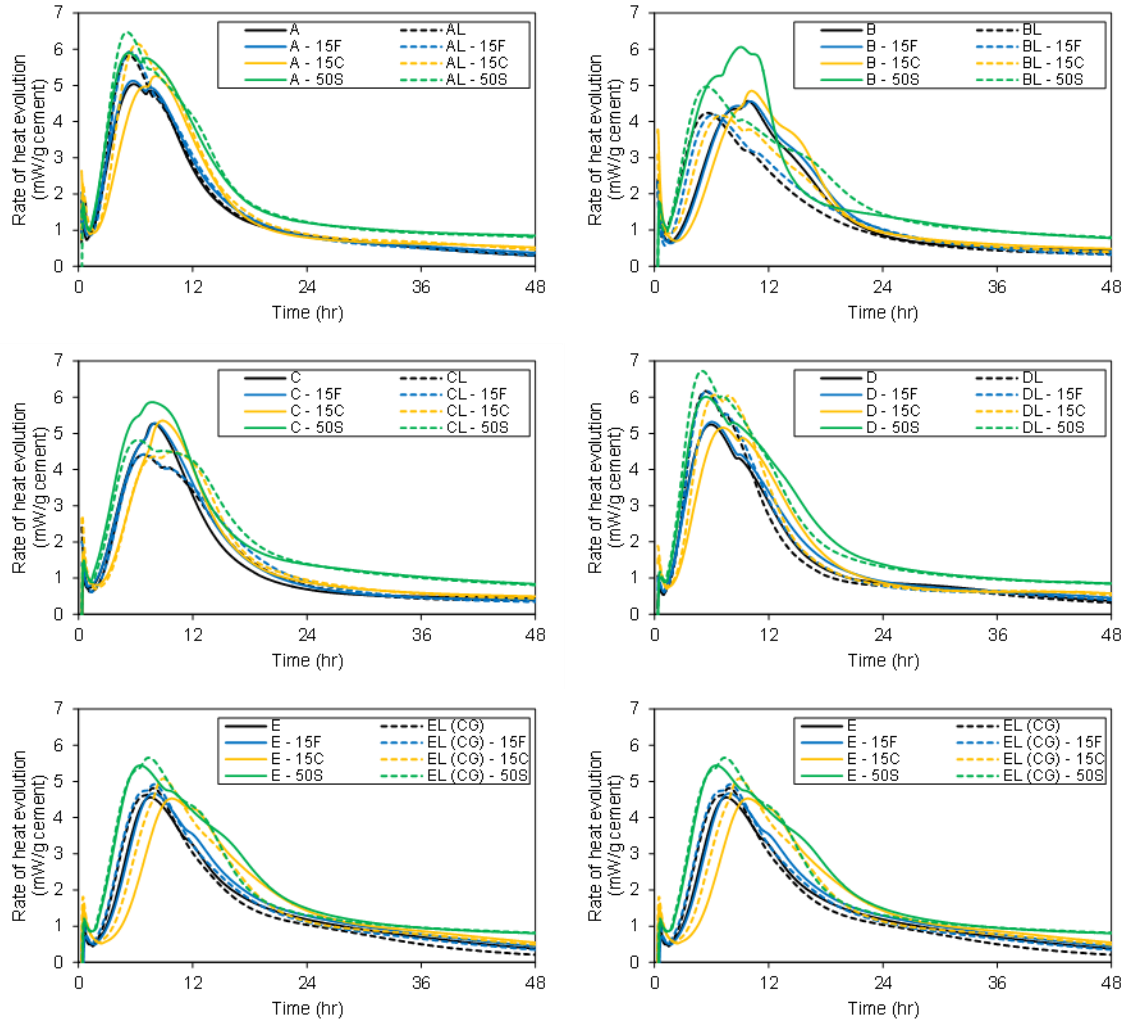
Figure 8.5: Rate of heat evolution for SCM-blended cement pastes, normalized by the mass of cement.

Comparing the Type I/II and Type IL cements to one another, it can be observed that the finer Type IL cements from sources A, D, and E again increase the heat released when combined with SCMs, while the coarser Type IL cements from sources B and C again decrease the heat released when combined with SCMs. The accelerating and decelerating effects of the SCMs were generally found to follow the particle size trends previously observed for the neat cement pastes, with slightly shorter delays (or more

rapid accelerations) seen for finer cements AL, DL, and EL, and greater retardation (or less rapid accelerations) seen for coarser cements BL and CL. Additionally, while the shapes of the heat release curves for the Type I/II cement pastes were generally consistent with one another – aside from stretching or compressing as dictated by retardation and acceleration, respectively – the shapes of the heat release curves for the Type IL blends were found to change depending on the type of SCM used. In particular, blends of Type IL cement with Class C fly ash generally showed a broadening of the peak typically associated with C_3A hydration, while the blends of Type IL cements with slag showed a third peak between 2 and 24 hr of hydration suggesting possible changes to the hydration of the C_3S and C_3A – or possibly other – phases. No significant changes in the shape of the heat evolution curves were observed for the mixtures containing Class F fly ash, suggesting that the limestone interactions with Class F fly ash are not as pronounced during the first 3 days of hydration.

Degree of hydration was computed from the cumulative heat results for the 33 cement paste mixtures to determine if the limestone-SCM interactions had any significant effects on cement hydration over the first 72 hr. It can be seen from the results in Figure 8.6 that by 72 hr of hydration, a 15% substitution of cement by Class F fly ash increases degree of hydration by an average of 4.0% (SD = 3.0%), a 15% substitution of cement by Class C fly ash reduces degree of hydration by an average of 6.1% (SD = 3.3%), and a 50% substitution of cement by slag reduces degree of hydration by 26.8% (SD = 3.2%). As with heat of hydration, there were no significant differences between the Type I/II and Type IL cement blends at 72 hr of hydration; however, for both cement sources, the Class

C fly ash increased degree of hydration for the Type IL cement paste relative to the Type I/II cement paste, regardless of cement fineness.
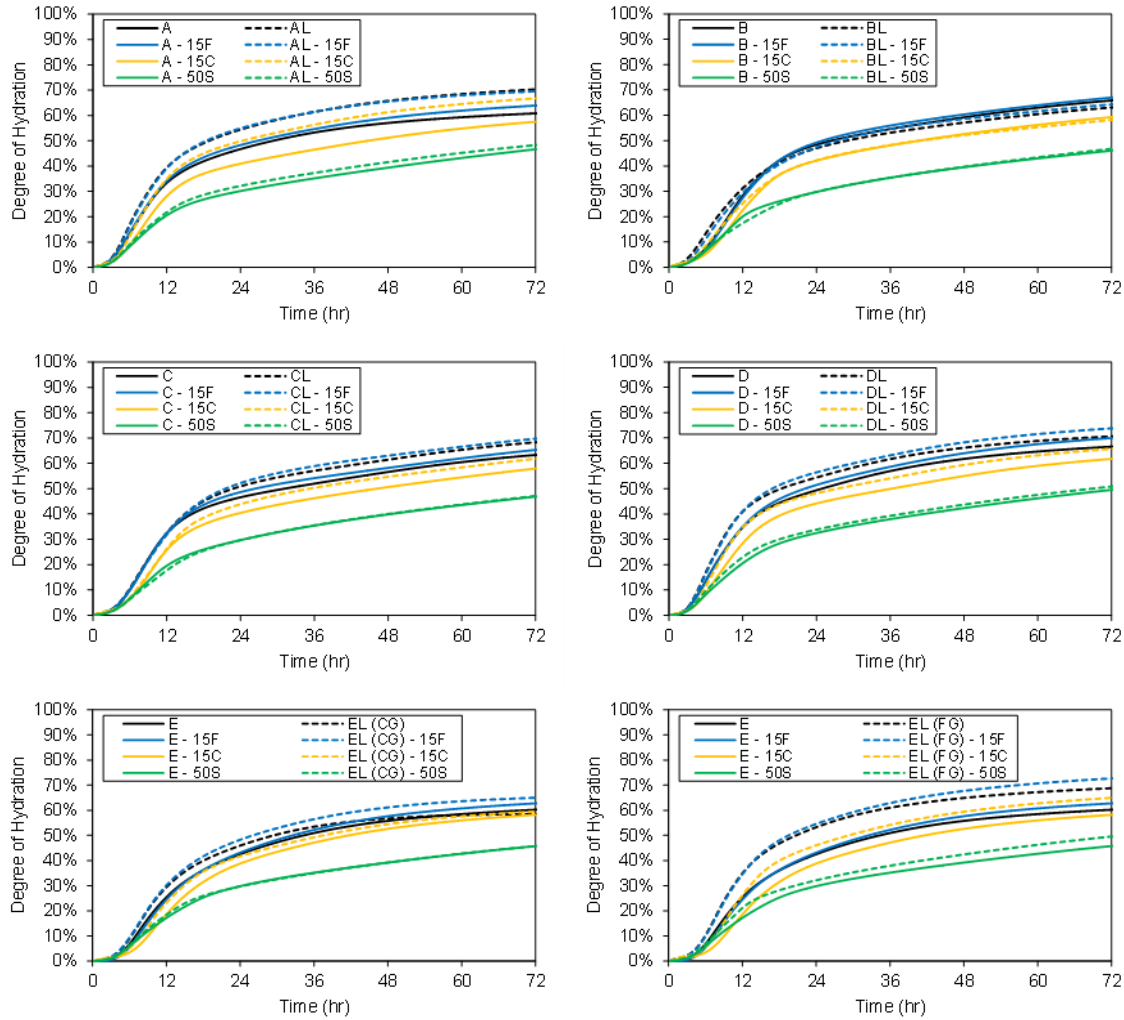
Figure 8.6: Degree of hydration for SCM-blended cement pastes.

8.3.2   Chemical shrinkage

The results of the chemical shrinkage test, normalized with respect to the starting volume of cement paste, are shown in Figure 8.7. Error bars are omitted for clarity, but

the average coefficient of variation over the 7 day period for each of the 33 tests did not exceed 6% for any mix.

The shapes of the chemical shrinkage curves are generally consistent with the degree of hydration curves of Figure 8.6, as would be expected given the hydration-rate-dependence of chemical shrinkage. The relative magnitudes of the chemical shrinkage for SCM blended cement pastes were greater than the relative magnitudes of degree of hydration for the same SCM blended pastes, suggesting that the SCM interactions contribute more to chemical shrinkage than they do to degree of hydration. In particular, it was observed after 72 hr of hydration that 15% Class F fly ash increased degree of hydration by 4%, 15% Class C fly ash decreased degree of hydration by 6%, and 50% slag decreased degree of hydration by 27%. By contrast, after 72 hr of hydration, 15% Class F fly ash reduced chemical shrinkage by an average of 12.0% (SD = 3.9%), 15% Class C fly ash reduced chemical shrinkage by an average of 1.5% (SD = 3.0%), and 50% slag reduced chemical shrinkage by 22.2% (SD = 3.3%). Similar reductions were also observed prior to normalizing the results by the starting volume, indicating that the differences between the degree of hydration and chemical shrinkage are not due to the different volumes of the pastes, but are more likely a function of the secondary hydration of the SCMs.

By 7 days, the secondary reactions of the SCMs appear to introduce even more chemical shrinkage of the paste, reducing the shrinkage-mitigating effects seen at earlier ages in the SCM blends. While the more slowly reacting Class F fly ash mixtures continued to show approximately a 10% reduction in chemical shrinkage by 7 days (10.5%, SD = 4.5%), the hydraulically reactive slag only reduced chemical shrinkage by

9.0% (SD = 3.8%), and the Class C fly ash was found to actually increase chemical shrinkage by 3.7% (SD = 3.6%). Between 3 and 7 days of hydration, then, the chemical reactivity of the SCMs appears to play a significant role in increasing the chemical shrinkage of mixtures containing Class C fly ash and slag.
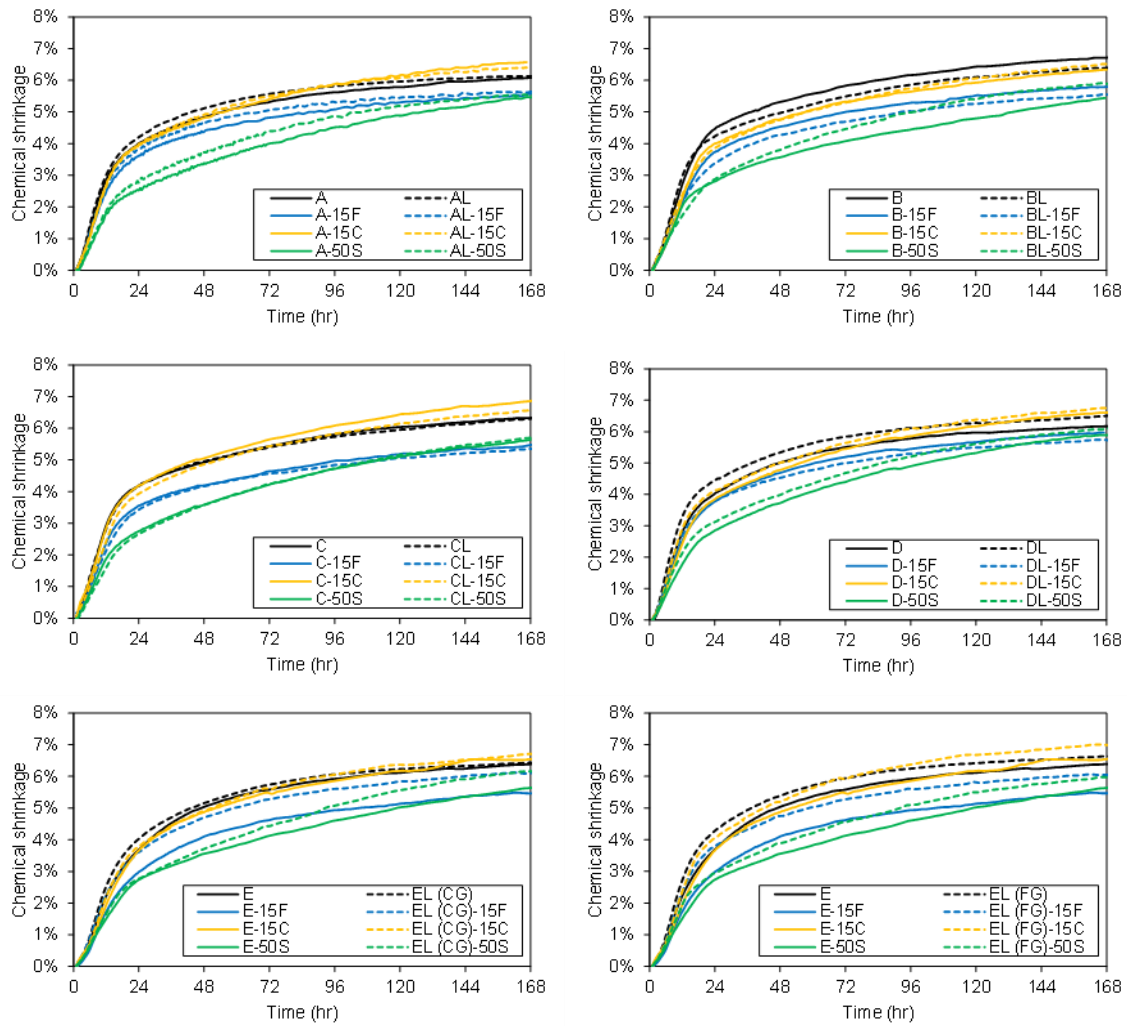
Figure 8.7: Chemical shrinkage for SCM blended cement pastes at *w/b* = 0.40, as a fraction of the initial paste volume.

The changes in chemical shrinkage relative to the neat cement pastes were generally consistent between Type I/II and Type IL cements, but small differences could be discerned for the mixtures containing 15% Class F fly ash and 50% slag. The Type I/II blends containing Class F fly ash reduced chemical shrinkage by approximately 1.5% more than the corresponding Type IL cement pastes did, or 11.2% compared to only 9.8% for the Type IL mixtures. Similarly, the Type I/II blends containing slag reduced chemical shrinkage by approximately 3% more than the corresponding Type IL cement pastes, or 10.7% compared to only 7.6% for the Type IL mixtures. It would be logical to attribute such differences to the secondary reactions between the limestone and alumina phases in the SCMs; however, for both the Class F fly ash and the slag, the differences between the two cement types were within one standard deviation of the mean for the eleven cements. This suggests that – for the Class F fly ash blends, in particular – the effect of the limestone-SCM synergies on chemical shrinkage is still small after 7 days of hydration. Longer duration studies encompassing more of the secondary reactions may be required to fully investigate the influence of limestone-SCM synergies on the early-age chemical shrinkage of SCM-blended PLC pastes.

8.3.3 Autogenous shrinkage

The autogenous shrinkage results are shown in Figure 8.8 for the SCM blends with cements from source A and in Figure 8.9 for the SCM blends with cements from source C. Figure 8.8b and Figure 8.9b are normalized with respect to the cement factor, CF, of the binder; that is, the proportion of cement in the binder (1.0 for neat cement

pastes, 0.85 for blends with fly ash, and 0.5 for blends with slag). Error bars are removed for clarity.

During the first 7 days of hydration, the autogenous shrinkage of all six SCM-blended cement pastes was found to be lower than the companion Type I/II and Type IL neat cement pastes, due primarily to the dilution of the cement by the more slowly reacting SCMs. Such a decrease suggests that SCM-blended cement pastes may be effective at reducing shrinkage at early ages, when less strength has been developed and the potential for cracking is higher. However, as the primary hydration of the cement slows and the secondary hydration of the SCMs becomes more dominant, significant changes in autogenous shrinkage can be observed. These changes appear to be sensitive to both the type of SCM used and the type of cement used, indicating potential effects from limestone-SCM interactions.
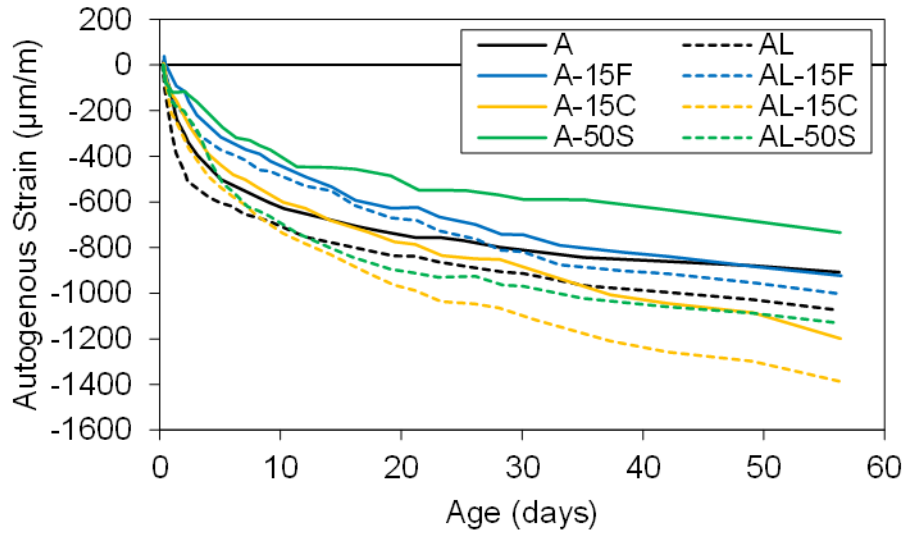
(a)
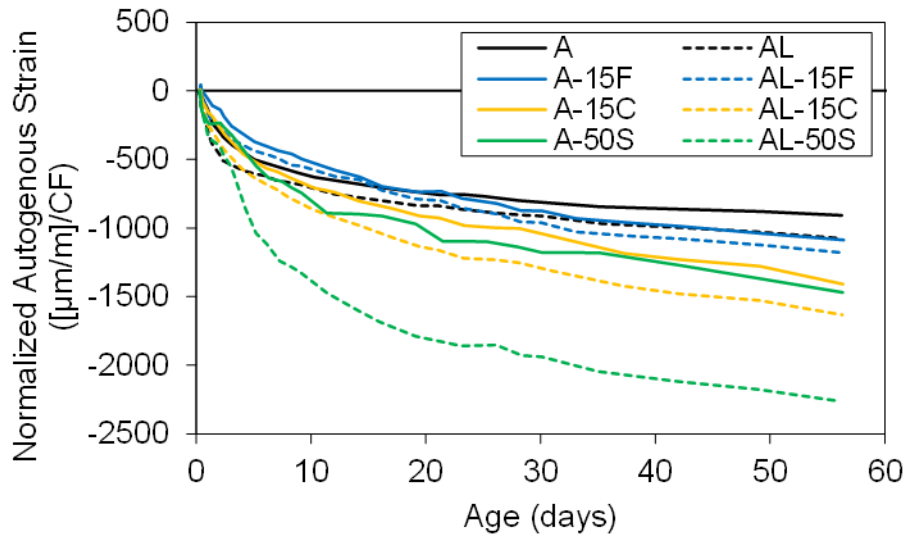
(b)

Figure 8.8: Autogenous shrinkage of SCM blended cement pastes at *w/b* = 0.40, prepared with cements from source A.(a) Results as measured. (b) Results normalized by cement factor (CF). Error bars are removed for clarity.
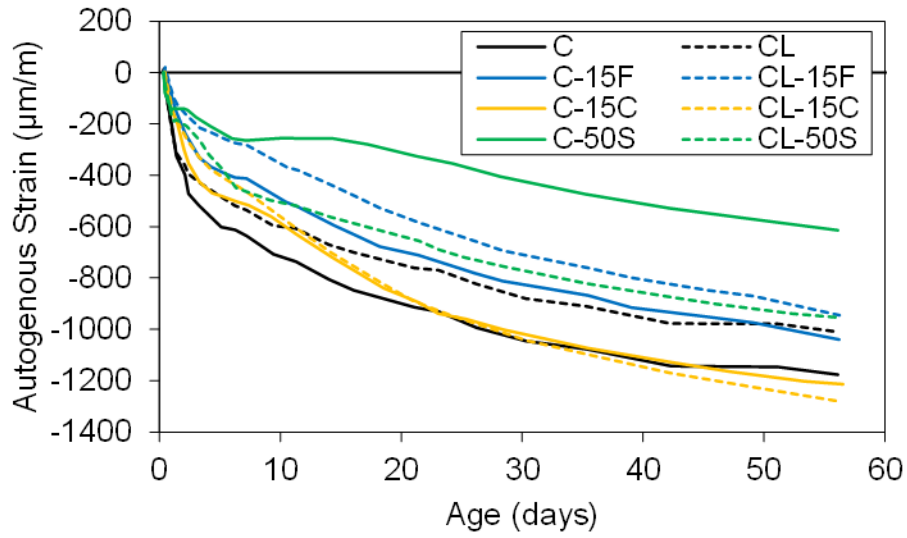
(a)
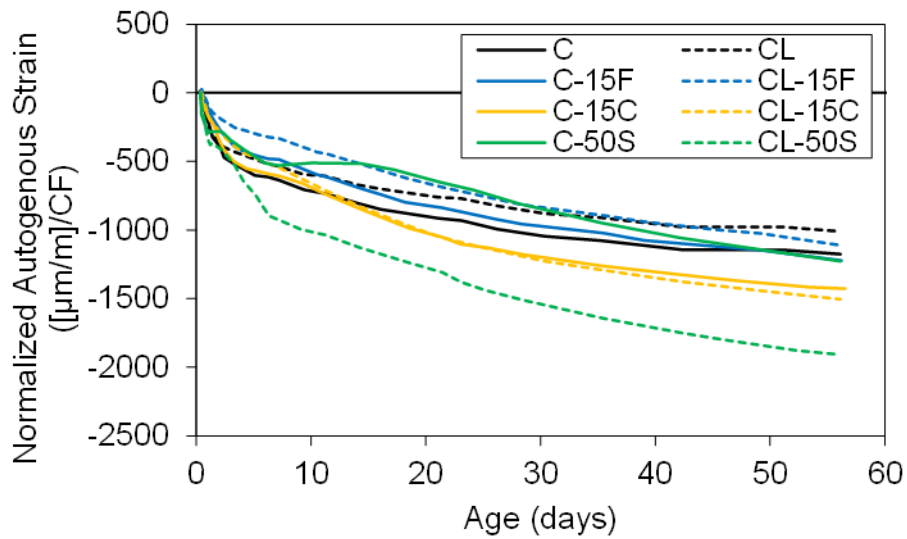
(b)

Figure 8.9: Autogenous shrinkage of SCM blended cement pastes at *w/b* = 0.40, prepared with cements from source C.(a) Results as measured. (b) Results normalized by cement factor.

The 50% replacement of cement with slag had the most extreme effects on autogenous shrinkage of the Type I/II and Type IL cement pastes. Even at early ages, the autogenous shrinkage of the Type IL cement-slag mixes was more than 50% larger than the autogenous shrinkage of the Type I/II cement-slag mixes, and by 56 days, it was observed that the shrinkage of the AL and CL blends exceeded that of the A and C blends by 72% and 56%, respectively. Comparing the slag mixes to their neat cement paste counterparts, it can additionally be observed that the 50% slag replacement for the Type I/II blends reduced autogenous shrinkage by an average of 38% (48% for cement A and 28% for cement C) at 56 days, but only reduced autogenous shrinkage in the Type IL blends by a combined 1% (5% increase for cement AL, 6% decrease for cement CL) at that same age. The substantial increase in autogenous shrinkage for the Type IL cement-slag relative to their Type I/II-slag counterparts suggests extensive pore refinement in those blends as a result of the limestone-slag synergies, but also indicates that a 50% replacement of Type IL cement by slag may not have the same shrinkage-mitigating effects as the same replacement level would for a more traditional Type I/II cement.

Additional – albeit smaller – differences were observed in the autogenous shrinkage results for the two fly ash blends. After about 7 days of hydration, the Class C fly ash blends begin to show steeper increases in autogenous shrinkage compared to the neat cement paste control mixtures, which suggest that pozzolanic activity initiating around 7 days of hydration leads to greater pore refinement in Class C fly ash blends. The autogenous shrinkage of the Class C fly ash blends continues to increase through 56 days, leading to a 56 day autogenous shrinkage, on average, 23% greater than for the neat cement paste controls. Separating by cement type, it can be seen that the Type I/II cement

blends increase autogenous shrinkage by an average of 18%, while the Type IL cement blends increase autogenous shrinkage by an average of 28%, further suggesting reductions in average pore size due to interactions between the limestone and fly ash. Overall, the blend of Type IL cement with Class C fly ash had the largest autogenous shrinkage observed for both cement sources by 28 days, indicating that such a combination may not be desirable if shrinkage is to be limited during the first 28 days of hydration.

Finally, it was observed that the Class F fly ash blends undergo autogenous shrinkages more similar in magnitude to the neat cement paste controls, despite continued pore refinement as a result of their secondary hydration reactions. On average, the substitution of cement by 15% Class F fly ash reduced the 56 day autogenous shrinkage by 6%, with little differences observed between the Type I/II and Type IL mixtures beyond what was already observed for the control mixtures. Although the Class F fly ash is slower to react due to its low CaO content and coarser particle size, it is anticipated that beyond 56 days, the ongoing secondary reactions of the Class F fly ash will continue to refine the porosity, leading to greater autogenous shrinkage for those cement pastes relative to the neat cement paste mixtures.

8.3.4 Setting time

8.3.4.1 Fly ash

Figure 8.10 and Figure 8.11 show the results of the time of setting for the group of samples with 15% fly ash Class F and Class C, respectively, from sources A to E tested at 73 °F.

For Class F fly ash, the results show that Type IL cement showed faster setting time (~6% to ~25%) for sources A, D, and E which was the group of Type IL cements with higher fineness. Type I/II and Type IL from sources B and C showed similar times of setting and that was the group of Type IL cements with similar particle sizes to their companion Type I/II cement.

For Class C fly ash, the results show that Type IL cement showed faster setting time (~7% to ~10%) for sources A, B, C, and E. Type I/II from source D showed faster setting than Type IL.
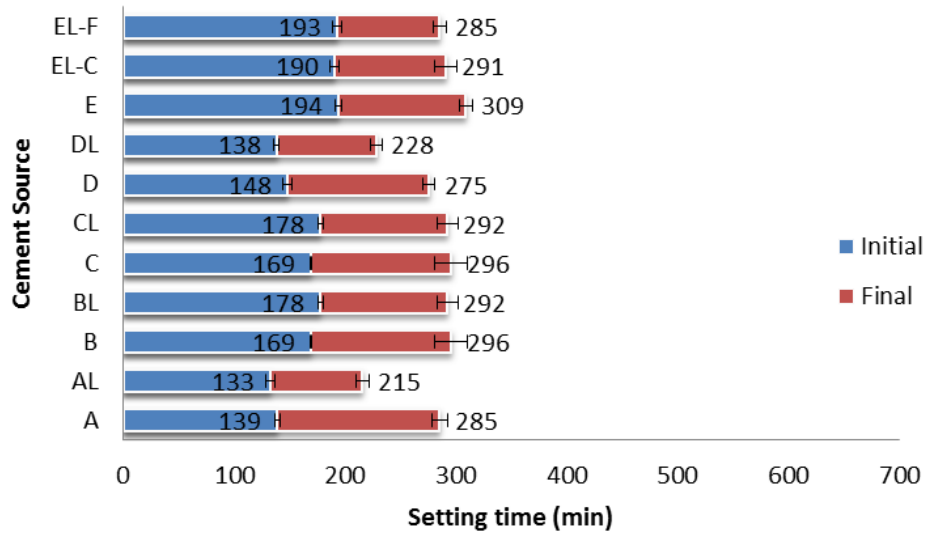
Figure 8.10: Time of setting of cements A to E with 15% fly ash Class F at 73 °F
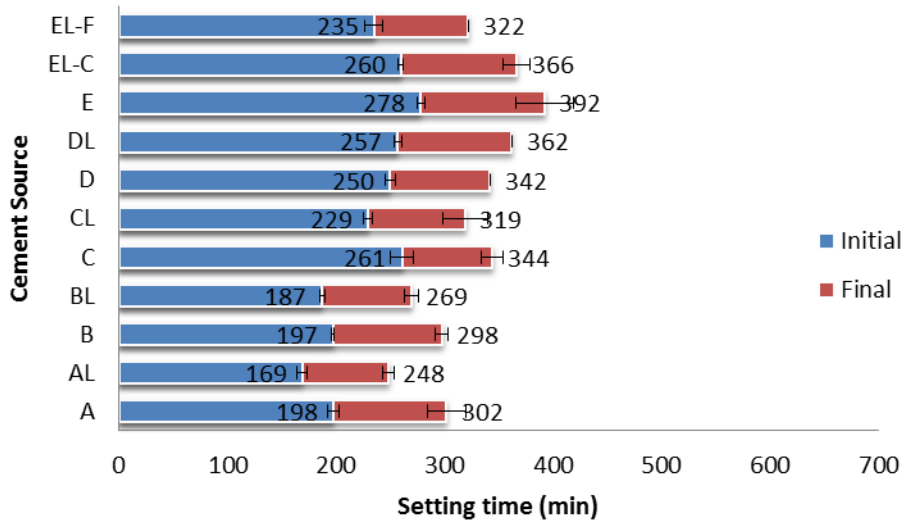
Figure 8.11: Time of setting of cements A to E with 15% fly ash Class C at 73 °F

157

In general, Class F showed faster setting than Class C (~14% average). This is believed to be due to the higher fineness of Class F fly ash, as well as its potential for water adsorption due to its higher LOI (loss-on-ignition) content.

Figure 8.12 and Figure 8.13 show the effect of calcite content on the setting time of pastes with 15% replacement by weight of cement with fly ash. The results show that higher calcite content led to faster setting time for both Classes of fly ash. However, low R^2 values indicate that other factors (such as fineness and chemical composition) also contribute to the observed behavior.
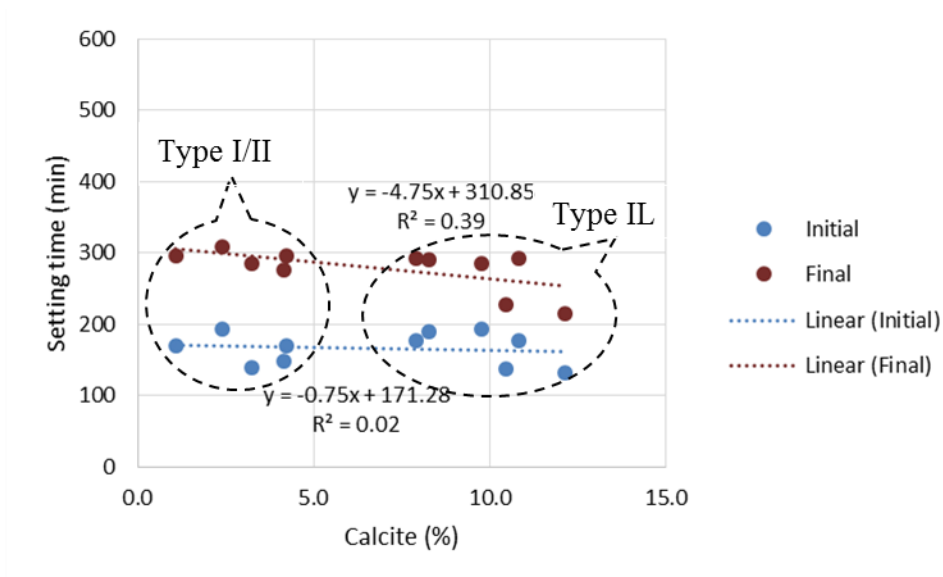
Figure 8.12: Effect of calcite content on the setting time of pastes with 15% Class F fly ash
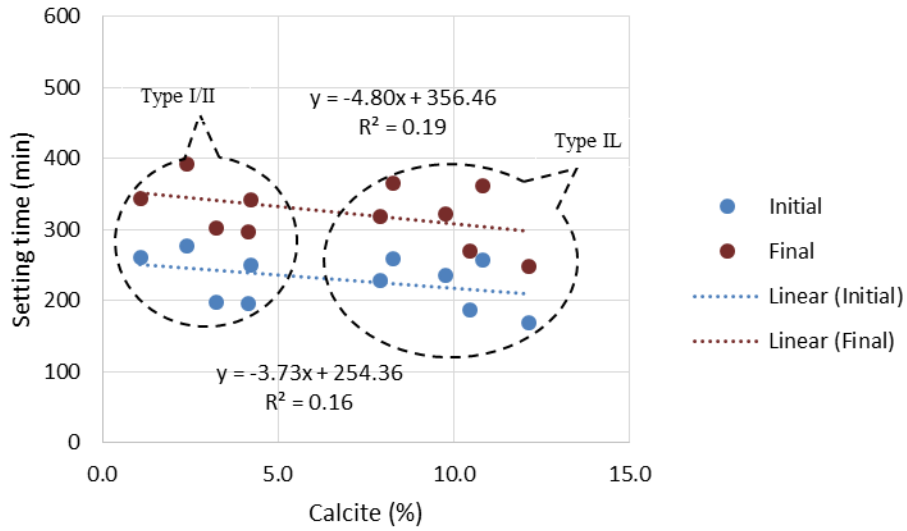
Figure 8.13: Effect of calcite content on the setting time of pastes with 15% Class C fly ash

8.3.4.2 Slag

Figure 8.14 shows the results of the time of setting for the group of samples with 50% slag from sources A to E tested at 73 °F.

The results show that Type IL cement showed relative similar setting times of Type I/II and Type IL cements (with one standard deviation). Slag was finer than all the cements, which had a dominant effect over the limestone replacement.
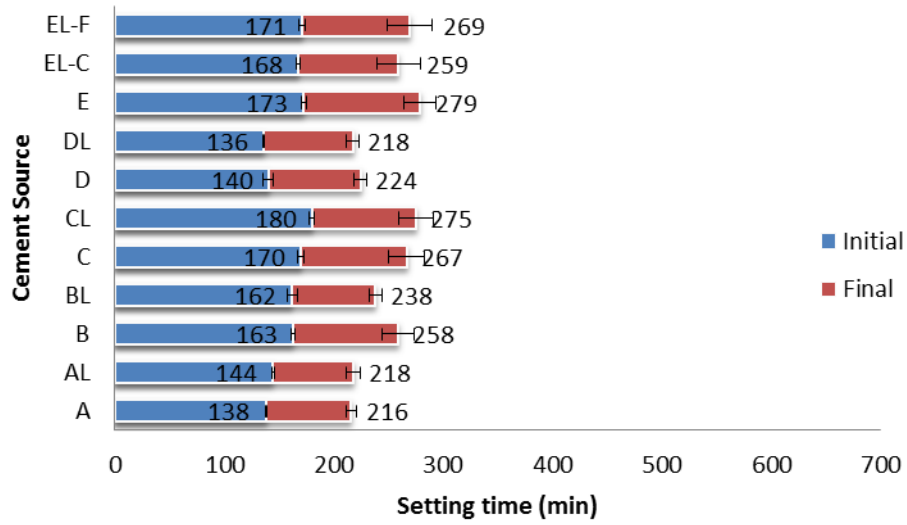
Figure 8.14: Time of setting of cements A to E with 50% slag at 73 °F

Figure 8.15 shows the effect of calcite content on the setting time of pastes with 50% replacement by weight of cement with slag. The results show that the calcite content had no significant effect on the setting time. However, low R^2 values indicate that other factors (such as fineness and chemical composition) also contribute to the observed behavior.
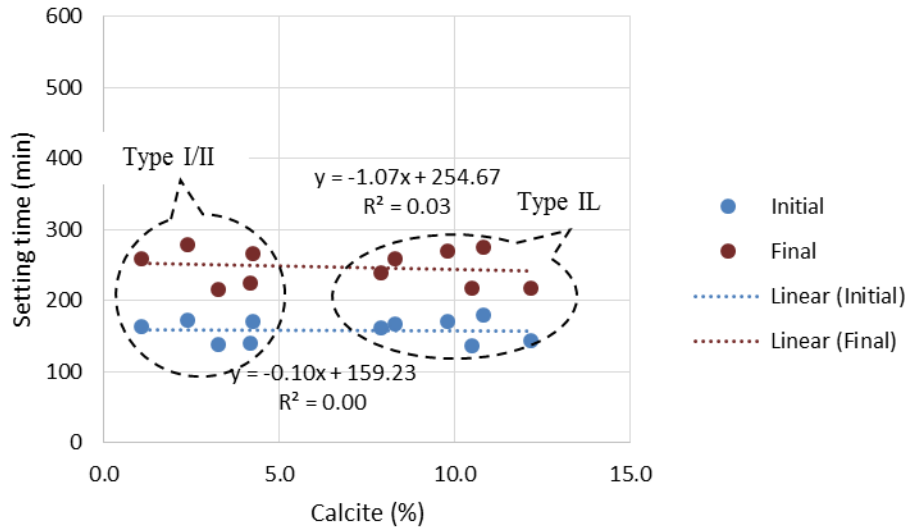
Figure 8.15: Effect of calcite content on setting time of cement pastes with 50% slag replacement

8.3.5 Mechanical properties

8.3.5.1 Compressive strength

Figure 8.16 shows the compressive strength values of Type I/II and Type IL cements from plant A with and without SCMs.
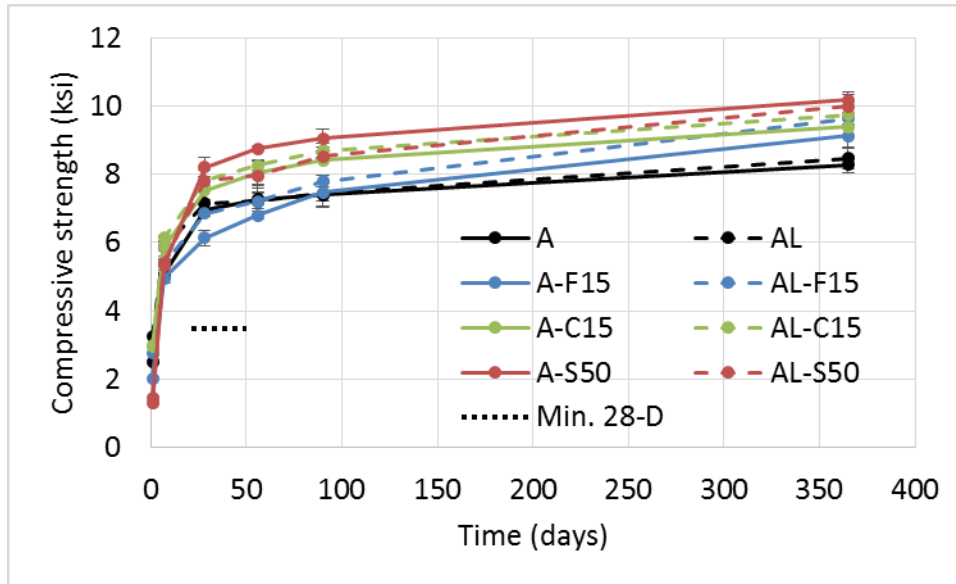
Figure 8.16: Compressive strength of Class AA concrete from plant A with SCMs

At one day, all SCM mixes showed lower compressive strength than the base mixes. The Class F fly ash and Class C fly ash mixes showed 10% to 20% lower strength than the base mixes, while the slag mixes showed ~50% lower strength than the base mixes. This was a result of the dilution of the cement by SCMs which do not participate in the compressive strength at early ages (due to the delay of the initiation of the pozzolanic reaction). Type IL showed higher strength than Type I/II with the Class F fly ash and slag mixes, but similar strength for the Class C fly ash mixes.

By 7 days, the strength of the SCM mixes caught up to and sometimes surpassed the base cement mixes; where the strength of the Class F fly ash and slag mixes was less than 10% lower than the strength of the base mixes, while the Class C fly ash mixes surpassed the strength of the base mixes which can be attributed to the hydraulic properties of Class C fly ash and the lower replacement percentage compared to slag.

AL-F15 showed higher strength than A-F15. Type I/II and Type IL showed similar values with Class C fly ash and slag mixes.

By one year, all the SCM mixes resulted in strength values higher than the base mixes, with the slag mixes showing the highest strength. The compressive strength values of Type I/II with SCMs were similar to the values of Type IL with SCMs (no statistically significant differences).

Figure 8.17 shows the compressive strength values of Type I/II and Type IL cements from plant C with and without SCMs.
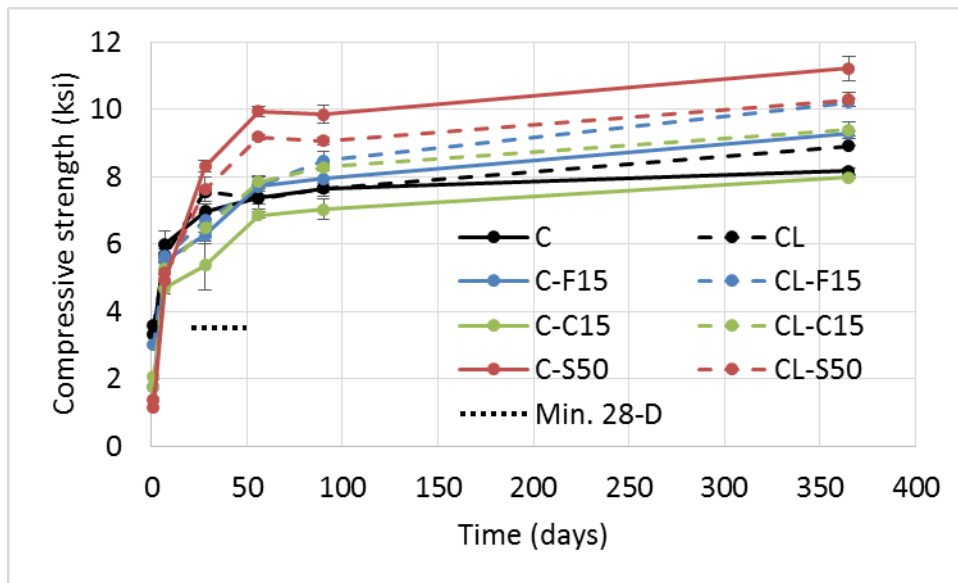
Figure 8.17: Compressive strength of Class AA concrete from plant C with SCMs

At one day, all SCM mixes showed lower compressive strength than the base mixes. The Class F fly ash and Class C fly ash mixes showed 50% lower strength than the base mixes (except for CL-F15 which showed 15% lower strength than CL), while the slag mixes showed 60% lower strength than the base mixes. This was a result of the

dilution of the cement by SCMs which do not participate in the compressive strength at early ages (due to the delay of the initiation of the pozzolanic reaction). In general, at one day, the differences between the SCM mixes and the base mixes were larger for plant C than plant A as a result of the largest average particle size of the cement particles.

By 7 days, the Class F fly ash mixes caught up to the base cement mixes; while Class C fly ash and slag mixes showed lower values than the base mixes. For the Class C fly ash and slag mixes, Type IL cement showed strength values that were closer to the base mixes (10% lower than the base mixes) than Type I/II cement did (20% lower than the base mixes). This indicates that limestone particles enhanced the nucleation effect with the SCM mixes.

By one year, all the SCM mixes resulted in strength values higher than the base mixes (except for Cement C with Class C fly ash, i.e. C-C15, which showed a similar strength to the base mix). The compressive strength of CL-F15 was higher than C-F15 (~15%). The C-C15 and CL-C15 mixes showed similar strength to the base mixes. For the slag mixes, the C-S50 and CL-S50 showed 35% and 15% higher compressive strength than the C and CL mixes, respectively. The difference was larger for Type I/II cement mainly due to the dilution effect as a result of the limestone replacement. All the SCM mixes showed either similar or higher strength than the base mixes, with the slag mixes showing the highest strength.

Figure 8.18 to Figure 8.20 show scatter plots of calcite content vs. the compressive strength of concrete at 1 day, 28 days, and 1 year for the Class F fly ash, Class C fly ash, and slag mixes, respectively. After applying a linear regression best fit line, it can be seen that the higher the calcite content, the larger the compressive strength

for the fly ash mixes. However, the 1 year strength of the slag mixes is lower with higher

calcite content. The nucleation effect was more dominant in the fly ash mixes, due to the

larger particle size of the fly ash. However, the dilution effect was more dominant for the

slag mixes due to the smaller particle size of the slag. Low R^2 values indicate that other

factors (such as fineness and chemical composition) also contribute to the observed

behavior.
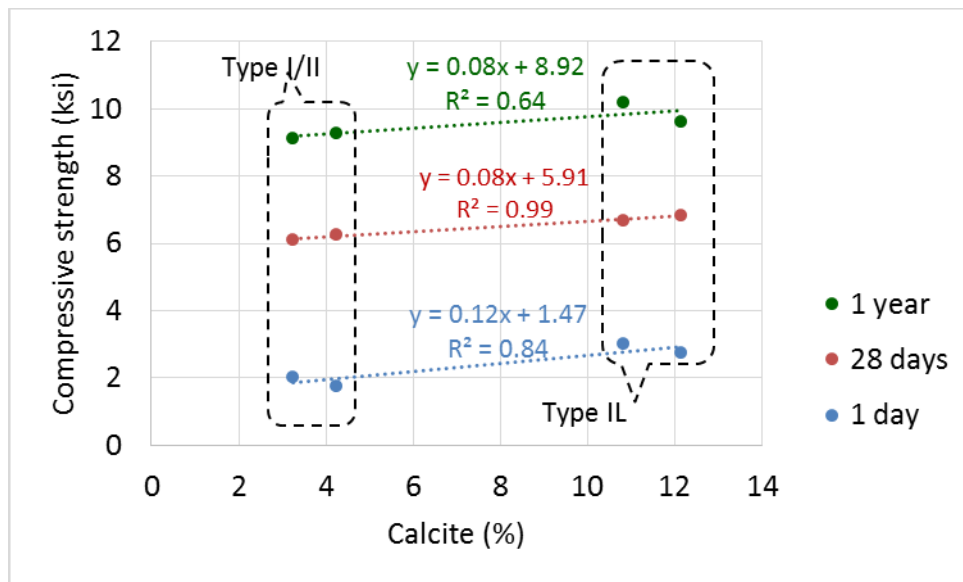
Figure 8.18: Effect of calcite content on compressive strength of concrete with Class F
fly ash
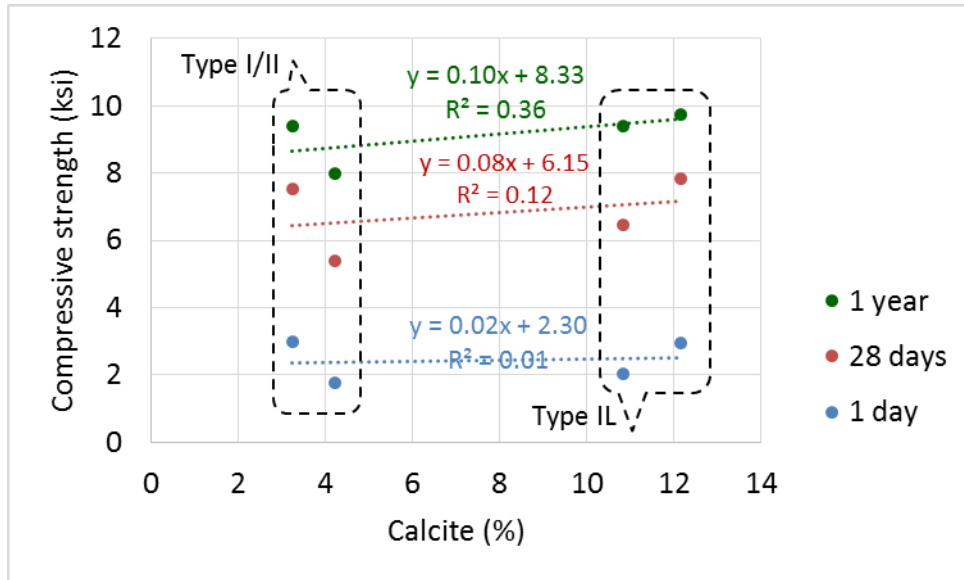
Figure 8.19: Effect of calcite content on compressive strength of concrete with Class C fly ash
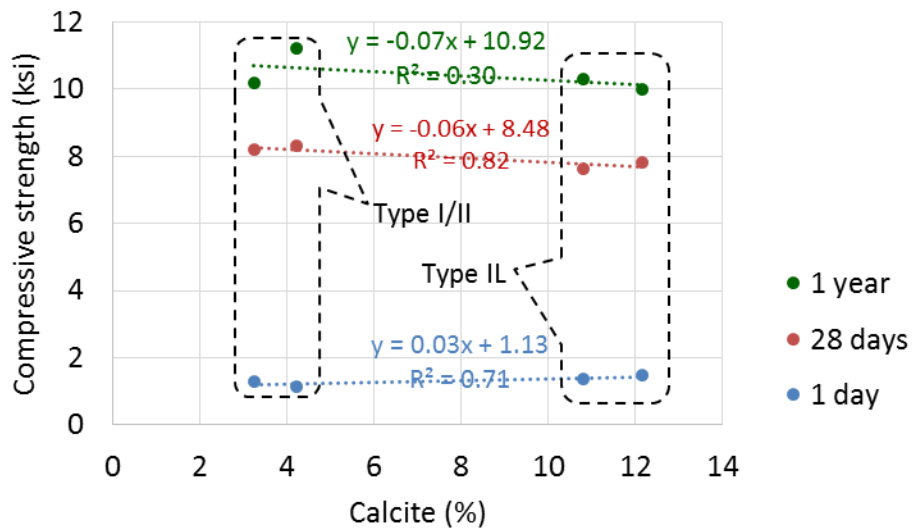
Figure 8.20: Effect of calcite content on compressive strength of concrete with slag

Analysis of variance (ANOVA) was conducted to investigate the statistical significance of the difference in values of the compressive strength of Type I/II and Type

IL cement of plants A and C. The null (no difference) hypothesis was that average strength of Type I/II and Type IL are similar ($\mu1=\mu2$). A summary of the results for Class F fly ash mixes is shown in Table 8.5. Accepting the null hypothesis indicates that there is no statistical significance in the difference between the strength of Type I/II and Type IL cement while rejecting the null hypothesis indicates that there is a significant statistical difference between the strength of Type I/II and Type IL cement.

Table 8.5: ANOVA results for comparing Type I/II and Type IL cements from each plant
for the compressive strength of the Class F fly ash mixes
(null hypothesis, strength of Type I/II = strength of Type IL, "Similar": $\mu1=\mu2$)

Time	Cement source and SCM			
	A/AL (no SCM)	A/AL + Class F fly ash	C/CL (no SCM)	C/CL + Class F fly ash
7 days	Different	Different	Similar	Similar
28 days	Similar	Different	Different	Different
1 year	Similar	Similar	Different	Different

The results showed that for early-age strength, the Class F fly ash mixes with finer Type IL cement (AL-F15) resulted in statistically higher strength when compared to the values of mix with the companion Type I/II (A-F15). The coarser Type IL cement, CL-F15, resulted in statistically higher strength at one year than C-F15. This indicates that for the Class F fly ash mixes, the finer limestone cement resulted in higher strength at early age, while the coarser limestone cement resulted in higher strength at one year.

Table 8.6 shows the results of ANOVA for Class C fly ash mixes, as well as the ANOVA results of the base mixes from plants A and C for comparison (discussed in Chapter 6). The results showed that the Class C fly ash mixes with the finer Type IL cement (AL-C15) resulted in small differences that were not statistically significant when

167

compared to the Class C fly ash mixes with the companion Type I/II cement (A-C15). However, the Class C fly ash mixes with the coarser Type IL cement (CL-C15) resulted in statistically higher strength when compared to the Class C fly ash mixes with the companion Type I/II cement (C-C15). When compared to the base mixes (without SCMs), the main difference in behavior was observed at early age (7 days) where the Class C fly ash decreased the differences between A and AL (finer) resulting in statistically similar strength, while it increased the differences between C and CL (similar fineness) where CL-C15 showed statistically higher strength.

Table 8.6: ANOVA results for comparing Type I/II and Type IL cements from each plant for the compressive strength of the Class C fly ash mixes
(null hypothesis, strength of Type I/II = strength of Type IL, "Similar": $\mu 1 = \mu 2$)

Time	Cement source and SCM			
	A/AL (no SCM)	A/AL + Class C fly ash	C/CL (no SCM)	C/CL + Class C fly ash
7 days	Different	Similar	Similar	Different
28 days	Similar	Similar	Different	Different
1 year	Similar	Similar	Different	Different

Table 8.7 shows the results of ANOVA for slag mixes, as well as the ANOVA results of the base mixes from plants A and C for comparison (discussed in Chapter 6). The results showed that the slag mixes with the finer Type IL cement (AL-S50) resulted in small differences that were not statistically significant when compared to the slag mixes with the companion Type I/II cement (A-S50). However, the slag mixes with the coarser Type IL cement (CL-S50) resulted in statistically lower strength than the mix with Type I/II cement (C-S50).

168

Table 8.7: ANOVA results for comparing Type I/II and Type IL cements from each plant
for the compressive strength of the slag mixes
(null hypothesis, strength of Type I/II = strength of Type IL, "Similar": μ1=μ2)

Time	Cement source and SCM			
	A/AL (no SCM)	A/AL + slag	C/CL (no SCM)	C/CL + slag
7 days	Different	Similar	Similar	Similar
28 days	Similar	Different	Different	Different
1 year	Similar	Similar	Different	Different

8.3.5.2 Elastic modulus

Elastic modulus was measured for concrete cylinders (6 in. x 12 in.) at 28 days of age (ASTM C469). Figure 8.21 and Figure 8.22 show the elastic moduli of cements from plant A and plant C, respectively, with SCMs. All mixes showed relatively similar values to the base mixes. The figures also show the predicted values calculated using Equation 6.2 (from ACI 363R-10 [85]),

$$E = 40\sqrt{f_c'} + 10^3 \qquad \text{Equation 6.2}$$

The values obtained using Equation 6.2 were higher than all of the experimental values indicating that the equation over estimates the 28-day elastic modulus of the concretes made with SCMs.
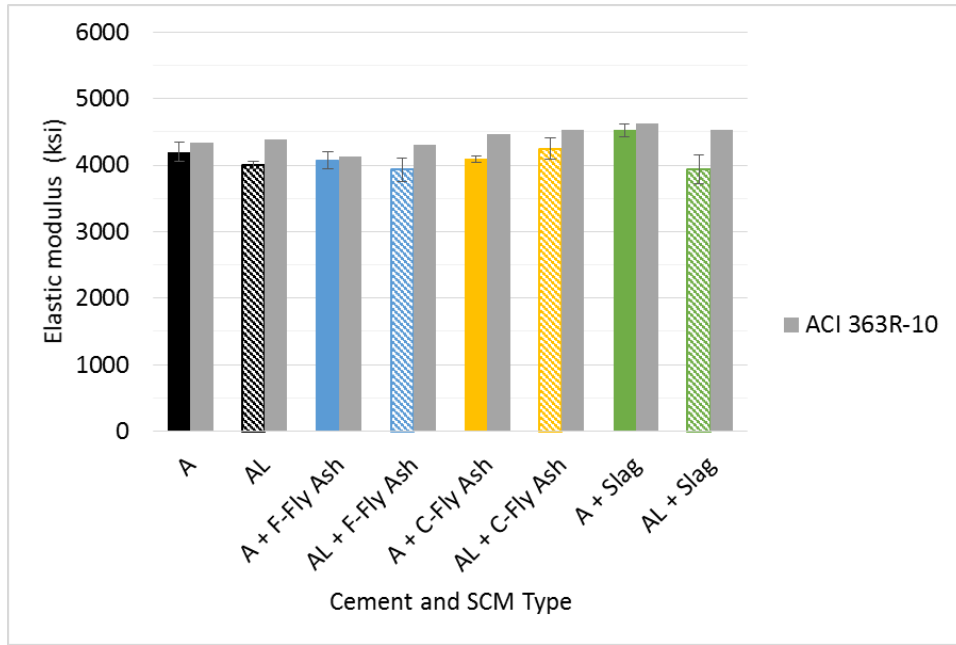
Figure 8.21: Comparison of concrete elastic modulus values for plant A and SCMs with ACI 363R-10 predicted values
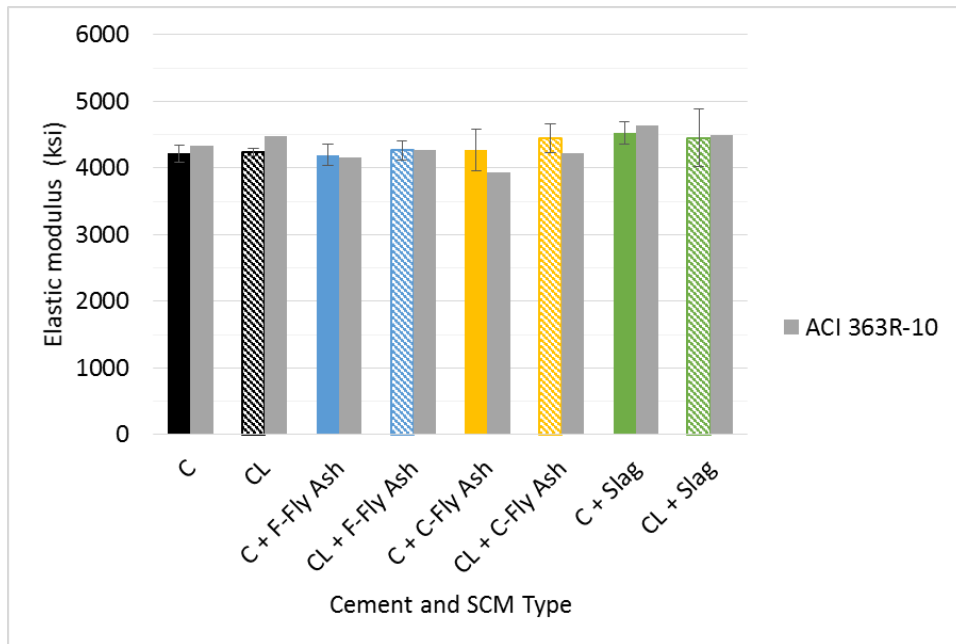
Figure 8.22: Comparison of concrete elastic modulus values for plant C and SCMs with ACI 363R-10 predicted values

Figure 8.23 shows a scatter plot of calcite content vs. the elastic modulus of the SCM mixes and the base mixes of cements from plants A and C. After applying a linear regression best fit line, the general trend seen is that the higher the calcite content, the lower the elastic modulus. The exception to this trend was the mixes with the Class C fly ash where higher calcite content corresponded with slightly higher elastic modulus. One possible reason for the behavior of the Class C fly ash mixes is the hydraulic behavior of the Class C fly ash. A second explanation is related to the low fineness of Class C fly ash, where the finer limestone particles increased the nucleation sites and, therefore, enhanced the pozzolanic and hydration reactions of Class C fly ash with higher limestone content. Low R^2 values indicate that other factors (such as fineness and chemical composition) also contribute to the observed behavior.
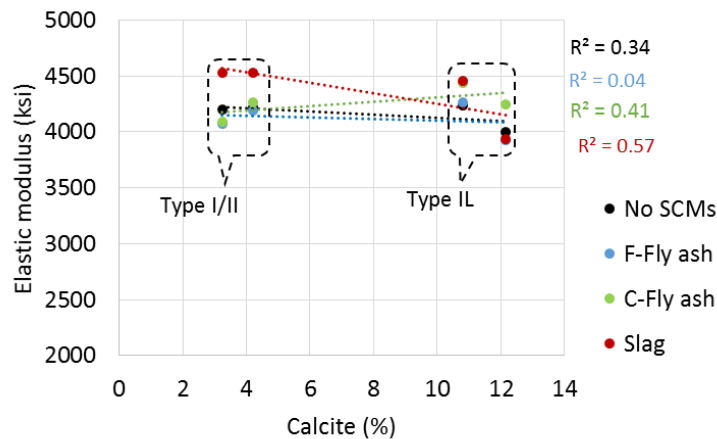
Figure 8.23: Effect of calcite content on elastic modulus of concrete with SCMs

8.3.5.3 Splitting tensile strength

Splitting tensile strength [ASTM C496, AASHTO T 198] was measured for concrete samples (4 in. x 8 in.) at 28 days of age. Figure 8.24 and Figure 8.25 show the

171

splitting tensile strength values of cements from plant A and plant C, respectively, with SCMs. The figures also show the calculated values computed using Equation 6.3 obtained from ACI 363R-10 (equation 6-13 in ACI 363R-10 section 6.6) which was discussed in Chapter 6:

$$f_{sp} = 7.4\sqrt{f'_c}$$
<div align="right">Equation 6.3</div>

where:

- f_{sp} = splitting tensile strength (psi)
- f_c' = compressive strength (psi)

For plant A (Figure 8.24), all SCM mixes showed lower splitting tensile strength than the base mixes. The Class F fly ash mixes showed ~30% lower strength than the base mixes, and the Class C fly ash mixes showed ~20% lower strength than the base mixes. For the fly ash mixes, Type I/II and Type IL showed relatively similar values. For the slag mixes, Type IL showed ~30% lower tensile strength than Type I/II. Cement AL as well as slag have small particle size. The small particle size of slag did not enhance the nucleation effect that was present due to the small limestone particles. The dilution effect was more dominant for the slag mix.
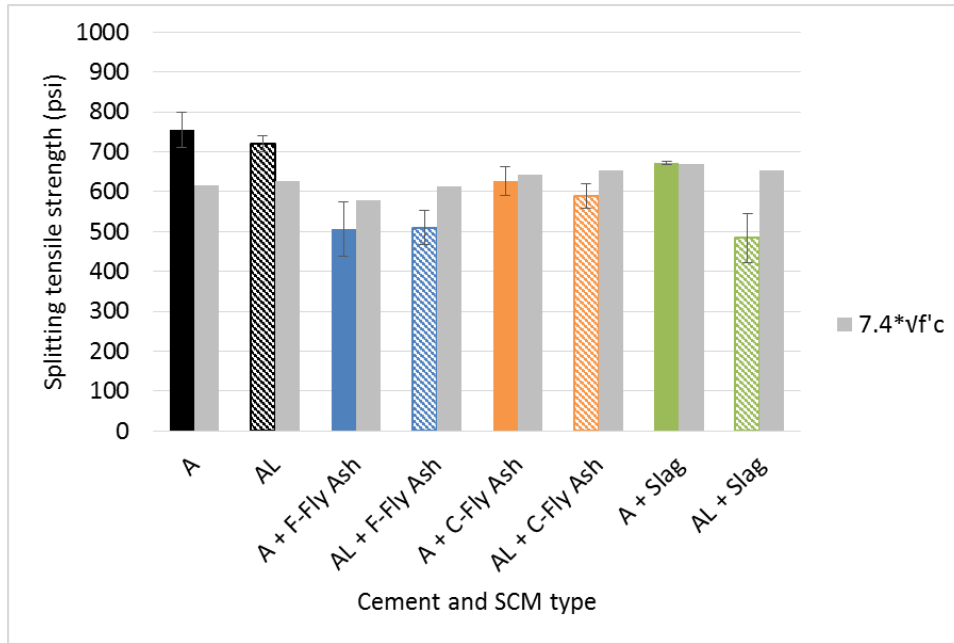
Figure 8.24: Splitting tensile strength of Type I/II and Type IL cements from plant A with SCMs.

When comparing the measured values to the calculated values (Equation 6.3), the measured values of the SCM mixes with Type IL cement showed lower values than the calculated ones, suggesting that that such relations do not hold for SCM mixes with finer Type IL cement.

For plant C (Figure 8.25), the fly ash mixes showed lower splitting tensile strength than the base mixes while the slag mixes showed relatively similar values to the base mixes. For Class F fly ash and Class C fly ash mixes, Type I/II cement with fly ash showed relatively similar values to the base mix while Type IL with fly ash showed ~15% lower strength than the base mix. This implies that the dilution effect is more dominant for the fly ash mixes with cements from plant C (due to the relatively larger size of cement C and CL). The slag mixes showed relatively similar values to the base mixes.

173
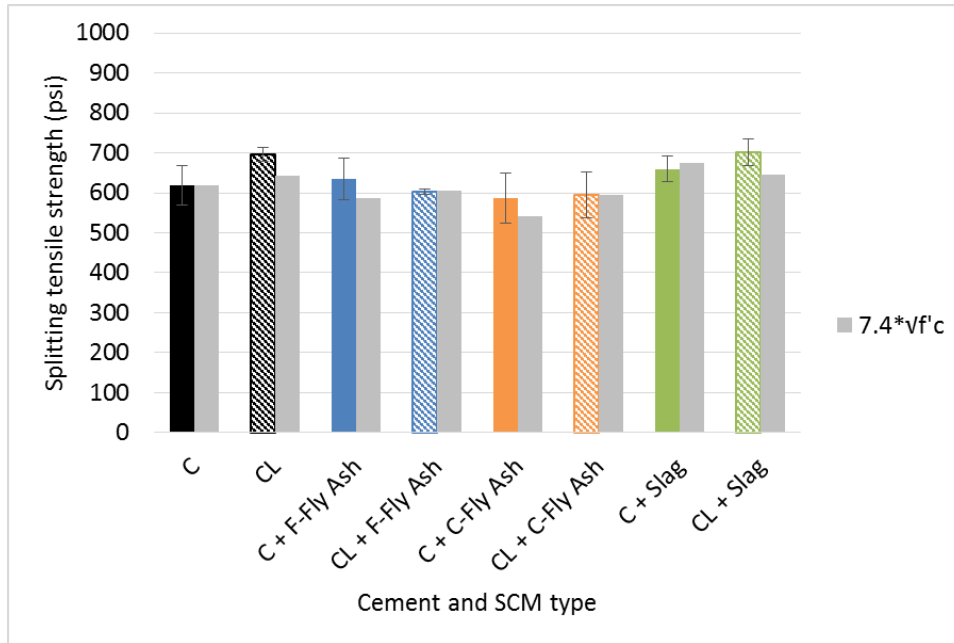
Figure 8.25: Splitting tensile strength of Type I/II and Type IL cements from plant C with SCMs

For plant C, the values obtained using Equation 6.3 were relatively similar to the experimental values. This indicates that Equation 6.3 was a good estimate of the tensile strength of concrete made with coarser limestone cement and SCMs.

Figure 8.26 shows a scatter plot of calcite content vs. the splitting tensile strength of the SCM mixes and the base mixes of cements from plants A and C. After applying a linear regression best fit line, it can be seen that the scatter was large, but a trend can be observed for the slag mixes where larger calcite content resulted in lower tensile strength. Low R^2 values indicate that other factors (such as fineness and chemical composition) also contribute to the observed behavior.
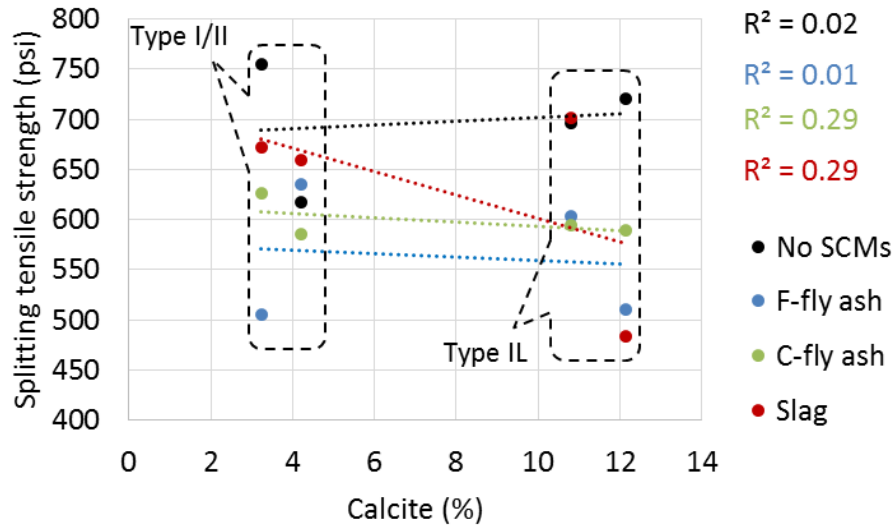
Figure 8.26: Effect of calcite content on the splitting tensile strength of concrete with SCMs

8.3.6 Drying shrinkage

The results of drying shrinkage measurements for the concrete mixes with SCMs are discussed below.

8.3.6.1 Class F fly ash

Figure 8.27 shows the drying shrinkage values of Class AA concrete made with Type I/II and Type IL cements from plants A and C compared to mixes with 15% cement replacement (by weight) with Class F fly ash.

For plant A, using 15% Class F fly ash resulted in similar drying shrinkage values of Type I/II and Type IL. When compared to the base mixes, using 15% Class F fly ash reduced the drying shrinkage of Type I/II by 15% and Type IL by 25%.

For plant C, using Class F fly ash resulted in relatively similar drying shrinkage values for Type I/II and Type IL cements.

(a) Plant A   (b) Plant C
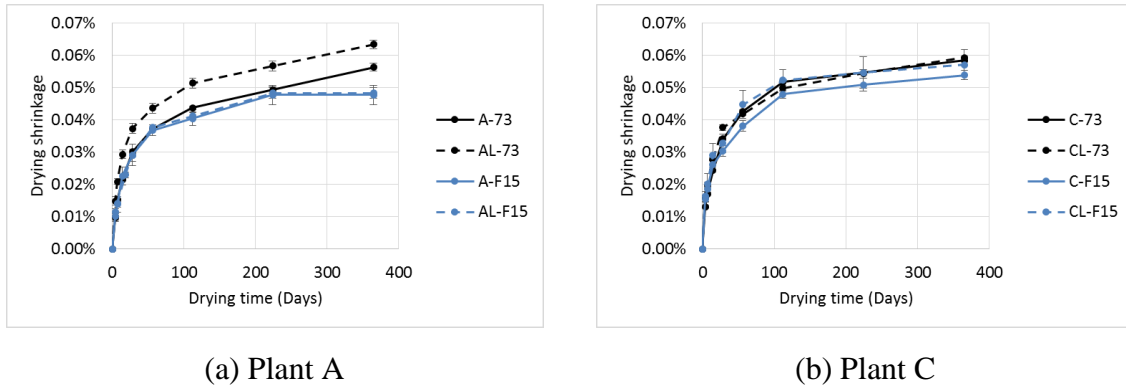
Figure 8.27: Drying shrinkage of Type I/II and Type IL cements with 15% Class F fly ash replacement compared to base mixes

Analysis of variance (ANOVA) was conducted to investigate the statistical significance of the difference in values of the drying shrinkage of Type I/II and Type IL cement of plants A and C when used with Class F fly ash in concrete. The null (no difference) hypothesis was that average drying shrinkage of Type I/II and Type IL are similar ($\mu 1=\mu 2$). A summary of the results for the Class F fly ash mixes is shown in Table 8.8. Accepting the null hypothesis indicates that there is no statistical significance in the difference between the drying shrinkage of Type I/II and Type IL cement while rejecting the null hypothesis indicates that there is a significant statistical difference between the drying shrinkage of Type I/II and Type IL cement.

Table 8.8: ANOVA results for comparing Type I/II and Type IL cements from each plant for the drying shrinkage of Class F fly ash mixes
(null hypothesis, concrete shrinkage with Type I/II = concrete shrinkage with Type IL, "Similar": μ1=μ2)

Time	Concrete mixes compared	
	A-F15 and AL-F15	C-F15 and CL-F15
7 days	Similar	Similar
28 days	Similar	Similar
1 year	Similar	Similar

The results of ANOVA show that the difference in drying shrinkage between Type I/II and Type IL cements were not statistically significant at all ages.

8.3.6.2 Class C fly ash

Figure 8.28 shows the drying shrinkage values of Class AA concrete made with Type I/II and Type IL cements from plants A and C compared to mixes with 15% cement replacement (by weight) with Class C fly ash.

For plant A, using Class C fly ash resulted in higher drying shrinkage of Type IL than Type I/II (~10% at 1 year). When compared to the base mixes, using 15% Class C fly ash resulted in slightly lower drying shrinkage than the base mixes (~7% at 1 year).

For plant C, using 15% Class C fly ash resulted in lower drying shrinkage of Type IL than Type I/II (~15%). When compared to the base mixes (i.e. without SCMs), using 15% Class C fly ash resulted in higher drying shrinkage for Type I/II (~15%) than the base mix, while Type IL cement showed higher values during the first month (17% at 4 weeks) but then showed 7% lower shrinkage than the mix without the fly ash at 1 year.

177
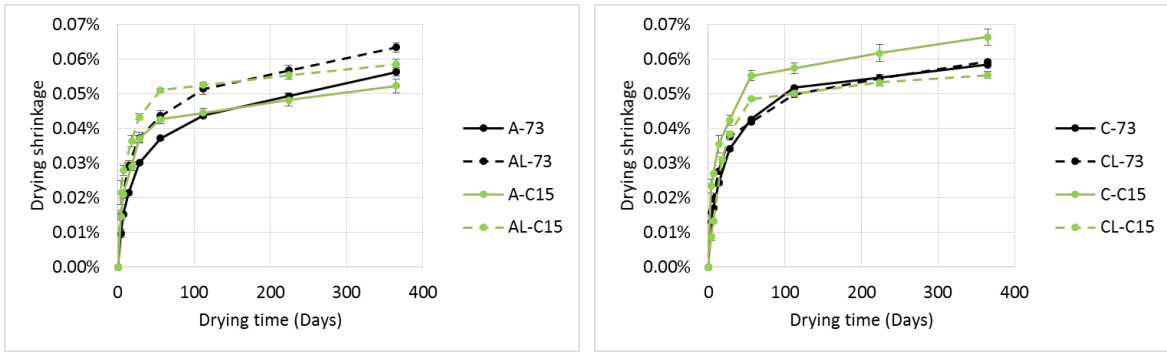
(a) Plant A (b) Plant C

Figure 8.28: Drying shrinkage of Type I/II and Type IL cements with 15% Class C fly ash replacement compared to base mixes

Comparing early age drying shrinkage behavior of the Class C fly ash mixes with the Class F-fly ash mixes (shown in Figure 8.29), the particle size seems to have a significant effect. At 7 days, cement A and AL with Class C fly ash showed 35% higher drying shrinkage than the base mixes. Cement C with Class C fly ash showed 60% higher drying shrinkage than the base mix, while cement CL with Class C fly ash showed similar drying shrinkage to the base mix, indicating that the limestone in cement CL decreased the early age shrinkage when using Class C fly ash.
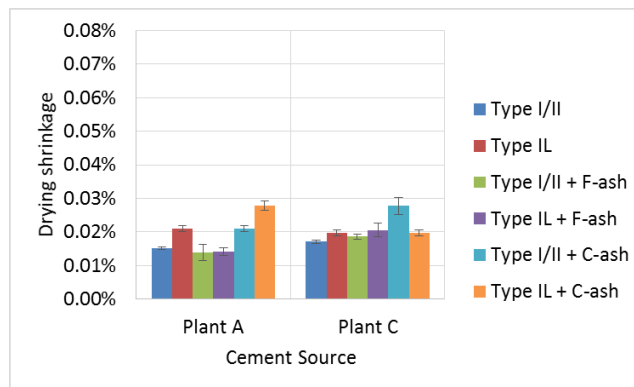
Figure 8.29: Drying shrinkage values at 7 days

Comparing the shrinkage at 1 year (shown in Figure 8.30), Class F fly ash decreased the drying shrinkage for both cements. The difference when compared to the base mixes was higher for plant A than plan C (~20% and ~5%, respectively). Class C fly ash reduced the shrinkage for A, AL, and CL (~7%) but increased the 1 year shrinkage of cement C (~15%).
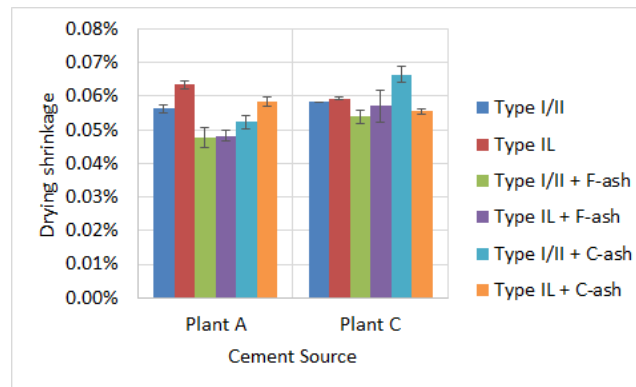
Figure 8.30: Drying shrinkage values at 365 days

Analysis of variance (ANOVA) was conducted to investigate the statistical significance of the difference in values of the drying shrinkage of Type I/II and Type IL cement of plants A and C when used with Class C fly ash in concrete. The null (no difference) hypothesis was that average drying shrinkage of Type I/II and Type IL are similar ($\mu1=\mu2$). A summary of the results for the Class C fly ash mixes is shown in Table 8.9. Accepting the null hypothesis indicates that there is no statistical significance in the difference between the drying shrinkage of Type I/II and Type IL cement while rejecting the null hypothesis indicates that there is a significant statistical difference between the drying shrinkage of Type I/II and Type IL cement.

Table 8.9: ANOVA results for comparing Type I/II and Type IL cements from each plant
for the drying shrinkage of Class C fly ash mixes
(null hypothesis, drying shrinkage of Type I/II = drying shrinkage of Type IL, "Similar":
$\mu1=\mu2$)

Time	Concrete mixes compared	
	A-C15 and AL-C15	C-C15 and CL-C15
7 days	Different	Different
28 days	Different	Different
1 year	Different	Different

The results of ANOVA show that the difference in drying shrinkage between Type I/II and Type IL cements were statistically significant at all ages. One reason is that Class C fly ash was coarser than Class F fly ash; and since the limestone particles in Type IL cement tend to be of higher fineness, more nucleation sites were available for the Class C fly ash to enhance the hydraulic reaction. Cement AL had a higher fineness than cement CL, and therefore mix AL-C15 showed higher shrinkage than mix CL-C15. Limestone particles tend to be of higher fineness than clinker particles because limestone is softer than clinker and therefore the inter-grinding process would lead the limestone particles to be smaller in size [114].

8.3.6.3 Slag

Figure 8.31 shows the drying shrinkage values of Class AA concrete made with Type I/II and Type IL cements from plants A and C compared to mixes with 50% cement replacement (by weight) with slag.

For plant A, using 50% slag resulted in similar drying shrinkage values for A-S50 and AL-S50 mixes. When compared with base mixes, using 50% slag resulted in lower drying shrinkage values for Type I/II and Type IL (19% and 27%, respectively).

For plant C, using 50% slag resulted in 8% lower drying shrinkage values for CL-S50 when compared to C-S50. When compared with base mixes, using 50% slag resulted in lower drying shrinkage values for Type I/II and Type IL (~5% and ~15%, respectively).

(a) Plant A   (b) Plant C
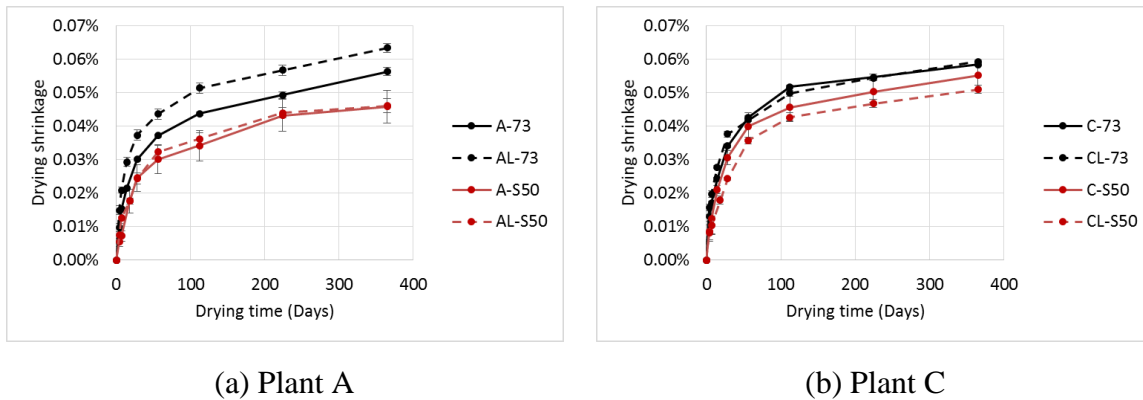
Figure 8.31: Drying shrinkage of Type I/II and Type IL cements with 50% slag replacement compared to base mixes

Analysis of variance (ANOVA) was conducted to investigate the statistical significance of the difference in values of the drying shrinkage of Type I/II and Type IL cement of plants A and C when used with Class C fly ash in concrete. The null (no difference) hypothesis was that average drying shrinkage of Type I/II and Type IL are similar ($\mu 1=\mu 2$). A summary of the results for the slag mixes is shown in Table 8.10. Accepting the null hypothesis indicates that there is no statistical significance in the difference between the drying shrinkage of Type I/II and Type IL cement while rejecting

the null hypothesis indicates that there is a significant statistical difference between the drying shrinkage of Type I/II and Type IL cement.

Table 8.10: ANOVA results for comparing Type I/II and Type IL cements from each plant for the drying shrinkage of slag mixes
(null hypothesis, drying shrinkage of Type I/II = drying shrinkage of Type IL, "Similar": $\mu 1 = \mu 2$)

Time	Concrete mixes compared	
	A-S50 and AL-S50	C-S50 and CL-S50
7 days	Different	Similar
28 days	Similar	Different
1 year	Similar	Similar

The results of ANOVA show that when blended with slag, AL-S50 showed higher shrinkage than A-S50 at 7 days, while C-S50 and CL-S50 showed similar drying shrinkage. This indicates that when finer Type IL cement (AL) was blended with slag, the result was a larger drying shrinkage at early age which is not favorable, and therefore it is not recommended to use finer Type IL cement with slag for applications where low early age drying shrinkage is required. The ANOVA results showed similar shrinkage values of the slag mixes at 1 year.

8.4   Discussion

The primary objective of this segment of the research effort was to better understand how interactions between limestone-blended cements and alumina-containing SCMs affect the early-age hydration processes and microstructural development of PLC-SCM blended systems. The results indicate that each SCM interacts with Type IL cement

182

in a way that uniquely affects the hydration and microstructural development of the PLC-SCM blend.

The Class F fly ash was observed to have the smallest effect on hydration, early-age shrinkage, and compressive strength development. Aside from a slight, 10 min retardation, which can be attributed to a dilution effect and to the coarser particle size distribution of the fly ash, the differences between the rates of hydration of the fly ash-blended and the neat cement pastes over the first 72 hr were found to be minimal. The primary difference observed was a slight increase in the isothermal heat released by the C_3A hydration and a general extension of the reaction time by 1-2 hr, but the same effect was observed for both the Type I/II and Type IL blends. Cumulative heat and chemical shrinkage for the Class F fly ash blends were both reduced by 10% at 3 and 7 days, respectively, indicating that the 15% replacement of cement by Class F fly ash had a primarily diluting role during the first 7 days of hydration. It was not until 14 days that the normalized autogenous shrinkage began to differ significantly from the control pastes, indicating that the secondary pozzolanic reaction of the Class F fly ash does not initiate – and therefore does not have any effect on microstructural development – until that age. Based on the relative autogenous shrinkages and compressive strengths, it is believed that the extent of the pore refinement in the Class F fly ash-blended materials is small, as the increases in normalized autogenous shrinkage and compressive strength were within the expected variability of each test performed. Synergetic interactions between the limestone and Class F fly ash were likewise considered to have a minimal effect on the hydration and microstructural development of the PLC blends at the particular *w/b* and fly ash dosage investigated, based on the observation that differences between the Type

183

I/II and Type IL blends were either within the expected variability of the test methodologies or were consistent with the differences already observed for the neat cement mixtures. Overall, it was found that substituting either cement with 15% Class F fly ash was an effective method of decreasing the early-age heat of hydration and chemical and autogenous shrinkage while still producing concrete of equivalent compressive strength to the control mixtures.

Compared to the Class F fly ash, the Class C fly ash was observed to have a more pronounced effect on hydration, early-age shrinkage, and compressive strength development as a result of the Class C's pozzolanic and hydraulic reactivity. Blends containing Class C fly ash released more heat and exhibited significantly more chemical shrinkage in the first 3-7 days of hydration compared to the blends containing Class F fly ash, suggesting that even at early ages, the hydraulic properties of the Class C fly ash enable it to participate in the hydration and microstructural development of the cement pastes. Between 7 and 14 days of hydration, the pozzolanic reactivity of the Class C fly ash initiates, as evidenced by a relative increase in the normalized autogenous shrinkage for those cement pastes. The pozzolanic reaction appears to occur 3-7 days sooner for the Type IL pastes than for the Type I/II pastes, suggesting that chemical interactions between the limestone and the Class C fly ash accelerate the onset of secondary reactions in PLC-fly ash blends and produce concretes with more refined porosities at earlier ages than PC-fly ash blends do. While refinements in porosity were observed to contribute to increases in the rate of compressive strength development, they were also observed to contribute to significant increases in autogenous shrinkage, such that blends of PLCs with

Class C fly ashes may be less desirable than blends of PLCs with Class F fly ashes for applications where early-age cracking is to be avoided.

With respect to the slag replacement, it was observed that the 50% replacement of both cements with blast furnace slag had significant – and significantly varied – impacts on the hydration, early-age shrinkage, and compressive strength development of the PC and PLC blends. The hydraulic reactivity of the slag was observed within just a few hours of hydration in the normalized calorimetric heat profiles, which indicated significant increases in the rate and amount of heat evolved in blends containing 50% slag. These hydraulic effects led to an increase in the relative rate of chemical shrinkage within the first few days of hydration, such that the 50% reduction in cement content only reduced chemical shrinkage by 9% at 7 days, compared to the 50% reduction that would be expected from substitution with a chemically inert filler. Changes to the intensity and shape of the calorimetric C_3A peak in blends containing Type IL cements pointed to limestone-slag interactions occurring within the first few hours of hydration, which resulted in a more than two-fold increase in autogenous shrinkage for Type IL blends compared to the Type I/II blends when normalized by the cement fraction in the binder. Such increases suggest substantial reductions in the average pore size of Type IL-slag blends as a result of these chemical interactions, but these hypothesized reductions did not result in further increases in compressive strength. Instead, it was observed that the Type IL-slag concretes had slightly reduced compressive strengths when compared to their Type I/II counterparts, possibly indicating that the extent of their microstructural development is less than suggested by their autogenous shrinkage. Since autogenous shrinkage additionally depends on the surface tension of the pore solution, it is possible

185

that the changes to the pore solution by the substitution of cement with 10% limestone and 50% slag had a significant impact on its surface tension, as well, but further investigation is required.

Finally, it appears as though the different alumina loadings of the SCMs had no direct relationship to the synergetic limestone-SCM interactions observed. It had been predicted that the Class F fly ash and slag, which added the largest amounts of alumina to the cementitious binder, would have a more noticeable interaction with the limestone than the Class C fly ash, which added 20% less alumina. However, while all three SCMs exhibited some synergetic interaction with the limestone, the relative magnitudes of the increased strengths and autogenous shrinkage were greater for the mixes containing slag and Class C fly ash than for the mixes containing Class F fly ash. One possible explanation for these observed differences could be that the limestone synergies are not strictly related to the amount of reactive alumina in the SCMs, but also to their relative rates of reaction. The slag, which showed significant hydraulic reactivity within the first few hours, also showed the clearest differences between the hydration and early-age shrinkage of the Type I/II and Type IL blends, while the Class F fly ash, which showed slow pozzolanic reactivity only after 14 days of hydration, also showed the smallest differences in autogenous shrinkage and compressive strength development for the Type I/II and Type IL blends. Recent research by Puerta-Falla, et al., [107] supports this hypothesis by demonstrating that the source of the alumina plays a significant role in the synergetic interactions exhibited between limestone and SCMs. The results of this study propose an extension to their findings, suggesting that it is not strictly the source of the alumina but also the reactivity of the source that influences the nature of the limestone-

186

SCM interactions. Further research looking at the reaction rates of limestone with alumina sourced from various SCMs would be needed to investigate this hypothesis more fully.

8.5   Conclusions

The results of this study demonstrate that blends of Type IL cements with SCMs can be suitably used as replacements for Type I/II cements in construction applications. Despite the dilution of the cement by the limestone filler, equivalent or more refined porosities – resulting in equivalent or higher strengths – can be achieved when Type IL cements are partially substituted with 15% fly ash or 50% slag, by mass. Chemical interactions between the PLCs and both Class C and F fly ashes were found to increase compressive strength by 56 days relative to blends of ordinary portland cement and fly ash, supporting the "synergetic" PLC-SCM interactions previously established in the literature. While blends of Type IL cements with 15% Class C fly ash were able to achieve higher strengths at 56 days when compared to the Type I/II control mixtures, the increases in strength came at the expense of increased chemical and autogenous shrinkage at early-ages, which could increase cracking in structural applications. By contrast, blends of Type IL cements with 15% Class F fly ash were found to provide the best balance in properties, slightly increasing compressive strength by 56 days, while still reducing early-age chemical and autogenous shrinkage. Such mixes are recommended for use in construction applications, pending further investigating into their long-term durability (Chapter 7).

Blends of PLCs with 50% slag did not show the same synergetic increases in compressive strength as the blends with 15% fly ash did, but still showed substantial increases in compressive strength relative to the Type I/II concretes. While blends of Type I/II cements with slag were found to dramatically reduce the autogenous shrinkage exhibited by the cement paste, no such shrinkage-mitigating effects were found for blends of Type IL cements with slag, believed to be due to the chemical interactions between the limestone and the slag. Based on the pronounced influence of the limestone on the autogenous shrinkage of the 50% slag mixes, it is recommended that lower slag replacement levels be considered for structural concretes containing Type IL cements.

The effect of several parameters on the compressive strength was investigated. It was found that the higher calcite content, the greater the compressive strength of the fly ash mixes. The slag mixes showed lower strength with higher calcite content, which may be a result of the higher cement replacement used for slag mixes.

For the elastic modulus, it was found that the higher calcite content, the lower the elastic modulus of the Class F fly ash and slag mixes. While the for the Class C fly ash mixes, higher calcite content resulted in higher elastic moduli values.

For the splitting tensile strength, it was found that SCM mixes with finer Type IL cement resulted in lower splitting tensile strength than coarser Type IL. Also, as the calcite content in SCM mixes increased, the splitting tensile strength slightly decreased.

For drying shrinkage of concrete, it was found that Type I/II and Type IL cements blended with Class F fly ash or slag resulted in similar drying shrinkage values at one year, but lower than the values of the base Type I/II or Type IL mixes. However, when

blended with Class C fly ash, the finer Type IL (AL) showed higher drying shrinkage than Type I/II (A), while the coarser Type IL (CL) showed lower drying shrinkage than Type I/II (C). It was also found that blending finer Type IL cement (AL) with slag resulted in higher early age drying shrinkage. Therefore, considering both the autogenous shrinkage and drying shrinkage results, 50% by mass slag in combination with PLC is not recommended for use in applications where lower early age drying shrinkage is required.

In general, the effect of calcite content on several parameters did not show strong correlation. The low R^2 values indicate that other factors (such as fineness and chemical composition) also contribute to the observed behavior. In addition to that, the number and variation of Type IL cements was not large enough to provide a sample pool with clearer trends. However, the data collected did indicate that calcite content, particle size, and chemical composition are the main factors affecting behavior.

Chapter 9. EVALUATING THE EFFECT OF TEMPERATURE

9.1 Experimental program

The effect of low (40 ºF) and high temperature (90 ºF) curing conditions on setting time, mechanical properties, and drying shrinkage is discussed in this chapter. All materials were held at these curing temperatures prior to mixing, to better simulate field conditions. Comparisons are made to results presented previously where curing conditions were at 73 ºF.

Setting time (ASTM C191) was measured as described in Section 4.1. Mechanical properties (compressive strength, elastic modulus, and splitting tensile strength) were measured as described in Section 6.1.1. Drying shrinkage was measured as described in Section 6.1.2. Class AA concrete was used for the tests discussed in this chapter; SCMs were not examined. Table 9.1 shows the labels used concrete mixes based on the cement source and the curing temperature.

Table 9.1: Labels used for concrete mixes cured at different temperatures

Curing Temperature	Plant A		Plant C	
	Type I/II	Type IL	Type I/II	Type IL
40 ºF	A-40	AL-40	C-40	CL-40
73 ºF	A-73	AL-73	C-73	CL-73
90 ºF	A-90	AL-90	C-90	CL-90

9.2 Results

9.2.1 Setting time at 90 °F

Figure 9.1 shows the results of the time of setting for the group of samples from sources A to E and tested at 90 °F.
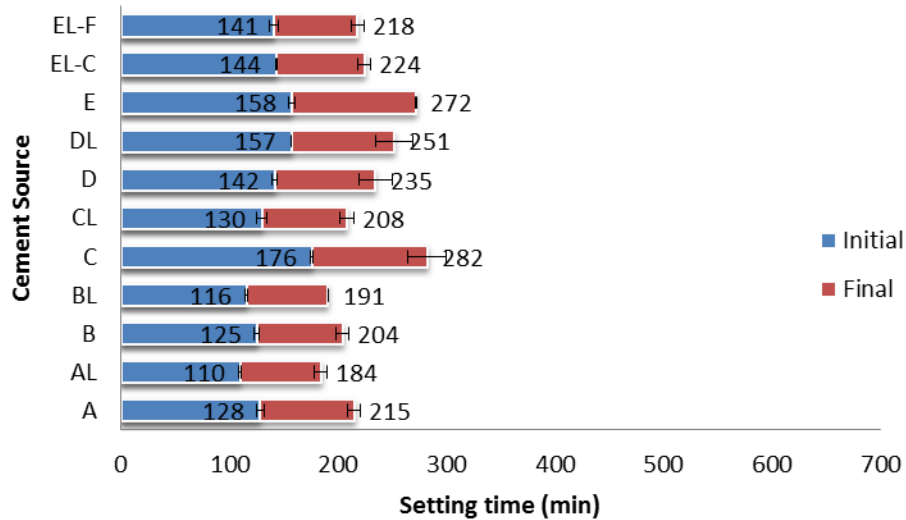
Figure 9.1: Time of setting of cements A to E at 90 °F

The results show that Type IL cement exhibited faster setting time (7% to 25%). The exception was cement D and DL where the setting time was relatively similar (within the standard deviation).

When comparing the setting times at 90 °F with those at 73 °F, the higher temperature caused a larger difference of the setting time of Type I/II cement than Type IL cement. For example, the higher temperature decreased the setting time of cement A by 31% where it decreased the setting time of cement AL by 13%. This indicated that the dilution effect of limestone replacement of clinker was more dominant at higher temperature.

It should be noted that this effect was not observed for cements C and D. The QXRD analysis showed that cement C had ~15% more C_3S than cement CL while the amount of C_2S was relatively similar in both. Cement D had ~4% more of C_3S but ~12% more of C_2S than cement DL. This may have affected the rate of hydration at higher

191

temperature. The lack of consistency in the C_3S and C_2S in Type I/II and Type IL from sources C and D affected the trends observed for the setting time at higher temperature.

Figure 9.2 shows the scatter plot of the relation between calcite content and setting time at 90 °F. The results have low R^2 values but indicate that there may be a decrease in setting time with higher calcite content. The data in Figure 9.2 were separated to produce separate scatter plots for Type I/II and Type IL, as shown in Figure 9.3, which show a conflicting behavior of Type I/II and Type IL cements at 90 ºF. For Type I/II, higher calcite content led to a slower setting time. However, for Type IL, higher calcite content led to faster setting time. This suggests additional factors – such as greater fineness of the limestone during intergrinding at higher fractions – play a role in setting time, beyond calcite content. The low R^2 values indicate that other factors (such as fineness and chemical composition) also contribute to the observed behavior.
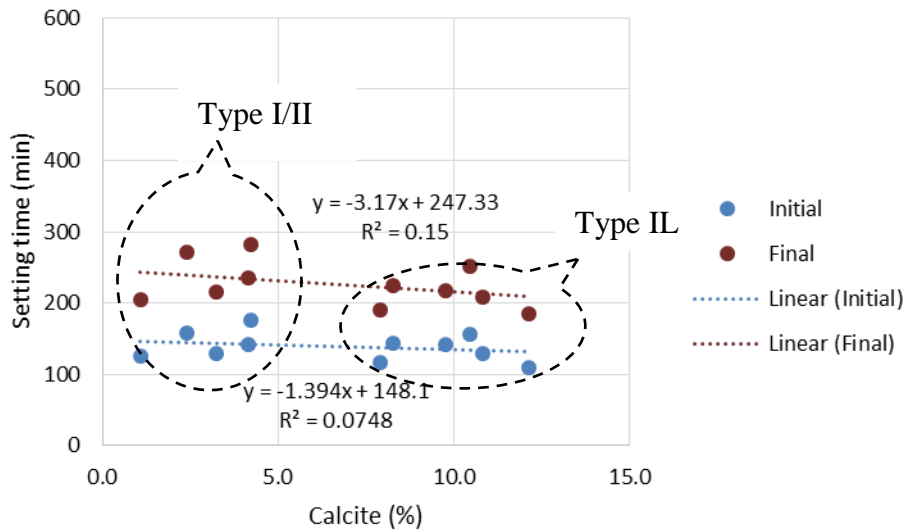
Figure 9.2: Effect of calcite content on setting time at 90 °F

(a) Type I/II   (b) Type IL
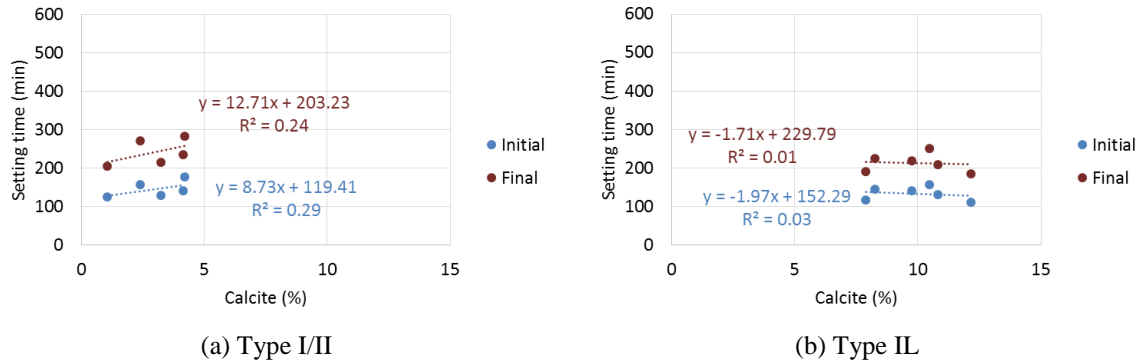
Figure 9.3: Effect of calcite content on setting time of Type I/II and Type IL cements at 90 °F

Figure 9.4 shows the scatter plots of the relation between the setting time and the C_3A content for Type I/II and Type IL cements at 90 °F. For Type I/II cement, higher C_3A content led to faster setting time. However, for Type IL cement, higher C_3A content led to slower setting time, indicating an interference of limestone with the hydration of C_3A phase at 90 °F (which was not observed at 73 °F, Figure 9.5). The low R^2 values indicate that other factors (such as fineness and chemical composition) also contribute to the observed behavior.

(a) Type I/II   (b) Type IL
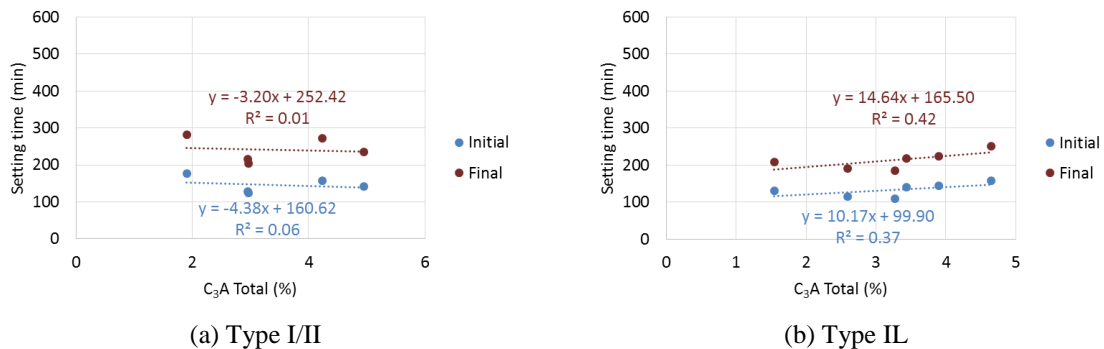
Figure 9.4: Effect of C_3A content on setting time of Type I/II and Type IL cements at 90 °F

193
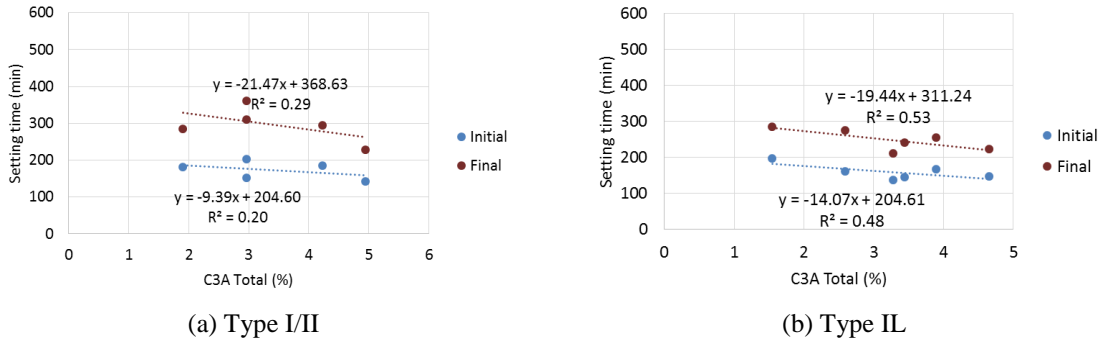
(a) Type I/II

(b) Type IL

Figure 9.5: Effect of C_3A content on setting time of Type I/II and Type IL cements at 73 °F

9.2.2 Setting time at 40 °F

Figure 9.6 shows the results of the time of setting for the group of samples from sources A to E and tested at 40 °F.
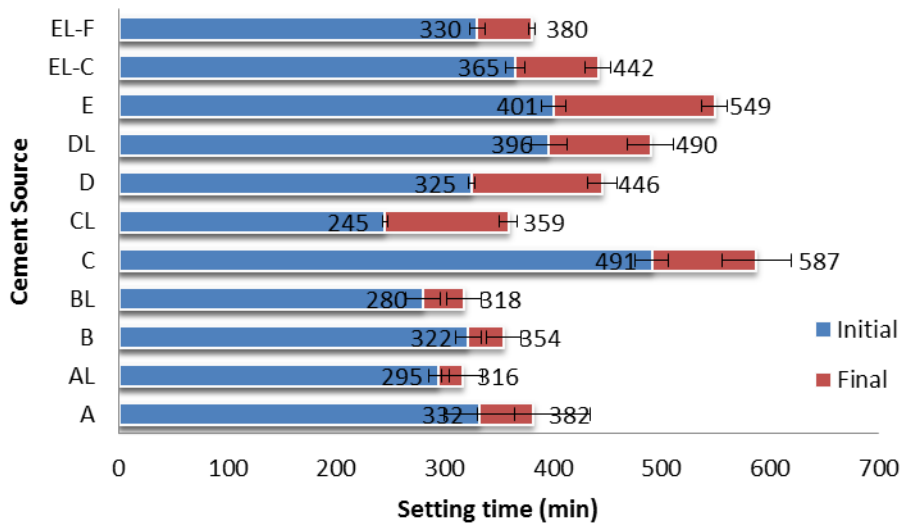
Figure 9.6: Time of setting of cements A to E at 40 °F

The results show that Type IL cements experienced faster setting time (~10% to ~40%) than their companion Type I/II cements. The exception was cement DL where the setting time was larger (~10%).

194

As described for the higher temperature, cement D had ~4% more of C_3S but ~12% more of C_2S than cement DL. This may have affected the rate of hydration at lower temperature.

Figure 9.7 shows scatter plots of the relation between calcite content and setting time for Type I/II and Type IL cements at 40 °F. For Type I/II, the higher calcite content led to slower setting time. However, for Type IL, the low R^2 values do not permit determining a specific relation. The low R^2 values indicate that other factors (such as fineness and chemical composition) also contribute to the observed behavior.

(a) Type I/II   (b) Type IL
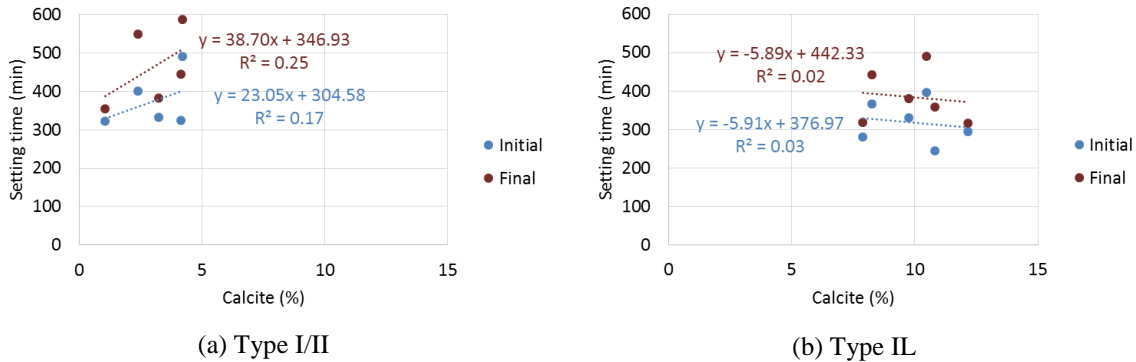
Figure 9.7: Effect of calcite content on setting time of Type I/II and Type IL cements at 40 °F

Figure 9.8 shows scatter plots of the relation between C_3A content and setting time for Type I/II and Type IL cements at 40 °F. For Type I/II, the higher C_3A content led to faster setting time. However, for Type IL, higher C_3A content led to slower setting time, indicating an interference of limestone with the hydration of C_3A phase at 40 °F (which was not observed at 73 °F, Figure 9.5).

195
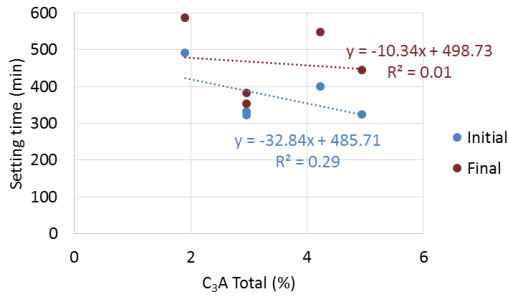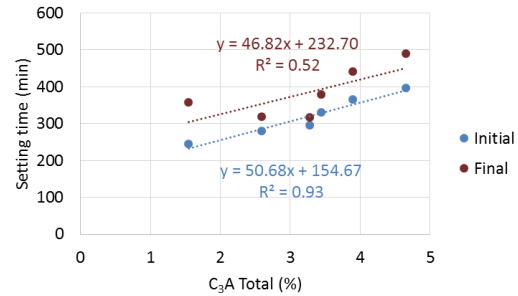
(a) Type I/II   (b) Type IL

Figure 9.8: Effect of C_3A content on setting time of Type I/II and Type IL cements at 40 °F

9.3 Mechanical properties

9.3.1 Compressive strength

Class AA concrete mixtures were prepared using Type I/II and Type IL from sources A and C, and were cured at room temperature (73 °F), 90 °F, and 40 °F until the time of testing.

Figure 9.9 and Figure 9.10 show the compressive strength results for Type I/II and Type IL cement from sources A and C, respectively. In the legend, the letter "L" was used to label Type IL cements. The numerical value in the legend indicates the curing temperature in ºF.

The results in Figure 9.9 (Cement A/AL) showed that Type IL cement resulted in relatively higher 1-day compressive strength than Type I/II cured at all curing temperatures. At 28 days, Cement AL cured at 90 °F showed significant increase (~30%) in compressive strength when compared to cement A cured at 90 °F. However, the difference in strength between A and AL was smaller for other curing temperatures (~3%

for 73 °F curing, and ~7% for 40 °F curing). At 1 year, cement AL cured at 90 °F showed about 40% higher strength than cement A cured at 90 °F. Also at 1 year, cement AL cured at 40 °F showed slightly lower strength (~4%) than cement A cured at 40 °F.
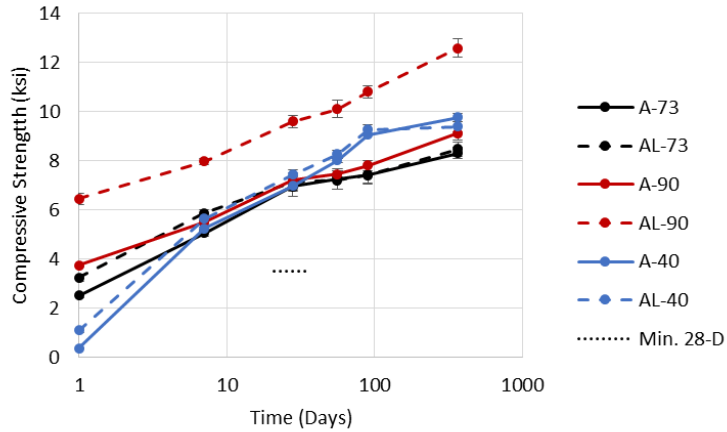
Figure 9.9: Compressive strength of Type I/II and Type IL cements from Plant A cured at 73 °F, 90 °F, and 40 °F

The results in Figure 9.10 (Cement C/CL) showed that at 1 day, Type IL cement resulted in slightly higher (~7%) compressive strength than Type I/II when cured at 73 °F. The difference between Type I/II and Type IL was higher (~35% at 1 day) for the mixes cured at 40 °F, while Type IL cement showed slightly lower (3%) 1-day compressive strength than Type I/II when cured at 90 °F.

At 28 days, Type IL cement showed similar compressive strength to Type I/II for the mixes cured at 90 °F and 40 °F, while Type IL showed slightly higher (~9%) compressive strength than Type I/II for the mixes cured at 73 °F.

At 1 year, Type IL cement showed similar compressive strength to Type I/II for the mixes cured at 90 ℉ and 40 ℉, while Type IL showed slightly higher (~9%) compressive strength than Type I/II for the mixes cured at 73 ℉.
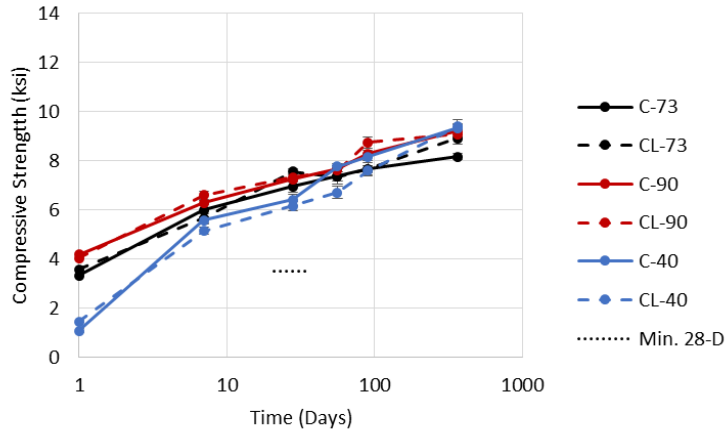
Figure 9.10: Compressive strength of Type I/II and Type IL cements from Plant C cured at 73 ℉, 90 ℉, and 40 ℉

The particle size analysis of Type I/II and Type IL cements from plant A and C are summarized in Table 9.2. The median particle size of cement AL is about 25% lower than cement A (7.5 μm and 10 μm respectively). This smaller particle size provides more nucleation sites for cement hydration and therefore increases the rate of hydration leading to faster strength development. The higher temperature (90 ℉) seems to have enhanced the difference in the rate of hydration significantly as seen in the strength development of cement AL at 90 ℉ in Figure 9.9. However, cement C and CL had a relatively similar median particle size, which explains the similar rate of strength development shown in Figure 9.10.

Table 9.2: Particle size summary for cements from Plant A and C

Cement	Surface mean [μm]	Volume mean [μm]	D_{10} [μm]	D_{50} [μm]	D_{90} [μm]
A	6.28	14.1	2.77	10.0	30.2
AL	5.09	10.2	2.29	7.5	21.8
C	6.53	15.1	3.03	10.1	34.1
CL	5.60	14.6	2.25	10.2	33.6

Figure 9.11 and Figure 9.12 show scatter plots of calcite content vs. the compressive strength of concrete at 1 day, 28 days, and 1 year for concrete cured at 90 ºF and 40 ºF, respectively. After applying a linear regression best fit line, it can be seen that when curing at 90 ºF, the higher the calcite content, the larger the compressive strength at all ages. However, for the concrete cured at 40 ºF, the calcite content does not seem to have a significant effect on the compressive strength. The low R^2 values indicate that other factors (such as fineness and chemical composition) also contribute to the observed behavior.
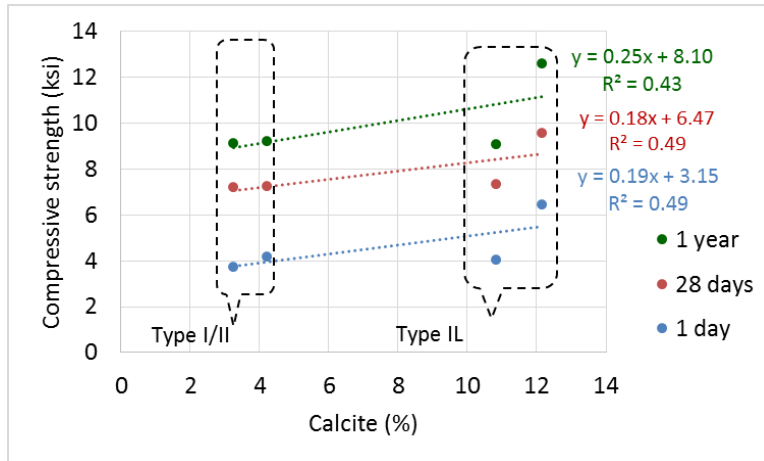
Figure 9.11: Effect of calcite content on compressive strength of concrete cured at 90 ℉

Figure 9.12: Effect of calcite content on compressive strength of concrete cured at 40 ℉

Analysis of variance (ANOVA) was conducted to investigate the statistical significance of the difference in values of the compressive strength of concrete made with Type I/II and Type IL cement of plants A and C. The null (no difference) hypothesis was that average strength of Type I/II and Type IL are similar ($\mu1=\mu2$). A summary of the results for the 90 ℉ mixes is shown in Table 9.3, and for the 40 ℉ mixes in Table 9.4, and the values for the base mixes (73 ℉) are shown in both tables. Accepting the null

hypothesis indicates that there is no statistical significance in the difference between the strength of Type I/II and Type IL cement while rejecting the null hypothesis indicates that there is a significant statistical difference between the strength of Type I/II and Type IL cement.

Table 9.3: ANOVA results for comparing Type I/II and Type IL cements from each plant for the compressive strength of the 90 ºF mixes
(null hypothesis, strength of Type I/II = strength of Type IL, "Similar": $\mu1=\mu2$)

Time	Cement source and SCM			
	A/AL (73 ºF)	A/AL (90 ºF)	C/CL (73 ºF)	C/CL (90 ºF)
7 days	Different	Different	Similar	Different
28 days	Similar	Different	Different	Different
1 year	Similar	Different	Different	Similar

Table 9.4: ANOVA results for comparing Type I/II and Type IL cements from each plant for the compressive strength of the 40 ºF mixes
(null hypothesis, strength of Type I/II = strength of Type IL, "Similar": $\mu1=\mu2$)

Time	Cement source and SCM			
	A/AL (73 ºF)	A/AL (40 ºF)	C/CL (73 ºF)	C/CL (40 ºF)
7 days	Different	Different	Similar	Different
28 days	Similar	Similar	Different	Similar
1 year	Similar	Similar	Different	Similar

For the mixes cured at 90 ºF, the results showed that the differences between the compressive strength of concrete made with Type I/II and Type IL cements were significant for both plants A and C, except for the one year strength of plant C mixes. This indicates that limestone has a statistically significant effect on the compressive

strength when curing at high temperature. The coarser Type IL (CL) resulted in similar values at one year.

For the mixes cured at 40 °F, the results showed that the differences between the compressive strength of concrete made with Type I/II and Type IL cements were not significant for both plants A and C, except for the 7 days strength. This indicates that limestone has a statistically significant effect on early age compressive when curing at low temperature, but does not have a significant effect on later ages.

9.3.2 Elastic modulus

Elastic modulus was measured for concrete cylinders (6 in. x 12 in.) at 28 days of age (ASTM C469). Figure 9.13 and Figure 9.14 show the effect of curing temperature on the elastic moduli of concrete made with cements from plant A and plant C, respectively. All mixes showed relatively similar values to the base mixes. The figures also show the elastic moduli compared to the values calculated using Equation 6.2 (from ACI 363R-10 section 6.3).

$$E = 40\sqrt{f_c'} + 10^3 \qquad\qquad \text{Equation 6.2}$$

Where:

E: Modulus of elasticity (ksi)

f_c': specified compressive strength of concrete (psi)
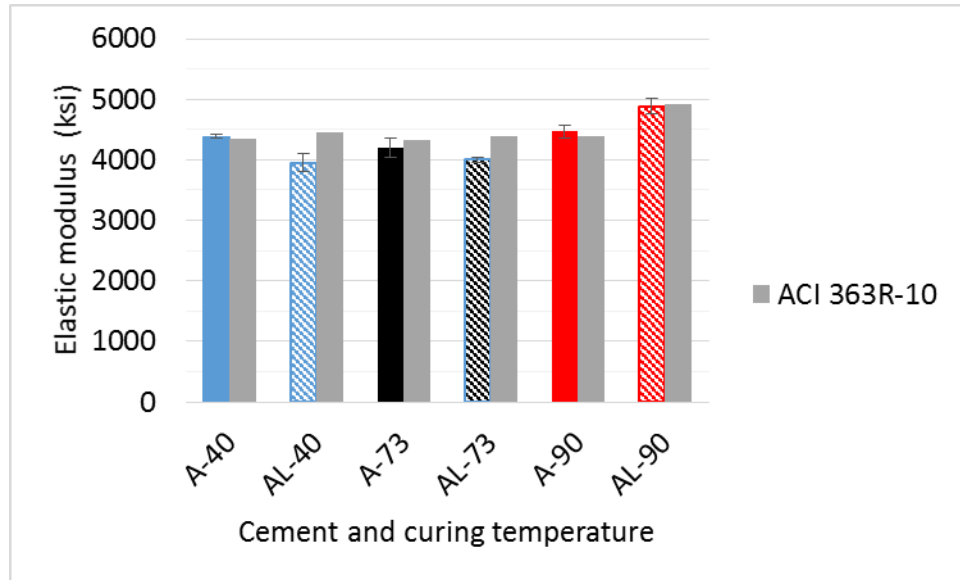
Figure 9.13: Elastic modulus values of concrete made with Type I/II and Type IL cements from plant A cured at 40, 73, and 90 ºF with ACI 363R-10 predicted values

For concrete made with cements from Plant A, curing at 40 ºF resulted in 10% lower elastic modulus of Type IL (AL-40) than Type I/II (A-40) which followed the trend previously discussed for the 73 ºF mix. On the other hand, curing at 90 ºF resulted in 10% higher elastic modulus of concrete made with cement AL-90. ACI 363R-10's equation overestimated (13%) the elastic modulus value for AL-40 indicating the equation is not accurate for cold temperature curing. For the 90 ºF mixes, the equation predicted relatively close values to the measured ones.
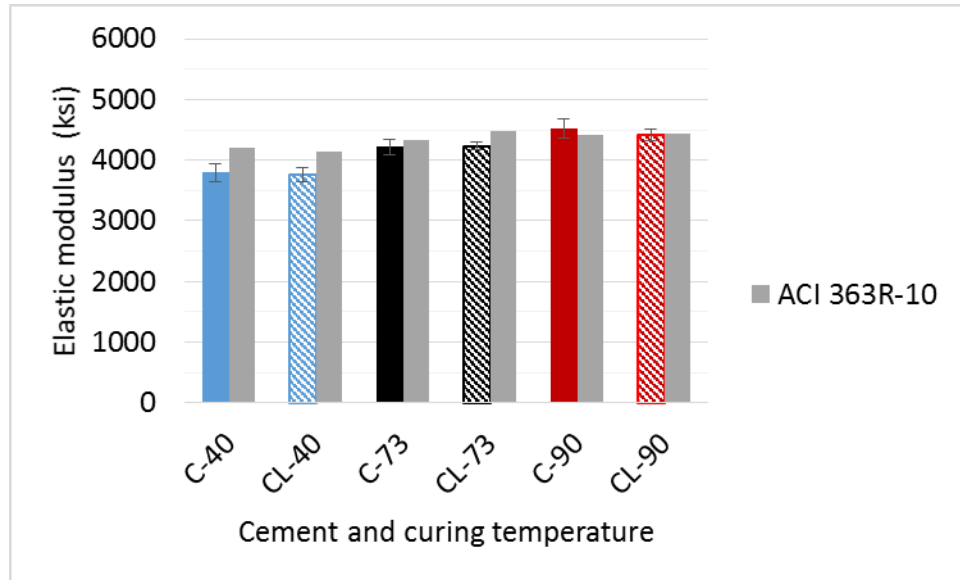
Figure 9.14: Elastic modulus values of concrete made with Type I/II and Type IL cements from plant C cured at 40, 73, and 90 ºF with ACI 363R-10 predicted values

For concrete made with cements from Plant C, curing at 40 ºF resulted in statistically similar elastic modulus of Type I/II (C-40) and Type IL (CL-40) which followed the trend previously discussed for the 73 ºF mix. Statistically similar values were obtained for the C-90 and CL-90 mixes. ACI 363R-10's equation overestimated (10%) the elastic modulus value for both C-40 and CL-40 mixes, indicating that the equation is not accurate for cold temperature curing. For the 90 ºF mixes, the equation predicted relatively close values to the measured ones.

The above results followed the same trends observed for the compressive strength. Figure 9.15 shows the compressive strength values of concretes made with Type I/II and Type IL cements from plants A and C and cured at 40, 73, and 90 ºF. Figure 9.16 shows the elastic modulus values of concretes made with Type I/II and Type IL cements

204

from plants A and C and cured at 40, 73, and 90 °F. The trends seen for the elastic

modulus values followed the trends seen for the compressive strength.
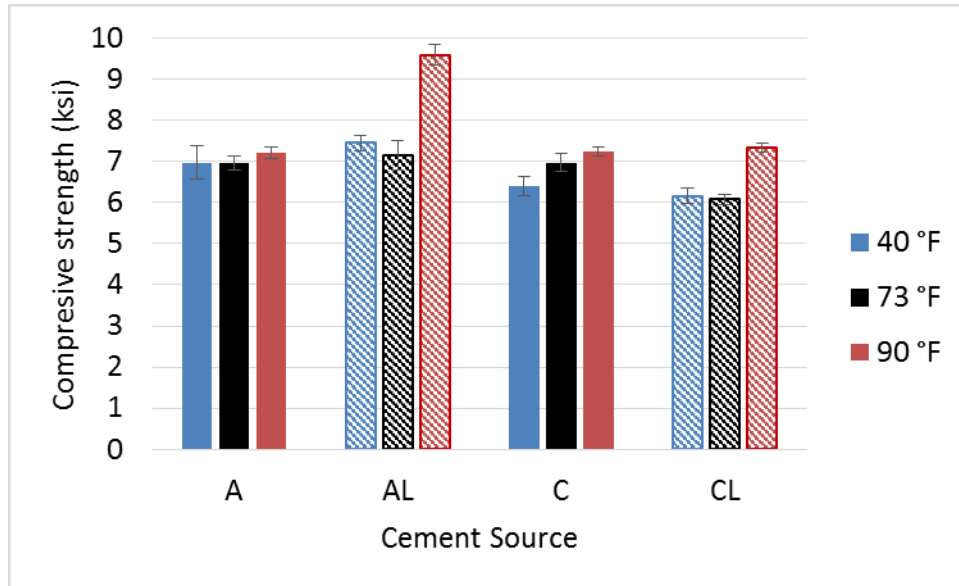
Figure 9.15: Compressive strength values of concretes made with Type I/II and Type IL
cements from plants A and C and cured at 40, 73, and 90 °F
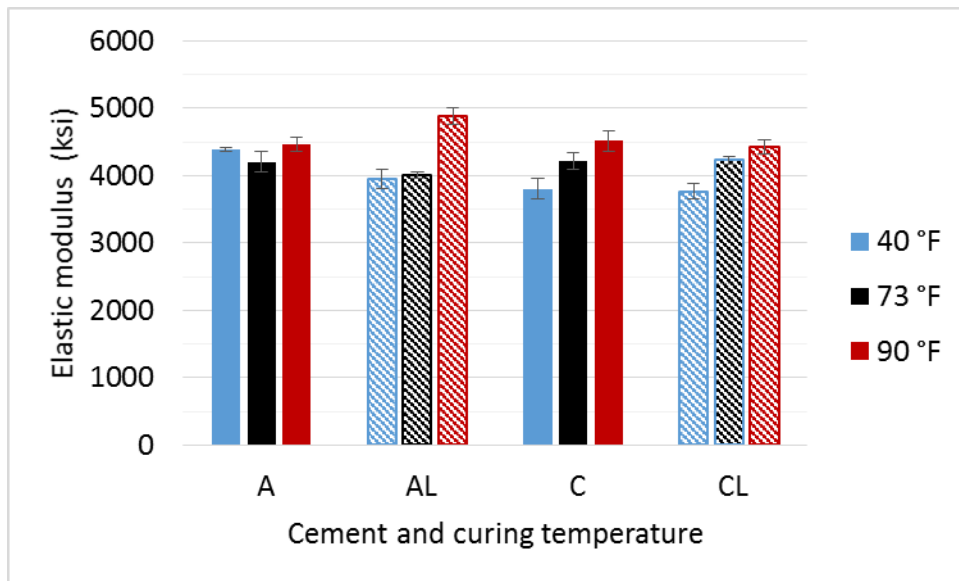
Figure 9.16: Elastic modulus values of concretes made with Type I/II and Type IL
cements from plants A and C and cured at 40, 73, and 90 °F

Figure 9.17 shows a scatter plot of calcite content vs. the elastic modulus of concretes using cements from plants A and C and cured at 40, 73, and 90 ℉. After applying a linear regression best fit line, the general trend seen is that the higher the calcite content, the lower the elastic modulus for the mixes cured at 40 ℉. However, for the concrete mixes cured at 90 ℉, higher calcite content resulted in larger elastic modulus values. The low R^2 values indicate that other factors (such as fineness and chemical composition) also contribute to the observed behavior.
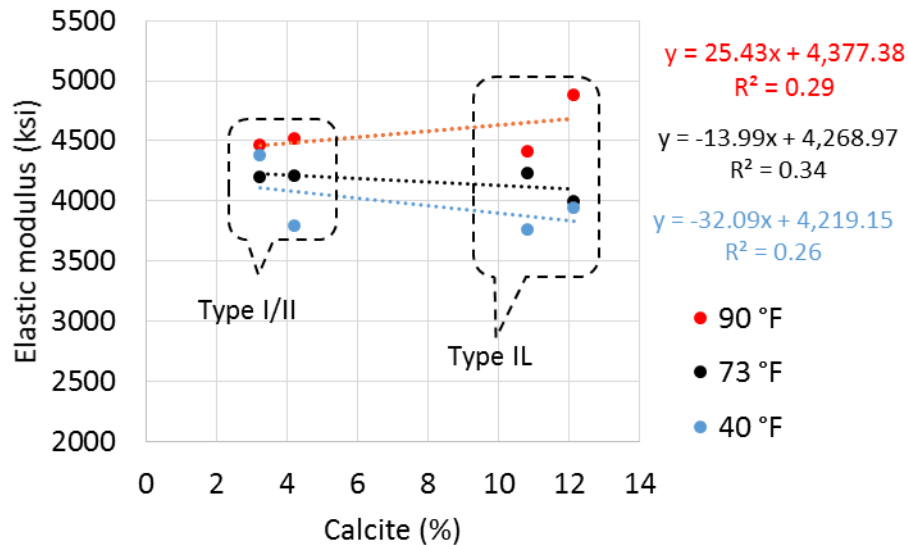
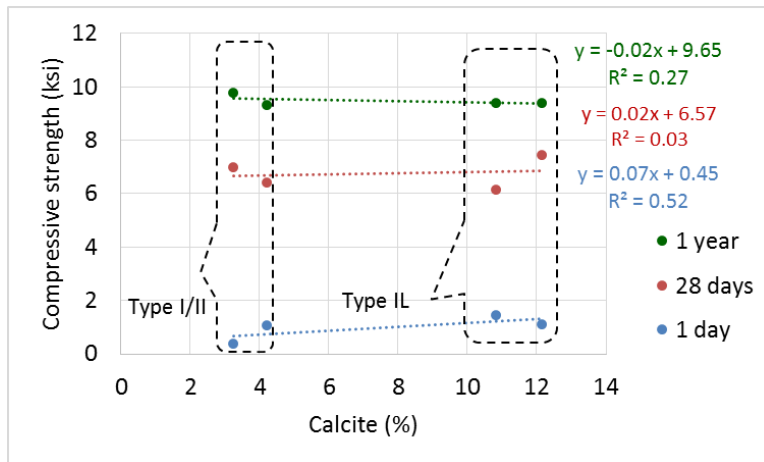Figure 9.17: Effect of calcite content on elastic modulus of concrete with SCMs

9.3.3 Splitting tensile strength

Splitting tensile strength [ASTM C496, AASHTO T 198] was measured for concrete samples (4 in. x 8 in.) at 28 days of age. Figure 9.18 and Figure 9.19 show the effect of curing temperature on the splitting tensile strength values of concrete made with cements from plant A and plant C, respectively, cured at 40 ℉, 73 ℉, and 90 ℉. The

figures also show the calculated values computed using ACI 363R-10 (equation 6-13 in

ACI 363R-10 section 6.6) which was discussed in Chapter 6:

$$f_{sp} = 7.4\sqrt{f'_c}$$

where:

- f_{sp} = splitting tensile strength (psi)
- f_c' = compressive strength (psi)
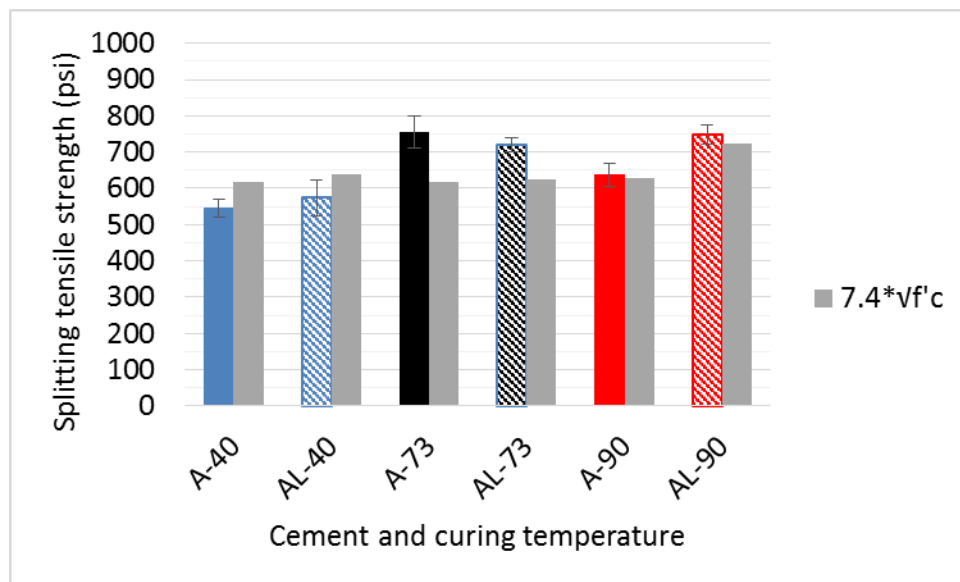
Figure 9.18: Splitting tensile strength of concrete made with Type I/II and Type IL
cements from plant A cured at 40, 73, and 90 ºF
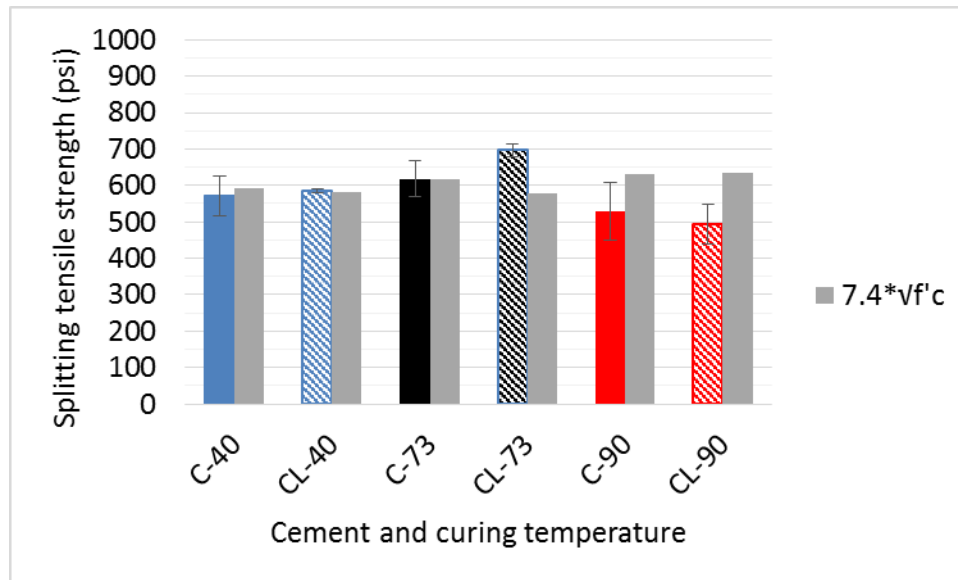
Figure 9.19: Splitting tensile strength of concrete made with Type I/II and Type IL cements from plant C cured at 40, 73, and 90 ºF

For plant A (Figure 9.18), curing at 90 ºF resulted in 17% higher value of the mix made with AL, while the curing at 40 ºF resulted no statistically significant difference between A and AL. For plant C (Figure 9.19), curing at high and low temperature did not yield statistically significant differences between C and CL. This indicates that the finer Type IL cement (AL) has a significant effect on the results when cured at high temperature.

Figure 9.20 shows a scatter plot of calcite content vs. the splitting tensile strength of the concretes made with cements from plants A and C and cured at 40, 73, and 90 ºF. After applying a linear regression best fit line, the low R^2 values for concretes cured at 73 and 90 ºF indicate that no clear relation can be established. But for concretes cured at 40 ºF, it appears that the higher calcite content, does not alter the splitting tensile strength.
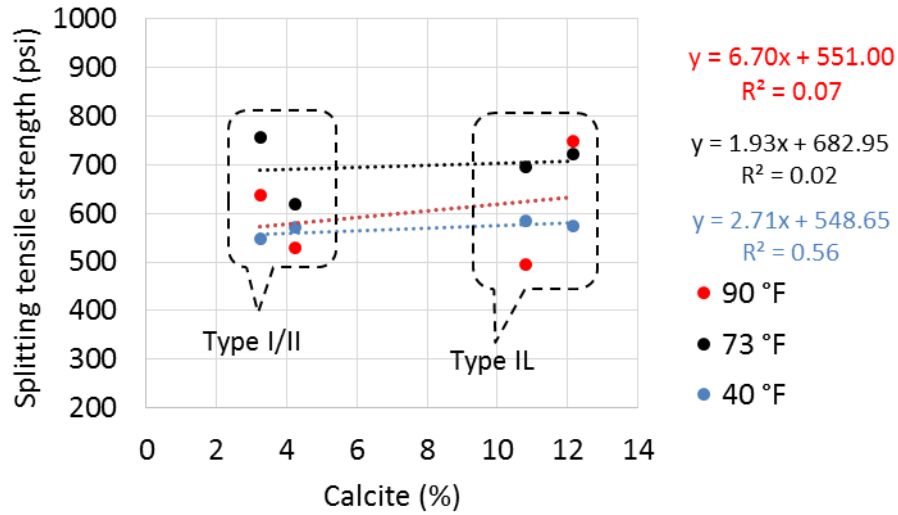
Figure 9.20: Effect of calcite content on the splitting tensile strength of concrete cured at 40, 73, and 90 ℉

9.4 Drying shrinkage

Figure 9.21 shows the drying shrinkage values of Class AA concrete made with Type I/II and Type IL cements from plants A and C cured at 73 ℉ compared to mixes cured at 90 ℉ (for 28 days). After curing, drying was done at 73 ℉ for all samples.

For plant A, curing at 90 ℉ resulted in similar drying shrinkage values of Type I/II and Type IL cement. When compared to the base mixes (i.e. cured at 73 ℉), Type IL showed lower values (~10%), while Type I/II showed similar values.

For plant C, curing at 90 ℉ resulted in similar drying shrinkage values of Type I/II and Type IL cement.

209

(a) Plant A   (b) Plant C
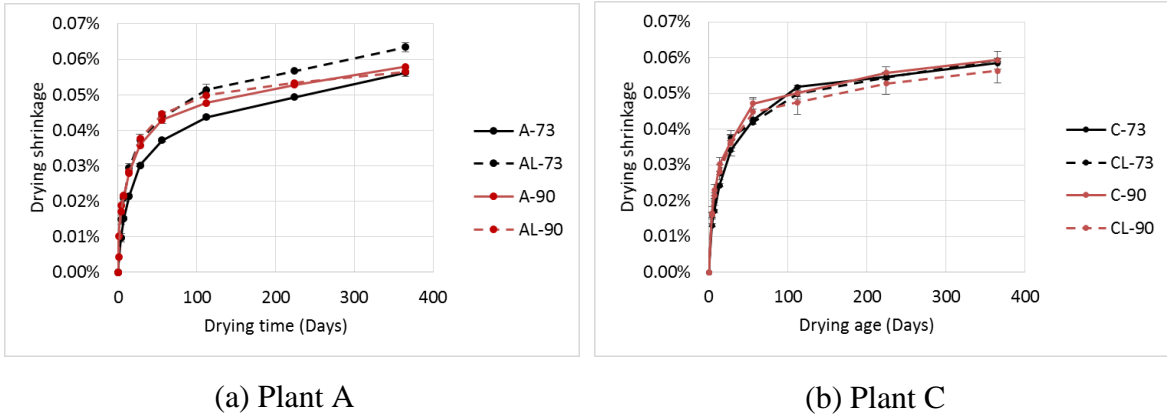
Figure 9.21: Drying shrinkage of concrete made with Type I/II and Type IL cements cured at 90 ℉ compared to 73 ℉

Figure 9.22 shows the drying shrinkage values of Class AA concrete made with Type I/II and Type IL cements from plants A and C cured at 73 ℉ compared to mixes cured at 40 ℉ (for 28 days). After curing, drying was done at 73 ℉ for all samples.

For plant A, curing at 40 ℉ resulted in significantly larger drying shrinkage values (~25%) of Type IL cement than Type I/II cement. When compared to the base mixes (i.e. cured at 73 ℉), Type I/II and Type IL cements cured at 40 ℉ showed lower values (~20% and ~10% respectively) than the base mixes.

For plant C, curing at 40 ℉ resulted in lower drying shrinkage values (~15%) of Type IL cement than Type I/II cement. When compared to the base mixes (i.e. cured at 73 ℉), Type I/II and Type IL cements cured at 40 ℉ showed lower values (~10% and ~25% respectively) than the base mixes.
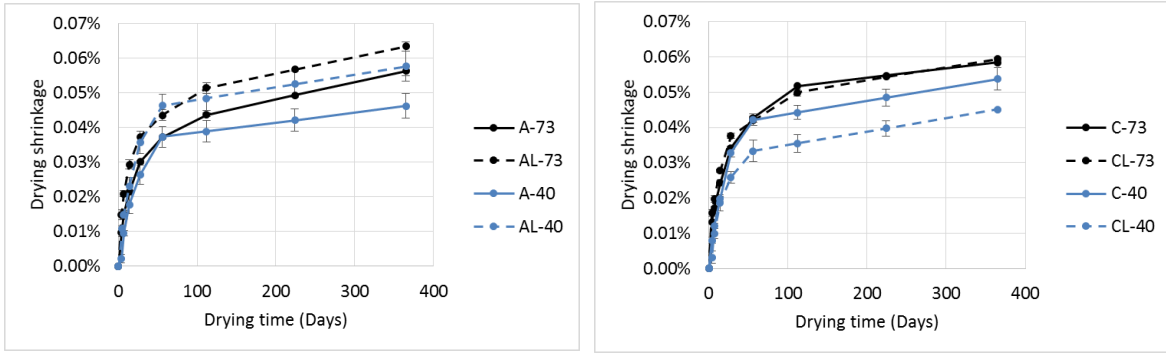
(a) Plant A   (b) Plant C

Figure 9.22: Drying shrinkage of concrete made with Type I/II and Type IL cements cured at 40 ℉ compared to 73 ℉

The Federal Highway Administration (FHWA) Section 718-47 [115] specifies maximum drying shrinkage of 0.06% at 56 days, which all the above mixes have successfully met.

Figure 9.23 and Figure 9.24 show scatter plots of calcite content vs. drying shrinkage of the concretes made with cements from plants A and C and cured at 90 ℉ and 40 ℉, respectively. After applying a linear regression best fit line, it can be seen that higher the calcite content decreases the one-year shrinkage of the concretes cured at 90 ℉. However, for the concretes cured at 40 ℉, the low R^2 values do not permit an accurate conclusion. The low R^2 values indicate that other factors (such as fineness and chemical composition) also contribute to the observed behavior.

211
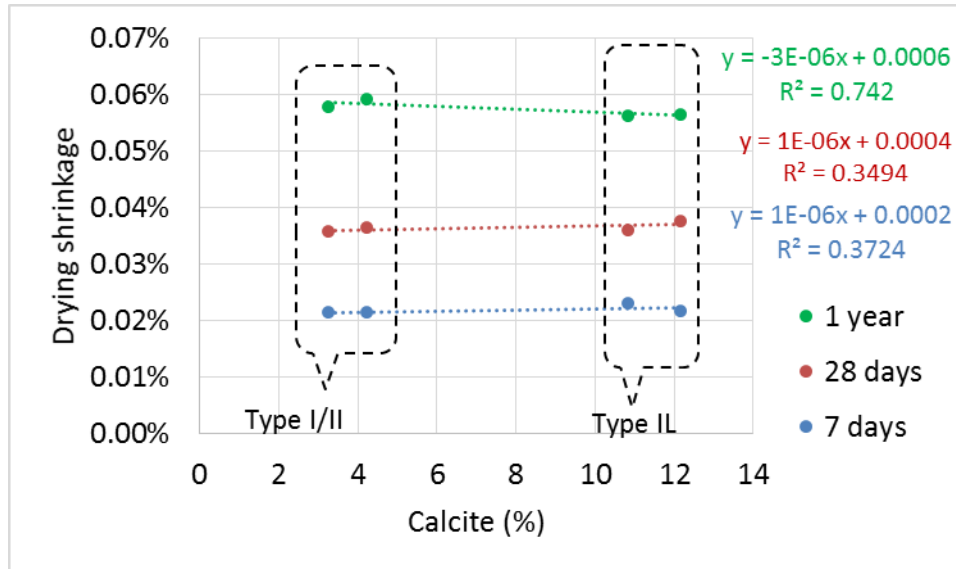
Figure 9.23: Effect of calcite content on the drying shrinkage of concrete cured at 90 ºF
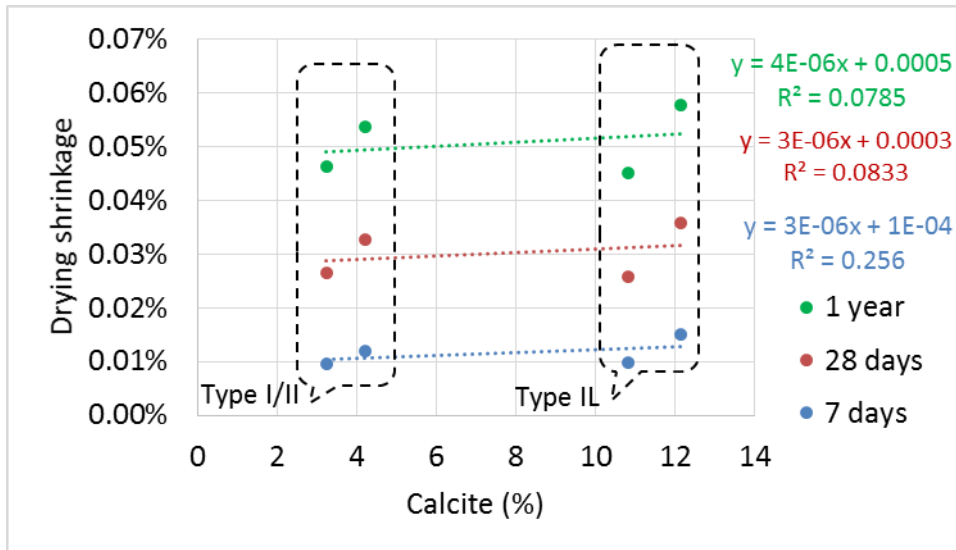
Figure 9.24: Effect of calcite content on the drying shrinkage of concrete cured at 40 ºF

212

9.5 Conclusions

The effect of temperature on setting time, mechanical properties of concrete, and drying shrinkage of concrete was discussed in this chapter.

For the setting time, higher calcite content decreased the setting time at high and low temperatures which can be attributed to the nucleation effect of the limestone particles.

For the compressive strength, the effect of limestone was more pronounced in the mixes cured at 90 ºF where higher calcite content resulted in higher compressive strength. However, for the mixes cured at 40 ºF, higher calcite content increased the early strength while it decreased the long term strength of concrete.

For the elastic modulus, the trend seemed to follow that of the compressive strength, where higher calcite content resulted in larger elastic moduli when concrete was cured at high temperature, while higher calcite content resulted in lower elastic moduli when concrete was cured at low temperature.

For the splitting tensile strength, higher calcite content resulted in higher splitting tensile strength at both temperatures, but the effect was more pronounced for concrete cured at high temperature.

For the drying shrinkage, higher calcite content increased the drying shrinkage for concretes cured at high and low temperatures, except for the 1 year values of the mixes cured at high temperature where higher calcite content resulted in lower drying shrinkage.

In general, the effect of calcite content on some parameters did not show strong correlation. The low R^2 values indicate that other factors (such as fineness and chemical composition) also contribute to the observed behavior. In addition to that, the number and variation of Type IL cements was not large enough to provide a sample pool with clearer trends. However, the data collected did indicate that calcite content, particle size, and chemical composition are the main factors affecting behavior.

Chapter 10. CONCLUSIONS AND RECOMMENDATIONS

10.1   Conclusions

The primary objective of this research was to understand how the chemical and physical properties of finely ground limestone inclusions influence the early-age hydration and structure and the long-term durability of portland limestone cement (PLC)-based materials, particularly in comparison to ordinary portland cement. This research compared the performance of limestone blended cements to conventional portland cements in concretes designed to meet GDOT specifications for Class A, AA, and AA1 (or AAA) concrete [13].

As stated in Chapter 1, the specific objectives were to:

(1) compare regionally produced limestone blended cements (PLCs) with conventional portland cements in terms of composition and fineness,

(2) evaluate the influence of increasing ground limestone addition rates through the assessment of key material properties (e.g., setting time, strength development, shrinkage, permeability, air content, and durability to freezing/thawing cycling),

(3) examine the relative sensitivity of those properties to field conditions (e.g., variations in temperature), and

(4) assess the combinations of limestone blended cements with fly ash (15%) and slag (50%).

Experimental and computational investigations into several commercially-available and laboratory-produced PLC systems yielded insights into the relative influences of the limestone's composition, blending rate with portland cement, and particle size distribution on the hydration and microstructural development of PLC-based materials. These insights provided the context for subsequent analysis of the long-term durability of PLC-based systems as it relates to shrinkage, permeability, and freezing and thawing resistance. The following sections present the key findings of this research effort.

10.1.1 Physical effects of limestone fillers

Based on the literature review presented in Chapter 2, it was established that interground limestone can affect cement hydration through three primary physical mechanisms: (1) dilution, (2) heterogeneous nucleation, and (3) improvements in particle packing (filler effect). This study investigated the relative influence of each of these effects on the hydration and microstructural development of six commercially-produced Type IL portland limestone cement pastes. It was concluded that:

- Type IL cements ground to similar fineness as Type I/II cements produced from the same clinker (typically with median particle size $D_{50} \approx 10$ µm) exhibited dilution-dominated hydration behavior, which was characterized by slower rates of hydration and increased total porosity, but also by reductions in early-age chemical and autogenous shrinkage. Such behavior was primarily attributed to the reduced clinker content of the cement, which, in turn, reduced the volume of hydration products formed (dilution effect) and the amount of chemical shrinkage experienced by the paste. Additional decreases in hydration rate and increases in

216

porosity were attributed to the coarser size of the clinker fractions in the Type IL cements compared to the Type I/II cements, which resulted from the relatively finer grinding of the soft limestone during finishing.

- Type IL cements ground significantly finer than Type I/II cements produced from the same clinker (typically with D_{50} < 10 μm) exhibited nucleation- and filler-dominated hydration behavior, which was characterized by more rapid rates of hydration and decreased average pore sizes, but also by increases in early-age chemical and autogenous shrinkage. This behavior was primarily attributed to the enhanced nucleation of hydration products on the surfaces of the limestone particles (heterogeneous nucleation) and the improved space-filling efficiency of the finer particle size distributions (filler effects). In the most finely ground Type IL cements (typically with D_{50} < 9 μm), a finer grind of the clinker fraction further contributed to more rapid rates of hydration and increases in chemical and autogenous shrinkage, which could increase the potential for cracking at early-ages.

10.1.2 Chemical effects of limestone fillers

Investigations into the chemical effects of limestone fillers on the hydration and microstructural development of commercially- and laboratory-produced portland limestone cements yielded the following conclusions:

- For the particular cement compositions, limestone sources, and 0.40 *w/b* investigated, it was found that approximately 10-20% of the calcium carbonate ($CaCO_3$) in the limestone becomes available to participate in cement hydration

217

within the first few days of hydration. The availability of the $CaCO_3$ shifts the thermodynamic balance of the system such that ettringite is no longer converted into the AFm phase monosulfate, but rather becomes indirectly stabilized as the $CaCO_3$ and any remaining C_3A (and at later ages, C_4AF) react with one another to produce the carbonate-AFm hydration products, hemi- and monocarbonate.

- Limestone contents as low as 3% by weight are sufficient to form carbonate-AFm phases, and hemi- and monocarbonate were detected after about 3 days of hydration in all of the limestone-containing Type I/II and the Type IL cement pastes investigated.

- Analysis by the modified Powers' model reveals that formation of carbonate-AFm increases the chemical shrinkage experienced by limestone-containing Type I/II and Type IL cement pastes. These increases are not properly accounted for by the model, leading to the conclusion that Powers' model is not appropriate for the prediction of chemical shrinkage in limestone-containing Type I/II or Type IL cement systems. Comparison of experimental data to Powers' model predictions can, however, illustrate the chemical effects of reactive fillers on the hydration of blended cement pastes.

- While the particular mineralogical composition of the limestone slightly influences the amount of $CaCO_3$ available for reaction and the degree of hydration and chemical shrinkage exhibited by the paste, the effects of geological source are minimal in comparison to the other physical and bulk chemical ($CaCO_3$-related) effects previously discussed.

10.1.3 Mechanical properties of concrete

The effects of several parameters on the compressive strength of concrete were investigated.

The effect of Type IL cement on the strength varied in different concrete Classes. It was found that the higher the concrete Class (i.e., higher cement factor and lower w/b ratio), the greater the effect of Type IL cement on the strength. For higher w/b and lower cement factor, the effect of limestone filler was negligible. For lower w/b and higher cement factor, it was found that the effect of limestone was more significant where ground limestone with up to 15% replacement of the portland cement increased the strength with finer Type IL cement while it decreased the strength for coarser Type IL cement.

Regarding the elastic modulus of concrete, the finer Type IL cement increased the elastic modulus while coarser Type IL resulted in no statistically significant differences compared to companion concretes made with Type I/II cements. The trends generally followed those of the compressive strength. The equation for elastic modulus provided in ACI 363R-10 was more accurate in predicting elastic modulus than the one from ACI 318-14 (see section 6.2.2 for details).

Regarding the splitting tensile strength of concrete, Type IL did not show statistically significant differences. However, a trend was observed where finer particle size resulted in higher tensile strength.

Also, it was found that in some cases, the difference in mechanical properties of the many concrete samples was higher between plants than between Type I/II and Type

IL cement from the same plant. This result indicates that performance based specifications are recommended for cement producers to satisfy the applications of concrete used.

10.1.4 Drying shrinkage of concrete

The effects of several parameters on drying shrinkage were investigated..

The effect of Type IL cement on the drying shrinkage varied with different *w/b* and cement factors. Class AAA concrete made with Type IL cement and with a low *w/b* of 0.32 and high cement factor of 800 pcy , showed lower shrinkage than Class AA concrete made with Type IL cement and with a *w/b* of 0.445 and a cement factor of 635 pcy. The Class AA concrete with the high fineness Type IL cement yielded significantly higher drying shrinkage than comparison concrete made with Type I/II cement.

For Class A concrete (*w/b* of 0.49 and cement factor of 611 pcf), no statistically significant differences in shrinkage were found between concretes made with Type IL and Type I/II cement at 7 days. However, the finer limestone Type IL cement in Class A concrete decreased the drying shrinkage at one year by about 5% compared to that made with Type I/II cement.

10.1.5 Interactions with supplementary cementitious materials

Synergetic interactions between limestone and alumina-containing SCMs were investigated in this study to determine how the alumina source (SCM type) and its interaction with the limestone affected the hydration, microstructural development, and early-age shrinkage of PLC-SCM blended systems. Investigations of PLC-SCM

synergies in systems blended with either 15% Class F fly ash, 15% Class C fly ash, or 50% blast furnace slag, by total mass of cementitious material, led to the following conclusions:

- An underlying mechanism of the limestone-SCM "synergy" is the acceleration of the secondary hydraulic and pozzolanic SCM reactions by the limestone filler. Blends of PLCs with SCMs were found to exhibit secondary SCM-induced pore refinements an average 3-7 days earlier than found with blends of ordinary portland cements (OPCs) and SCMs. However, the specific influence of the SCMs varied with composition and fineness, with Class C fly ash and slag producing a greater increase in strength, but also shrinkage.

- PLC-SCM synergies are not strictly related to the alumina content of the SCM, but also to the relative reactivity of the SCM. The hydraulically reactive SCMs, Class C fly ash and slag, reacted more rapidly and showed greater limestone synergies than did the more slowly reacting pozzolanic Class F fly ash, despite having comparatively lower total alumina contents.

- Although the purported "synergies" between PLCs and SCMs beneficially increase the compressive strength and further refine the microstructure of PLC-SCM blended systems, they also negatively increase the chemical and autogenous shrinkage experienced by the PLC-blended systems at early-ages, thereby increasing the potential for cracking in structural applications.

- The results of drying shrinkage of concretes showed that when blending finer Type IL cements with slag, the early age drying shrinkage was higher than the concrete without SCMs. Therefore, given also the increased autogenous shrinkage

221

in this system, it is not recommended to use finer Type IL cement with 50% slag, where low early age drying shrinkage is required.

10.1.6 Durability implications

The implications of limestone-induced microstructural changes on the permeability of PLC-blended systems were indirectly assessed using electrical test methods (surface resistivity [SR] and rapid chloride permeability [RCP] tests). It was concluded that:

- Formation factor – rather than the measured values of resistivity (SR) or total charge passed (RCP test) – provides a more reliable indicator of microstructural development and permeability in blended cement systems. Changes to pore solution composition caused by the incorporation of limestone and/or SCMs artificially increases the resistivity and decreases the total charge passed by OPC- and PLC-blended systems, which may lead to erroneous lower permeability Classifications under current testing protocols.

- Interground limestone has no significant effect on the permeability of neat PLC systems. Changes in permeability were primarily affected by the relative grind of the clinker particles within the cement, rather than by the physical or chemical effects of the limestone particles.

- Synergetic interactions between SCMs and limestone fillers produced PLC-blended concretes with equivalent or reduced permeabilities compared to OPC-blended concretes. 50% cement replacement with slag offered the greatest decreases in permeability at 56 days, followed closely by the 15% replacement

222

with Class F fly ash, and less closely by the 15% replacement of cement by Class C fly ash.

- Service life predictions indicated that PLC concretes do not have significantly different expected service lives than OPC concretes, but when blended with SCMs, the synergetic reductions in permeability may extend the service lives of PLC-blended mixes by up to 15% compared to OPC-blended mixes. The predictions, however, rely upon the underlying assumptions (1) that the service life is governed by the ingress of chloride ions and subsequent corrosion of the reinforcing steel, (2) that the diffusion coefficient of concrete is directly proportional to the total charge passed during an RCP test, and (3) that the concrete is uncracked. The use of PLCs (and combinations of PLCs with SCMs) in concrete applications challenges the validity assumptions (2) and (3), as it was determined that PLCs (and PLC-SCM blends) may alter the total charge passed by the RCP test through electrochemical means and may also increase the potential for early-age cracking in structural applications.

- The non-air-entrained Class AA PLC concrete, similar to that of Class AA OPC concrete, failed the minimum of 60% RDM after cycles of freezing and thawing, which is the minimum requirement for freezing and thawing resistance according to ASTM C666. The air-entrained PLC and OPC concretes showed the relative dynamic modulus (RDM) of higher than 60%. Comparing two types of air-entrainers, synthetic (A260) and organic air-entrainer (A14), the air-entrained concrete with the organic air entrainer (A14) showed more consistent RDM

223

results after 300 cycles of freezing and thawing compare to concretes with synthetic air-entrainer (A260).

10.2   Recommendations for practice

10.2.1 Early-age behavior

Based on the results of the present study, it was concluded that the relative fineness of a portland limestone cement has the most significant impact on its rate of hydration and extent of chemical and autogenous shrinkage at early ages. Consequently, PLCs may be selected based on their fineness in order to obtain a certain combination of desired early-age properties. In applications where more rapid hydration and strength development rates are required, a fine PLC is recommended, but such selection comes at the expense of increased early-age shrinkage. In applications where early-age shrinkage is to be limited, use of a coarse PLC or a fine PLC in combination with 15% Class F fly ash is recommended.

Determination of whether a Type IL cement is "fine" or "coarse", however, is not a trivial task. While Blaine fineness is widely considered the industry standard for characterizing the fineness of a cement, it was found to be relatively insensitive to differences in the particle size distributions of the Type IL cements considered in this study, such that the largest Blaine "fineness" values were actually obtained for the most dilution-dominated cements. These insensitivities in Blaine fineness can be related to the particle-packing and specific gravity assumptions implicit in the calibration of the Blaine fineness test. Since Type IL cements have typically lower densities (due to the limestone inclusion) and improved particle packing efficiencies (due to broader particle size

224

distributions) compared to ordinary portland cements, the mass of sample that is used based on standard calibration procedures yields a lower porosity than is assumed by the standard, which, in turn, results in higher Blaine fineness values [116]. Instead, fineness parameters obtained by laser diffraction analysis were found to be comparatively more sensitive to changes in the particle size distributions and correlated well with the resulting dilution- or nucleation-dominated behaviors. Based on this preliminary study, it is recommended that "fine" Type IL cements be Classified as those cements having median particle sizes $D_{50} < 10$ μm or 90th percentile particle sizes $D_{90} < 30$ μm. But, further characterization of a larger selection of portland and portland limestone cements would be required to set accurate limits on the Classification.

10.2.2 Mechanical properties and drying shrinkage

Based on the conclusions discussed in section 10.1.3, it is recommended to specify the fineness and calcite content of Type IL cement depending on the application. For higher strength concrete with low *w/b* and high cement factor, finer Type IL is recommended for higher strength and lower drying shrinkage. For intermediate *w/b* and cement factor, coarser Type IL cement is recommended since it resulted in statistically similar concrete compressive strength values while it showed lower drying shrinkage of concrete than finer Type IL cement.

To address the risk with drying shrinkage, mix design acceptance approval for AAA and AA mixes will require testing by ASTM C1581 (where MSA < ½ in) or AASHTO T334 (where MSA > ½ in.), where:

- Concrete with Type IL cement, as defined by ASTM C595 and/or AASHTO M240, exhibits average time to cracking in days equal to or

greater than companion concrete produced with ASTM C 150/AASHTO M80 Type I/II cement

- Concrete with Type IL cement, as defined by ASTM C595 and/or AASHTO M240, exhibits average crack width equal to or less than companion concrete produced with ASTM C 150/AASHTO M80 Type I/II cement

- Type I/II and IL cements should be produced from same clinker (at the same plant) and concrete mixture proportions (e.g., aggregate type and content, cement content, *w/b*) should be consistent.

Further work is needed to implement performance criteria in a special provision or as a performance specification to ensure resistance to shrinkage cracking.

10.2.3 Use with SCMs

When combined with SCMs, PLC mixtures were found to exhibit equivalent or greater compressive strengths and equivalent or reduced permeabilities when compared to OPC mixtures without SCMs. These higher strengths and lower permeabilities occurred irrespective of the fineness of the Type IL cement, suggesting that coarsely ground PLCs may be beneficially combined with SCMs in order to counter some of the strength reductions and porosity increases attributed to the dilution of the clinker.

The increases in compressive strength and reductions in permeability also tended to be greater in blends of SCMs with PLCs than in blends of SCMs with OPCs due to the synergetic interactions between the limestone and the alumina within the SCM. While the synergetic interactions beneficially refined the porosity of the systems, these refinements were accompanied by often substantial increases in early-age shrinkage in PLC-SCM

blended systems. In applications where low shrinkage is required, it is *not* recommended that combinations of PLCs with Class C fly ash or high volumes of slag be used. Further research is recommended to determine if the current GDOT limits on slag replacement in structural concrete should be reduced for blends containing PLCs due to the significant increases in early-age shrinkage observed at the present 50% maximum replacement level.

10.2.4 Use in aggressive environments

The results of this study indicate that PLC and PLC-SCM blended systems have comparable or slightly improved resistance to the ingress of contaminants when compared to neat OPC and OPC-SCM blended systems at $w/b = 0.445$. Similar or greater improvements in permeability would be expected at even lower w/b's, where the dilution of the clinker by the limestone has a less impactful role in hydration and microstructural development due to the inability of the clinker to fully hydrate [117]. When adequately air-entrained, PLC concrete showed good resistance to freezing and thawing cycles under accelerated testing. Therefore, PLCs may be used as a suitable alternative to OPCs in structural applications requiring low permeability to contaminants and freeze/thaw resistance, provided that the potential increases in early-age shrinkage cracking are also controlled.

10.2.5 Methods for characterizing and modeling PLC systems

The research presented in this study also revealed several areas where conventional approaches to characterizing and modeling neat OPC systems did not suitably apply to PLC or PLC-SCM blended systems. In addition to the insufficiencies with the Blaine fineness test previously discussed, the study also indicated that Powers' model for chemical shrinkage under-predicts the amount of chemical shrinkage occurring in PLC (and limestone-containing OPC) systems due to its inability to account for the secondary hydration of carbonate-AFm species. It is therefore recommended that Powers' model not be used for the prediction of early-age shrinkage in PLC-based materials.

Furthermore, the influence of pore solution conductivity on SR and RCPT measurements was found to have a significant impact on the perceived permeability Classifications of both OPC and PLC systems – especially those containing blends with SCMs. Formation factor was determined to provide a more reliable and realistic indicator of microstructural development in both systems and is recommended for use as a more appropriate indicator of concrete's ability to resist the ingress of contaminants such as chloride ions. Further research is required to determine what values of formation factor correspond to acceptable chloride diffusion parameters, not only so that appropriate limits may be set for concrete specifications, but also so that more accurate estimates of expected service life may be predicted. Until such research is done, it is recommended that the SR and RCPT tests only be used in quality control applications where samples of field-batched concrete are compared to laboratory-prepared reference samples having similar compositions and pore solution chemistries. Use of either test with strictly defined performance requirements (e.g., a maximum permitted chloride permeability of 2000

coulombs at 56 days to provide adequate impermeability) is not recommended due to the conflating influence of pore solution composition.

10.3   Recommendations for future research

The research presented in this report provides further insights into the chemical and physical influences of limestone fillers on the hydration and microstructural development of PLC-based materials. However, the research also demonstrates the need for additional research related to the optimization of limestone-blended systems for use in structural applications. Specific areas for future research are recommended as follows:

- The research conducted in this study – for most considerations – only considered *w/b*'s of either 0.40 or 0.445. While the *w/b*'s selected provided substantial insights into the influence of limestone fillers on the hydration and microstructural development of PLC systems compared to those of OPC systems, they were still among the highest *w/b*'s permitted by GDOT for structural concrete applications and only provide an "upper-bound" on the behavior of PLC systems. A wider range of *w/b*'s should also be examined to more fully understand the balance between dilution-dominated behavior (which is more pronounced at higher *w/b*'s) and nucleation- and filler-dominated behavior (which is more pronounced at lower *w/b*'s) at other *w/b*'s that may be encountered in engineering applications.

- Also, the research conducted in this study only considered PLC systems with 8-12% replacement of clinker with limestone. While the dosage rates examined encompassed the typical range of limestone contents expected for Type IL

cements produced within the United States (based on a 15% limit set in current American [6] and Canadian [118] cement specifications), higher dosages of up to 35% are permitted in other parts of the world, including Europe [119]. Additional research is needed to characterize the early-age hydration and microstructural development – and their long-term durability implications – for PLC-based systems at these yet higher limestone dosages.

- With respect to SCM synergies, this research only considered binary blends of PLCs with either 15% weight replacement with Class F fly ash, 15% weight replacement with Class C fly ash, or 50% weight replacement with slag. Further research is recommended over a wider range of SCM dosages in order to determine the minimum replacement level for each SCM required to overcome dilution-induced reductions in compressive strength and impermeability and the maximum replacement level for each SCM such that early-age shrinkage is reduced. Additional research considering ternary blends of PLCs with both fly ash and slag is also recommended in order to investigate how PLC-SCM synergies affect hydration, microstructural development, and long-term durability in ternary blended systems.

- Finely ground PLC systems were found to exhibit particularly pronounced increases in early-age chemical and autogenous shrinkage at the 0.40 *w/b* investigated in this study. Since autogenous shrinkage, in particular, becomes more pronounced at lower *w/b*'s, further research is needed to determine whether there should be an upper limit on the fineness of the Type IL cements used at low

w/b's in order to protect concrete structures from detrimental increases in early-age chemical and autogenous shrinkage.

- Through studies of laboratory-blended PLCs containing custom blends of limestone powders, it was demonstrated that limestone mineralogy has a small effect on the early-age hydration and chemical shrinkage of PLC-based materials, but that ultimately it is the physical and bulk-chemical properties of the limestone that contribute most to the early-age properties. The four limestone powders investigated, however, all had relatively similar mineralogical compositions to one another. Further research should also examine a wider array of limestone sources, to better understand how mineralogical impurities such as amorphous silica or clay affect the hydration and property development of PLC-based materials.

- Limestone was found to interact with both C_3A and C_4AF phases to produce carbonate-AFm phases. While much has already been published in the literature about C_3A interactions with limestone [14, 16], less is known about the C_4AF interactions. Thus, further study into carbonate-AFm reactions from C_4AF hydration is recommended.

- The diffusion coefficients for OPC and PLC concretes were estimated from the RCP test results using the Nernst-Einstein equation, following the model of Barde, et al. [120]. The model implicitly normalizes the total charge passed during the RCP test by an *average* pore solution conductivity for neat OPC concretes, and therefore does not adequately account for the effect of pore solution conductivity on the total charge passed by the SCM-blended systems.

Predicted diffusion coefficients are consequently lower and expected service lives consequently longer due to the inability of the model to separate the structural diffusion parameters from the electrochemical artifacts. Thus, additional research is needed to develop a more appropriate relationship between the total charge passed by RCP and the ionic conductivity of the chloride ions, so that the Nernst-Einstein equation may be more appropriately used to characterize diffusion coefficients and predict service lives of OPC-SCM and PLC-SCM blended systems.

REFERENCES

1. Marland, G., et al., *Global, regional, and national fossil fuel CO2 emissions.* Trends: A Compendium of Data on Global Change, 2007: p. 37831-6335.
2. Mehta, P.K. and P.J.M. Monteiro, *Concrete : microstructure, properties, and materials*. 3rd ed. 2006, New York: McGraw-Hill. 659 pp.
3. Boden, T.A., G. Marland, and R.J. Andres, *Global, regional, and national fossil-fuel CO2 emissions*. 2010, Carbon Dioxide Information Analysis Center, U.S. Department of Energy: Oak Ridge, TN.
4. Malhotra, V., *Making concrete" greener" with fly ash.* Concrete international, 1999. **21**(5): p. 61-66.
5. Muller, N. and J. Hamisch, *A blueprint for a climate friendly cement industry.* 2008, World Wildlife Fund International. p. 101.
6. *ASTM Standard C595*, in *Standard Specification for Blended Hydraulic Cements*. 2012, ASTM International: West Conshohocken, PA.
7. ASTM C595, *Standard Specification for Blended Hydraulic Cements*, in *ASTM International*. 2014, ASTM: West Conshohocken, PA.
8. AASHTO, M., *STANDARD SPECIFICATION FOR BLENDED HYDRAULIC CEMENT*. 2015: American Association of State Highway and Transportation Officials.
9. ASTM C150 / C150M-12, *Standard Specification for Portland Cement*. 2012: ASTM International, West Conshohocken, PA.
10. 85, A.M., *STANDARD SPECIFICATION FOR PORTLAND CEMENT*. 2015: American Association of State Highway and Transportation Officials.
11. European Standard EN 197-1, *Cement - Part 1: Composition, specifications, and conformity criteria for common cements*. 2011: European Committee for Standardization, Brussels, Belgium.
12. ASTM C150, *Standard Specification for Portland Cement*. 2016, ASTM International.
13. Georgia Department of Transportation (GDOT), *Standard Specifications for Construction of Transportation Systems, Section 500.*, in *Concrete Structures.* 2015: Georgia Department of Transportation.
14. Matschei, T., B. Lothenbach, and F.P. Glasser, *The role of calcium carbonate in cement hydration.* Cement and Concrete Research, 2007. **37**(4): p. 551-558.
15. Lothenbach, B., et al., *Influence of limestone on the hydration of Portland cements.* Cement and Concrete Research, 2008. **38**(6): p. 848-860.
16. De Weerdt, K., et al., *Hydration mechanisms of ternary Portland cements containing limestone powder and fly ash.* Cement and Concrete Research, 2011. **41**(3): p. 279-291.
17. Nadelman, E., *Ph.D dissertation: Hydration And Microstructural Development Of Portland Limestone Cement-Based Materials*, in *School of Civil and Environmental Engineering,*. 2016: Georgia Institute of Technology.
18. Isaia, G.C., A.L.G. Gastaldini, and R. Moraes, *Physical and pozzolanic action of mineral additions on the mechanical strength of high-performance concrete.* Cement & Concrete Composites, 2003. **25**(1): p. 69-76.

19. Opoczky, L., *Progress of Particle-Size Distribution during the Intergrinding of a Clinker-Limestone Mixture.* Zement-Kalk-Gips, 1992. **45**(12): p. 648-651.

20. Lawrence, P., M. Cyr, and E. Ringot, *Mineral admixtures in mortars - Effect of inert materials on short-term hydration.* Cement and Concrete Research, 2003. **33**(12): p. 1939-1947.

21. Sun, H.F., et al., *Jet mill grinding of portland cement, limestone, and fly ash: Impact on particle size, hydration rate, and strength.* Cement & Concrete Composites, 2013. **44**: p. 41-49.

22. Jayapalan, A.R., et al., *Influence of Additions of Anatase TiO2 Nanoparticles on Early-Age Properties of Cement-Based Materials.* Transportation Research Record, 2010(2141): p. 41-46.

23. Lee, B.Y. and K.E. Kurtis, *Influence of TiO2 Nanoparticles on Early C3S Hydration.* Journal of the American Ceramic Society, 2010. **93**(10): p. 3399-3405.

24. Thomas, J.J., H.M. Jennings, and J.J. Chen, *Influence of Nucleation Seeding on the Hydration Mechanisms of Tricalcium Silicate and Cement.* Journal of Physical Chemistry C, 2009. **113**(11): p. 4327-4334.

25. Kadri, E.H., et al., *Combined effect of chemical nature and fineness of mineral powders on Portland cement hydration.* Materials and Structures, 2010. **43**(5): p. 665-673.

26. Oey, T., et al., *The Filler Effect: The Influence of Filler Content and Surface Area on Cementitious Reaction Rates.* Journal of the American Ceramic Society, 2013. **96**(6): p. 1978-1990.

27. Kosmatka, S.H., B. Kerkhoff, and W.C. Panarese, *Design and Control of Concrete Mixtures*. 14th ed. 2002, Skokie, IL: Portland Cement Association.

28. Balonis, M. and F.P. Glasser, *The density of cement phases.* Cement and Concrete Research, 2009. **39**(9): p. 733-739.

29. Hawkins, P., P.D. Tennis, and R.J. Detwiler, *The use of limestone in Portland cement: a state-of-the-art review*. 2003: Portland Cement Association Skokie.

30. Dhir, R., et al., *Evaluation of Portland limestone cements for use in concrete construction.* Materials and Structures, 2007. **40**(5): p. 459-473.

31. Svermova, L., M. Sonebi, and P.J. Bartos, *Influence of mix proportions on rheology of cement grouts containing limestone powder.* Cement and Concrete Composites, 2003. **25**(7): p. 737-749.

32. Soroka, I. and N. Setter, *The effect of fillers on strength of cement mortars.* Cement and Concrete Research, 1977. **7**(4): p. 449-456.

33. Heikal, M., H. El-Didamony, and M. Morsy, *Limestone-filled pozzolanic cement.* Cement and Concrete Research, 2000. **30**(11): p. 1827-1834.

34. Meddah, M.S., M.C. Lmbachiya, and R.K. Dhir, *Potential use of binary and composite limestone cements in concrete production.* Construction and Building Materials, 2014. **58**: p. 193-205.

35. Livesey, P., *Strength characteristics of Portland-limestone cements.* Construction and Building Materials, 1991. **5**(3): p. 147-150.

36. D.P. Bentz, E.F.I.B.E.B. and W.J. Weiss, *Limestone Fillers Conserve Cement; Part 2: Durability issues and the effects of limestone fineness on mixtures.* Concrete International. **31**(12).

37. Nocuń-Wczelik, W., B. Trybalska, and E. Żugaj, *Application of calorimetry as a main tool in evaluation of the effect of carbonate additives on cement hydration.* Journal of Thermal Analysis and Calorimetry, 2013. **113**(1): p. 351-356.

38. El-Didamony, H., et al., *Limestone as a retarder and filler in limestone blended cement.* Ceramics, 1995. **39**(1): p. 15-19.

39. Tsivilis, S., et al., *A study on the parameters affecting the properties of Portland limestone cements.* Cement and Concrete Composites, 1999. **21**(2): p. 107-116.

40. Bonavetti, V., et al., *Limestone filler cement in low w/c concrete: a rational use of energy.* Cement and Concrete Research, 2003. **33**(6): p. 865-871.

41. Bentz, D.P. and E.J. Garboczi, *Percolation of phases in a three-dimensional cement paste microstructural model.* Cement and Concrete Research, 1991. **21**(2-3): p. 325-344.

42. Monteiro, P., *Concrete: Microstructure, Properties, and Materials*. 2006: McGraw-Hill Publishing.

43. ASTM C143, *Standard Test Method for Slump of Hydraulic-Cement Concrete.* 2015, ASTM International.

44. Bentz, D.P., et al., *Limestone Fillers Conserve Cement; Part 1: An analysis based on Powers' model.* Concrete International, 2009. **31**(11): p. 41-46.

45. Bentz, D.P. and M.A. Peltz, *Reducing thermal and autogenous shrinkage contributions to early-age cracking.* ACI Materials Journal, 2008. **105**(4): p. 414.

46. Powers, T.C. and T.L. Brownyard. *Studies of the physical properties of hardened Portland cement paste*. in *Journal Proceedings*. 1946.

47. Powers, T.C., *Physical properties of cement paste*. 1900.

48. Tsivilis, S., et al., *The permeability of Portland limestone cement concrete.* Cement and Concrete Research, 2003. **33**(9): p. 1465-1471.

49. Pipilikaki, P. and M. Beazi-Katsioti, *The assessment of porosity and pore size distribution of limestone Portland cement pastes.* Construction and Building Materials, 2009. **23**(5): p. 1966-1970.

50. Claisse, P.A., E. Ganjian, and T.A. Adham, *A vacuum-air permeability test for in situ assessment of cover concrete.* Cement and Concrete Research, 2003. **33**(1): p. 47-53.

51. Bonavetti, V., et al., *Influence of initial curing on the properties of concrete containing limestone blended cement.* Cement and Concrete Research, 2000. **30**(5): p. 703-708.

52. Cochet, G. and F. Sorrentino, *Limestone filled cements: Properties and uses.* Mineral admixtures in cement and concrete, 1993. **4**: p. 266-295.

53. Ramezanianpour, A.A., et al., *Influence of various amounts of limestone powder on performance of Portland limestone cement concretes.* Cement and Concrete Composites, 2009. **31**(10): p. 715-720.

54. Al-Khaiat, H. and M.N. Haque, *Effect of initial curing on early strength and physical properties of a lightweight concrete.* Cement and Concrete Research, 1998. **28**(6): p. 859-866.

55. Alunno-Rosetti, V. and F. Curcio. *A contribution to the knowledge of the properties of portland-limestone cement concretes, with respect to the requirements of european and Italian*. in *Proceedings of the 10th International Congress on the Chemistry of Cement*. 1997.

56. Detwiler, R.J., *Properties of Concretes made with Fly Ash and Cements Containing Limestone*. 1996: Portland Cement Association.

57. ASTM C157, *Standard Test Method for Length Change of Hardened Hydraulic-Cement Mortar and Concrete*. 2014: Pennsylvania, UnitedStates.

58. *ASTM Standard C114*, in *Standard Test Methods for Chemical Analysis of Hydraulic Cement*. 2013, ASTM International: West Conshohocken, PA.

59. *ASTM Standard C1365*, in *Standard Test Method for Determination of the Proportion of Phases in Portland Cement and Portland-Cement Clinker using X-Ray Powder Diffraction Analysis*. 2011, ASTM International: West Conshohocken, PA.

60. 1698, A., *Standard Test Method for Autogenous Strain of Cement Paste and Mortar*. 2014, ASTM International.

61. *ASTM Standard C150*, in *Standard Specification for Portland Cement*. 2004, ASTM International: West Conshohocken, PA.

62. ASTM C204, *Standard Test Methods for Fineness of Hydraulic Cement by Air-Permeability Apparatus*. 2016, ASTM International.

63. ISO 13320-1. 1999, *Particle size analysis—Laserdiffraction methods—Part 1: General principles* International Organization for Standardization:Geneva, CH.

64. ASTM C1679-14, *Standard Practice for Measuring Hydration Kinetics of Hydraulic Cementitious Mixtures Using Isothermal Calorimetry*. 2014, ASTM International: West Conshohocken, PA.

65. C1608, A., *Standard Test Method for Chemical Shrinkage of Hydraulic Cement Paste*. 2012: West Conshohocken, PA.

66. ASTM C1698-09, *Standard Test Method for Autogenous Strain of Cement Paste and Mortar,.* 2014, ASTM International: West Conshohocken, PA,.

67. ASTM C191-13, *Standard Test Methods for Time of Setting of Hydraulic Cement by Vicat Needle*. ASTM International: West Conshohocken, PA.

68. ASTM C191, *Standard Test Methods for Time of Setting of Hydraulic Cement by Vicat Needle*. 2013, ASTM International.

69. Bullard, J.W., et al., *Mechanisms of cement hydration.* Cement and Concrete Research, 2011. **41**(12): p. 1208-1223.

70. ACI 301, *301-Specifications for Structural Concrete for Buildings.* American Concrete Institute International, 2005. **32**: p. 1313-2.

71. Tennis, P.D., M.D.A. Thomas, and W.J. Weiss, *State-of-the-art report on use of limestone in cements at levels of up to 15%*. 2011, Portland Cement Association: Skokie, Illinois. p. 78.

72. Bouasker, M., et al., *Chemical shrinkage of cement pastes and mortars at very early age: Effect of limestone filler and granular inclusions.* Cement and Concrete Composites, 2008. **30**(1): p. 13-22.

73. Georgia Department of Transportation, *Standard Specifications for Construction of Transportation Systems, Section 500 Concrete Structures*. 2015: Georgia Department of Transportation.

74. *ASTM Standard C192*, in *Standard Practice for Making and Curing Concrete Test Specimens in the Laboratory*. 2016, ASTM International: West Conshohocken, PA.

75. *Standard Test Method for Slump of Hydraulic-Cement Concrete*. 2015, ASTM International.

76. ASTM C138, *Standard Test Method for Density (Unit Weight), Yield, and Air Content (Gravimetric) of Concrete*. 2016: West Conshohocken, PA.

77. *Standard Test Method for Air Content of Freshly Mixed Concrete by the Pressure Method*. 2014, ASTM International.

78. *ASTM C39/C39M-16b Standard Test Method for Compressive Strength of Cylindrical Concrete Specimens*. 2016, ASTM International, West Conshohocken, PA.

79. ASTM C469, *Standard Test Method for Static Modulus of Elasticity and Poisson’s Ratio of Concrete in Compression*. 2014, ASTM International.

80. C496, A., *ASTM C496-11 Standard Test Method for Splitting Tensile Strength of Cylindrical Concrete Specimens*. 2011, ASTM International.

81. American Association of State, H. and O. Transportation, *T 22-14 - Compressive Strength of Cylindrical Concrete Specimens*, in *Standard Specifications for Transportation Materials and Methods of Sampling and Testing and AASHTO Provisional Standards (2016 Edition)*. 2016, American Association of State Highway and Transportation Officials (AASHTO).

82. American Association of State, H. and O. Transportation, *T 198-15 - Splitting Tensile Strength of Cylindrical Concrete Specimens*, in *Standard Specifications for Transportation Materials and Methods of Sampling and Testing and AASHTO Provisional Standards (2016 Edition)*. 2016, American Association of State Highway and Transportation Officials (AASHTO).

83. AlabamaDOT, *Standard Specifications for Highway Construction - Section 501*. 2012.

84. Carrasquillo, R.L., *Microcracking and engineering properties of high-strength concrete.* 1980.

85. 363R-10, A., *ACI 363R-10 Report on High-Strength Concrete.*

86. AASHTO TP95-11, *STANDARD METHOD OF TEST FOR SURFACE RESISTIVITY INDICATION OF CONCRETE'S ABILITY TO RESIST CHLORIDE ION PENETRATION*. 2011: Washington, DC.

87. ASTM C666, *Standard Test Method for Resistance of Concrete to Rapid Freezing and Thawing*. 2015, ASTM International.

88. AASHTO TP 95, *Standard method of test for surface resistivity indication of concrete's ability to resist chloride ion penetration*. 2011: American Association of State Highway and Transportation Officials.

89. Tennis, P., M. Thomas, and W. Weiss, *State-of-the-Art Report on Use of Limestone in Cements at Levels of up to 15%.* Portland Cem Assoc, 2011: p. 10-20.

90. AASHTO 259-80, *Resistance of Concrete to Chloride Ion Penetration,"American Association of States Highway and Transportation Officials,*

Standard Specifications—Part II, Tests,. 1990: Washington, D.C.

91. C1202, A., *Electrical Indication of Concrete's Ability to Resist Chloride Ion Penetration*. 1997: ASTM, Philadelphia, PA, 1997.

92. Georgia Department of Transportation, *Section 500-Concrete Structures*. 2006, Department of Transportation: Atlanta, Goergia.

93.   ASTM C457, *Standard Test Method for Microscopical Determination of Parameters of the Air-Void System in Hardened Concrete*. 2012: West Conshohocken, PA.

94.   Castellote, M., C. Andrade, and M.C. Alonso, *Standardization, to a reference of 25 C, of electrical resistivity for mortars and concretes in saturated or isolated conditions*. Materials Journal, 2002. **99**(2): p. 119-128.

95.   Irassar, E., *Sulfate attack on cementitious materials containing limestone filler—A review*. Cement and Concrete Research, 2009. **39**(3): p. 241-254.

96.   Chini, A.R., L.C. Muszynski, and J.K. Hicks, *Determination of acceptance permeability characteristics for performance-related specifications for Portland cement concrete*. 2003.

97.   Rupnow, T. and P. Icenogle, *Surface resistivity measurements evaluated as alternative to rapid chloride permeability test for quality assurance and acceptance*. Transportation Research Record: Journal of the Transportation Research Board, 2012(2290): p. 30-37.

98.   Du, L. and K.J. Folliard, *Mechanisms of air entrainment in concrete*. Cement and concrete research, 2005. **35**(8): p. 1463-1471.

99.   American Concrete Institute Committee 201, *Guide to Durable Concrete (ACI201.2-R08)*. 2008, American Concrete Institute.

100.   American Concrete Institute Committee 318, *Building Code Requirements for Structural Concrete (ACI 318-14)*. 2014, American Concrete Institute.

101.   Mindess, S., J.F. Young, and D. Darwin, *Concrete*. 2nd ed. 2003, Upper Saddle River, NJ: Pearson.

102.   *ASTM C512 - Standard Test Method for Creep of Concrete in Compression*. 2015, ASTM International.

103.   De Weerdt, K., et al., *Synergy between fly ash and limestone powder in ternary cements*. Cement & Concrete Composites, 2011. **33**(1): p. 30-38.

104.   Menendez, G., V. Bonavetti, and E.F. Irassar, *Strength development of ternary blended cement with limestone filler and blast-furnace slag*. Cement & Concrete Composites, 2003. **25**(1): p. 61-67.

105.   Vance, K., et al., *Hydration and strength development in ternary portland cement blends containing limestone and fly ash or metakaolin*. Cement & Concrete Composites, 2013. **39**: p. 93-103.

106.   Antoni, M., et al., *Cement substitution by a combination of metakaolin and limestone*. Cement and Concrete Research, 2012. **42**(12): p. 1579-1589.

107.   Puerta-Falla, G., et al., *Elucidating the Role of the Aluminous Source on Limestone Reactivity in Cementitious Materials*. Journal of the American Ceramic Society, 2015. **98**(12): p. 4076-4089.

108.   Georgia Department of Transportation, *Standard Specifications for Construction of Transportation Systems, Section 500 - Concrete Structures*. 2015, Georgia Department of Transportation.

109.   *ASTM Standard C1679*, in *Standard Practice for Measuring Hydration Kinetics of Hydraulic Cementitious Mixtures Using Isothermal Calorimetry*. 2009, ASTM International: West Conshohocken, PA.

110.   Schindler, A.K. and K.J. Folliard, *Heat of hydration models for cementitious materials*. ACI Materials Journal, 2005. **102**(1): p. 24-33.

111. *ASTM Standard C1608*, in *Standard Test Method for Chemical Shrinkage of Hydraulic Cement Paste*. 2012, ASTM International: West Conshohocken, PA.
112. *ASTM Standard C1698*, in *Standard Test Method for Autogenous Strain of Cement Paste and Mortar*. 2009, ASTM International: West Conshohocken, PA.
113. *ASTM Standard C39*, in *Standard Test Method for Compressive Strength of Cylindrical Concrete Specimens*. 2016, ASTM International: West Conshohocken, PA.
114. Tsivilis, S., N. Voglis, and J. Photou, *A study of the intergrinding of clinker and limestone.* Minerals Engineering, 1999. **12**(7): p. 837-840.
115. (FHWA), F.H.A., *SECTION 718- 47 HIGH PERFORMANCE CONCRETE FOR PRECAST AND PRESTRESSED BRIDGE ELEMENTS*. https://www.fhwa.dot.gov/resourcecenter/teams/structures/hpm_3.cfm.
116. *ASTM Standard C204*, in *Standard Test Methods for Fineness of Hydraulic Cement by Air-Permeability Apparatus*. 2011, ASTM International: West Conshohocken, PA.
117. Bonavetti, V., et al., *Limestone filler cement in low w/c concrete: A rational use of energy.* Cement and Concrete Research, 2003. **33**(6): p. 865-871.
118. *CSA Standard A3001*, in *Cementitious materials for use in concrete*. 2013, Canadian Standards Association: Mississauga, Ontario, Canada.
119. *European Standard EN 197-1*, in *Cement - Part 1: Composition, specifications, and conformity criteria for common cements*. 2011, European Committee for Standardization: Brussels, Belgium.
120. Barde, V., et al., *Relating Material Properties to Exposure Conditions for Predicting Service Life in Concrete Bridge Decks in Indiana*. 2009, Indiana Department of Transportation: Purdue University, West Lafayette, IN.